Master's thesis

NTNU
Norwegian University of Science and Technology
Faculty of Natural Sciences
Department of Chemistry

Sunniva Kvamme

Levels of Per- and polyfluoroalkyl substances (PFAS), trace elements, and steroid hormones in Arctic char (*Salvelinus alpinus*) from Lake Diesetvatnet, Svalbard

Master's thesis in Environmental Toxicology and Chemistry
Supervisor: Øyvind Mikkelsen
August 2022

NTNU
Norwegian University of
Science and Technology

Sunniva Kvamme

Levels of Per- and polyfluoroalkyl substances (PFAS), trace elements, and steroid hormones in Arctic char (*Salvelinus alpinus*) from Lake Diesetvatnet, Svalbard

Master's thesis in Environmental Toxicology and Chemistry
Supervisor: Øyvind Mikkelsen
August 2022

Norwegian University of Science and Technology
Faculty of Natural Sciences
Department of Chemistry

NTNU
Norwegian University of
Science and Technology

Acknowledgement

This thesis is the finalizing part of a Master's degree in "Environmental Toxicology and Chemistry", with a specialization in Environmental Chemistry, conducted at the Department of Chemistry at the Norwegian University of Science and Technology (NTNU). This part is dedicated to everyone that has contributed and made this master project possible.

Firstly, I want to thank my supervisor Øyvind Mikkelsen for giving me the possibility to undertake an interesting project at Svalbard, and for all of your guidance, feedback, and positivity throughout the whole project. I am grateful for all the knowledge and ideas you have shared. I also appreciate the guidance through the Arctic Field Grant application, and I want to thank Perrine Geraudie for proofreading and for providing feedback in this process.

I also want to thank The Research Council of Norway for funding the fieldwork in Ny-Ålesund through the Arctic Field Grant. A great thanks to the Norwegian Polar institute for support in the field with safe transportation and for providing necessary equipment. Thanks to Team Mikkelsen; Mathilde, Thomas, Nicola, Lill-Kathrin, Karoline, and Øyvind for a memorable fieldwork trip, and all support during the fieldwork.

From the Department of Chemistry, I want to thank Alexandros Asimakopoulos for providing me with PFAS methodology, and Shannen Thora Lea Sait for helping me out in the lab. I am forever grateful for your help, and for making everything a bit more understandable. Great thanks to Susana Villa Gonzalez for sharing your immense knowledge on MS, and for answering all of my questions. I also want to thank Kyyas Seyitmuhammedov and Anica Simic for helping me during freeze-drying and microwave digestion.

From the Department of Biology, I want to thank Tomasz Maciej Ciesielski for supporting my project. I am grateful for your help with the elemental methodology, for borrowing your equipment, and for your biological perspective on the project. I also want to thank Grethe Stavik Eggen for helping me in the lab on short notice, and Åse Krøkje for answering my questions and providing suggestions for the project.

I also want to thank my fellow students for making everyday life better. Especially great thanks to Mathilde, Hege, Natalia, Hanna Sofie, Sara, Sunniva, Laura, Nicola, and Christina for nice lunch breaks and cinnamon bun Wednesdays.

Great thanks to David Velasco Sanchez for helping me with R Studio. And lastly, I want to thank my boyfriend, Johannes, for putting up with me during this stressful period, and for your tech support.

Abstract

The Arctic environment is considered a pristine area, however, the presence of contaminants such as Per- and polyfluoroalkyl substances (PFAS) and mercury have been detected in the environment and wildlife due to their potential to undergo long-range transport. These chemicals have proven to be persistent, toxic, and bioaccumulate in Arctic animals. Arctic char is a suitable sentinel species for monitoring Arctic freshwater ecosystems due to its northern circumpolar distribution. The main objective of this study was to quantify the levels of steroid hormones, PFAS, and trace elements in Arctic char from Lake Diesetvatnet. Moreover, the study aimed to determine whether long-chained PFAS (≥ 8 carbons) dominated in the plasma of Arctic char and to study the distribution of selected trace elements in various tissues from Arctic char. Plasma samples were extracted for steroid hormones and PFAS with Hybrid solid phase extraction (Hybrid SPE), and analyzed with ultra-performance supercritical fluid chromatography-tandem mass spectrometry (UPSFC-MS/MS) and ultra-performance-liquid chromatography-tandem mass spectrometry (UPLC-MS/MS), respectively. A total of 41 trace elements in tissues from Arctic char were analyzed with inductively coupled-plasma mass spectrometry (ICP-MS). The distribution of selected trace elements was investigated with principal component analysis (PCA), and the concentration of trace elements Hg, Cd, Pb, and As was statistically tested for elevated concentrations in the kidney and liver. Steroid hormones androstenedione, testosterone, 5α-Dihydrotestosterone, and 11-Ketotestosterone were observed in the plasma of Arctic char. In total, 9 PFAS compounds were observed in the plasma of Arctic char including 6:2 FTS, PFNA, PFOSA, PFOS, PFDA, PFUnA, PFDoDA, PFTriDA, and PFECHS which were dominated by carbon chain lengths C8 to C13. PCA indicated that trace elements were differently distributed within tissues of Arctic char. Kidney samples correlated strongly with trace elements Hg, Cd, Se, and Tl, and Cu correlated with liver samples. The concentration of Hg in the kidney was significantly higher than Hg in plasma, and Cd concentration in the kidney was significantly higher than Cd in the brain, gonad, and hard roe, whereas As concentrations in the kidney and gonad were significantly higher than As in red blood cells and plasma. No statistical difference in Pb concentrations between tissues was found, and the liver tissue showed no significantly higher concentrations of Hg, Cd, Pb, and As. The levels of PFAS and trace elements observed in Arctic char from Lake Diesetvatnet were low but indicate the presence of contaminants that have been long-range transported to Lake Diesetvatnet as there are no local contamination sources in the vicinity of the Lake. Moreover, these results indicate that PFAS and the trace elements Hg, Cd, and As exhibit the potential to accumulate in Arctic char.

Contents

List of Figures

List of Tables

List of Abbreviations

POPs	Persistent organic pollutants
K_{OW}	Octanol-water partition coefficient
K_{OA}	Octanol-air partition coefficient
LRAT	Long-range atmospheric transport
PAHs	Polycyclic aromatic hydrocarbons
PCBs	Polychlorinated biphenyls
OHCs	Organohalogenated compounds
DDT	Dichlorodiphenyltrichloroethane
DDE	Dichlorodiphenyldichloroethylene
MeHg	Monomethyl mercury
PFAS	Per- and polyfluoroalkyl substances
FFTS	Fire-fighting training sites
WWTP	Wastewater treatment plant
AFFF	Aqueous film-forming foam
PFSA	Perfluoroalkyl sulfonates
PFCA	Perfluorocarboxylates
PFOS	Perfluorooctanesulfonic acid
PFOA	Perfluorooctanoic acid
FTOH	Fluorotelomer alcohols
PFHxS	Perfluoroheaxne-1-sulfonic acid
PFNA	Perfluorononanoic acid
PFDA	Perfluorodecanoic acid
PFUnA	Perfluoroundecanoic acid
PFOSA	Perfluorooctane sulfonamide
6:2 FTS	1H, 2H-Perfluorooctane sulfonate (6:2)
PFDoDA	Perfluorododecanoic acid
PFTriDa	Perfluorotridecanoic acid
PFECHS	Perfluoroethylcyclohexane sulfonic acid
AF	Ammonium formate
CA	Citric acid
HNO_3	Nitric acid
PP	Protein precipitation
GEM	Gaseous elemental mercury
ADME	Atmospheric mercury depletion events
MT	Metallothionein
BBB	Blood-brain barrier
CNS	Central nervous system
HSI	Hepatosomatic index
HP-axis	Hypothalamic-pituitary axis
HPI-axis	Hypothalamic-pituitary-interrenal axis
AN	Androstenedione
TS	Testosterone
DHT	5α-Dihydrotestosterone
11-ketoTS	11-Ketotestosterone
Hybrid SPE	Hybrid solid phase extraction
SPE	Solid phase extraction
SLE	Solid-liquid extraction
UPLC	Ultra-Performance liquid chromatography
UPSFC	Ultra-Performance supercritical fluid chromatography
MS/MS	Tandem mass spectrometry
ESI	Electrospray ionization
ICP-MS	Inductively coupled plasma-mass spectrometry
LOD	Limit of detection
LOQ	Limit of quantification
CRM	Certified reference material
IS	Internal standard
TA	Target analyte
ME	Matrix effect
PCA	Principal component analysis
RBC	Red blood cells
MeOH	Methanol
ACN	Acetonitrile
MTBE	Methyl tert-butyl ether
ME	Matrix effect

1 Introduction

The Arctic environment is considered one of the most pristine areas on the globe due to its remote location, untouched nature, and few local inhabitants. However, the presence of man-made chemicals and elevated levels of trace elements such as mercury have been detected in nature and wildlife in Arctic regions for several decades due to increased anthropogenic activities at lower latitudes [1, 2]. Many of these chemicals have the potential to undergo long-range transport from lower latitudes by wind and ocean currents and can therefore be transported far away from the emission point [3].

Per- and polyfluoroalkyl substances (PFAS), which is a large group of fluorinated compounds, have exhibited a variety of properties such as persistency, toxicity, and bioaccumulation in wildlife [4, 5]. Moreover, some of the PFAS compounds have proven to biomagnify in food webs in which high concentrations have been detected in apex predators such as polar bears [6, 2]. As a consequence, Perfluorooctanesulfonic acid (PFOS) and its salts were added to the Stockholm Convention in 2009 under "New POPs" and Perfluorooctanoic acid (PFOA) and its salts followingly added in 2019 [4, 5]. Mercury, and especially the organic form monomethyl mercury ($MeHg^+$), has been of great concern due to the bioaccumulative properties in fish and neurotoxic effects seen by the Minamata disaster in the 1950s due to human $MeHg^+$ poisoning. Even though mercury today is regulated by the Minamata Convention adopted in 2013, which aims to protect the environment and human health against mercury, high levels of mercury are still detected in wildlife in the Arctic [1, 7, 8]. Additionally, mercury levels have been postulated to increase in the future due to the thawing of permafrost, changed biogeochemical cycling of mercury, and increased methylation, as a consequence of global warming which occurs 3 times faster in polar regions than the global average [8].

Most studies on levels of contaminants and adverse effects have been conducted in marine ecosystems in the Arctic, but the information available on Arctic freshwater systems is still scarce [2, 1, 6]. Arctic Lakes are characterized by low nutrient input, primary production, and biodiversity [9, 10]. Moreover, Arctic Lakes have simple food webs with Arctic char (*Salvelinus alpinus*) as the apex predator of these ecosystems [11]. Arctic char is a fish species with a northern circumpolar distribution and is, therefore, a suitable sentinel species for Arctic freshwater ecosystems. Additionally, Arctic Lakes are closed aquatic systems that can become a deposit of a mixture of contaminants transported from lower latitudes [12].

The main objective of this study was to quantify the levels of Per- and polyfluoroalkyl substances (PFAS), trace elements, and steroid hormones in Arctic char from Lake Diesetvatnet at Svalbard. Lake Diesetvatnet is suitable for studying the impact of long-range transported

contaminants to Arctic freshwaters due to the remote location and the absence of local point contamination sources. Moreover, this study will investigate whether long-chained PFAS ($\geq$ 8 carbons) dominate in the plasma of Arctic char compared to short-chained PFAS ($<$ 8 carbons) by empirical study. And lastly, the distribution of selected trace elements; Hg, Cd, Pb, As, Cu, Zn, Ni, Cr, Se, Co, Mn, and Tl in various tissues including the brain, gonad, hard roe, liver, and kidney of Arctic char will be studied and investigated with multivariate principal component analysis. Additionally, non-essential trace elements including Hg, Cd, Pb, and As are expected to be present at elevated levels in the kidney and liver. This will be statistically tested by the null hypothesis: "There is no significant difference in levels of Hg, Cd, Pb, and As in the kidney and liver of Arctic char compared to the other collected tissues" against the alternative hypothesis: "There is a significant difference in the levels of Hg, Cd, and Pb in the kidney and liver of Arctic char compared to the other collected tissues".

To the best of my knowledge, contaminants in Arctic char from Lake Diesetvatnet has not been extensively studied previously, apart from the Ymer expedition in 1980 that collected two Arctic char samples in the vicinity of Lake Diesetvatnet in which persistent organic pollutants were analyzed [13]. However, this is more than 40 years ago, and new contaminants have been introduced to the environment since then. This project outcome consists of a new batch of innovative data on contamination in Arctic char and supports the scientific research of Arctic freshwater ecosystems. Additionally, other trace element levels except for mercury in various tissues of Arctic char have been poorly represented in the literature, this study will therefore add to the database of elemental levels in Arctic char. Muscle tissue is often sampled as this is relevant for human consumption. However, muscle tissue is not always sufficient to indicate trace element contamination in the fish due to the weak accumulating potential in this tissue [14, 15]. Therefore, sampling other tissues related to detoxification including the kidney and liver might provide better information about the bioaccumulative potential of some trace elements. Additionally, Svalbard is one of the locations that are particularly understudied in terms of freshwater ecosystems compared to other locations in the Arctic, such as Greenland and Canada, therefore more scientific data on Arctic freshwaters from this region will be provided [8, 6, 2]. Moreover, this research is important from the perspective of human health as it will bring knowledge to local inhabitants that might consume Arctic char as a part of their diet.

2 Theoretical background

2.1 Long-range transport of contaminants to the Arctic

The Arctic environment is often considered a pristine area. However, several studies have reported contamination in different environmental matrices indicating levels well above background levels of trace elements and persistent organic pollutants (POPs) originating from anthropogenic activities at lower latitudes [1, 2, 16]. Svalbard archipelago, which is located in the high Arctic, has become a reservoir of contamination because of its specific environmental conditions and geographic location.

Contamination is transported to the Arctic over long distances due to mass movements of air and water [3]. Moreover, migrating species have also been identified as conveyors of contaminants to the Arctic. In locations where migrating seabirds are nesting elevated levels of contamination have been detected in soil, freshwater, and fish [17]. The importance of the various transport routes depends on the physiochemical properties of the contaminants and environmental factors [3]. Physio-chemical properties that affect contaminants transport and distribution in the environment are; vapor pressure, polarity, water-solubility, persistence, octanol-water partition coefficient (K_{OW}), and to which extent adsorption to particles occurs [18]. Environmental factors that influence the transport and distribution of contaminants are temperature, wind speed and direction, and water currents. During the winter there is a greater air mass transport to the Arctic where increased concentrations of aerosols in the lower atmosphere have been observed [3]. This has been described as the Arctic Haze phenomenon. The haze derives from long-range atmospheric transport (LRAT) of anthropogenic emissions at lower latitudes, and usually appears in late Winter and early Spring concurrent with the polar sunrise [19]. The Arctic haze consists of sulfate, sea salts, crustal materials, black carbon, and trace amounts of heavy metals and organic contaminants [20]. Stronger air mass flow combined with reduced vertical mixing, less precipitation, and the absence of photochemical reactions during the polar night traps the pollutants in the atmosphere in the Arctic during wintertime [19]. Moreover, the mode of emission affects the fate of contaminants distribution in the environment, i.e in which environmental compartment the release of contaminants occurs during production, use, or disposal [18]. Examples of primary emissions routes are the leaching of pesticides used in agriculture into the soil and the emission of polycyclic aromatic hydrocarbons (PAHs) into the atmosphere by fossil fuel burning. In addition, secondary sources of pollution are becoming increasingly important with climate change, especially in the Arctic where warming occurs at a rate higher than the global average (Figure 1) [21]. Secondary emission sources are defined as the remobilization of contaminants from environmental reservoirs e.g. melting glaciers, thawing

permafrost, and forest fires. With that being said, environmental compartments such as the hydrosphere, cryosphere, and terrestrial compartments are in continuous exchange with the atmosphere, independent of climate change. However, increased warming is postulated to increase secondary emissions and redistribute pollutants in environmental compartments [18, 22, 21]. These secondary emission sources could be a significant contributor of contaminants to Arctic Lakes.

Many POPs such as polychlorinated biphenyls (PCBs), organohalogenated compounds (OHCs), and PAHs are subjected to LRAT. The potential for POPs to undergo LRAT has been suggested to depend on the volatility of the compounds as well as the ambient temperature. There are several proposed mechanisms for LRAT of contaminants to the Arctic [23]. The Global distillation theory suggests that compounds are fractionated in the atmosphere due to different vapor pressures, and therefore, are dispersed and mobilized to various latitudes [3, 23]. The "grasshopper effect" is a process defined as repeated cycles of volatilization, transport, and deposition (multi-hopping) of compounds before final deposition into environmental compartments [23]. Various compounds have different vapor pressure and subsequently different mobility. Volatile or semi-volatile compounds travel longer distances compared to less volatile compounds that will rapidly partition into environmental compartments such as water, snow, ice, soil, or vegetation. Moreover, transport is also dependent on the ambient temperature, as warmer temperatures at mid-latitudes favor evaporation, and cooler temperatures at high latitudes favor deposition from the atmosphere to terrestrial or oceanic compartments. Another important factor that affects a compound's ability to undergo LRAT is the octanol-air partition coefficient, K_{OA}, which describes the concentration ratio of the compounds in octanol and air at equilibrium [23]. LRAT has been considered the main pathway for volatile and semi-volatile POPs to reach the Arctic, however, ocean currents may be the dominant transport pathway over decadal time scales for some chemicals [18]. This hypothesis can be supported by high levels of contaminants found in high Arctic Lakes, that are not connected to the Ocean system or inhabited by migrating birds, which can only be explained by atmospheric transport [3].

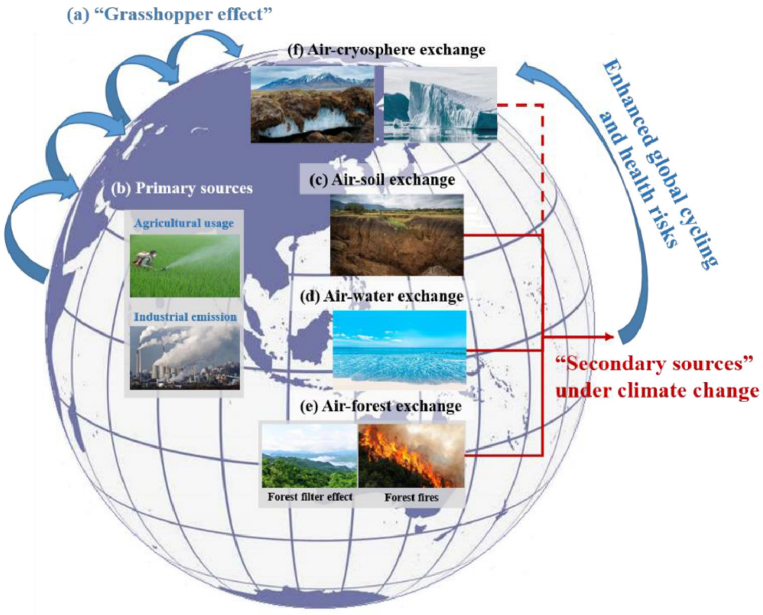

Figure 1: Global cycling patterns of POPs with enhanced secondary sources under climate change. Panel (a) shows the conceptual patterns of "grasshopper effect" for POPs as they are transported from low latitudes to polar regions. Panel (b) illustrates sources of POPs that are released through primary emission. Panel (c) - (f) are the detailed redistribution processes from secondary sources of POPs between environmental compartments, including (c) air-soil exchange, (d) air-water exchange, (e) air-forest exchange, and (f) air-cryosphere exchange. Figure adopted from Gong, P., and Wang, X. (2022) under the Creative Common lisence [21]

2.2 Local contamination sources at Svalbard

Long-range transport of pollutants is the major contributor to contaminants in the Norwegian Arctic, however, there exist several minor local pollution sources at Svalbard. There are a few permanent settlements in Svalbard, the main settlement is Longyearbyen which has around 2400 residents. In addition, there are a few smaller residential areas such as Ny-Ålesund, Sveagruva, and Barentsburg. All of these settlements were originally mining localities, however, Ny-Ålesund became a research center after 1964, and Longyearbyen serves as a tourism and research location. There are a few local point pollution sources in these settlements, in Longyearbyen mine 7 is still in operation, mine 7, and the coal power plant that supplies inhabitants with power. The coal mining and power plant have shown to emit organic contaminants such as PAHs and potentially toxic trace elements such as lead (Pb) and mercury (Hg) [24, 25, 16]. In Longyearbyen, the wastewater goes directly into Adventsfjorden untreated, and the wastewater has shown to contain a wide range of contaminants; including both heavy metals and Per- and polyfluoroalkyl substances (PFAS) [26, 27]. Moreover, fire-fighting training sites (FFTS) have been identified as local point sources for PFAS contamination both in Longyearbyen and Ny-Ålesund settlements. In ad-

dition, a sewage treatment facility at Ny-Ålesund close to Solvatnet has also been identified to contribute to PFAS contamination [28]. Solvatnet, which is located close to the settlement, is a freshwater pond that provides an important bird sanctuary [29]. In 2015, a small-scale wastewater treatment plant (WWTP) was installed in Ny-Ålesund settlement by Kings Bay AS [30]. This recently installed WWTP has shown to be effective in retaining microplastic from the wastewater shown by a pilot study conducted by Granberg *et al.* (2019), however, it still may constitute a point source of pollutants the to Kongsfjorden area [30, 31]. The Zepplin station at Ny-Ålesund have been monitoring several PFAS compounds in airborne particles which have shown that the concentrations are higher during the spring and summer [6].Additionally, trace elements have also been detected for a long time at the Zeppelin station, and a seasonal trend observed shows increased concentrations which coincide with the Arctic haze that appears in early Spring [32, 33].

2.3 Bioaccumulation, biconcentration, and biomagnification

Bioaccumulation is defined as the accumulation of contaminant(s) in an organism through ingestion of food or inhalation of the ambient air, whereas bioconcentration is a term that describes the accumulation of contaminants in aquatic organisms through passive diffusion from the water [15]. As a consequence, the concentration in organisms exceeds that of the ambient environment or that in the ingested food. Accumulation is a result of the toxicodynamics of a compound in an organism, i.e. the rate of absorption is higher than the rate of elimination for the contaminant [34]. Bioaccumulation and bioconcentration can be expressed as the bioaccumulation factor (BAF) and bioconcentration factor (BCF), respectively, which is the ratio of the concentration of a contaminant in the organism compared to that in the surrounding environment. For lipophilic compounds, bioaccumulation can be described by the logarithm_{10} of the K_{OW} ($\log K_{\text{OW}}$). Chemicals with a $\log K_{\text{OW}} > 5$ are considered to have the potential to bioaccumulate [35]. However, this bioaccumulation criteria is not suitable for all types of contaminants. Some contaminants accumulate based on other properties, i.e. PFAS with affinity for proteins [36, 37, 38]. Biomagnification is defined as the enrichment of a contaminant concentration with the trophic levels in a food web [15]. This process results from the accumulation of the contaminant from prey to predator successively throughout the food web up to the apex predator whose concentration can be several orders of magnitude compared to that in the primary producers. Biomagnification can be determined in a food web by measuring contaminant tissue concentrations at each trophic level, and the trophic level is determined by measuring the ratio of stable nitrogen isotope (δ^{15}N) [38, 15]. The biomagnification factor (BMF) can then be calculated, and a

BMF > 1 indicate biomagnification in a food web.

2.4 Per- and polyfluoroalkyl substances

2.4.1 Physio-chemical properties

Poly- and perfluoroalkyl substances (PFAS) are a group of compounds that are of anthropogenic origin. PFAS are composed of fluorinated carbon chains of different lengths and functional groups, which can be partly or fully fluorinated alkyl chains. The highly electronegative and small atomic size of fluorine provides a short, strong, and polar C-F bond, resulting in the high chemical and thermal stability of PFAS. Moreover, fluorine's low polarizability creates low surface tension and weak cohesive forces of fluorocarbons [39]. PFAS are amphiphilic compounds that are immiscible with water. Functional groups such as carboxylic acid group (-COOH), and sulfonate group (-SOH_3) are added to make the compounds more hydrophilic [6]. These physio-chemical properties provide PFAS with surfactant-like properties as well as water- and oil repellency, which makes them applicable for various industrial and commercial applications. In addition, the electron-withdrawing force of fluorine makes the C-C skeleton strong and stable, which has resulted in PFAS being ubiquitous and persistent in the environment [40].

There are several sub-groups of PFAS based on their functional groups. Two of the most studied PFAS compounds are Perfluorooctanesulfonic acid (PFOS) and Perfluorooctanoic acid (PFOA) which belong to Perfluoroalkyl sulfonates (PFSA) and Perfluorocarboxylates (PFCA) subgroups, respectively (Figure 2).

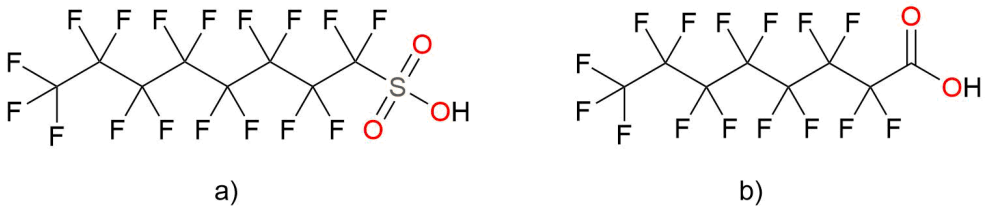

Figure 2: Chemical structure of Perfluorinated compounds; a) Perfluorooctane sulfonate (PFOS) and b) Perfluorooctanoate (PFOA). Made with ChemDraw Professional 16.0.

Another large subgroup of PFAS is the Fluorotelomer alcohols (FTOH), which are considered neutral precursors of the more stable acidic compounds, PFCA [41]. Other neutral PFAS are perfluoroalkyl sulfonamides (FASA) and N-ethyl perfluorooctane sulfonamidoethanol (N-EtFOSE) [42, 43]. Many of the neutral precursor compounds are less water-soluble and more volatile than ionic PFAS. Long-range transport and subsequent degradation in the atmosphere or biota of these neutral precursors to the more persistent PFCA and PFSA

compounds have been suggested to be an important mechanism for the distribution of these compounds in the environment.

A distinction is often made between long-chain PFAS (6 C $\geq$ for PFSA and 8 C $\geq$ for PFCA) and short-chain PFAS (6 C $<$ for PFSA and 8 C $<$ for PFCA), as their environmental fate among others are dependent on chain length and functional group, which determine the partitioning of PFAS in environmental matrices such as air, water, soil, sediment, ice, snow, and biota [44]. PFCA and PFSA both have low acid dissociation constants (K_{a}) and are almost fully ionized under most environmental conditions. As anionic substances, the PFCA and PFSA easily bind to proteins and phospholipids, these compounds are therefore found at elevated concentrations in biological tissues such as the blood, liver, and kidney. Long-chained PFAS has shown to have a strong affinity to sediment particles, whereas short-chained PFAS are often found in the dissolved phase [45, 46]. Partitioning has shown to vary with environmental conditions, e.g. organic carbon content and pH, with increased sorption with organic carbon content. As a consequence, short-chain PFAS have a higher potential for long-range transport, while long-chained PFASs are preferentially distributed in biota or abiotic environments such as sediment and soil [44]. Long-range transport of PFAS to remote areas such as the Arctic has been explained by two processes: (i) transport by ocean currents and (ii) atmospheric transport that result in oxidative transformations and degradation and subsequent wet and dry deposition of airborne precursors (Figure 3), such as FTOH and sulfonamide ethanol (EtFOSE) [47, 48]. Smog chamber studies have demonstrated that FTOH can degrade into various PFCA in the atmosphere [49]. Ionic PFAS that have higher water solubility, are mainly distributed in surface waters [50, 51]. Both PFCA and PFSA have been detected in global oceans and in remote lakes [52, 53]. Secondary sources of PFAS, such as the melting of glaciers, snowpacks, and sea ice have become increasingly important as a contribution to redistributing PFAS in the environment and have shown to be an important source of input of PFAS compounds to Arctic Lakes [54, 53].

2.4.2 History of PFAS - Source, production, use

PFAS is a group of chemicals that have been produced since the late 1940s. Due to their versatile properties such as high thermal stability, chemical inertness, dielectric strength, and hydrophobic- and lipophobic properties they are used in a wide range of products. PFAS are used in products such as surfactants and polymers. In polymers, they are used as water- and oil-repellent treatment in textile and food-contact paper. Due to PFAS's ability to lower aqueous surface tensions, they are used in emulsifiers and dispersants such as aqueous film-forming foams (AFFF) used as fire extinguishers at FFTS [6]. Other uses are electrical

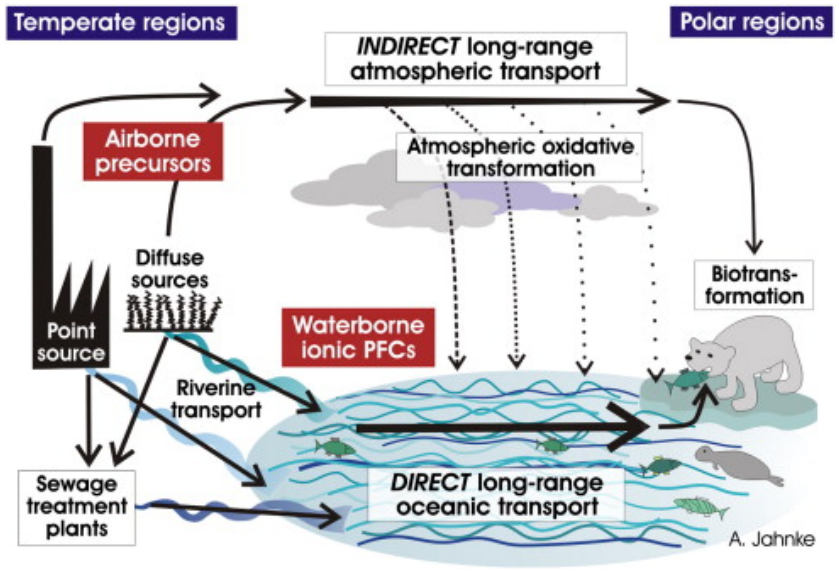

Figure 3: Major transport pathways of PFAS (PFCs) to the Arctic environment. Figure adopted from Butt *et al.* (2010) with permission from Elsevier [55].

insulations, non-stick coating (e.g. Teflon), lubricants for skis, anti-reflective coatings, and membranes for Chlor-alkali production. In 2018, the OECD/UNEP report identified 4730 different PFAS substances [56]. However, Buck *et al.* only identified 256 of these substances as commercially relevant, meaning substances used in commercial products [57].

There are two main methods for PFAS production (Buck *et al.* 2011); electrochemical fluorination (ECF) and telomerization [57]. In ECF, all the hydrogen atoms of the parent compound are replaced by fluorine by conducting electrolysis in anhydrous hydrogen fluoride (HF). The ECF process can lead to carbon chain rearrangement and breakage because of the free radical nature of the process, resulting in the synthesis of a mixture of linear and branched isomers and other fluorinated bi-products. The 3M company began large-scale production of PFCA with $8 \geq$ carbon atoms in 1947 using the ECF process. Later on, they started producing perfluorooctane sulfonyl fluoride (PFOSF) based products such as perfluorooctanesulfonamide ethanols (FOSE) and PFOS. In the telomerization manufacturing process, perfluoroalkyl iodide reacts with tetrafluoroethylene resulting in mixtures of perfluoroalkyl iodide with longer perfluorinated chains than the raw material. When the starting material is linear, the end product will also be linear. This method has been used for PFAS production since the 1970s by various companies for the production of FTOH and PFCA.

PFAS have been produced in large quantities for decades before their ubiquitously in the abiotic environment and biota was discovered around the 1990s and early 2000s [58]. The 3M company phased out production of long-chain PFCA and PFSA voluntarily around 2000, and measures have been taken by international authorities to regulate the production and use of

PFAS compounds. In 2009, PFOS, its salts, and Perfluorooctane sulfonyl fluoride (PFOSF) were listed under Annex B (Restriction) in the Stockholm Convention of New POPs because of their persistent, toxic, bioaccumulative properties, and potential for long-range transport [4]. Eventually, PFOA, its salts, and other related compounds were listed under Annex A (Elimination) in 2019 [5]. Perfluorohexane-1-sulfonic acid (PFHxS), its salts, and PFHxS-related compounds were proposed for listing in the Stockholm Convention by Norway in 2017 but are still under review [59, 60]. Even though some PFAS compounds have been eliminated and restricted in production and use, new replacement compounds have been produced, with unknown effects. A recent trend among the global PFAS producers is to replace the long-chain PFSA and PFCA with shorter-chain homologs or other types of fluorinated chemicals [61]. An example is the dimer acid of hexafluoropropylene oxide (HFPO-DA), an ether-based replacement compound for PFOA that has been increasingly studied over the last years. This compound is also marketed as its ammonium salt under the trade name GenX and has been used in the manufacturing of fluoropolymers [60, 61]. In China, compounds named chlorinated polyfluorinated ether sulfonate (F-53) and 6:2 chlorinated polyfluorinated ether sulfonate (F-53B) have been replaced by PFOS salts in the metal plating industry, and the 3M company started producing AFFF based on gaseous fluorinated ketones and 6:2 fluorotelomers (6:2 FTS) after the phase-out of PFOS and PFOA [61]. Short-chain PFAS has shown to be more water-soluble and has less affinity to particles, as a result, they are more mobile than the legacy PFAS compounds. However, some of the replacement compounds have shown to be equally or even more toxic than the original PFAS compounds that were replaced.

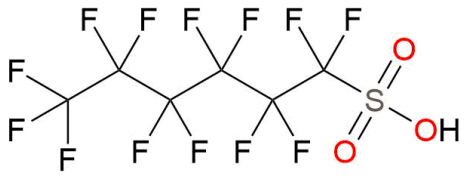

Figure 4: Chemical structure of Perfluorohexane-1-sulfonic acid (PFHxS). This compound and other PFHxS-related compounds are still under review by the Stockholm Convention. Made with ChemDraw Professional 16.0.

2.4.3 PFAS in freshwater environments

Studies on PFAS in Arctic Lake environments indicate that there are different sources of PFAS input to Arctic Lakes and that the location is an important factor affecting the PFAS levels. Freshwater environments that are located in the vicinity of point pollution sources

such as airports or FFTS have higher levels of PFAS in both the water column and in the sediments which has been demonstrated by a study conducted by Lescord *et al.* (2015) that analyzed six different Lakes in Canada in which two of the Lakes had higher PFAS contaminant loads due to the proximity of airports [46]. Lakes that mainly receive PFAS through LRAT generally have lower levels of PFAS. Several studies also highlight the importance of hydrological input as a vector of PFAS to the Lakes. Meltwater from glaciers, snowpacks, and thawing permafrost, i.e secondary emission sources, are repositories for atmospheric PFAS deposition that contributes to redistributing PFAS in the Arctic environment [22, 62, 53, 63].

2.4.4 Levels and toxicological effects of PFAS in fish

PFAS compounds are ubiquitous in the Arctic environment and wildlife [6]. Most studies have been conducted on marine species and food webs, especially on top predators such as polar bears and seabirds. However, there is limited knowledge about Arctic freshwater ecosystems and species, such as Arctic char [55]. In wildlife studies, PFOS is the most frequently detected compound found in the highest concentration [55, 6]. PFOS, Perfluorononanoic acid (PFNA) and Perfluorodecanoic acid (PFDA) are frequently detected in freshwater fish. PFOA on the other hand is not commonly detected in fish, but there are reports on longer chain PFCA such as Perfluoroundecanoic acid (PFUnA) and perfluorotetradecanoic acid (PFTA) that have been detected, however, infrequently. Levels and PFAS compounds that have been detected from previous studies in Arctic char are listed in Table A.1 [40, 46, 64, 65, 66].

Toxicokinetics is dependent on several factors inherent of the fish including gender, age, life stage, and genetics [34]. Additionally, there might be considerable species differences in the absorption, elimination, distribution, and metabolic capacities of fish. Moreover, diet, habitat, and location are also important, especially for ecosystems located close to point pollution sources [46]. The toxicokinetic and toxicodynamic effects are also dependent on the physio-chemical properties of the chemical, i.e. for PFASs; carbon chain length, functional group, and whether the compound is ionic or neutral.

One of the uptake routes of waterborne contaminants for fish is directly through the gills or skin, which could occur for water-soluble PFAS [37, 67]. Moreover, PFAS can bioaccumulate in fish through exposure to diet [36]. The importance of the two uptake pathways is uncertain and might vary depending on fish species, physio-chemical properties of the contaminants as well as the habitat and diet [36]. Elimination of contaminants in fish occurs through the gills as a passive excretion pathway, or as active excretion by the kidney and the bile [68]. The importance of the different elimination pathways depends on the physiochemical properties of the compounds and might vary between species.

Studies on bioconcentration and tissue distribution of PFAS compounds have found that the BCF, half-life, and uptake rate increase with perfluoroalkyl chain length in all tissues, and that PFSA has higher accumulating properties compared to PFCA [37]. The highest concentrations of PFAS have found in blood, liver, and kidney, whereas lower concentrations are found in gonad, muscle, and adipose tissue [37]. Unlike the legacy POPs that tend to bioaccumulate in lipid-rich tissues, PFAS accumulate in protein-rich tissues [6]. In humans, it has been reported that the serum protein albumin is important for binding with PFAS, as well as fatty acid binding proteins (FABP) found in the liver, and organic anion transporter (OATs) proteins [69]. The serum half-life of PFAS has been reported to be several years in humans, however, only days in fish [70, 71]. Bioaccumulation of the longer chained PFAS have been proven for several species in the Arctic wildlife [6]. Additionally, the functional group of PFAS might affect the internal distribution in fish [72]. Moreover, several studies have indicated that short-chain substitutes for legacy PFAS such as Perfluorobutanoic acid (PFBA), Perfluorobutanoic acid sulfonate (PFBS), and GenX, might have shorter half-lives and are eliminated faster [73, 74]. Lower bioaccumulative properties of the short-chain PFAS could be a result of greater water-solubility [73]. Studies have also indicated species-specific differences in uptake rates, total uptake, and elimination rates of PFAS [37]. Moreover, the route of exposure has proved to determine tissue distribution, total body burden and elimination rate [37, 36]. Fish exposed through the diet tend to have the highest PFAS concentrations in the liver, followed by blood and kidney, whereas fish exposed through the water have higher concentrations in blood compared to kidney and liver [37, 71].

In fish, adverse effects on the reproductive system and multigenerational effects including increased deformity and mortality in embryos have been observed. Moreover, growth suppression and vitellogenin induction in males have also been found [75, 76, 77]. Histological alterations to tissues such as the liver, thyroid, and gonads have been observed at PFOS concentrations of 10-300 μg L^{-1} [75]. A substitute of PFOS, F-53B, has shown to bioaccumulate in zebrafish and induce histopathological changes in the liver, and a reduction in the activity of oxidative stress-related biomarkers [78]. In addition, there have been reports indicating alterations in gene expression related to steroidogenesis [79]. There are also several studies suggesting that some PFAS compounds might be endocrine disrupting chemicals (EDCs), affecting both thyroid- and sex-hormones [80, 81, 77, 82]. These findings highlight the fact that there are multiple toxicity outcomes, and that there are potential species differences in the effects. Many of these mentioned exposure studies have only looked at the exposure of single compounds or simple PFAS mixtures [76]. Moreover, in reality, organisms are exposed to a complex mixture of contaminants that could alter toxicity outcomes, either by leading to synergistic, antagonistic, or additive effects, also known as "cocktail effects".

2.5 Trace elements

A wide range of elements compromise the Earth's crust and therefore exist in natural background levels. However, the levels of different elements can vary widely between environmental compartments as well as between locations. Elements are redistributed naturally in the environment by geological and biological cycles, and the hydrosphere is transporting elements from the crust to the biosphere, where elements can accumulate in plants and organisms, and eventually be incorporated into the food chain [34]. However, human activity has led to increasing levels of trace elements released into the environment due to activities such as mining, farming, and fossil fuel burning [83]. This has resulted in various elements becoming available at higher levels in several environmental compartments such as the atmosphere, hydrosphere, and biosphere [83]. Increased distribution and discharge of specific elements have raised concern due to negative effects seen in terrestrial and aquatic organisms, and in humans [84, 1].

In analytical chemistry, trace elements are defined as elements that exist in a concentration < 100 μg g^{-1} [83]. In biological systems, elements can be divided into three categories; major elements such as carbon, hydrogen, nitrogen, and oxygen; minor elements comprising calcium, chlorine, magnesium, phosphorus, potassium, sodium, and trace elements which can be further be dived into essential and non-essential trace elements. Essential trace elements are substances that are crucial for biological life concerning growth and development and are often required in a specific concentration range for an organism to be in homeostasis [34, 83]. Both deficiency and exceedance of the required concentration may provide toxic effects. Some trace elements that are essential for human and animal life are copper (Cu), zinc (Zn), iron (Fe), manganese (Mn), selenium (Se), and cobalt (Co). In contrast, non-essential trace elements that have no known biological functions can produce toxic effects even at low concentrations. Examples of elements that are toxic for most biological life are mercury (Hg), cadmium (Cd), lead (Pb), and arsenic (As). Because these elements have been shown to exert toxicity at low concentrations in both aquatic organisms and humans, these elements will be the main focus of this thesis. However, several studies have indicated that some essential trace elements might be exceeded at some locations in fish, therefore, this study will also look into a selection of essential trace elements.

2.5.1 Sources, input, and cycling of trace elements in freshwater ecosystems

Major sources of anthropogenic atmospheric emission of trace elements are fossil fuel combustion, non-ferrous metal production, and waste incineration [84]. Coal combustion releases chromium (Cr), Hg, Mn, antimony (Sb), Se, tin (Sn), and thallium (Tl), while the com-

bustion of gasoline is a source of lead (Pb). However, the release of Pb from gasoline has rapidly decreased since the 1980s due to conversion to unleaded gasoline. Oil combustion is a source of nickel (Ni) and vanadium (V). Non-ferrous metal production releases arsenic (As), cadmium (Cd), Cu, indium (In), and Zn, and waste incineration have shown to release heavy metals such as Cd, As, Cr, Pb [84]. Another important source of mercury emission is small-scale gold mining, which has been identified as a greater source than earlier anticipated [1, 8]. In addition, metal mining and smelting are also contributing sources of heavy metals. Moreover, today mercury is regulated through the Minamata Convention on Mercury which is a global treaty that was adopted in 2013 and entered into force in 2017 [7].

The physical and chemical forms of trace elements released impact their behavior, transport, and fate. The majority of elements are emitted as aerosols with different particles size, in the gaseous phase, or a mix of both [84, 3]. The distance they are transported is dependent on particle size and solubility in which larger elemental particles deposits closer to the pollution source. However, other environmental factors such as temperature, wind, and precipitation conditions also impact the distance they travel [84]. Elements emitted as gases are more prone to undergo LRAT. For example, gaseous elemental mercury (Hg^0, GEM), which has a lifetime of approximately 1 year in the atmosphere, is transported to the Arctic by air currents within a few days [1]. Moreover, it has been estimated that anthropogenic activity is contributing to two-thirds of the atmospheric Hg [1]. Besides, Hg exists in several oxidation states in addition to GEM; inorganic divalent form (Hg^{2+}) and organic forms in which monomethyl mercury ($MeHg^+$) is the most common organic form of Hg. Pb and Cd have also proven to undergo LRAT to the Arctic, and Cd has exhibited similar transport pathways as Hg even though this element is released primarily as aerosols rather than in the gaseous state [84]. When elements have been transported to the Arctic, they are subsequently sequestered from the atmosphere by wet or dry deposition. Hg has been linked to increased deposition during polar sunrise described as atmospheric mercury depletion events (AMDE), a phenomenon first reported by Schroeder *et al.* (1998) [85]. A change in the oxidation state of GEM occurs due to increased ozone and reactive halogen species in the atmosphere such as bromine (Br^-) and chlorine (Cl^-) leading to oxidation of GEM to Hg^{2+} that is subsequently deposited. On the contrary, Cd deposition occurs due to the aggregation of particles together with fog droplets and sea salt aerosols [84].

In freshwater ecosystems snowmelt has been identified as an important contributor to the input of Hg, where concentrations have been measured highest early in spring [86]. Moreover, thawing permafrost has been suggested as a potential source for the input of Hg to Lake ecosystems, as permafrost has been identified as a reservoir of Hg [1]. The location of freshwaters also determines the input and concentration of trace elements, and concentrations

are usually highest in locations close to point pollution sources such as mining and smelting industries [87]. The concentration and speciation of trace elements affect the bioavailability and subsequently the toxicity of these elements to fish. Elements in soluble fraction or as ionic species are more readily bioavailable [15]. Several factors affect the concentration and speciation of trace elements in freshwater environments. Firstly, the local bedrock determines which elements are enriched in the environment. At Mitra peninsula at Svalbard, there is a metamorphic rock type with a mix of marble, phyllite, metapelitic schist, and small amounts of quartzite. Metamorphic rocks are chemically altered products of sedimentary or igneous rocks, and metamorphism takes place under high temperature and pressure for a long time in the interior of Earth's crust [88]. These types of rock consist of major elements such as C, Si, Al, and Mg and minor trace elements such as Fe, Cu, Sr, Ni, Zn. Moreover, water parameters such as ionic strength, water hardness (Ca^{2+} concentration), organic matter, pH, redox potential, and valence state of the elements determine the speciation [15, 84, 89, 90, 91]. Organic matter and pH determine the retention of elements in sediments and the water phase, where a decrease in pH increases the ionic concentrations of elements [92]. Elevated levels of several trace elements in freshwater environments have been associated with particulate organic matter and vegetation, and concentrations in sediments of freshwater are generally higher than in the waterbody [87, 93, 84]. Additionally, the Hg concentration might depend on the size of the Lake catchment area which is an indicator for the input of atmospheric wet and dry deposition [94, 95, 91].

The cycling and speciation of Hg in freshwaters are influenced by microbes that are involved in altering Hg speciation. Microbes methylate dissolved Hg^{2+} to MeHg, and the production of MeHg is of high concern due to this compound's high toxicity and biomaginfying properties displayed in Artic food webs [1]. Methylation mainly occurs in the top part of the sediments where there are increased levels of organic and particulate matter, but, can occur in the water column as well [92]. Moreover, demethylating bacteria also exist, in which MeHg is demethylated to Hg^{2+}. Two factors are known to activate the methylation process; decreased pH and dissolved organic matter (DOM) content in the water [96]. Photochemical transformations of Hg also play a key role in modifying the speciation, mobility, and toxicity of Hg in freshwaters. Hg^{2+}, which is a reactive species, can be photochemically reduced to Hg^0 which results in the evasion of Hg from freshwaters, while oxidation of Hg^0 results in retention of mercury in freshwaters. Some studies have indicated that there is increased Hg reduction in freshwaters compared to marine waters, and that reduction of Hg in freshwaters is mainly due to photoreduction, and not attributed to demethylation [97, 98].

2.5.2 Levels of trace elements and toxicological effect in fish

The chemical speciation of trace elements affects their bioavailability and toxicity. Generally, trace elements dissolved in the water phase as ions are more bioavailable and toxic. The uptake of trace elements in fish depends on both physiological factors inherent to the fish and the aquatic environment. Dissolved trace elements are mainly taken up by the gills or through the skin. When trace elements are absorbed by the gills, they can either be eliminated back to the water phase or distributed to other tissues such as the liver for incorporation into the metabolism or detoxified. Moreover, trace elements can also be taken up through the diet, where trace elements are absorbed by the alimentary tract. Additionally, the uptake rate is determined by the concentration of trace elements in the ambient environment and habitat conditions, as well as dietary concentrations [92]. For example, wild fish are primarily exposed to MeHg through their diet ($\geq$ 90% of total uptake) [99, 100]. Most of the MeHg in ingested food is absorbed across the intestine with uptake efficiencies up to 80% and then transferred to the blood [99]. MeHg circulates in the bloodstream and is further distributed to tissues and organs with a high affinity for MeHg. Initial concentrations of MeHg in fish are greatest in the blood, spleen, kidney, and liver. However, after a few weeks, MeHg is redistributed and found to accumulate in skeletal muscle bound to cysteine, an amino acid [101, 102]. Uptake of MeHg through the gills is less efficient with only 15% absorption [100]. Elimination of MeHg from fish is generally slow, where the half-life of MeHg has been suggested to be approximately 490 days [103]. When the elimination rate is slower than the uptake rate bioaccumulation will occur over time [104]. Fish also seem to have fewer defense mechanisms against MeHg compared to mammals which have shown to exhibit demethylation mechanisms in the liver which favors more readily elimination of Hg [105]. Moreover, both essential and non-essential trace elements exhibit greater accumulation in metabolic active tissues such as the liver, kidney, and gills compared to other types of tissues such as muscle and skin [15]. Greater accumulation in these tissues can be explained by their role in the detoxification of toxic elements. In addition, the liver and kidney have a higher occurrence of metallothionein (MT), which is a family of cysteine-rich proteins that sequesters heavy metals such as Hg, Cd, Pb, and Cu [14].

Bioaccumulation of trace elements is often greater in freshwater fish than in marine fish species. Studies have found that landlocked Arctic char accumulates higher concentrations of Hg compared to anadromous Arctic char [106, 107, 108]. In anadromous Arctic char biomass dilution of Hg concentrations has been observed with increased growth and size [84]. Hg concentrations have been found to correlate positively with age, length, trophic position, size, lipid content, body condition, and diet [109, 110, 91, 111]. Additionally, diet is an important factor that affects the bioaccumulation of trace elements in fish. For example,

some studies have found that benthic invertebrates have higher levels of Hg compared to pelagic invertebrates [112]. Additionally, an increase in bioaccumulation of Hg has been observed for landlocked Arctic char that have become cannibalistic, due to a shift in a diet at a higher trophic level [113]. Bioaccumulation of trace elements is also dependent on abiotic environmental factors. Higher concentrations of organic matter and humic acids have shown to increase the bioavailability of Hg for uptake as it increases the retention of Hg in the water phase [92, 91, 84]. Increased bioaccumulation has also been observed with decreased water pH for several trace elements such as Hg, Cd, Pb, Al, Ni, and Cu, and an increased water temperature has been suggested to affect the uptake of trace elements such as Cd and Pb and is mainly attributed to increased metabolic rate in the summer season [89, 92, 90]. Additionally, bioaccumulation of Hg might depend on the size of the Lake catchment area which is an indicator for the input of atmospheric wet and dry deposition [94, 95, 91].

Toxic outcomes observed in fish by exposure to MeHg are changes in biochemical processes, damage to cells and tissues, and reduced reproduction [104]. Moreover, MeHg has been linked to sublethal effects such as reduced growth, development, and behavioral changes [114]. Cd toxicity is often related to kidney dysfunction and nephrotoxicity [92]. Fish exposed to Cd have shown behavior changes, especially a reduction in predatory behavior [115]. Moreover, Cd has proven to induce the MT gene expression and production, which play an important role in the binding of trace elements in the liver and kidney [116, 117]. Pb has been suggested to disturb Ca^{2+}-homeostasis due to its similarity with Ca^{2+} [92].

2.5.3 Selenium and mercury interactions

Trace elements such as Hg have a high affinity for sulfur in cysteine-rich proteins and enzymes. However, Hg has about 10^6 times greater affinity for Se compared to sulfur compounds, suggesting that Se is superior in binding Hg [118]. Hg interacts strongly with Se in an organism forming insoluble mercury selenide (Hg-Se) species that is non-toxic and has a protective effect on Hg toxicity. However, the binding of Hg also reduces the bioavailability of Se. Se is a crucial element in antioxidant enzymes called selenoezymes that prevents oxidative damage from reactive oxygen species (ROS). An excess of Se over Hg is therefore needed to maintain the enzyme activity and antioxidant system to prevent oxidative damage from ROS. The toxicity of Hg is dependent on the Se status in an organism, and a tissue molar ratio of Se:Hg > 1 has been proposed to be beneficial for protection against Hg toxicity [119].

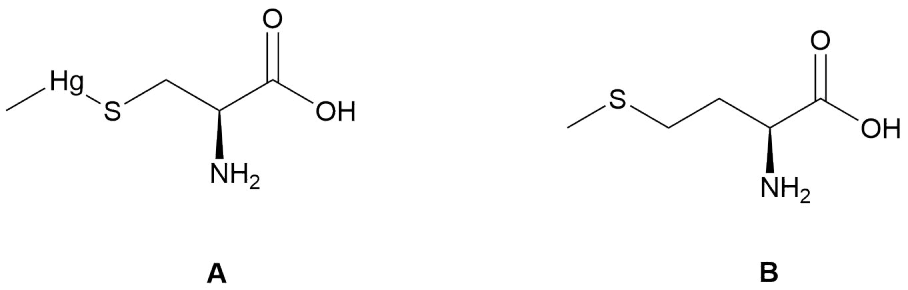

Figure 5: MeHg can bind to the amino acid cysteine to form a cysteine-mercury complex (A) which is similar to the essential amino acid methionine (B), and in that way be transported across the BBB due to amino acid mimicry. Figure redrawn from Aschner, M. and Aschner, J.L (1990) [123]. Made in ChemDraw Professional 19.0.

2.5.4 Blood-brain barrier and maternal transfer in fish

Similarly to mammals, teleost fish have several protective membranes in the brain that isolates the neuronal microenvironment from the blood [120, 121]. The blood-brain barrier (BBB) is a highly selective semipermeable tissue consisting of tight junctions of endothelial cells in the brain capillaries that impede non-selective diffusion from the circulating blood into the extracellular fluid of the central nervous system (CNS) [34]. This barrier only allows the passage of small molecules by passive diffusion or active transport of macromolecules, nutrients, and ions that are crucial for neural function. Thus, the BBB prevents blood bourne contaminants from entering the CNS which possibly could produce neurotoxic effects. Moreover, the highly selective transport across the brain vessels is important to protect the integrety of the CNS as any small disturbances might affect the signaling and functioning of the brain [120].

For instance, MeHg is a known neurotoxic compound that can cross the BBB [122, 34]. The mechanism behind this is the ability of MeHg to mimic a natural amino acid. In the blood, MeHg can bind to the amino acid cysteine to form a cysteine-mercury complex (Figure 5) [123]. The only structural difference between this complex and the amino acid methionine is the Hg atom that is located between the sulfur and the methyl group. Because of the similarity in chemical structure, this complex can be transported across the BBB by the neutral amino acid transporter.

Maternal transfer of contaminants from the gravid fish to the hard roes (eggs) has been demonstrated by several studies [124, 125]. During the spawning period, contaminants can be redistributed within the body, and increase in the ovaries, resulting in increased exposure of the oocytes. A study suggested that the transfer of organohalogenated contaminants from fish to eggs was influenced by lipid percentage in the fish and eggs [126]. Moreover, Hg has also been proven to be transferred maternally to the eggs mainly as MeHg ($> 90\%$).

However, the amount of MeHg transferred maternally is suggested to be low [122]. The diet of the fish during oogenesis has also been suggested to affect the MeHg load in eggs. Exposure of contaminants to fish could lead to reduced reproductive success due to lowered survival rates of the eggs and larvae of fish, and delay in the spawning [122].

2.6 Arctic Lakes

Arctic Lakes are characterized as oligotrophic with low input of nutrients, primary production, and biodiversity [9]. The Arctic environment has strong seasonal shifts, with a long winter period of 9-10 months and a short ice-free period in the summer from mid-July to the end of September [9]. During the winter, Arctic Lakes have a thick and clear ice cover of approximately 1.5-2 meters. In addition, little annual precipitation (< 400 mm) minimizes the snow layer on the ice allowing sunlight to penetrate the thick ice, which results in some primary production all year round. This is a critical characteristic of Arctic Lakes as they are ice-covered most of the year. Moreover, Arctic Lakes have low water temperatures and reach maximum summer temperatures of $5 - 7°C$ [127, 128]. However, the main limiting factor for primary production in Arctic Lake ecosystems is nutrients, and not sunlight and temperature [10]. Because Lakes are closed aquatic systems, they can become a deposit of a mixture of contaminants.

Arctic Lakes can be divided into two types; glacial Lakes and non-glacial Lakes [10]. The main difference is that glacial Lakes receive glacial meltwater in the spring when the sun returns. The input of glacial meltwater decreases the water temperature and the visibility in the water column because of the increased input of sediment particles. Particles transported with meltwater significantly reduce the income of sunlight and hence the primary production. Low primary production results in lowered concentrations of plankton and organic material. Arctic Lakes are quite shallow, and the water column is not stratified due to cold summer temperatures and much wind [128]. Non-glacial Lakes usually have higher water temperatures in the summer (7-8°C). In addition, non-glacial Lakes have increased visibility in the water column, up to 5-8 meters, whereas glacial Lakes have a visibility depth of only 10-60 centimeters. Due to the special bedrock on Svalbard, several Artic Lakes have a high content of dissolved ions [10]. Some Arctic Lakes are also connected to the Ocean by rivers, however, the rivers are normally frozen completely during the wintertime [128]. Lakes that are inhabited by nesting and breeding sea bird colonies have higher input of nutrients and therefore increased primary production [12]. In addition to transporting nutrients, the birds act as a vector for pollutants to these Lakes. An example is Lake Ellasjøen at Bjørnøya, where the Lake catchment has increased levels of PCBs and Hg due to bird influence [17].

Svalbard is a remote island with a harsh climate which has resulted in freshwaters with few species being able to survive. Arctic Lakes have low species diversity and simple food webs with Arctic char as the apex predator. The flora and fauna of Artic Lakes are usually simple consisting of a few pelagic and benthic invertebrates [129]. As Arctic Lakes are oligotrophic, the diet of Artic char might differ between freshwaters and during the season.

Lake Diesetvatnet located at the Mitra peninsula (Mitrahalvøya) on Spitsbergen at Svalbard, consists of two connected Lake systems; Nordre Diesetvatnet and Søre Diesetvatnet (catchment areas are given in Table 2). Søre Diesetvatnet is connected to the Ocean by a 3-4 km long river named Diesetelva [127]. The hydrological budget of Disetvatnet is influenced by glacier meltwater, groundwater sources, and the seasonal melting of snow. The most dominating glacier is Dronningbreen, which is the greatest glacier system at Mitrahalvøya. As a consequence, the water temperature is low ($4 - 5°C$) in the summer [128]. The water chemistry in the river stream from glaciers is dependent on the local bedrock, however, meltwater from glaciers usually has low concentrations of nutrients, organic matter and low conductivity [10]. In Lake Diestvatnet, the visibility depth has been measured to be around 0.25 to 1 meters [130].

Table 2: Catchment area of Søre- and Nordre Diesetvatnet located at Mitrahalvøya, Svalbard.

Lake	**Area (km^2)**
Søre Disetvatnet	1.74
Nordre Disetvatnet	2.30

2.7 Arctic char (*Salvelinus alpinus*)

Arctic char (*Salvelinus alpinus*) is a cold-water fish species of the Salmonidae family that has a northern circumpolar distribution. Arctic char is the only freshwater fish at Svalbard that inhabit and reproduce in Arctic Lakes throughout the year. This fish species has adapted to strong seasonal changes and challenging environmental conditions [11]. There are two main forms of Arctic char; landlocked and anadromous Arctic char [9]. The landlocked form spends its whole life in the Lake, whereas anadromous Arctic char migrate to the sea during summer. These two groups of Arctic char can co-exist in Arctic Lakes that are connected to the Ocean by river streams, however, in closed Lakes, only landlocked forms exist. It is estimated that approximately 100-150 freshwaters are inhabited by landlocked Arctic char on Svalbard, on the contrary, around 20 Arctic lakes are inhabited by anadromous Artic char. The life strategy of Arctic char is developed depending on conditional traits such as growth rate, body size, and lipid stores in the early juvenile stage [11]. Various environmental

conditions also affect the ratio of anadromous and landlocked Arctic char, such as the length of the river stream, temperature, salinity, predation, and food availability in the Lake [128]. However, it has been confirmed that the two forms of Arctic char originate from the same gene pool, as the offspring of each form can develop into both forms [131].

Landlocked Arctic char has a restricted growth pattern, however, when they switch to a cannibalistic diet i.e. eating smaller Arctic char, their growth increases. Moreover, cannibalism is an important mechanism for regulating the density and dynamics of a population [128, 132]. The majority of the population consists of small dwarf individuals, which are restricted to a size of 12-18 cm [9, 11]. Cannibalistic individuals are often bigger than 30 cm and can reach the age of 35. Glacial Arctic Lakes that have reduced visibility often have fewer cannibalistic individuals. However, cannibalistic feeding of Arctic char is population-specific, and Artic char from Svalbard have stronger cannibalistic tendencies than Artic char from more temperate regions in mainland Norway [132]. Landlocked Arctic char becomes sexually mature at age 2-7 years. Moreover, landlocked Arctic char has shown to exhibit spawning cycles of two years, probably due to limited food in oligotrophic Artic Lakes and the need to regain energy reserves after spawning [133].

The anadromous life strategy implies that the Arctic char is born in the Lake, and undertakes one or several migrations to the ocean to feed before returning to the freshwater for over-wintering and to spawn (for sexually mature individuals) [11]. During their residence in seawater, anadromous Artic char feed intensively until they have increased their body weight, fat storage, as well as diminished appetite [11]. The migration period normally starts in mid-July and lasts for approximately 30 days at Svalbard, and Artic char return before the river freezes. During the sea residence, Arctic char can grow up to 5 cm in length and double their weight, especially during the first years of migration [128]. When juvenile Arctic char change their habitat from the Lake to the river they begin their anadromous life strategy, where they can stay for 3-6 summer periods before migrating to the sea. Anadromous Arctic char do not migrate any longer than 30 km from where they grew up, and the age of first migration is around 4-9 years. Anadromous individuals reach sexual maturity after 3-4 seaward migrations, at age 8 years or older [128]. Their length when they reach sexual maturity is usually around 30-35 cm, but female char is normally a bit longer (40-45 cm) when they become sexually mature [128]. Moreover, anadromous Arctic char can reach up to 70 cm in length [11]. Arctic char may not migrate and spawn each year depending on their energy reserves [11].

Lake Diesetvatnet is inhabited by both landlocked and anadromous Arctic char due to the connection with the Ocean. Studies from Diesetelva have found that 43% of the smaller Arctic char (< 25 cm) return from seaward migration, whereas 75% of the bigger individuals

(> 45 cm) return to the Lake [128]. This indicates that the mortality rate is bigger for smaller individuals during migration. The major cause of mortality during the migration is predation, and in Diesetelva there have been observations of seal bites on Arctic char that return to the river. However, seawater tolerance has also been hypothesized to affect the survival of smaller individuals [130]. Monitoring studies in Diesetelva have revealed that the amount of anadromous char was relatively constant from the 70s to the 90s with a count of 700-900 anadromous char migrating up the river [9].

2.7.1 Rythmic life of Arctic char

The long periods of continuous darkness and sunlight during the winter- and summer months are one unique feature of the Arctic. The seasonal absence of circadian rhythm in feeding behavior is a ubiquitous trait among resident polar vertebrates. During the winter when Arctic Lakes are ice-covered, studies have shown that Arctic char exhibit minimal activity and that they mostly stay in the same place to save their energy reserves [11]. Nevertheless, there is evidence that Arctic char keep track of time during winter, and that the ambient photoperiod is a determining factor affecting their plasma melatonin levels, a hormone that influences the circadian rhythm [134]. Arctic char have shown to exhibit strong seasonality in food intake and growth, as a result of seasonal differences in water temperature and food availability in high Arctic Lakes.

In early spring, the anadromous form of Arctic char prepares for seaward migration in the summer by initiating a pre-adaptive process called smoltification. Endogenous rhythms and endocrinological changes as well as external factors such as increased solar radiation and water temperatures interact to determine the timing of smoltification in anadromous Arctic char [135]. Smoltification is a process that involves a series of physiological, biochemical, and behavioral changes that prepare Arctic char for seaward migration and their residence stay in the Ocean [11]. During smoltification, Arctic char gain seawater tolerance, i.e the ability to maintain plasma osmolality and ion concentrations far below that of seawater. This is a necessary feature for migrating anadromous Arctic char due to the salinity difference in the marine water and freshwater. A measure of seawater tolerance is the activity of the enzyme Na^+K^+–ATPase, which is the main driver of ion secretion by the gill during hypoosmoregulation in seawater. Arctic char upregulate this activity during spring when the sunlight returns. In teleost fish, the steroid hormone cortisol has an osmoregulatory function and has shown to play an important role in seawater adaptation [136, 137, 135, 11]. At lower latitudes, i.e. mainland Norway, it has been suggested that Arctic char prepare for their return to the freshwater by downregulating the gill Na^+K^+–ATPase activity by the end of their sea residence. During sea migration, anadromous Arctic char increase their body

weight and fat reserves to prepare for overwintering in the freshwater in which emaciation eventually will occur resulting in reduced body condition [11]. Moreover, Arctic char has an inherent seasonal up-and down-regulation of their appetite that is influenced by a pre-determined adipose level which subsequently leads to a cessation of appetite [11].

Arctic char spawn in the autumn, from late August to October, and the eggs hatch during spring [9]. However, the reproductive cycle in Arctic char begins as early as 6–8 months before spawning, in March. The timing of reproduction in the anadromous Arctic char is tightly coupled to the seasonal changes in photoperiod [11]. Anadromous individuals often spawn right after returning from sea migration, and both anadromous and landlocked Arctic char spawn in the Lake they grew up.

2.7.2 Health indicies in fish

The condition factor, also named body condition, is a general indicator of health in fish. The condition factor is expressed as a numerical value and can be used to assess the growth condition of fish. There are several proposed ways of calculating the condition factor (K) in fish, one of them is Fulton's formula given in Equation 1 [138, 139]:

$$\mathrm{K} = \left(\frac{\mathrm{W}}{\mathrm{L}^3}\right) \cdot 100 \tag{1}$$

W is the body mass of the fish in grams and L is the fork length in centimeters which is multiplied by 100 to bring the factor close to 1. A normal fish will have a condition factor close to 1. A fattier fish with K above 1 is considered in good condition, and a slim fish with K below 1 indicates a poor body condition. The body condition of fish might vary depending on several factors including the environment and habitat, food availability, season, and sexual maturity. Other stressors such as contamination might affect the body condition negatively [104, 140].

Hepatosomatic index (HSI) in fish is the ratio of the liver weight to the body mass, and this factor can provide information about the functioning of the liver (Equation 2). Prolonged fasting in fish is normally associated with a reduced HSI and tissue size of the liver, accompanied by reduced liver metabolic capacity and enzymatic activity, and reduced plasma glucose levels [135, 141, 142]. HSI can also increase due to contamination exposure as a result of inflammation and hypertrophy of the cells. Several studies have indicated that exposure to PFAS compounds might have a negative effect on the HSI index [143, 144, 145]. HSI has been applied as an indicator of environmental contamination, however, a confounding factor is that the HSI varies with reproduction and other environmental factors such as food availability.

$$\mathrm{HSI} = \left(\frac{\mathrm{W_L}}{\mathrm{W_T}}\right) \cdot 100 \tag{2}$$

$\mathrm{W_L}$ is the liver weight and $\mathrm{W_T}$ is the total body weight.

2.8 The endocrine system

The endocrine system also referred to as the hormone system, is found in most living organisms including mammals, birds, and fish. The hormone system consists of glands that are responsible for producing and releasing hormones into the bloodstream, as well as nuclear receptors that are located within cells of organs and tissues that respond to the hormones released [146]. Hormones are signaling biomolecules that regulate many biological processes and functions such as reproduction, growth, stress response, and osmoregulation [147]. The binding of hormones to receptors in target organs leads to alterations in the cells to maintain homeostasis. Hormonal levels in fish are affected by environmental variables, such as light, temperature, and feeding, and endogenous variables, including developmental and reproductive status [147]. There are several classes of hormones, both steroid and non-steroid hormones, in which the former are a class of lipid hormones.

The hypothalamic-pituitary (HP) axis constitutes the link between the CNS and the endocrine system [147]. Specific cells in the hypothalamus control hormone production and release in the pituitary gland, and cells in the pituitary produce and secrete hormones that induce effects on peripheral glands located throughout the body. The glands in the target organs produce a negative feedback loop back to the hypothalamus and pituitary when the hormones have reached the target organ and induced alterations to regain homeostasis.

2.8.1 Steroid hormones

Endogenous steroid hormones and their metabolites are vital compounds that control physiological functions in most living organisms. Steroid hormones derive from cholesterol and are synthesized in living cells in different tissue in a process called steroidogenesis (Figure 6) [148]. The steroidogenic pathway is complex and involves various enzymes that catalyze the synthesis pathways from one steroid to another, however, there can be several pathways for synthesizing one steroid hormone. There are four main classes of steroids: progestogens, androgens, mineralocorticoids, glucocorticoids, and estrogens. Moreover, steroid hormones share the same tetracyclic structure in which positions of the double bonds and hydroxyl- and keto-functional groups are the main difference between the steroid hormones [149]. Additionally, the steroidogenic pathway for teleost fish haven proven to be different from that in humans, even though there are many similarities. [150].

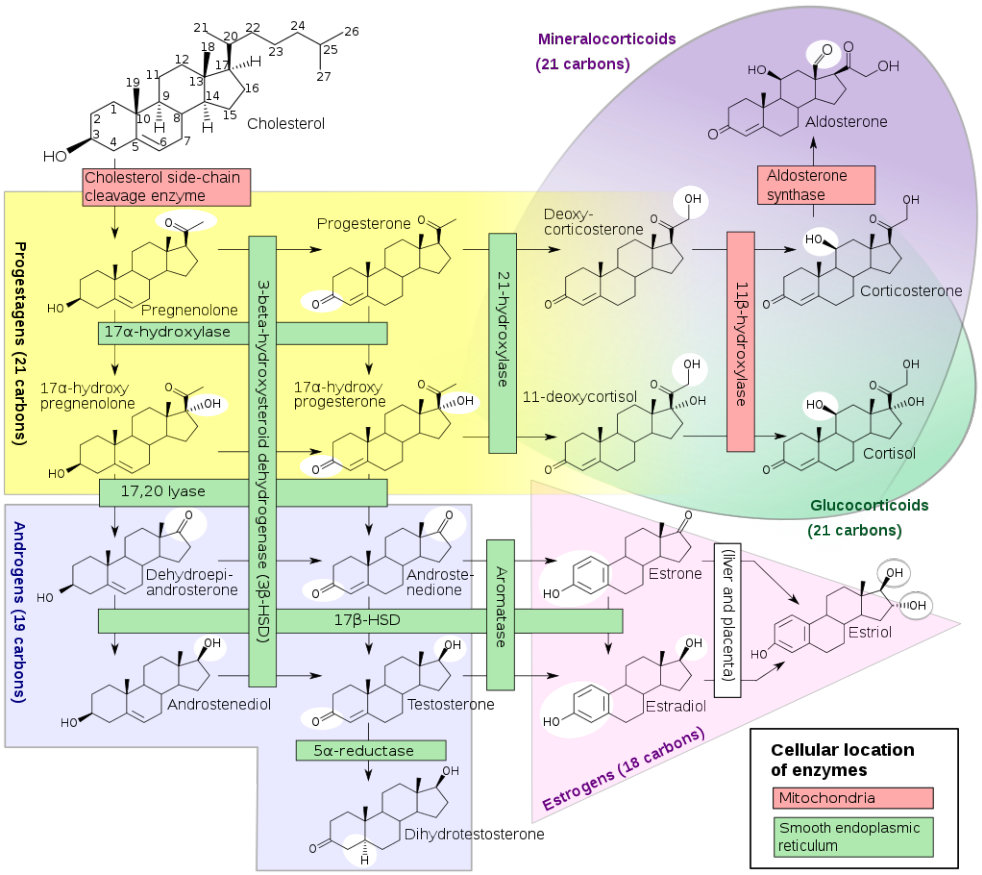

Figure 6: Diagram of the steroidogenic pathway. The figure shows the five main classes of steroid hormones: steroids: progestogens, androgens, mineralocorticoids, glucocorticoids, and estrogens, which are displayed with different background colors. All steroid hormones derive from cholesterol. The steroidogenic pathway is complex and involves various enzymes that catalyze the synthesis pathways from one steroid to another. The figure displays which enzymes are involved in catalyzing the synthesis of one steroid to another, and the colored boxes indicate the cellular location of the enzymes. Figure adopted from Haggestrom *et al.* (2014) licensed under creative Commons license (CC-0) [148].

2.8.2 Cortisol and the stress response

Cortisol is a steroid hormone in teleost fish that is secreted and released by the interrenal cells of the head kidney, the anterior part of the kidney which is an analog to the mammalian adrenal gland, by activation of the hypothalamic-pituitary-interrenal (HPI) axis [136]. Under normal conditions, cortisol regulates several physiological functions including regulating the metabolism, the immune response, and modulating reproductive endocrine control [136]. Stress is defined as a physiological response that disturbs the homeostasis of an organism due to exposure to stressors [151]. Under exposure to stressors, rapid physiological changes may occur due to increased cortisol levels released into the bloodstream. Stressors can be a wide

variety of external or internal factors. Examples of environmental factors are food availability, salinity, and water temperature. Other stressors can be chemical contaminants or biological agents such as parasites or viruses. Internal factors that determine the sensitivity of an individual to stressors are life stage, sex, body condition, and inherited characteristics. The stress response elicits several physiological and behavioral alterations in order to overcome or adapt to the changes. Moreover, fish has proven to be more sensitive toward exposure to stressors compared to other vertebrates [137, 151].

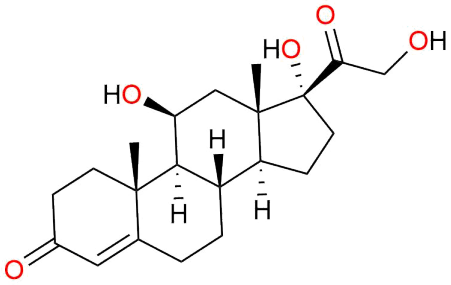

Figure 7: Chemical structure of the cortisol steroid hormones showing the tetracyclic structre and positions of functional groups. Made with ChemDraw Professional 16.0.

The stress response in teleost fish can be divided into three major responses. The primary response encompasses the neuroendocrine and physiological response which activates the HPI axis and the brain-sympathetic-chromaffin cell (BSC) axis. During the BSC axis activation, chromaffin cells of the head kidney release catecholamines, such as adrenaline and noradrenaline, which are triggered by the sympathetic nervous system [152]. The action of catecholamines increases hemoglobin oxygen affinity, and arterial blood pressure and mobilizes glucose to the muscles [153]. However, there is evidence that an increase in plasma catecholamine levels only occurs if the fish is exposed to severe stress accompanied by reduced oxygen blood levels [154]. The activation of the HPI axis releases corticotropin-releasing factor (CRF) from the hypothalamus triggered by the central nervous system. CRF stimulates the pituitary to secrete adrenocorticotropic hormone (ACTH), which activates the interrenal cells of the head kidney to synthesize and release cortisol into the circulatory system (Figure 8).

The secondary stress response leads to alterations at the physiological and biochemical level, such as increased glucose in the blood, osmoregulatory disturbances in water and ion exchange, and immune responses leading to increased antibody production as examples. The tertiary response is related to individual changes such as growth, swimming capacity, and behavioral changes in feeding and reproduction. Moreover, cortisol also plays an important role in osmoregulation in fish together with other hormones [150].

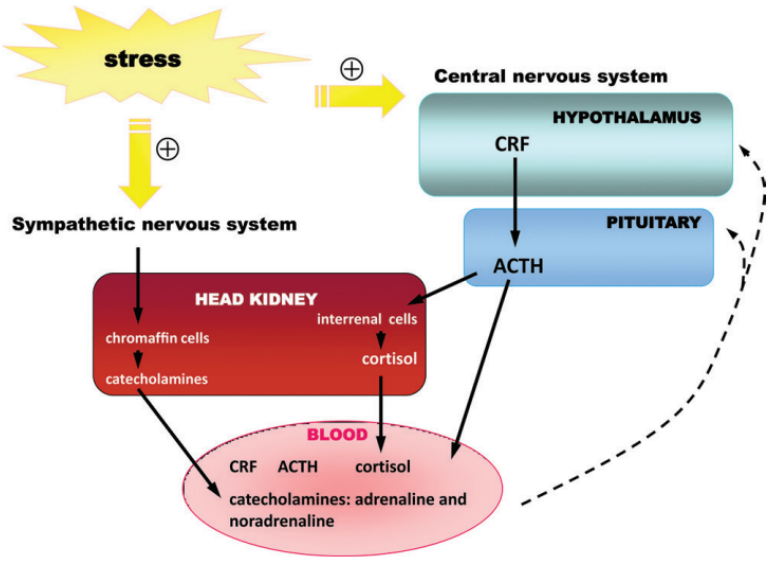

Figure 8: The stress response in teleost fish activates of BSC- and HPI-axis, which is the primary stress response. During the BSC-axis activation, chromaffin cells of the head kidney release catecholamines, such as adrenaline and noradrenaline, which are triggered by the sympathetic nervous system. The activation of the HPI-axis releases CRF from the hypothalamus triggered by the central nervous system. The pituitary gland responds by releasing ACTH, which activates the interrenal cells of the head kidney to synthesize and release cortisol into the circulatory system. Figure adopted by Kalamarz-Kubiak (2018) [136] under the Creative Commons license (CC-0).

2.8.3 Basal levels of cortisol in fish

Cortisol is a commonly used biomarker of stress in fish, however, cortisol is secreted by various stress stimuli including confinement, handling, toxicant exposure, and change in temperature which makes it a non-specific biomarker of stress [155]. Basal cortisol levels in wild teleost fish vary widely between species, however, within a species there are also individual differences due to inherent factors such as sex, life stage, maturity, season, time since feeding, and time of the day [137]. For species in the Salmonidae family, increased cortisol levels have been reported to coincide with smoltification [156]. There has also been a reported increase in cortisol in adult salmonids in association with sexual maturation and riverine migration. A study conducted on wild migrating Arctic char found that plasma cortisol levels were twice as high in upstream migrants compared to downstream migrants, 464 ng mL^{-1} and 244 ng mL^{-1}, respectively [138].

Barton and Iwama (1991) report that general basal plasma cortisol levels in unstressed fish are less than 30-40 ng mL^{-1}. In the review from Pankhurst (2011), there is a suggestion that most undisturbed teleosts have a mean basal plasma cortisol level of $\leq$10 ng mL^{-1}, however, there can be some species that deviate from this value with considerably higher

basal cortisol levels [137]. Pickering and Pottinger (1989) reported basal plasma cortisol levels in the range of 0-5 ng/ml for brown trout and rainbow trout, and an elevation in plasma cortisol in the range of 40-200 ng mL^{-1} after handling and 1-hour confinement [157]. Most fish species show an increase in plasma cortisol levels within a few minutes to a few hours after exposure to a stressful event [137]. Pankhurts (2011) reported that most teleosts show a measurable increase in plasma cortisol within 10 minutes. However, there may be an interspecies variation or even differences within the same species. Daily rhythms in cortisol levels of fish have been described in many species [147]. Cortisol levels are endogenously driven by circadian rhythm, as well as other environmental factors. For example, in brown trout, the levels of cortisol have a diel oscillation of 1-30 ng mL^{-1} with a peak concentration at night [158]. In white spotted char, a similar diel variation of 3-30 ng mL^{-1} with the highest concentration at night has been found [159]. However, in Atlantic salmon diel variation of cortisol levels from 1-160 ng mL^{-1} have been reported with considerable seasonal changes in diel peak concentrations [160].

2.8.4 The effect of steroid hormones on the reproductive cycle

Reproduction is one of the life events of fish that have been reported to affect plasma cortisol levels. Moreover, there are other steroid hormones involved in the reproductive cycle. The reproductive cycle of Arctic char begins early in the spring and involves several endocrine changes [11]. Levels of 17β-oestradiol (E2) and TS in female fish increase, and in males an increase in 11-KetoTS has been observed [11]. The increase of E2 in females is accompanied by the production of oocytes. From June and July, there is also a marked increase in plasma levels of E2 and TS followed by vitellogenesis, the process of egg yolk formation in the oocytes, and rapid growth of the oocytes up until spawning. For anadromous Arctic char, the rapid growth of the oocytes often starts after the return from the sea migration, indicating that the choice to proceed with maturation is decided once necessary energy reserves to reproduce have been acquired during the seawater residency. A few weeks before spawning in late August to September, there is a drop in plasma E2 levels and subsequently the plasma TS in female char, which signals the completion of vitellogenesis. In males, an increase in 11-KetoTS is associated with spermatogenesis and this steroid remains elevated until spawning commences [11].

2.8.5 Endocrine disruption

Endocrine disruption (ED) is defined as the disruption of the normal activity of the endocrine system by an endocrine-disrupting chemical (EDC). EDC was defined by Chrisp *et al.* (1997)

and the U.S. Environmental Protection Agency as “An exogenous agent that interferes with the synthesis, secretion, transport, binding, action, or elimination of natural hormones in the body that are responsible for the maintenance of homeostasis, reproduction, development, and/or behavior" [146]. EDCs elicit various effects that range from subtle changes in the physiology and sexual behavior of fish to permanently altered sexual differentiation and impairment of fertility and subsequently, loss of reproduction capability [34]. EDCs can be natural products or synthetic chemicals that mimic the action of hormones either by enhancing (an agonist) or inhibiting (an antagonist) their effects or by blocking the receptors without any effect [146]. Factors that affect the outcome of an EDC are dose, total body burden, timing, and duration of exposure. Effects may be reversible or irreversible, and acute or delayed [146, 34].

2.9 Sample preparation

Sample preparation is an important part of an analytical method and is primarily used to isolate an analyte or analyte group of interest and to remove interfering compounds from a sample matrix. [161]. Environmental and biological samples are often complex matrices, and therefore need several steps with sample preparation before the samples can be analyzed without considerable interferences [83]. Matrix effect is defined as the effect of co-eluting matrix components on the ionization or detection of the target analyte during analysis. Sample preparation can involve drying, homogenization, extraction, derivatization, and clean-up. All or some of these steps can be conducted to improve detection in the instrument analysis or remove compounds that can be detrimental to the separating system [161]. However, it is important to keep in mind that all sample preparation steps that are implemented in an analytical approach can lead to analyte loss and introduction of contamination [83].

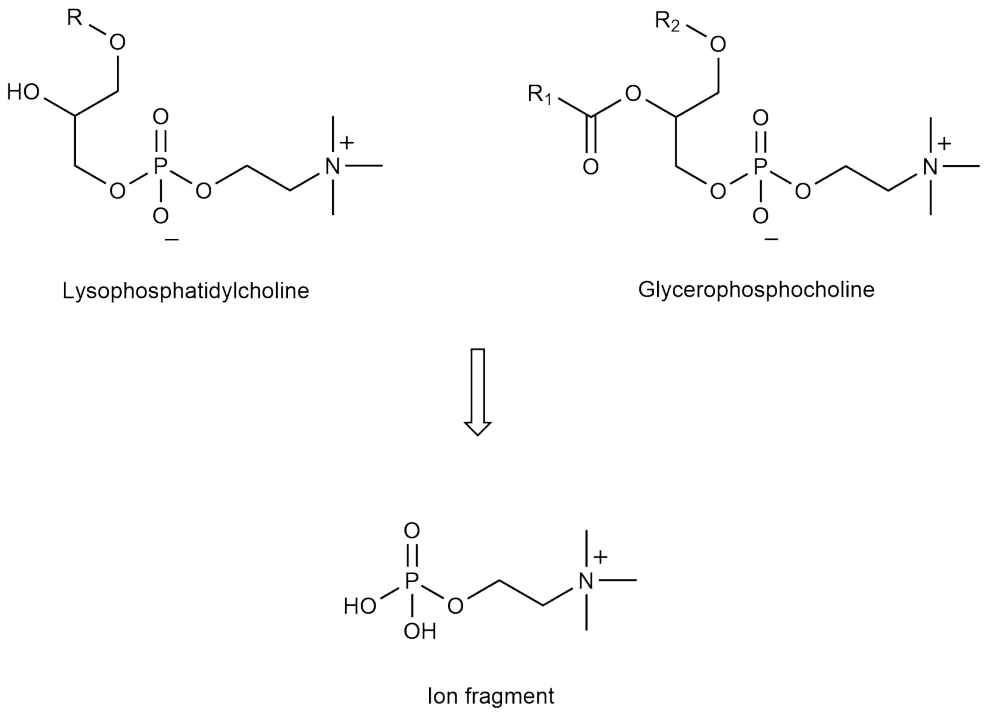

Figure 9: The chemical structure of two major phospholipids, lysophosphatidylcholine and glycerophosphocholine, and their ion fragment contributing with matrix interferences. Redrawn from Ahmad *et al.* (2012) with ChemDraw Professional 16.0 [162]

Biological samples often cause ion suppression due to the presence of phospholipids during analysis [162]. Phospholipids, and in particular glycerophosphocholine and lysophosphatidylcholine represent the major class of endogenous compounds causing significant matrix effects, and they are abundant in plasma samples (Figure 9). The molecular structure of phospholipids exhibits two major functional groups: a polar substituent and one or two long-chain fatty acid ester groups. Phospholipids are highly ionic compounds due to the ionizable phosphate group, that easily influences the ionization of target analytes. The extent of ion suppression depends on the sample preparation method as well as the chromatographic separation. However, it is worth mentioning that proteins also contribute to ion suppression in the analysis of biological samples, but they are more easily removed. Several techniques have been applied for the removal of proteins to obtain cleaner sample extracts, however, phospholipids are co-extracted when using traditional sample preparation techniques such as protein precipitation (PP), solid-liquid extraction (SLE), and solid-phase extraction (SPE) [162].

2.10 Extraction methods

2.10.1 Hybrid Solid Phase Extraction

Hybrid Solid Phase extraction (Hybrid SPE) is a simple and rapid extraction and clean-up method used for sample preparation before analysis with liquid chromatography (LC) coupled to mass spectrometric (MS) detection [163, 164, 165]. However, this extraction technique is not as commonly reported in the literature in contrast to solid phase extraction (SPE) and solid-liquid extraction (SLE) [164]. The Hybrid SPE cartridge consists of zirconium (Zr) packed silica sorbent, low porosity filter, and 0.2 μm hydrophobic frit assembly. Phospholipids are retained on the Zr sorbent while remaining proteins are retained on the low porosity filter [165, 164]. The mechanism for the removal of phospholipids is the highly selective Lewis acid-base interaction between the phosphate group, inherent in all phospholipids, and the Zr atoms [162]. By removing these matrix components, the impact of matrix effects is significantly reduced during analysis which improves the sensitivity of the method, as well as the recovery of the analytes [162].

The procedure of the Hybrid SPE method is to first subject the sample to a PP agent before the sample extract is eluted through the Hybrid SPE cartridge [162]. PP agents act as modifiers that inhibit the analytes of interest from co-retaining with the phospholipids on the Zr sorbent. Methanol with ammonium formate (AF) is an example of a PP agent that can be used for basic, acidic, and neutral compounds. The formate ion ($HCOO^-$) is a strong Lewis base that prevents acidic compounds from interacting with Zr atoms, while ammonium ion ($NH_4{}^+$) prevents basic compounds from interacting with exposed silanol groups [162]. Citric acid (CA) in acetonitrile is recommended for chelators and acidic chelator compounds. Citric acid is a stronger Lewis base than the formate ion, inhibiting most chelator compounds from interacting with Zr sorbent.

The advantage of this sample preparation method over SLE and SPE is the simplicity and time efficiency. Hybrid SPE extraction and clean-up consist of a few steps only, and less use of solvents. In addition, it has been reported to be less expensive than the traditional SPE cartridges [162]. However, the Hybrid SPE method is recommended for biological liquid samples such as plasma and serum by the manufacturer, and not for solid matrices [163].

2.10.2 Solid Phase Extraction

Solid Phase Extraction (SPE) is a time-consuming extraction and clean-up method that requires more steps compared to Hybrid SPE [165]. SPE is a column filled with a sorbent that consists of porous particles or polymerized monolith. The capacity of the sorbent is dependent on the surface area and type of sorbent. There are various SPE cartridges

based on different chemical interactions; normal phase, cation/anion exchange, and reversed phase. The reversed-phase SPE is commonly used for separating non-polar to moderately polar compounds from a polar sample matrix [161]. The extraction mechanism is based on hydrophobic interactions between carbon-hydrogen bonds from the compound and the sorbent. C-H-rich groups will be retained, while ionized compounds or compounds with relatively many polar functional groups will be removed. A reversed-phase sorbent normally consists of silica-based material with different carbon chain lengths (C_2, C_4, C_{18}) than can be modified with different groups, for example, a phenyl group.

The procedure of this method includes 1) activating the sorbent with a non-polar solvent, also called conditioning, 2) rinsing the sorbent (often with water), 3) applying the sample to the SPE cartridge, 4) rinsing sorbent with a solvent of appropriate elution strength, and 5) elution of analyte(s) of interest with a solvent with appropriate elution strength [83].

In the analysis of biological samples, the advantage of the SPE method is that it reduces matrix effects in samples with high selectivity in extraction and purification. Moreover, the potential for automation of the extraction with the chromatographic system, and the use of lower volumes of organic solvents compared to SLE [162]. The efficiency of SPE depends on the type of sorbent, sample volume, pH, and the content of organic modifiers. In SPE, only small a amount of the phospholipids are removed, however, in reversed-phase SPE phospholipids will co-extract with analytes due to the hydrophobic tail.

2.10.3 Solid-liquid extraction

Solid-liquid extraction (SLE) is a simple but time-consuming extraction technique where an analyte(s) of interest is separated from a solid matrix by a liquid solvent. The efficiency of SLE depends on how deeply the solvent penetrates or diffuses into the pores of the solid matrix [166]. The transfer of the solvent inside the solid particles occurs due to the concentration gradient at the solid-liquid interface and can be modified by several factors.

Several factors influence the SLE efficiency; solvent properties, extraction time of solvent and sample, the particle size of the solid sample, temperature, pressure, and agitation of the solvent mixture [166]. The choice of solvent is probably the most important factor affecting extraction efficiency. The solvent must have suitable chemical properties that match the analyte of interest i.e. the analyte must be soluble in the solvent. The polarity of the solvent is therefore important. Moreover, the particle size of the solid sample highly affects the extraction efficiency. The extraction efficiency increases with a decreased particle size as the surface area of the solid sample increases, and the rate of transfer of the solvent increases. Grinding or cutting the solid sample into smaller pieces before the extraction will therefore enhance the extraction efficiency [83].

Another factor that might affect the extraction efficiency is the water content of the sample as the water can affect the mass transfer of solvent by competing with the solvent dissolution. However, in some cases, water is needed to permit the transport of the analyte. Increased temperature also enhances the extraction efficiency, however, too high temperatures might cause undesirable reactions or degradation of thermolabile compounds. Moreover, the solvent might evaporate at high temperatures which is undesirable. The agitation of the solvent also increases the extraction by increasing the diffusion and transfer rate. [166]. Additionally, repetitive extractions with smaller volumes often provide better recovery and reduce the amount of solvent used.

2.10.4 Ultrasound assisted extraction

Ultrasound-assisted extraction, also called ultrasonication, is the application of ultrasound waves to a liquid medium [166]. The mechanical waves have frequencies of around 20 kHz or greater and are applied to cause agitation of the liquid medium. As mentioned previously, agitation of a solvent during extraction increases the extraction efficiency. During the ultrasonication process, the ultrasound waves will create longitudinal waves in the liquid medium that will form regions with compression and expansion waves. These waves will create bubbles in the liquid near the sample surface which generates negative pressure. When the bubble collapses near the sample surface, high pressure and temperature shock waves will be created resulting in physical disruption of the sample that enhances solvent penetrations which subsequently result in increased extraction of the analyte [166].

2.11 Freeze-drying

Biological samples contain about 70% water, however, the water content reduces the storage life of samples as they are easier degraded. To preserve biological samples water is removed. Water can be removed by different drying techniques i.e. air-drying and drying at high temperatures, however, for biological samples freeze-drying is the most commonly used method. Freeze-drying is a process that dehydrates a sample in the frozen state by sublimation under a vacuum [139]. Freeze drying consists of a three-step process that involves freezing the sample, primary drying, and secondary drying. The advantage of freeze-drying samples is that volatile compounds are more preserved compared to air-drying and heat-drying. Moreover, removing water from samples also makes the comparison of contaminant concentration easier as the uncertainty of the difference in water content between samples is eliminated. The water content can be determined by weighing the sample before and after freeze-drying and calculated by equation 3 [139].

$$\text{Water content } (\%) = \left(\frac{\mathrm{W}_{wet} - \mathrm{W}_{dry}}{\mathrm{W}_{wet}} \right) \cdot 100\% \tag{3}$$

$\mathrm{W_{wet}}$ is the weight of the sample in wet weight (ww) and $\mathrm{W_{dry}}$ is the weight of the sample after drying, referred to as dry weight (dw).

2.12 Microwave digestion for elemental analysis

Microwave digestion is a commonly used method for sample preparation prior to elemental analysis. Solid samples are chemically broken down by using mineral acid in combination with microwave heating to dissolve elements into the solution. Different microwave digestion systems have been employed; open vessels and closed vessels at different pressures [167]. Closed-vessel microwave digestion provides faster and more efficient sample decomposition. Moreover, the risk of sample contamination and analyte losses by volatilization is eliminated [168, 167]. Depending on the sample matrix and which elements will be analyzed, nitric acid (HNO_3), hydrofluoric acid (HF), or sulphuric acid (H_2SO_4) are commonly used, however, HNO_3 is the most used for environmental analyses [169]. For samples containing organic material, such as biological samples, it is necessary to oxidize the organic matrix properly [167]. This can be done by adding a strong oxidizing agent such as hydrogen peroxide (H_2O_2) in addition to the mineral acids.

2.13 Analytical methods

2.13.1 Ultra-Performance Liquid Chromatogrpahy

Ultra-Performance liquid chromatography (UPLC) is an analytical separation technique where compounds are separated by the difference in affinity to the stationary phase that the column is made of and the mobile phase. Most conventional LC pumps operate at pressure up to 400 bar, while ultra-high pressure systems operate at pressures up to 1000-1200 bar [161]. The chromatographic method requires special columns and connections due to the high pressure. The UPLC columns are long and packed with tiny particles (< 2 μm) that result in high backpressure and a reduction in the analytical time and mobile phase consumption. Analytes co-elute less with interferences during ionization resulting in reduced matrix effects [170]. Moreover, this method provides better resolution and more narrow peaks compared to conventional LC and high-pressure liquid chromatography (HPLC). UPLC coupled to tandem mass spectrometric detection (MS/MS) is widely used in the analysis of biological samples due to the high sensitivity and selectivity, and has shown to be applicable for analyzing a broad range of PFAS compounds [171, 172].

2.13.2 Ultra-performance supercritical fluid chromatography

Ultra-performance supercritical fluid chromatography (UPSFC) is a highly efficient analytical separation technique for the analysis of a wide range of compounds; non-polar, polar, and ionizable. This technique provides fast and high resolution and separation of compounds due to the unique feature of supercritical fluids [173]. In UPSFC, the mobile phase has a higher diffusion rate which decreases the column backpressure and increases the efficiency compared to LC [161]. A supercritical fluid is a compressed gas that exists at a critical temperature and pressure and has lower density and viscosity than a liquid, but higher than gas. Therefore supercritical fluids exhibit gas-like diffusivity and the dissolving capacities of a liquid [161]. LC-MS has been increasingly applied as an analytical technique for steroid hormone analysis in the last decades due to the elimination of cross-reactivity which often has been a problem in steroid quantification with the traditional immunoassays [155]. Several authors have recently highlighted the use of UPSFC-MS/MS in steroid profiling due to the increased sensitivity and chromatographic efficiency compared to UPLC-MS/MS, and also highlight the applicability for steroid profiling [173, 174, 175]. Moreover, UPSFC improves the separation of isomers and enantiomers compared to other separation techniques and enables simultaneous quantification of endogenous steroids. In addition, derivatisation of steroids is not necessary prior to UPSFC-MS/MS analysis, such as in GC-MS analysis [175].

2.13.3 Tandem mass spectrometry

Ionizable compounds that can be transferred to the gas phase can be detected with MS [161]. In tandem mass spectrometry (MS/MS), a triple quadrupole (3Q) analyzing configuration can be used. The first quadrupole (Q1) selects which ion(s) that are going to be measured [176] (Figure 10). The second quadrupole (Q2) is a collision cell in which a collision gas will collide with the ions and split them into fragments. In the third quadrupole (Q3), specific fragment(s) from Q2 is selected and measured. The operating mode can be run in single reaction monitoring (SRM) or multiple reaction monitoring (MRM). The latter is often applied for multiple analytes, and the fragmentation is usually specific for each compound.

The advantage of MS/MS detection is high sensitivity and selectivity for multi-compound analysis. Moreover, combined quantification and qualitative identification is another important feature in MS/MS [177]. The use of LC-MS/MS in combination allows for the determination of multiple analytes in a single run with high specificity and reliable identification. MS/MS provides exact structural information by measuring selected ion fragments and the chromatographic technique provides analytes with specific retention time [176]. However,

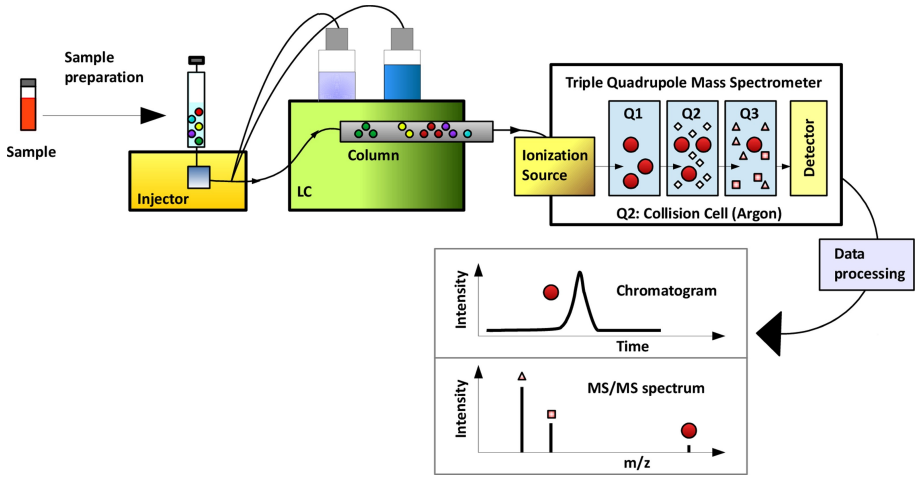

Figure 10: Schematic principle of the LC-MS/MS instrument. A sample is injected into the LC column, and after chromatographic separation, the analytes are ionized in the ionization sources of the MS where they are separated and detected. The first quadrupole (Q1) selects which ion(s) that are going to be measured. The second quadrupole (Q2) is a collision cell in which a collision gas will collide with the ions and split them into fragments, and in the third quadrupole (Q3), specific fragment(s) from Q2 are selected and measured by the detector. Data is processed, and the resulting chromatogram is thereafter provided together with ion the fragment. Reprinted from Wudy *et al.* (2018) with permission from Elsevier [176].

the inherent drawback of MS/MS is that only targeted analytes are monitored in which non-target compounds will not be detected. In addition, LC operates with liquid under high pressure while MS/MS operates under vacuum, therefore compounds are transferred from liquid to gas phase by ionization at the interface between LC-MS. Electrospray ionization (ESI) is a commonly used ionization technique with a wide application.

2.13.4 Electrospray ionization

Electrospray ionization (ESI) is a commonly used ionization technique with a wide application. ESI is carried out at atmospheric pressure and is used for polar compounds [161, 176]. Neutral polar compounds can either accept or donate protons under the given conditions, yielding positive or negative ions during the ESI process. When the mobile phase containing analytes enters the ESI capillary, high voltage is applied and at the outlet of the capillary, a nebulizing gas (often nitrogen gas) is mixed to facilitate the formation of droplets [161]. In addition, dry gas is introduced in the opposite direction of the flow. The highly charged droplets decrease in size moving toward the entrance of the detector. When the force inside the droplets exceeds the surface tension, the droplets explode into smaller droplets. This is a repetitive process that provides ions in the gas phase. Depending on the configuration of the MS, detection is performed in the positive mode (+) or the negative mode (-), detecting

the protonated or deprotonated ions, respectively.

In ESI, compounds deriving from a sample matrix that are eluted together with the analytes of interest can affect the ionization process and are often termed matrix effects. ESI is an ionization method that is highly susceptible to matrix effects [176]. This is evident when the results are compared with those obtained from the quantification of the analyte dissolved in a pure solvent solution. Matrix effects can increase the ionization of the analyte (ion-enhancement) or, more commonly, decrease the ionization efficiency (ion-suppression).

2.13.5 Inductively coupled plasma-mass spectrometry

Inductively coupled plasma-mass spectrometry (ICP-MS) is a widely used technique for multi-trace element analysis. ICP is an ion source that is used in elemental analysis [161]. The instrument has a wide linear dynamic range which allows for simultaneous determination of trace elements in the same sample injection and isotopic information. ICP-MS has a low detection limit which allows for the detection of elements at trace and ultra-trace concentrations. Moreover, ICP-MS has shown to exhibit high precision and accuracy detection of trace elements and has high specificity and sensitivity. However, high concentrations of organic content might provide matrix interferences and spectral interferences for polyatomic ions. These effects can be minimized or eliminated by the use of alternative isotopes or interference correction equations [168]. In addition, organic interfering matrices can be removed by oxidative conversion to carbon dioxide and water before analysis. HNO_3 can oxidize organic matrices completely if sufficiently large volumes of acid are used, however, this might cause a dilution problem for several trace elements that would be diluted at or below the detection limit. Another way of increasing the oxidizing power of the digestion is to use a mixture of HNO_3 with 30% hydrogen peroxide (H_2O_2) [178].

2.14 Quality Assurance and Quality Control

Quality assurance (QA) is the management and assessment that the quality standards are met in a laboratory. This encompasses all the activities that are implemented to ensure high quality in the performance and the results that are produced. An example of implemented QA activity is the establishment of standard operating procedures for a method or instrument analysis. Quality control (QC) is a part of the QA and includes steps and activities that are conducted as a part of the scientific work to ensure high quality in the work during the whole process from sample collection to analysis, and to ensure that the data produced are accurate, precise, and reliable.

Method validation is a process carried out to ensure that the method is suitable for the

intended use and that the quantification of compounds is accurate and reliable [161]. Several aspects need to be considered when selecting a method that consists of multiple steps. For example, for sample preparation, a suitable solvent for extraction of the analyte and a proper clean-up step needs to be selected and evaluated. For analysis, a proper analytical method should be chosen based on the analyte of interest. When a method is selected, validation needs to be carried out before the method can be implemented. Common validation parameters to consider are the limit of detection (LOD), the limit of quantification (LOQ), linearity, range, repeatability, accuracy, recovery, and matrix effect [161]. Moreover, analysis of validated standard reference materials (SRM) is essential to verify the performance of the method. Standard reference materials should be of a similar matrix and contain the same concentration range of analytes as the samples to be analyzed. Standards that are used to validate the method can be from the working laboratory, however, it is important to include certified reference materials (CRM) from internationally accepted manufacturers to assure the quality of the method [83].

2.14.1 Quantification

For a chromatographic method, different calibration methods can be used for quantification. A widely used calibration method is the internal standard (IS) method, where a known amount of a known compound is added to the samples and calibration solutions [161]. The IS used should have similar chemical properties as the analyte and preferably close retention times, however, the IS must be separatable from the analyte in the chromatographic system. For multi-compound analysis, several IS can be used. A calibration curve is established from the spiked calibration standards, where the concentrations of the analytes are variable while the concentration of the IS is kept constant. The calibration curve is made by plotting relative response, i.e. the ratio of the area of the analyte peak against the IS peak as a function of the concentration.

2.14.2 Precision and accuracy

Accuracy is the closeness of an experimental result to the true value, whereas precision is the variability of repeated measurements [83]. By analyzing CRM, method blanks, and establishing a calibration curve from standard solutions, the systematic error or bias of a method can be identified. The variability of measurements, or the random error of a method, can be described by the standard deviation (σ) (Equation 4) and the relative standard deviation (RSD) [83].

$$\sigma = \sqrt{\sum_{i=1}^{n} \frac{(x_i - \overline{x})^2}{n-1}} \tag{4}$$

$\overline{x}$ is the mean (Equation 5), x_i refers to individual measurements and n is the number of measurements.

$$\overline{x} = \frac{1}{n} \sum_{i=1}^{n} x_i \tag{5}$$

The RSD is given in Equation 6, and is expressed as the percentage ratio of the standard deviation to the mean. It is the preferred measure to compare results of different magnitude and across units.

$$\text{RSD}(\%) = \left(\frac{\sigma}{\overline{x}} \right) \cdot 100\% \tag{6}$$

2.14.3 Retention time

The retention time (t_R) is defined as the time it takes for an analyte to travel through a chromatographic column from the injection to detection [161]. The t_R of a peak in a sample is used to confirm that the peak is the correct compound, by comparing it with a standard of the analyte. The t_R are influenced by the chromatographic system that is used as it affects the affinity the analytes have to the stationary phase in the column and the mobile phase. The length of the column and the flow rate of the mobile phase are also factors that influence the separation and t_R of the peaks, and the t_R might shift in various solvents due to the matrix effect. Moreover, chromatographic peaks should be well separated from neighboring peaks to be reliably quantified [161]. For compounds that are not properly separated, errors may occur in peak height and area determination.

2.14.4 Limit of detection and limit of quantitation

Limit of detection (LOD) is defined as the lowest concentration of a chromatographic signal of the analyte in a sample that can be detected, whereas the limit of quantitation (LOQ) is

defined as the lowest concentration of a chromatographic signal of the analyte that can be reliably quantified with acceptable accuracy and precision [179]. Different approaches can be applied for estimations of LOD and LOQ values, and these estimations are used to define the sensitivity of a method. However, different estimation approaches provide considerably different values for LOD and LOQ which can make the comparison between scientific data challenging [180, 181].

One method for estimating LOD and LOQ is based on the calibration curve method, where the standard deviation of the established calibration curve and the numerical value of the slope are considered. LOD and LOQ can be calculated according to equation 7 and 8 [180, 182, 179];

$$\mathrm{LOD} = 3.3 \cdot \frac{\sigma}{\mathrm{S}} \tag{7}$$

where σ denotes the standard deviation of the y-intercept of the regression line established from the calibration curve, and S is the slope of the calibration curve. This method is applicable to most analytical methods, however, the limitations of this estimation method are that it depends on the number of concentration points in the calibration curve, the range of concentrations used, the number of measurements, and the variability of the data points in the calibration curve [181].

$$\mathrm{LOQ} = 10 \cdot \frac{\sigma}{\mathrm{S}} \tag{8}$$

Another way of calculating LOD and LOQ is the signal-to-noise ratio (S/N) times 3 and 10, respectively [180, 182, 179]. S/N is the relative ratio of the peak height of a signal compared to the noise peak height. Noise is defined as fluctuations in the background signals of the instrument. This method is applicable in analytical methods that exhibit baseline noise and is one of the most used methods for estimating LOD and LOQ due to its simplicity. However, a limitation of this method might be that it depends on a subjective interpretation of how to obtain noise, even though the built-in software is used for integrations [181].

2.14.5 Linearity and range

Linearity is the concentration range where the detector response is directly proportional to the analyte concentration, and range is defined as the concentration range that is within

the linear range [161]. The linear range should cover the concentrations that are expected to be present in the samples, and LOQ should be within the linear range or the lowest concentration point in the range [183].

Linearity and range can be determined by analyzing spiked calibration standards with a minimum of 5 or more concentrations that are expected to cover the analyte concentration in a sample [184]. Linear regression by the method of least squares can be used to describe the response of the calibration standards, where the signal response is plotted as a function of the analyte concentration. The correlation coefficient, R^2, obtained from the linear regression is an indication of the linear relationship between the data points.

2.14.6 Matrix effect

Matrix effect (ME) is defined as the effect of co-eluting matrix components on the ionization efficiency and detection of the analyte [185, 186]. For instance, phospholipids are often co-extracted from biological samples, and due to phospholipids' ionic nature, they interfere with the analyte during the ionization which subsequently affects the detected signal response [162]. Moreover, ME will also affect the reproducibility and accuracy of the method due to signal enhancement or suppression, which results in over- or underestimation of the quantification of analyte concentrations [170]. However, ME can be reduced by proper sample preparation and post-extraction clean-up. Another way of minimizing the effect of ME is the use of isotopically labeled IS to correct for losses during extraction and the analytical method [163]. Another way of minimizing ME is to modify the chromatographic or detection parameters, and one of the easiest ways to combat ME is to reduce the injection volume or dilute the sample [185]. In LC-MS, ME is usually not avoidable, however, in some cases, calibration curves can be made with matrix spikes or a proper matrix surrogate to tackle ME.

One way of quantitatively evaluating ME is by the post-extraction addition method which is conducted by comparing the signal response of the analyte in a standard solution to that of a sample spiked post-extraction (matrix match) [187, 185]. The relative matrix effect, ME (%), can be calculated by equation 9;

$$\mathrm{ME}(\%) = \left(\frac{\mathrm{A_{MM}} - \mathrm{A_{MB}}}{\mathrm{A_{Std}}} - 1 \right) \cdot 100\% \tag{9}$$

the $\mathrm{A_{MM}}$ is the peak area of the analyte in a post-extraction matrix spiked sample also referred to as matrix matched (MM) sample, and $\mathrm{A_{Std}}$ is the peak area of the analyte in

a solvent. The peak area of the method blank A_{MB} should be subtracted from the peak area of MM sample to correct for any contamination introduced during the method. If the calculated ME is 0% there is no matrix effect, however, if ME is above or below 0%, there is an occurence of signal enhancement and suppression, respectively [185].

2.14.7 Recovery

Recovery of a method is defined as the percentage of the true concentration of an analyte recovered during the analytical procedure, also referred to as extraction efficiency. The recovery of a method accounts for analyte loss during sample preparation that leads to errors in the results. Absolute recovery is calculated by using external standards, while relative recovery is calculated by using the relative responses of the external standard and IS.

Extraction efficiency can be quantitatively determined by comparing matrix samples spiked pre- and post-extraction [188]. The absolute recovery, $R_{abs}(\%)$, can be calculated by the following equation 10;

$$R_{abs}(\%) = \left(\frac{A_{SSP} - A_{MB}}{A_{MM} - A_{MB}}\right) \cdot 100\% \tag{10}$$

A_{SSP} is the response for the sample spiked pre-extraction, and A_{MM} is the response for samples spiked post-extraction. The method blank, A_{MB}, is subtracted from the peak areas to correct for any contamination that has been introduced during the analytical method. The relative recovery, $R_{rel}(\%)$, can be calculated the same way by using relative response according to equation 11;

$$R_{rel}(\%) = \frac{\left(\frac{A_{SSP}}{A_{SSP(IS)}} - \frac{A_{MB}}{A_{MB(IS)}}\right)}{\left(\frac{A_{MM}}{A_{MM(IS)}} - \frac{A_{MB}}{A_{MB(IS)}}\right)} \cdot 100\% \tag{11}$$

On a general basis, recoveries between 70-120% are regarded as acceptable, and this has been recommended to use for analysis of pesticide residues in food by the Swedish National Food Administration [177, 189].

2.15 Statistical methods

2.15.1 Kruskal-Wallis test

The Kruskal-Wallis test is a rank-based non-parametric statistical method used for testing if three or more independent sample groups of equal or different sample sizes originate from the same distribution, named after Kurskal and Wallis (1952) [190, 191]. This test assumes that the data deviate from a normal distribution, and therefore the null hypothesis postulate that the median of all sample groups is similar. The alternative hypothesis assumes that at least one of the median of the sample groups is different from one of the median of the other sample groups. A significant test indicates that at least one sample group has a different distribution. However, the test does not indicate for which groups this difference occurs and for how many of the groups, therefore, a post-hoc analysis is normally conducted to identify which groups differ. Several methods can be used for post-hoc analysis, one way is Dunn's test.

Dunn's test (1964) is based on multiple pairwise comparisons using rank sums of independent sample groups that indicate which sample groups are significantly different at a set significance level α [191, 192]. However, when multiple pairwise comparisons are tested, the probability of getting a "false positive" significant difference increases. This is called the Family-wise error rate or type I error. The type I error is normally equal to α when one comparison test is performed but increases with the number of comparisons. There are ways of controlling the family-wise error rate, for instance by using adjusted p-values.

2.15.2 Principal component analysis

Principal component analysis (PCA) is a multivariate statistical technique that is based on mathematical algorithms that analyzes a dataset that is described by several inter-correlated quantitative dependent variables [193]. The basis of the dataset might be a matrix that consists of y number of samples and x number of variables. A PCA reduces the dimensionality of the data while retaining most of the variation by identifying directions, called principal components (PCs) [194]. The PCs are new linear combinations of the original variables that are represented as weighted averages. Moreover, the PCs are represented as new independent variables. Multivariate analysis is used in a wide range of scientific fields. PCA aims to extract the most important information from a dataset and to express this information as new orthogonal variables that can be displayed in a pattern in which similarities and dissimilarities can be observed. A PCA plot, therefore, simplify the description of the dataset, by compressing the data while retaining important information [195].

The first principal component (PC1) is aligned along the direction with the maximum

variances and therefore explains the largest possible variance of the dataset [193]. The direction of PC1 is found by the least-squares method, a line that has the best fit to all contributing data points. Principal component two (PC2) is the direction that explains the second largest variance of the dataset and is computed orthogonally to PC1. Higher orders of principal components (PC3, PC4, etc.) are orthogonal to the lower PCs and represent a successively smaller variance that contains less information. When the principal components are represented in a direction where the variance is so small that no information can be obtained it is called noise. A PCA plot has a common origin, and the most common is the average point which is the mean of all variables in all samples, called the mean center.

A PCA plot consists of both score and loading plots [196]. Scores are coordinates that are projected to a PC that is derived from a coordinate in the original dataset. A sample in a dataset has a coordinate that is relative to the PC origin and its own set of scores that are determined by the variables in the PCA. The score plot contains the scores of all the samples. Moreover, the score plot can also be used for outlier identification, identification of trends, and groups, or finding similarities or variations between samples. A principal component contains x variables, called loadings, which provide information about the relationship between the original variables and the PC [196]. In a loading plot, loading vectors are plotted against each other, and the plot contains variables of the samples. Information that can be drawn from the loading plot is how much each variable contributes to each PC.

The corresponding score and loading plots are complementary and should be used together for the interpretation of the data. The plots provide valuable information about the samples and variables together, and the influence of original data can be explored [196]. One way for interpretation is to look at the correlations along the principal components, i.e. to see if variables and samples correlate positively or negatively.

The data should be preprocessed before PCA analysis which means the data will be transformed to fit the analysis better [196]. This is especially important when variables are measured in different units and of different magnitudes. One way of transforming the data is to use a scaling factor, for instance, the inverse of the standard deviation that will ensure each variable has the same variance. The variables become more comparable and avoid that some variables dominate more than others and thereby influence the analysis. Another way of transforming the data is by mean centering.

3 Methods and Materials

3.1 Study area

Svalbard is an archipelago that is located in the Arctic Ocean and is situated between 74°-81° North and 10°-35° East [197]. Spitsbergen is the largest island on Svalbard, and the climate on the west coast is influenced by the warm water carried by the North Atlantic current [128, 197]. About 60% of Svalbard is covered by glaciers and perennial ice cover [10]. Most of the freshwaters are located on Spitsbergen, and it is estimated that around 400 km^2 (0.06%) of Svalbard consist of freshwater [128]. The mean annual air temperature at Spitsbergen is -6°C, and annual precipitation is usually below 500 mm [197].

3.1.1 Sampling location

Mitrahalvøya is situated North of Kongsfjorden and on the west side of Krossfjorden. Lake Diesetvatnet, which consists of two catchment areas, Nordre Diesetvatnet and Søre Diesetvatnet, is located at Mitrahalvøya approximately 35 km North of Ny-Ålesund settlement and 21 m above sea level [130]. Nordre- and Søre Diesetvatnet are connected, and both catchment areas receive meltwater and sediment particles from nearby glaciers during the spring and summer seasons [10]. Furthermore, from Søre Diesetvatnet an approximately 3-4 km long river, Diesetelva, flows out into the Arctic Ocean with variable depth (0.1-1.5 m) and width (5-40 m) [127, 130]. As a consequence, both anadromous and resident populations of Arctic char coexists in Lake Diesetvatnet. Samples were collected in the mouth of Søre Diesetvatnet (79.19308 °N, 11.34714 °E) at the beginning of the outflow of the Diesetelva. The sampling location is shown in the map (Figure 11).

Pictures from the sampling location are provided in Figure 12. The water where Arctic char were caught was shallow with reduced visibility. The surrounding area was covered by an open tundra landscape with reindeer nearby and glacier-covered mountains. Moreover, some patches of snow could be spotted by the river, Diesetelva, and seabirds flying over the Lake water during the sampling.

3.2 Sampling

Permission for the sampling was provided by the Governor of Svalbard. Samples of Arctic char were collected in Diesetelva 17th of August 2021. The sampling location is shown in Figure 11. The sampling site was reached by boat from Ny-Ålesund to the west side of Mitrahalvøya, by Laksebu. From there, the sampling location was reached by walking up

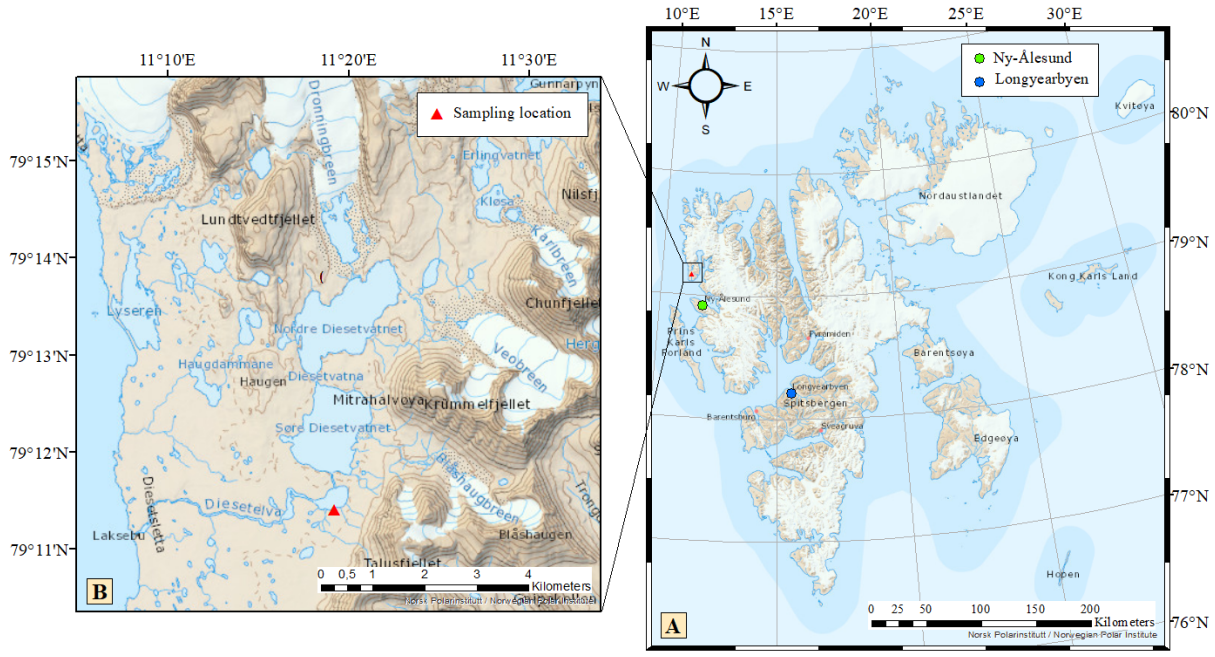

Figure 11: Map of Svalbard archipelago (A) shows main settlements; Longyearbyen (blue circle) and Ny-Ålesund (green circle). The study area is located on Mitrahalvøya, highlighted with a black box in map A and enlarged in map B.

along the river. Water samples from Diesetelva were collected and analyzed for different water parameters (Table 3).

Table 3: Water parameters from the sampling location at Diesetelva: coordinate of the sampling location given in decimal degree (DD). Measured water parameters included acidity (pH), conductivity (μS/cm), turbidity (NTU), and redox conditions (mV).

Coordinate	pH	Conductivity	Turbidity	Redox
79.19308 °N, 11.34714 °E	8.03	97.7	217	7.94

Arctic char was caught with a fishing rod and spinning baits. Spinning baits for freshwater- and river fishing were used; copper- and yellow-colored spinning baits of size 6.5 to 12 g. The sampling of fish was conducted according to ISO 23893-1:2007(E) [198]. Blood samples were taken immediately after the fish was caught. Disposable syringes (2 mL) with 23G 1 1/4 inch needle and Eppendorf tubes (1.5 mL) were rinsed with heparin (40 mg mL^{-1}). 1-3 mL of blood was drawn from the caudal vertebral vein, and the fish was killed right after the blood sampling was conducted. Biometric measurements of the fish were taken: body mass and length were measured with a kitchen scale and measuring tape (Table 4). For

Figure 12: Pictures from the sampling location.

sample collection of organs, the body cavity was cut open, taking care not to damage the gall bladder. Liver, gonad, and kidney were carefully taken out from the abdominal cavity, weighed and packed in alumina foil, and kept cold on snow in the field (Table B1). The skull was cut open to collect the brain, and the dorsal fin was collected. After the fieldwork, organ samples were stored at -20°C, and blood samples were kept in the fridge for 8 days at 4-5°C before the plasma was separated from whole blood. Samples ID are given in Table B2.

Table 4: Biometric measurements of individual Arctic char collected at the sampling location. Length of the fish is given in centimeters (cm), weight in grams (g), and gender given as female (F) or male (M).

Fish	Length (cm)	Weight (g)	Gender
1	45.0	900	F
2	47.5	1050	F
3	51.5	1350	F
4	36.0	350	M
5	49.0	950	F
6	49.0	1040	F
7	52.5	1390	F

3.3 Sample pretreatment

3.3.1 Centrifugation of blood samples

Plasma was separated from whole blood with an Eppendorf™ Centrifuge 5804 R. Whole blood samples WB-1, WB-3B, and WB-6B were centrifuged at 1000 rounds per minute (rpm) at 4°C for 4 minutes. Blood sample WB-3B was hemolysed and showed no clear separation, and was centrifuged again at 1000 relative centrifugal force (rcf) at 4°C for 5 minutes. Blood samples WB-2, WB-3A, WB-4, WB-5, WB-6A, and WB-7 were centrifuged at 1000 rcf at

4°C for 5 minutes. Blood sample WB-7 had no clear separation of the plasma, therefore sample WB-7 together with WB-3B were centrifuged again at 2000 rcf at 4° for 5 minutes. Plasma samples were subsampled into aliquotes of 100 μL (Table B2), and both plasma and red blood cell samples were stored at -80°C until further analysis.

3.3.2 Freeze-drying of organ samples

Gonad, hard roe (eggs), liver, and kidney samples were slightly thawed and cut with a titanium grade 2 knife into smaller pieces, and weighed out into metal-free Coulter® plastic cups (VWR). Brain samples were weighed out into the plastic cups without cutting. The equipment used for cutting was rinsed with nitric acid (HNO_3, 1 M), Milli-Q H_2O (ultrapure), and then EtOH between all samples to avoid cross-contamination. Sample cups were covered with parafilm and a lid, and kept at -21°C for two days prior to freeze-drying. A hole was made in the parafilm with the titanium grade 2 knife to let vapor out during drying. Samples were freeze-dried with Christ ALPHA 1-4 LD plus under vacuum (0.94 mbar) at -21°C for 28 hours followed by final drying under vacuum (0.090 mbar) at -43°C for 15 minutes. Samples were weighed after freeze-drying to determine the water content of samples, and stored at -21°C until further analysis. The water content of the samples is given in Table C7.

3.3.3 Homogenization of organ samples

Organ samples were crushed to powder using an agate mortar and pestle. A porcelain spatula covered in plastic foil was used to transfer the samples back into the plastic containers. The mortar and pestle were washed with soap and water, then five times with Milli-Q H_2O (ultrapure), and dried with dust-free paper tissues in between all samples. The plastic foil used outside the spatula was exchanged between all samples.

3.4 Determination of PFAS in plasma

3.4.1 Preparation of standard solutions

Stock solution of 1 μg mL^{-1} of 43 PFAS target analytes (TA) (Table B4) were prepared in MeOH as solvent. A 1 μg mL^{-1} IS mix of 3 isotopically labelled PFAS compounds were prepared in MeOH (Table B6).

3.4.2 Extraction of PFAS in plasma

Plasma samples were thawed slowly on the ice at room temperature. 100 μL of plasma was spiked with 20 ng mL^{-1} of IS. For protein precipitation, 450 μL MeOH containing

0.1% ammonium formate (AF, NH_4CO_2H) was added, and the mixture was vortexed for 30 seconds and centrifuged at 4000 rcf for 10 minutes at room temperature with an Eppendorf Centrifuge 5810. Superclo HybridSPE®-Phospholipid cartridge (30 mg, 1 mL) was rinsed with 1 mL of MeOH. The supernatant was transferred to the HybridSPE cartridge and the eluent was collected directly into amber LC-vials for analysis. For quality control, a recovery test of pooled plasma samples following the same extraction and clean-up protocol as described above was conducted. The recovery test included a method blank (MB) and a sample (S1) spiked with 20 ng mL^{-1} IS pre-extraction, and three replicates of samples spiked (SP1, SP2, SP3) with 20 ng mL^{-1} TA and 20 ng mL^{-1} IS pre-extraction, and two replicates of samples spiked with 20 ng mL^{-1} TA and 20 ng mL^{-1} IS post-extraction, referred to as matrix matches (MM1 and MM2). A calibration curve of PFAS TA with concentrations in the range of 0.1-50 ng mL^{-1} in MeOH containing 0.1% ammonium formate was prepared, in which all were spiked with 20 ng mL^{-1} of IS.

3.4.3 Analysis of PFAS with UPLC-ESI-MS/MS

UPLC-ESI-MS/MS was carried out by a protocol adopted by Vike-Jonas with minor modifications [163, 164]. Analysis of 43 PFAS TA in sample extracts was performed with an Acquity UPLC (Waters, Milford, USA) coupled to a Xevo^{TM} TQ-S triple quadrupole mass spectrometer. Separation of TA was performed on a Kinetex C18 column (30 mm x 2.1 mm, 1.3 μm, 100 ÅPhenomenex) connected to a Phenomenex C18 guard column (2.1 mm). The column temperature was set to 30°C with a mobile phase mixture consisting of 2 mM ammonium acetate in H_2O (A) and MeOH (B), with an injection volume of 4 μL and a flow rate of 0.2 mL min^{-1} with gradient elution according to Table 5.

Table 5: Gradient eluent program for UPLC-ESI-MS/MS analysis of PFAS compounds.

Time	Flow	A (%)	B (%)	Step
Initial	0.25	80	20	Initial
0.1	0.25	80	20	6
0.2	0.25	50	50	6
0.8	0.25	30	70	6
1.5	0.25	20	80	6
2.8	0.25	15	85	5
4.5	0.25	0	100	6
5.5	0.25	0	100	6
5.6	0.25	80	20	6
6	0.25	80	20	6

Mass spectrometric detection was performed using electrospray ionization in negative

mode (ESI-) with a Zspray (Waters, Milford, CT, USA), and a capillary voltage of 2 kV, cone voltage of 25 V, and source offset of 40 V. Desolvation temperature was held at 450°C, and the desolvation gas flow was set to 650 L h^{-1}. The source temperature was set to 150°C and the cone gas flow was maintained at 150L h^{-1}. The nebuliser gas flow was set to 6.0 bar. The tuning parameters for the ESI- are given in Table 6. Data were obtained by MassLynx™ 4.1 software and processed in TargetLynx (Waters, Milford, USA). Quantification of PFAS was performed using the IS method.

Table 6: Tuning parameters for ESI (-) during analysis of PFAS compounds with UPLC-ESI-MS/MS.

ESI (-)	
Capillary (kV)	2
Cone (V)	25
Source offset (V)	40
Desolvation temperature (°C)	450
Desolvation gas flow (L/h)	650
Cone (L/h)	150
Nebuliser (Bar)	6
Source temperature (°C)	150

3.5 Determination of steroid hormones in plasma

3.5.1 Preparation of standard solutions

Stock solution of 1 μg mL^{-1} of 18 steroid TA (Table B5) were prepared in MeOH as solvent. A 1 μg mL^{-1} IS mixture of 3 isotopically labelled steroid hormones were prepared in MeOH (Table B7).

3.5.2 Extraction of steroid hormones in plasma

Plasma samples were thawed slowly on the ice at room temperature. 100 μL of plasma was spiked with 20 ng mL^{-1} IS. 450 μL MeOH containing 0.1% ammonium formate (AF, NH_4CO_2H) was added, and the mixture was vortexed for 30 seconds and centrifuged at 4000 rcf for 10 minutes. Superclo HybridSPE®-Phospholipid cartridge (30 mg, 1 mL) was rinsed with 1 mL of MeOH. The supernatant was transferred to the Hybrid SPE cartridge and the eluent was collected directly into amber LC-vials for analysis. For quality control, a recovery test of pooled plasma samples following the same extraction and clean-up protocol as described above was conducted. The recovery test included a method blank (MB) and sample (S1) spiked with 20 ng mL^{-1} IS pre-extraction, three replicates of samples spiked

(SP1, SP2, SP3) with 20 ng mL^{-1} TA and 20 ng mL^{-1} IS pre-extraction, and two replicates of samples spiked with 20 ng mL^{-1} TA and 20 ng mL^{-1} IS post-extraction, referred to as matrix matches (MM1 and MM2). A calibration curve of steroid hormone TA with concentrations in the range of 0.1-50 ng mL^{-1} in MeOH containing 0.1% ammonium formate was prepared, in which all were spiked with 20 ng mL^{-1} of IS.

3.5.3 Analysis of steroid hormones with UPSFC-ESI-MS/MS

Ultra-Performance supercritical fluid chromatography-tandem mass spectrometry (UPSFC-MS/MS) analysis was adopted from de Kock *et al.* (2018) with minor modification [173]. Analysis of 18 steroid hormone TA in sample extracts was performed with an Acquity UPC^2 (Waters, Milford, USA) system coupled to a Xevo^{TM} TQ-S triple quadrupole mass spectrometer (Waters, Milford, USA). Separation of TA were performed on a Viridis® CSH Fluoro-Phenyl UPC^2 column (2.1 mm x 100 mm, 1.7 μm, 130 Å) connected to a Viridis® CSH Fluoro-Phenyl VanGuard^{TM} pre-column (2.1 mm x 5 mm). The mobile phase mixture constituted of CO_2 (A) and 0.1% formic acid in methanol:isopropanol (MeOH:*i*-PrOH, 1:1) as co-solvent (B). The mobile phase had an injection volume of 1 μL and a gradient elution program according to Table 7. The UPSFC system was equipped with an autosampler and the automated back pressure was set to 2000 psi. Elution from the chromatographic system into the MS system was supported by a make-up solvent consisting of 0.1% formic acid (HCOOH) in MeOH:*i*-PrOH (1:1) at a flow rate of 0.2 mL min^{-1}.

Table 7: Gradient eluent program for UPSFC-ESI-MS/MS analysis of steroid hormones.

Time (min)	Flow (mL/min)	A (%)	B (%)	Curve
Initial	1	98	2	Initial
0.5	1	98	2	6
3.0	1	83	17	6
3.5	1	83	17	6
4.0	1	98	2	6
5.0	1	98	2	6

Mass spectrometric detection was performed using electrospray ionization in the positive mode (ESI+) with a Zspray (Waters, Milford, CT, USA), and a capillary voltage of 2.8 kV, cone voltage of 20 V, and source offset of 80 V. The collision gas flow was maintained at 0.15 mL min^{-1}. Desolvation temperature was held at 500°C, and the desolvation gas flow was set to 1000 L h^{-1}. The source temperature was set to 150°C and the cone gas flow was maintained at 150L h^{-1}. The nebuliser gas flow was set to 6.0 bar. The tuning parameters for the ESI+ are given in Table 8. Data were obtained by MassLynx^{TM} 4.1 software and

processed in TargetLynx (Waters, Milford, USA). Quantification of steroid hormones was performed using the internal standard method.

Table 8: Tuning parameters for ESI(+) during analysis of steroid hormones with UPSFC-ESI-MS/MS.

ESI(+)	
Capillary (kV)	2.8
Cone voltage (V)	20
Source offset (V)	80
Source temperature (°C)	150
Desolvation temperature (°C)	500
Desolvation gas flow (L/h)	1000
Cone (L/h)	150
Nebuliser (Bar)	6.0
Collision gas flow (mL/min)	0.15

3.6 Method test for extraction of steroid hormones and PFAS in liver samples

Three different techniques for extraction of steroid hormones and PFAS in biological samples were assessed; Hybrid SPE, SPE, and SLE. The protocols were conducted on pooled liver samples (wet weight) with a recovery test set-up according to Table 9. Method blanks were used to monitor background contamination, while pre- and post-spiked samples were used to assess the recovery of extracted compounds. Liver samples from Arctic char were used to make up the pooled samples, and the combined liver samples were homogenized with an agate mortar and pestle.

Table 9: Recovery test set-up for the three extraction protocols. Recovery samples; method blank (MB), sample (S1), spiked samples (SP1, SP2, SP3), and matrix matches (MM1 and MM2). Pooled liver sample were spiked with internal standard (IS) and target analytes (TA) pre-extraction (pre) or post-extraction (post) accordingly.

	Sample	**IS (pre)**	**TA (pre)**	**IS (post)**	**TA (post)**
MB		x			
S1	x	x			
SP1	x	x	x		
SP2	x	x	x		
SP3	x	x	x		
MM1	x			x	x
MM2	x			x	x

3.6.1 Preparation of standard solutions

Stock solution of 0.5 μg mL^{-1} of 43 PFAS TA (Table B4) were prepared in MeOH as solvent. A 1 μg mL^{-1} IS mixture of 3 isotopically labelled PFAS were prepared in MeOH (Table B6). The same stock solution of TA and IS mixture of steroid hormones from the extraction procedure in plasma were used, section 3.5.1 (Table B5 and B7).

3.6.2 Hybrid SPE

Extraction of steroid hormones and PFAS with Hybrid SPE was conducted with two different precipitation agents, 0.1% AF in MeOH (w/v) and 0.5% citric acid (CA) in acetonitrile (ACN) (w/v), adopted from the following method with minor modifications [163, 164]. Both precipitation agents followed the same procedure. Approximately 100 mg of liver tissue were weighed out in a 15 mL polypropylene tube on a precision scale. Liver samples were spiked with 20 ng mL^{-1} IS and 20 ng mL^{-1} TA pre- or post-extraction according to Table 9. 450 μL of 0.1% AF in MeOH or 0.5% CA in ACN were added. The sample mixture was vortexed for 30 seconds, ultrasonicated for 45 minutes with Branson 3510 Ultrasonic Cleaner, and centrifuged at 4000 rcf for 10 minutes at room temperature. Superclo HybridSPE®-Phospholipid cartridge (30 mg, 1 mL) were rinsed with 1 mL 0.1% AF in MeOH or 0.5% CA in ACN. The supernatant was transferred to the pre-washed cartridge, and the eluent was collected directly in amber LC-vial for analysis.

3.6.3 Solid-phase extraction

Extraction and clean-up protocol with solid-phase extraction (SPE) were conducted according to Weisser *et al.* (2016) with minor modifications [199]. Approximately 100 mg of liver tissue was weighed out in a 15 mL polypropylene tube on a precision scale. Liver samples were spiked with 20 ng mL^{-1} with TA and 20 ng mL^{-1} IS pre- or post-extraction according to Table 9, and added 1 mL of H_2O:MeOH (25:75, v/v). The sample mixture was vortexed for 30 seconds, ultrasonicated for 45 minutes with Branson 3510 Ultrasonic Cleaner, and centrifuged at 4000 rcf for 10 minutes at room temperature. The supernatant was transferred to a new 15 mL PP tube and diluted with 4 mL Milli-Q H_2O (ultrapure) to a total volume of 5 mL. HyperSep^{TM}C18 cartridge (50 mg, 1 mL) was pre-conditioned in the following order with 3 mL heptane, 3 mL acetone, 3 mL MeOH, and 3 mL Milli-Q H_2O. The supernatant was transferred to the C18 SPE cartridge, and washed with 6 mL Milli-Q H_2O and thereafter 6 mL H_2O:MeOH (75:25, v/v). The analytes were eluted with 3 mL H_2O:MeOH (20:80, v/v) and concentrated to approximately 500 μL under a gentle stream of nitrogen gas at 60°C with a Stuart block heater SBH200D/3, and transferred to amber LC-vials for analysis.

3.6.4 Solid-liquid extraction

A generic protocol for solid-liquid extraction (SLE) was conducted with minor modifications [200]. Approximately 100 mg of liver tissue was weighed out in a 15 mL PP tube on a precision scale. Samples were spiked according to Table 9, and added 3 mL of Methyl tert-butyl ether (MTBE). The sample mixture was ultrasonicated for 45 minutes with Branson 3510 Ultrasonic Cleaner. The extract was transferred to a new polypropylene tube, and the extraction procedure of the liver sample was repeated 3 times to the combined extract volume of 9 mL (3 x 3 mL). The combined extract was centrifuged at 4000 rcf for 10 minutes at room temperature, and the extract was transferred to a new polypropylene tube and evaporated to near dryness under a gentle stream of nitrogen gas at 40°C with a Stuart block heater SBH200D/3. The analytes were reconstituted with 500 μL of H_2O:MeOH (1:1, v/v), vortex mixed and transferred to amber LC-vials for analysis.

3.6.5 Analysis of sample extracts

Sample extracts from the three extraction techniques were analyzed for steroid hormones with UPSFC-ESI-MS/MS and PFAS with UPLC-ESI-MS/MS as decribed in sections 3.5.3 and 3.4.3, respectively.

3.7 Determination of trace elements

3.7.1 Microwave digestion of organ samples with UltraCLAVE

The acid digestion procedure followed the standard routine NS-EN 13805:2014 [201]. Organ samples (40-350 mg) were weighed out into 15 mL acid-washed Teflon tubes on a precision scale. 2 or 5 mL of Scanpure HNO_3 50% was added to each sample depending on sample weight (approximately 1.25 mL HNO_3 per 100 mg sample). Three replicates of a CRM (DORM-5, fish protein, NRC) were prepared the same way. 6 blanks (3 replicates with 5 mL and 3 replicates with 2 mL of HNO_3 50% w/w) were prepared and randomly distributed among the samples. Samples were digested in high pressure (160 bar) and high temperature (240°C) microwave unit (UltraCLAVE Milestone, Shelton, CT, USA) for 1.5 hours. After digestion, the samples were diluted with ultrapure Milli-Q water 10±5% times the added volume of 50% HNO_3 w/w to reach a final concentration of 0.6 M HNO_3. The samples were placed in a 15 mL polypropylene tube for ICP-MS analysis.

3.7.2 Microwave digestion of plasma and red blood cells with UltraCLAVE

Red blood cells (RBC) and plasma samples were weighed out into 15 mL acid-washed Teflon tubes on a precision scale and added 2 mL and 1 mL of Scanpure HNO_3 65% w/w, respectively. Three replicates of CRM (Seronorm, trace elements in whole blood L-2), two replicates of CRM (Seronorm, trace elements in serum), and 1 replicate of CRM (DOLT-3, Dogfish liver, NRC) were prepared. 6 blanks (3 replicates with 2 mL and 3 replicates with 1 mL of HNO_3 65% w/w) were prepared. Samples were digested in high pressure (160 bar) and high temperature (240°C) microwave digestion reactor (UltraCLAVE, Milestone, GmbH, Leutkirch, Germany) for 1.5 hours. After digestion, the samples were diluted with ultrapure Milli-Q water 24±5% times the added volume of 65% w/w HNO_3 to a final concentration of 0.6 M HNO_3. The samples were placed in a 15 mL polypropylene tube for ICP-MS analysis.

3.7.3 Analysis of trace elements with ICP-MS

Samples were analyzed for elemental composition using an 8800 Triple Quadrupole inductively coupled plasma mass spectrometry (ICP-MS) system (Agilent, USA) equipped with prepFAST M5 autosampler (ESI, USA). The accuracy of the analysis was determined using CRM; DORM-5 fish protein (NRC), DOLT-3 dogfish liver (NRC), Seronorm™ trace elements whole blood L-2 (Sero), and Seronorm™ trace elements serum (Sero) (Table C10). Samples were diluted 10-25 times prior to analysis depending on the sample type. System parameters during analysis are listed in Table 10.

Table 10: System parameters during ICP-MS analysis.

General parameters	
RF Power	1550 W
Nebulizer Gas	0.80 L/min
Makeup Gas	0.38 L/min
Sample depth	8.0 mm
Ion lenses	x-lens
H2 mode	
H2 gas flow	4.5 mL/min
He gas flow	1.0 mL/min
O2 mode	
O2 gas flow	0.525 mL/min

3.8 Data treatment and statistical methods

Topographic base map services were provided by the Norwegian Polar Institute and processed with ArcGIS Desktop (ArcMAP) by Esri Version 10.8.1. Processing of chromatograms obtained from UPLC-MS/MS and UPSFC-MS/MS analyses were conducted with MassLynx^{TM} 4.1 software and processed in TargetLynx (Waters, Milford, USA). The chromatographic data were processed using Microsoft Excel version 2207. Statistical analyses and visualization of the data were performed using R version 4.2.0 with RStudio version 2022.02.3. The data were tested for normality with the Shapiro-Wilks test with a significance level set at $p < 0.05$. Non-parametric data were tested with Kruskal-Wallis to test for significance in trace element levels between tissues of Artic char. Pairwise multiple comparisons using Dunn's test post-hoc analysis with Holm adjustments were conducted to find which tissues that were statistically significantly different. The PCA analysis was performed in Aspen Unscrambler version 12.1. The data was preprocessed prior to PCA analysis by mean centering and weighted as the inverse of the standard deviation ($1/\sigma$), and cross-validated. The algorithm singular value decomposition (SVD) was applied.

4 Results

4.1 Steroid hormones in plasma of Arctic char

Quantification of steroid hormone TA were accomplished based on the IS method. In total, 4 out of 18 analyzed steroids were observed in plasma samples. Concentrations of 11-Ketotestosterone (11-KetoTS), 5α-Dihydrotestosterone (DHT), testosterone (TS), and androstenedione (AN) in individual plasma samples are listed in Table 11. AN was observed in all plasma samples, and TS was observed in 8 out of 9 plasma samples (Table 12). 11-KetoTS and DHT were observed in 1 and 4 individual plasma samples, respectively. Concentrations of DHT and TS in plasma sample P-5c were 34.2 ng mL^{-1} and 47.0 ng mL^{-1}, respectively, and both concentrations were above the estimated LOD from the calibration curve method. The rest of the steroid hormone concentrations in the plasma samples were below the estimated LOD calculated from the calibration curve method.

Values for LOD, LOQ, absolute recovery, relative recovery, and matrix effect are listed in Table C1 in Appendix for 11 out of 18 steroid hormones. The remaining steroid hormones: ALDO, A5, DHEA, P5, E1, and E2, are not reported due to missing signals and poor separation and are therefore written as NA (not applicable). The absolute recovery percentages for steroid hormones in plasma ranged from 52% to 12 000%, whereas the relative recoveries ranged from 42% to 510%. Matrix effects were negative for all steroids and ranged from -2.0% to -100%.

Table 11: Concentrations in ng mL^{-1} ww of 4 steroid hormones observed in individual plasma samples. All concentrations are < LOD, based on the estimation of LOD with the calibration curve method, except for DHT and TS in plasma sample P-5c which are > LOD.

Sample ID	11-KetoTS	DHT	TS	AN
P-1c	18.7	11.5	19.0	11.0
P-2c			5.13	3.36
P-3Ac			6.56	4.22
P-3Ba			5.16	3.38
P-4a				2.69
P-5c		34.2	47.0	12.2
P-6Ad		17.8	16.0	8.86
P-6Bc		16.7	17.8	8.87
P-7c			5.60	3.33

Table 12: Observation rate (OR) of steroid hormones in plasma samples (n=9), and mean, standard deviation (SD), median, minimum, and maximum concentration in ng mL^{-1} ww of 3 steroids in plasma samples. Calculation of mean, median, minimum, and maximum are based on values in Table 11. 11-KetoTS was only observed in one plasma sample and is not included.

Compound	OR	Mean	SD	Median	Min	Max
DHT	4/9	20.0	8.50	17.3	11.5	34.2
TS	8/9	15.3	13.2	11.3	5.13	47.0
AN	9/9	6.43	3.55	4.22	2.69	12.2

4.2 PFAS in plasma of Arctic char

The mean total PFAS concentration in plasma of Arctic char from Diesetvatent was 26.8±5.98 ng mL^{-1}, and the concentration of PFAS ranged from 20.8 to 38.7 ng $mL^{-}1$ (Table C2). 9 out of 43 analysed PFAS were observed in plasma; 6:2 FTS, PFNA, PFOSA, PFOS, PFDA, PFUnA, PFDoDA, PFTriDA, and PFECHS. Three PFAS compounds that were observed, FOSAA, MeFOSAA, and DiSAMPAP, are excluded due to low recoveries (< 40%). All the observed PFAS concentrations were below LOD. 6:2 FTS, PFNA, PFOS, and PFUnA were observed in all individual plasma samples. Mean concentrations are given in Table 13 for PFAS with an observation rate above 60%, and the percentage composition of 9 of the observed PFAS in individual plasma samples is shown in figure 13.

Table 13: Observation rate (OR) of PFAS in plasma samples (n=9) for PFAS with OR > 60%. Mean, standard deviation (SD), median, minimum, and maximum concentrations in ng mL^{-1} ww of PFAS compounds in plasma samples.

Compound	OR	Mean	SD	Median	Min	Max
6:2 FTS	9/9	9.64	0.204	9.61	9.28	9.97
PFNA	9/9	1.95	0.0862	1.98	1.85	2.09
PFOS	9/9	5.39	1.84	4.98	1.93	8.98
PFUnA	9/9	5.27	0.745	5.13	4.20	6.48

PFAS TA were quantified based on the IS method. The IS PFOA $^{13}C_8$ was applied to the respective PFOA TA, whereas the IS 6:2 FTS $^{13}C_2$ was used for the TA 6:2 FTS. The IS PFOS $^{13}C_8$ was applied on all the other PFAS target analytes listed in table B4. Absolute and relative recoveries of PFAS TA ranged from 1.2% to 130% and -82% to 120%, and matrix effects of PFAS TA ranged from -110% to 22% (Table C3). LOD and LOQ were calculated based on the calibration curve method.

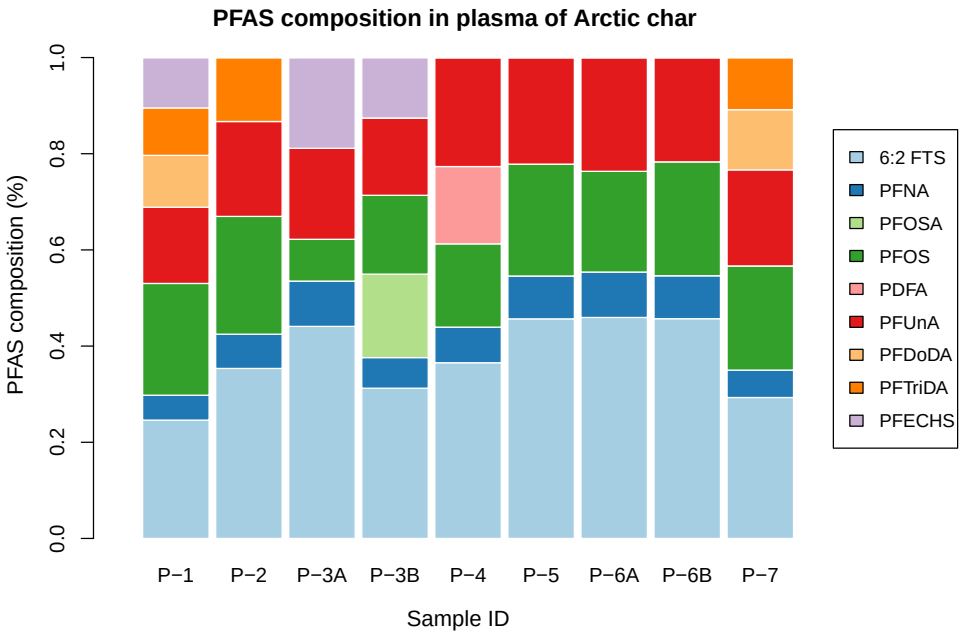

Figure 13: Percentage (%) composition of the 9 observed PFAS compounds: 6:2 FTS, PFNA, PFOSA, PFOS, PFDA, PFUnA, PFDoDA, PFTriDA, and PFECHS, in individual plasma samples of Arctic char. Overview of samples-ID are given in Table B2.

4.3 Method test for extraction of steroid hormones and PFAS in liver samples

Absolute and relative recoveries and matrix effects for steroid hormones and PFAS for all 4 extraction methods are listed in Table C5 and C6.

4.3.1 Extraction of steroid hormones in liver samples

The IS $^{13}C_3$-CORNE was not applied to any of the steroids due to irregular signals. IS $^{13}C_3$-DHT was used for P4, DHT, TS, AN, DHEA, 17 OH-P5 steroid TA, while the IS $^{13}C_2$-17α-OHP was used for COR, CORNE, ALDO, COS, 11-deoxyCOR, 17α-OHP, DOC, 11-KetoTS steroid TA. The Hybrid SPE extraction and clean-up of pooled liver samples with 0.1% ammonium formate (AF) in MeOH provided absolute recoveries ranging from -34000% to 150% and relative recoveries ranging from -1500% to 190%. All steroid hormones provided negative matrix effects ranging from -1.5% to -100%. The same extraction and clean-up method with 0.5% citric acid (CA) in ACN provided recoveries of steroid hormones ranging from 38% to 100% and 66% to 160% for absolute and relative, respectively. All steroids had negative matrix effects ranging from -6.1% to -95% except for ALDO which had a positive matrix effect of 6.1%. Recoveries for steroid hormones with SPE extraction and

clean-up ranged from 19-200% and 30-2500% for absolute and relative, respectively. Matrix effects were negative for all steroids and ranged from -34% to -83%. The SLE extraction provided absolute and relative recoveries of steroid hormones ranging from 21-110% and 63-240%, respectively. Most of the steroids had negative matrix effects in the range of -12% -89% except for DHT and DHEA which had matrix effects of 6.2% and 115%, respectively.

4.3.2 Extraction of PFAS in liver samples

The IS $^{13}C_8$-PFOS was not applied to any of the PFAS TA due to inconsistent signals. IS $^{13}C_8$-PFOA was applied to all PFAS TA except for 6:2 FTS in which IS $^{13}C_2$ 6:2 FTS was applied. The Hybrid SPE extraction and clean-up with 0.1% AF in MeOH provided absolute and relative recoveries ranging from 13-250% and 17-530%, respectively. All PFAS compounds provided strong negative matrix effects ranging from -43% to -100% except for MeFOSA, EtFOSA, PFHxDA, and SAMPAP which had positive matrix effects of 84% , 140% , 72% , and 2.3%, respectively. The same extraction with 0.5% CA in ACN provided absolute and relative recoveries in the range 16-510% and 15-480%, respectively. Most PFAS had strong positive matrix effects. Matrix effects ranged from 59000% to -70%. The SPE extraction and clean-up provided absolute and relative recoveries ranging from -0.1% to 160% and -0.2% to 160%, respectively. Most PFAS had negative matrix effects ranging from -12% to -250%, and a few PFAS with positive matrix effects ranging from 1.6-1300%. Absolute and relative recoveries for SLE ranged from 2.9-340% and 2.0-170%, respectively. Matrix effects were mainly negative ranging from -12% to -120%, and a few PFAS with positive matrix effects ranging from 23% to 190%.

4.4 Trace elements in Arctic char

The elemental composition was analyzed in 7 tissues from Arctic char including the brain, gonad, hard roe, liver, kidney, plasma, and red blood cells for 41 elements in total (Table C8). LOD values for the elemental analysis with ICP-MS are given in Table C9, and the percentage recovery for the certified reference material used including; DORM-5, DOLT-3, seronorm whole blood L-2, and seronorm serum are presented in Table C10.

In the present study, one of the objectives was to determine the distribution of non-essential trace elements including Hg, Cd, Pb, and As in the listed organs of Arctic char, and to determine whether the concentration is higher in the liver and kidney compared to other matrices. In addition, the distribution of a selection of essential trace elements Cu, Zn, Se, Ni, Cr, Mn, Tl, and Co are included.

Table 14: Concentration of trace elements in μg g^{-1} in various tissues of Arctic char. For each sample type (matrix) number of samples above LOD (n > LOD), and mean±standard deviation (SD), median, and range of concentrations are given. Concentrations in samples of brain, gonad, hard roe, liver, and kidney are given in dry weight, whereas RBC and plasma are given in wet weight.

Element	Matrix	n >LOD	Mean±SD	Median	Range
Hg	Brain	6	0.0229±0.0072	0.0176	0.00533-0.0561
	Gonad	6	0.0233±0.030	0.00855	0.00180-0.0877
	Hard roe	4	0.00804±0.0032	0.00706	0.00506-0.0130
	Liver	7	0.0786±0.12	0.0392	0.0118-0.365
	Kidney	7	0.0966±0.079	0.0668	0.0117-0.272
	RBC	9	0.0165±0.011	0.0127	0.00776-0.0246
	Plasma	4	0.00457±0.0035	0.00343	0.000796-0.0106
Cd	Brain	6	0.0181±0.014	0.0153	0.00630-0.0468
	Gonad	7	0.0481±0.057	0.0177	0.00255-0.142
	Hard roe	4	0.0344±0.038	0.0214	0.00148-0.0931
	Liver	7	0.305±0.36	0.169	0.0913-1.17
	Kidney	7	1.98±1.1	1.73	0.861-4.20
	RBC	3	0.000325±0.00013	0.000319	0.000183-0.000473
	Plasma	3	0.000594±0.000072	0.000588	0.000510-0.000685
Pb	Brain	5	0.298±0.38	0.131	0.00661-1.02
	Gonad	5	0.161±0.14	0.132	0.0118-0.418
	Hard roe	2	0.0176±0.015		0.00237-0.0328
	Liver	6	0.0266±0.043	0.00739	000239-0.122
	Kidney	7	0.195±0.19	0.0935	0.00169-1.64
	RBC	9	0.00525±0.002		0.00299-0.00942
	Plasma	2	0.0602±0.035		0.0251-0.0952
Se	Brain	6	1.54±0.58	1.33	1.11-2.82
	Gonad	7	1.76±1.1	1.42	0.348-3.60
	Hard roe	4	4.24±0.85	3.98	3.46-5.52
	Liver	7	4.09±3.3	2.73	1.95-12.1
	Kidney	7	6.77±3.5	5.65	3.47-14.9
	RBC	9	0.810±0.43	0.723	0.383-1.82
	Plasma	7	0.444±0.31	0.381	0.0338-0.974

Table 14 continued from previous page

Element	Matrix	n >LOD	Mean±SD	Median	Range
As	Brain	6	0.619±0.33	0.478	0.293-1.20
	Gonad	7	3.51±4.3	1.86	0.421-14.0
	Hard roe	4	1.18±1.0	0.972	0.204-2.56
	Liver	7	0.787±0.35	0.748	0.199-1.25
	Kidney	7	1.69±0.46	1.59	1.09-2.52
	RBC	9	0.0581±0.030	0.0555	0.0107-0.124
	Plasma	7	0.101±0.061	0.0812	0.0235-0.201
Cu	Brain	6	9.72±0.80	9.90	8.60-10.6
	Gonad	7	6.60±9.9	2.00	0.183-30.3
	Hard roe	4	25.8±17	21.5	9.20-51.2
	Liver	7	27.0±10	29.6	8.54-40.7
	Kidney	7	5.34±1.5	5.10	2.31-7.68
	RBC	9	0.212±0.036	0.201	0.158-0.280
	Plasma	7	0.416±0.17	0.407	0.223-0.807
Zn	Brain	6	44.6±4.4	43.9	38.4-51.1
	Gonad	7	75.3±47	61.0	8.04-168
	Hard roe	4	139±74	126	62.8-243
	Liver	7	84.4±19	82.1	59.3-122
	Kidney	7	110±28	95.2	86.1-157
	RBC	9	7.67±1.6	6.71	5.80-14.0
	Plasma	7	13.6±4.9	11.7	7.66-22.8
Ni	Brain	6	0.241±0.27	0.147	0.0340-0.803
	Gonad	6	0.0745±0.057	0.0653	0.00976-0.159
	Hard roe	4	0.0202±0.018	0.0143	0.00280-0.0494
	Liver	4	0.0467±0.072	0.00711	0.00105-0.172
	Kidney	7	0.472±0.56	0.327	0.0724-1.81
	RBC	9	0.00849±0.0057	0.00587	0.00410-0.0214
	Plasma	6	0.0278±0.030	0.0145	0.00747-0.0925
Co	Brain	6	0.200±0.18	0.118	0.0455-0.548
	Gonad	7	0.157±0.20	0.107	0.0213-0.634
	Hard roe	4	0.0463±0.25	0.198	0.0869-0.707
	Liver	7	0.150±0.10	0.120	0.0955-0.391
	Kidney	7	1.20±0.50	1.25	0.0823-1.73
	RBC	9	0.0278±0.036	0.0150	0.00754-0.118
	Plasma	7	0.109±0.15	0.0493	0.0328-0.474

Table 14 continued from previous page

Element	Matrix	n >LOD	Mean±SD	Median	Range
Cr	Brain	6	0.565±0.84	0.186	0.00294-2.40
	Gonad	7	0.0832±0.085	0.0580	0.00819-0.261
	Hard roe	1	<LOD	<LOD	<LOD
	Liver	1	<LOD	<LOD	<LOD
	Kidney	7	0.242±0.17	0.197	0.0263-0.559
	RBC	8	0.00613±0.0050	0.00361	0.00196-0.0166
	Plasma	4	0.00677±0.0075	0.00379	0.000241-0.0193
Mn	Brain	6	6.6±7.0	3.34	1.22-21.2
	Gonad	7	6.38±8.5	2.93	0.413-26.4
	Hard roe	4	5.14±2.4	5.20	2.55-7.61
	Liver	7	4.31±2.5	2.67	1.71-7.72
	Kidney	7	4.95±1.9	4.74	2.51-8.48
	RBC	9	0.0527±0.025	0.0533	0.0163-0.130
	Plasma	6	0.0320±0.017	0.0244	0.0149-0.0645
Tl	Brain	6	0.0175±0.014	0.0104	0.00498-0.0383
	Gonad	7	0.0158±0.026	0.00467	0.000692-0.0789
	Hard roe	4	0.00406±0.00091	0.00426	0.00277-0.00497
	Liver	7	0.0751±0.10	0.0208	0.319-0.0103
	Kidney	7	0.0489±0.070	0.0151	0.00912-0.217
	RBC	7	0.000246±0.00039	0.000125	0.0000214-0.00106
	Plasma	2	0.000319±0.00031		0.0000131-0.000624

4.4.1 Mercury (Hg)

Mean concentration of Hg in the different tissues of Arctic char presented in increasing order were 0.00457 μg g $^{-1}$ wet weight (ww) in plasma (n=4), 0.00804 μg g $^{-1}$ dry weight (dw) in hard roe (n=4), 0.0165 μg g $^{-1}$ ww in red blood cells (RBC) (n=7), 0.0229 μg g $^{-1}$ dw in brain (n=6), 0.0233 μg g $^{-1}$ dw in gonad (n=6), 0.0786 μg g $^{-1}$ dw in liver (n=7), and 0.0966 μg g $^{-1}$ dw in kidney (n=7). The distribution of Hg in tissues of Arctic char are presented in Figure 14.

The data was tested for normality with the Shapiro Wilks test that indicated deviation from normality ($p < 0.05$). Kruskal-Wallis test showed that there was a statistical significant difference in median Hg concentrations between the different organs in Arctic char: χ^2 (6) = 19.30, n = 41, $p = 0.00369$ [202]. Pairwise multiple comparisons using Dunn's test post-hoc analysis with Holm adjustments indicated that there was a statistically significant difference in the median concentrations between kidney and plasma ($p = 0.00743$) (Figure 14). None of the other Hg tissue concentrations were statistically significantly different.

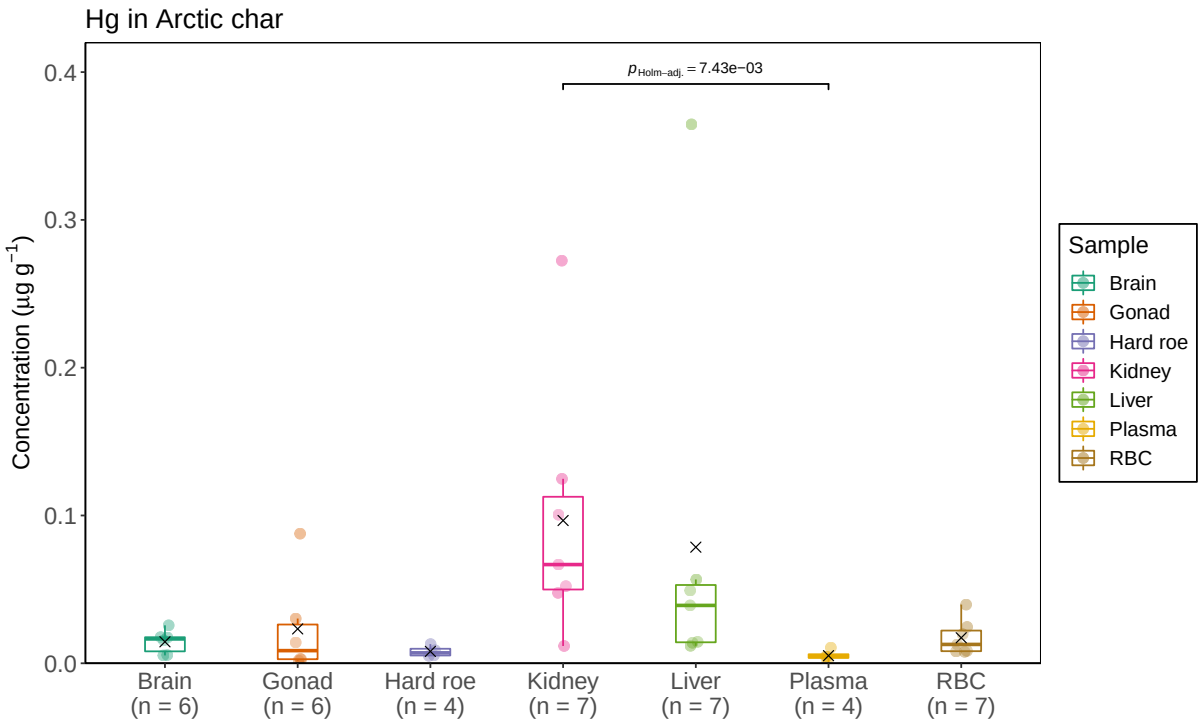

Figure 14: Distribution of Hg in tissues of Arctic char from Lake Diesetvatnet. Box and whisker plot shows minimum and maximum (whiskers), interquartile range (box), and median (horizontal line) concentrations of Hg in μg g $^{-1}$ in each sample type (n indicates the number of samples for each tissue). The cross indicates the mean concentration, and the bar indicates groups that are statistically significantly different with the corresponding p-value.

4.4.2 Cadmium (Cd)

Mean concentration of Cd in the different tissues of Arctic char presented in increasing order were 0.000325 μg g $^{-1}$ ww in RBC (n=3), 0.000594 μg g $^{-1}$ ww in plasma (n=3), 0.0181 μg g $^{-1}$ dw in brain (n=6), 0.0344 μg g $^{-1}$ dw in hard roe (n=4), 0.0481 μg g $^{-1}$ dw in gonad (n=7), 0.305 μg g $^{-1}$ dw in liver (n=7), and 1.98 μg g $^{-1}$ dw in kidney (n=7) (Table C8). The distribution of Cd in tissues of Arctic char are presented in Figure 15.

The data was tested for normality with the Shapiro Wilks test that indicated deviation from normality ($p < 0.05$). Kruskal-Wallis test showed that there was a statistical significant difference in median Cd concentrations between the different organs in Arctic char: χ^2 (4) = 22.94, n = 31, p = 0.0001302 [202]. Pairwise multiple comparisons using Dunn's test post-hoc analysis with Holm adjustments indicated that there was a statistical significant difference in the median concentrations between the kidney and brain (p = 0.00114), the kidney and gonad (p = 0.00444), and the kidney and hard roe (p = 0.00444) (Figure 15). None of the other tissue Hg concentrations were statistically significantly different.

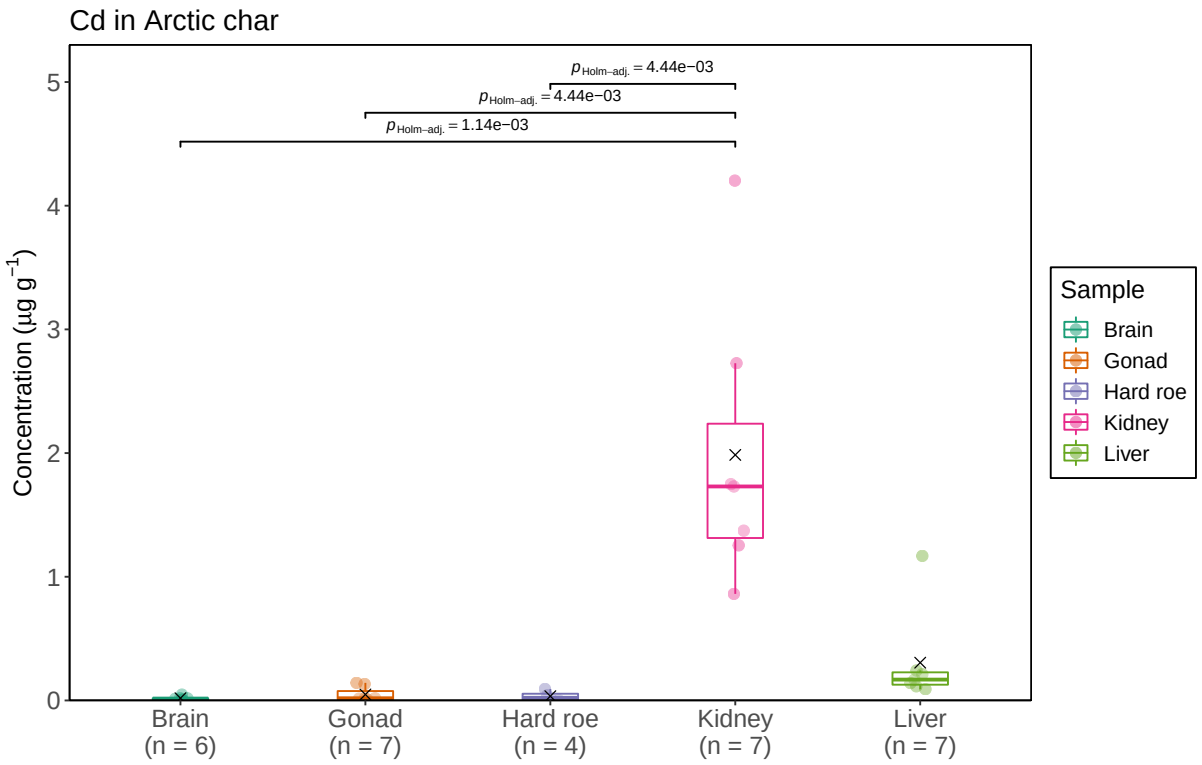

Figure 15: Distribution of Cd in tissues of Arctic char from Lake Diesetvatnet. Box and whisker plot shows minimum and maximum (whiskers), interquartile range (box), and median (horizontal line) concentrations of Cd in μg g $^{-1}$ in each sample type (n indicates the number of samples for each tissue). The cross indicates the mean concentration, and the bar indicates groups that are statistically significantly different with the corresponding p-value.

4.4.3 Lead (Pb)

Mean concentration of Pb in the different tissues of Arctic char presented in increasing order were 0.00525 μg g $^{-1}$ ww in RBC (n=7), 0.0176 μg g $^{-1}$ dw in hard roe (n=2), 0.0266 μg g $^{-1}$ dw in liver (n=6), 0.0602 μg g $^{-1}$ ww in plasma (n=2), 0.161 μg g $^{-1}$ dw in gonad (n=5), 0.195 μg g $^{-1}$ dw in Kidney (n=7), and 0.298 μg g $^{-1}$ dw in brain (n=5) (Table C8). The distribution of Pb in tissues of Arctic char are presented in Figure 16.

The data were tested for normality with the Shapiro Wilks test that indicated deviation from normality ($p < 0.05$). Kruskal-Wallis test showed that there was no statistically significant difference in median Pb concentrations between the different organs in Arctic char: χ^2 (4) = 12.9, n = 30, p = 0.01178 [202].

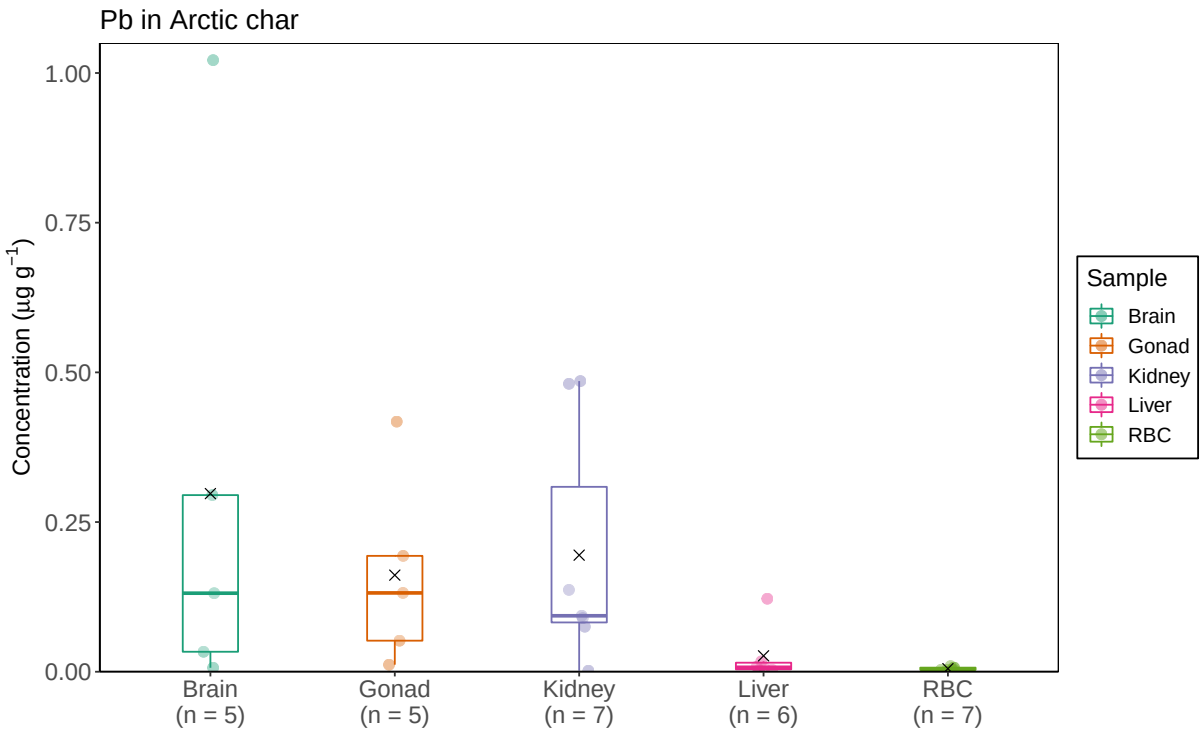

Figure 16: Distribution of Pb in tissues of Arctic char from Lake Diesetvatnet. Box and whisker plot shows minimum and maximum (whiskers), interquartile range (box), and median (horizontal line) concentrations of Pb in μg g $^{-1}$ in each sample type (n indicates the number of samples for each tissue). The cross indicates the mean concentration.

4.4.4 Arsenic (As)

Mean concentration of As in the different tissues of Arctic char presented in increasing order were 0.0581 μg g $^{-1}$ ww in RBC (n=7), 0.101 μg g $^{-1}$ ww in plasma (n=7), 0.619 μg g $^{-1}$ dw in brain (n=6), 0.787 μg g $^{-1}$ dw in liver (n=7), 1.18 μg g $^{-1}$ dw in hard roe (n=4), 1.69 μg g $^{-1}$ dw in Kidney (n=7), and 3.51 μg g $^{-1}$ dw in gonad (n=7) (Table C8). The distribution of As in tissues of Arctic char are presented in Figure 17.

The data was tested for normality with the Shapiro Wilks test that indicated deviation from normality ($p < 0.05$).Kruskal-Wallis test showed that there was statistically significant difference in median As concentrations between the different organs in Arctic char: χ^2 (6) = 34.61, p = 5.137e-06 [202]. Pairwise multiple comparisons using Dunn's test post-hoc analysis with Holm adjustments indicated that there was a statistical significant difference in the median concentrations between the gonad and plasma (p = 0.00178), the gonad and RBC (p = 0.000159), the kidney and plasma (p = 0.00415), and the kidney and RBC (p = 0.000422) (Figure 17).

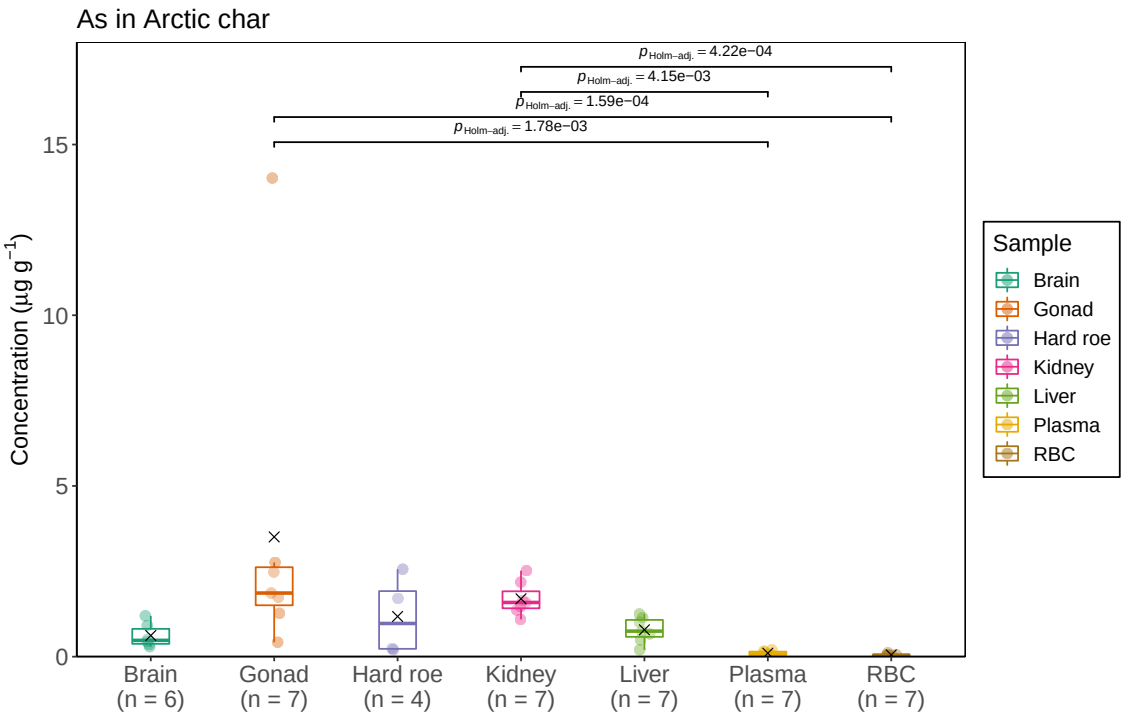

Figure 17: Distribution of As in tissues of Arctic char from Lake Diesetvatnet. Box and whisker plot shows minimum and maximum (whiskers), interquartile range (box), and median (horizontal line) concentrations of As in μg g $^{-1}$ in each sample type (n indicates the number of samples for each tissue). The cross indicates the mean concentration, and the bar indicates groups that are statistically significantly different with the corresponding p-value.

4.4.5 Essential trace elements in Arctic char

The data of the selected elements Cu, Zn, Se, Ni, Cr, Mn, Tl, and Co were tested for normality with the Shapiro Wilks test that indicated deviation from normality ($p < 0.05$).

Copper (Cu): Kruskal-Wallis test showed that there was statistically significant difference in median Cu concentrations between the different organs in Arctic char: χ^2 (6) = 36.84, p = 1.896e-06 [202]. Pairwise multiple comparisons using Dunn's test post-hoc analysis with Holm adjustments indicated that there was a statistical significant difference in the median concentrations between the brain and RBC (p = 0.00422), the hard roe and plasma (p = 0.0191), the hard roe and RCB (p = 0.00124), the liver and plasma (p = 0.00193), and the liver and RBC (p = 0.0000403) (Figure C21).

Zinc (Zn): Kruskal-Wallis test showed that there was statistically significant difference in median Zn concentrations between the different organs in Arctic char: χ^2 (6) = 35.11, p = 4.102e-06 [202]. Pairwise multiple comparisons using Dunn's test post-hoc analysis with Holm adjustments indicated that there was a statistical significant difference in the median concentrations between the gonad and RBC (p = 0.0314), the hard roe and plasma (p =

0.0411), the hard roe and RCB (p = 0.00243), the kidney and plasma (p = 0.000108), and the liver and RBC (p = 0.00221) (Figure C22).

Selenium (Se): Kruskal-Wallis test showed that there was statistically significant difference in median Se concentrations between the different organs in Arctic char: χ^2 (6) = 35.33, p = 3.719e-06 [202]. Pairwise multiple comparisons using Dunn's test post-hoc analysis with Holm adjustments indicated that there was a statistical significant difference in the median concentrations between the hard roe and plasma (p = 0.00655), the kidney and plasma (p = 0.0000297), the kidney and RCB (p = 0.000941), and the liver and plasma (p = 0.00776) (Figure C23).

Nickel (Ni): Kruskal-Wallis test showed that there was statistically significant difference in median Ni concentrations between the different organs in Arctic char: χ^2 (6) = 24.13, p = 0.0004948 [202]. Pairwise multiple comparisons using Dunn's test post-hoc analysis with Holm adjustments indicated that there was a statistical significant difference in the median concentrations between the brain and RBC (p = 0.0476), the kidney and hard roe (p = 0.0476), the kidney and liver (p = 0.0476), and the kidney and RBC (p = 0.00146) (Figure C24).

Chromium (Cr): Kruskal-Wallis test showed that there was statistically significant difference in median Cr concentrations between the different organs in Arctic char: χ^2 (4) = 17.77, p = 0.001369 [202]. Pairwise multiple comparisons using Dunn's test post-hoc analysis with Holm adjustments indicated that there was a statistical significant difference in the median concentrations between the brain and RBC (p = 0.0432), the kidney and plasma (p = 0.0262), and the kidney and RBC (p = 0.00805) (Figure C25).

Manganese (Mn): Kruskal-Wallis test showed that there was statistically significant difference in median Mn concentrations between the different organs in Arctic char: χ^2 (6) = 27.64, p = 0.0001097 [202]. Pairwise multiple comparisons using Dunn's test post-hoc analysis with Holm adjustments indicated that there was a statistical significant difference in the median concentrations between the brain and plasma (p = 0.0314), the gonad and plasma (p = 0.0479), the hard roe and plasma (p = 0.0314), the kidney and plasma (p = 0.00699), the kidney and RBC (p = 0.0174), and the liver and plasma (p = 0.0314) (Figure C26).

Thallium (Tl): Kruskal-Wallis test showed that there was statistically significant difference in median Tl concentrations between the different organs in Arctic char: χ^2 (5) = 22.50, p = 0.0004201 [202]. Pairwise multiple comparisons using Dunn's test post-hoc analysis with Holm adjustments indicated that there was a statistical significant difference in the median concentrations between the kidney and RBC (p = 0.00440), and the liver and RBC (p = 0.000873) (Figure C27).

Cobalt (Co): Kruskal-Wallis test showed that there was statistically significant difference in median Co concentrations between the different organs in Arctic char: $\chi^2\,(6) = 24.57$, $p = 0.0004096$ [202]. Pairwise multiple comparisons using Dunn's test post-hoc analysis with Holm adjustments indicated that there was a statistical significant difference in the median concentrations between the kidney and plasma ($p = 0.0196$), and the kidney and RBC ($p = 0.0000983$) (Figure C28).

4.4.6 Molar ratio Se:Hg in Arctic char

The molar ratio of selenium:mercury (Se:Hg) in various tissues of Arctic char from Lake Disetvatent is listed in Table 15, and was calculated from the measured concentration of Se and Hg in tissues from Table C8.

Table 15: Mean±SD molar ratio of Se:Hg in the various tissues of Arctic char, and n is the number of samples.

Tissue (n)	**Molar Se:Hg**
Brain (6)	250±200
Gonad (6)	1200±1500
Eggs (4)	1600±700
Liver (7)	300±200
Kidney (7)	290±220
RBC (9)	92±12
Plasma (4)	560±650

5 Discussion

5.1 Steroid hormones in plasma of Arctic char

The 4 steroid hormones that were observed in the plasma of Arctic char are a group of androgen steroid hormones (AN, TS, 11-Keto TS, and DHT) that stimulate male characteristics [203]. Even though these hormones are considered "male hormones", females synthesize these hormones as well, and the androgens are involved in the reproductive cycle of both genders. In female teleost fish, androgen hormones such as TS support the growth and development of oocytes [204]. Moreover, androgens are involved in several other biological functions in fish including growth and osmoregulation. Arctic char, both anadromous and landlocked, are spawning in late September and October. Arctic char from this study was caught on the 17^{th} of August, the timing of fieldwork is therefore expected to be prior to spawning for most of the sexually mature fish [11]. Sexual maturity could be confirmed for 4 of the individuals (fish number 3, and 5-7) in which hard roes (eggs) were observed by the ovaries of the fish. Sexual maturation and the reproductive cycle are processes that are associated with an increase in circulating steroid sex hormones i.e androgen and estrogen steroids, and it is therefore expected to see elevated levels of sex steroids in these individuals [11]. As described previously, the plasma levels of these steroid hormones are also constantly changing during the reproductive cycle. Moreover, some individuals might spawn earlier or later compared to the what is the normal average for Arctic char.

In this study, 11-Keto TS was observed in one plasma sample. In teleost fish, 11-Keto TS is considered to be the major androgen hormone and has proven to be more potent than TS [204, 203]. Male fish usually have higher plasma 11-Keto TS levels than females, and the levels are normally seasonally dependent [203]. For example, male Arctic char begins to increase 11-Keto TS plasma levels in early Spring several months before spawning, and studies have shown that the hormone level is peaking up until pre-spawning [11, 203]. 11-Keto TS is converted from TS, and this hormone is responsible for stimulating secondary sexual characteristics (i.e. thicker epidermis, breeding color), spermatogenesis, gonadal growth, and reproductive behavior [205]. A study conducted on Arctic char found that 11-Keto TS plasma concentrations were ranging from approximately 7-15 ng mL^{-1} in males in August, and that the concentration was at the highest in October [205]. A study conducted on coho salmon detected 11-Keto TS blood concentration up to 22 ng mL^{-1} in females [203]. In the present study, 11-Keto TS was only detected in a female char at a concentration of 18.7 ng mL^{-1}. However, only one male fish were caught and this was also the smallest fish that might not have been sexually mature. Additionally, the male fish also had the poorest body condition and might have taken a decision not to spawn due to low energy reserves (Table

B1). A previous study indicated that the condition factor and energy stores can have an impact on whether Arctic char decides to reproduce [205]. This might be the case for the male fish caught in the present study.

Testosterone was observed in 6 out of 7 individuals, and the mean plasma TS concentration was 15.3 ± 13.2 ng mL^{-1}. In female teleost fish, TS plasma levels have shown to be of the same magnitude as TS plasma levels in males, and for some species, TS plasma levels in females can exceed that in males [204, 203]. TS supports male sexual characteristics but is also involved in the metabolism of carbohydrates, fat, and protein, as well as in osmoregulation. Interestingly, TS was not observed in the one male Arctic char in the present study. In a study conducted on fathead minnow, mean plasma TS concentrations have been measured in males and females to be 7.53 ± 2.81 ng mL^{-1} and 9.56 ± 9.16 ng mL^{-1}, respectively [206]. A study conducted on Arctic char found that TS plasma concentration peaked in October for males and females which is the time of spawning, and the levels of TS in males and females ranged from approximately 15-30 ng mL^{-1} and 20-50 ng mL^{-1} in August, respectively. [205]. In both of these studies mean TS plasma concentrations were higher for females. Moreover, these concentrations are in the same order of magnitude as the present study.

AN was observed in all individuals with a mean plasma concentration of 6.43 ± 3.55 ng mL^{-1}. AN is one of the metabolic precursors of testosterone, and the levels of AN in plasma were lower than TS in the present study, in accordance with previous studies [204, 203]. Additionally, an observation that was made is that the male Artic char in the present study had the lowest AN plasma concentration of all the individuals, which further supports that this individual might not have been sexually mature or is spawning this year.

DHT was observed in 4 out of 9 plasma sample, however, two of the plasma samples were from the same individual, and was therefore only observed in three individuals. The mean plasma DHT concentration was 20.0 ± 8.50 ng mL^{-1} and was only observed in female Arctic char. DHT is an androgen steroid hormone that is converted from testosterone, and this steroid hormone is understudied in fish. However, a few studies have suggested that various fish species synthesize this hormone, as gene expressions and enzymatic activity of enzymes that convert TS into DHT have been detected in various tissue of teleost fish [204]. The main role of this hormone in the reproductive cycle of fish is still uncertain. An exposure study conducted on fathead minnow demonstrated that DHT is a potent androgen leading to sexual male characteristics such as dorsal fin spots and nuptial tubercle formation (small, raised, epidermal structures on regions of the head, body, or fin rays). Moreover, DHT caused females to induce male physiological characteristics [207]. A later study by Margiotta-Casaluci *et al.* (2013) measured DHT in plasma of fathead minnow with mean plasma concentrations of 0.59 ± 0.17 ng mL^{-1} and 0.42 ± 0.17 ng mL^{-1} in male and female,

respectively. The levels observed in the present study are therefore about two orders of magnitude greater compared to the levels in that study, however, nothing that this study was conducted on a different species, and levels might vary considerably between species. Additionally, hormone concentrations also vary greatly with the time of sampling. Borg (1994) also suggested that DHT might be an important androgen in some teleost species, however, still to this date, few studies have looked into this hormone as a potential important androgen in fish [203]. However, in mammals, DHT is one of the major androgens.

None of the estrogen steroid hormones were detected. Androgens are precursors of estrogenic steroids, for instance, TS is a metabolic precursor of E2. Similar to the androgens, previous studies on Arctic char have reported that E2 plasma concentrations begin to increase in female Arctic char during early spring to prepare for reproduction and that the E2 plasma concentration peak in August/September before spawning [11, 205]. An increase in E2 in plasma will lead to the growth of the oocytes and induce the production of Vitellogenin that will be incorporated into the oocytes. Moreover, a study has reported that E2 declined 1 month earlier than TS plasma concentration in females and that the E2 plasma concentrations in female Arctic char were approximately ranging from 12-20 ng mL^{-1} in August [205]. The earlier decline of plasma E2 compared to TS and potentially low concentrations of this steroid hormone could explain why this estrogen was not observed in the present study. Additionally, the method could affect the observation as well, some steroid hormones have been reported to have poor ionization due to carbonyl- and hydroxyl-groups that have low proton affinity [173, 176].

Due to the limited number of Arctic char samples in the present study, and the great variation in the individual samples it is difficult to determine if the steroid levels presented in this study reflect the levels of sexually mature Arctic char. Steroid hormone levels are dynamic and show natural fluctuations within a day, month, and year, as well as with the life stage. Additionally, different species will exhibit different levels of steroid hormones during the reproductive stage. Moreover, comparison within the same species might be difficult as there could be variation between different Arctic char populations at different locations. For example, Arctic char from mainland Norway usually migrate and reproduce about one month earlier than populations at Svalbard. This is mainly due to the difference in ice conditions [11]. Therefore it is expected that their timing of peak steroid hormone plasma concentrations will vary as well.

The stress hormone cortisol (COR) was not detected in the present study, however, this hormone will be discussed briefly as it was initially a part of the project to look at COR and contaminants in the blood of Arctic char. Unfortunately, the method was not optimal for COR to be detected. First of all, both the absolute and relative recoveries were far above

120%, and the compound had strong negative matrix effects -98% (Figure C1 and C3). This indicates that co-extracted matrix compounds were interfering with the ionization of this compound, causing strong suppression of the signal. Moreover, several of the lowest calibration curve concentration had to be excluded from the calibration curve as no peak could be distinguished from the noise. This resulted in high LOD and LOQ estimations, a calibration curve with only three points, and a linear range of 5-20 ppb for this compound. There was also a problem with the highest calibration curve concentration; 50 ppb, the signal was lower and had more background noise compared to 20 ppb. LOD and LOQ were estimated from the calibration curve method; 3.67 and 11.1 ppb, respectively (Table C4). This method for estimation of LOD and LOQ depends on the number of concentration points in the calibration curve, the concentration range used, the number of measurements, and the variability in the data points in the calibration curve [181]. With 3 calibration points and a narrow concentration range, this method for LOD/LOQ estimation may not be suitable. There is no standard procedure on how LOD and LOQ estimations should be conducted in research. This method was mainly chosen because it provided robust LOD and LOQ estimation. Most studies use the S/N ratio or the standard deviation of the blanks to estimate LOD and LOQ as it often provides lower values. However, different practices for LOD/LOQ estimations make comparison challenging, especially in method validation studies as different estimations will inevitably provide different LOD/LOQ values. Therefore, estimations based on S/N peak height were also conducted to see how much variation there is between the different estimation methods, the results are summarized in Table C4. For COR, estimations of LOD and LOQ based on S/N peak heights provided values 3- and 4-orders of magnitude lower compared to estimations from the calibration curve method. However, the LOQ value provided by the S/N peak heights is outside the linear range which is not optimal. It is therefore clear that the method was not optimal for COR.

Another explanation that COR was not observed in the plasma is that the levels were not high enough. Several studies and critical reviews indicate that basal plasma COR levels in wild teleost fish are less than 40 ng mL^{-1} [137, 157]. However, some studies report that levels might be lower than 10 ng mL^{-1}, and even in the range 0-5 ng mL^{-1} [157]. A study conducted on anadromous Arctic char from mainland Norway, that were divided into social ranks, demonstrated that the dominant Arctic char had a lower basal COR level of approximately 10 ng mL^{-1}, whereas intermediate and subordinate Arctic char had approximate basal COR levels in the range of 20-35 ng mL^{-1} [208]. The LOD estimation in the present study was 3.67 ppb which corresponds to approximately a concentration of 18 ng mL^{-1} in the plasma. This LOD value is quite high which means that the method might not be sensitive enough to detect low levels of COR. Moreover, the blood samples were taken

immediately and conducted within 5-10 minutes after Arctic char was caught. Therefore, the COR level might not have had the time to increase by the time the blood sampling was conducted. It might vary how fast the COR levels rise after exposure to acute stress between species, ranging from a few minutes to hours [137]. However, a review by Pankhurst (2011) indicates that most teleost fish have a measurable increase in plasma COR within 10 minutes [137]. The study on Arctic char from mainland Norway was exposed to stress in the form of dip-netting and transferred to a small holding tank, and showed an increase in COR plasma levels after 30 minutes. However, how fast the COR levels increased was different for dominant and subordinate char. After exposure to stress, the COR levels increased significantly for dominant char to approximately 40 ng mL^{-1}. The study demonstrates that basal plasma COR levels and the amount of COR increase after exposure to stress vary within a species and that it might be influenced by social rank. Bigger and dominant fish might be less stressed compared to smaller fish [208]. Moreover, COR levels have been shown to vary considerably within a day and can depend on life stage, time since feeding, gender, and maturity. Some studies have shown that an increase in COR levels coincides with smoltification and reproduction [156, 138]. The timing of blood sampling is therefore important, and only reflects the levels at a specific time, and it may not necessarily reflect their basal COR levels as many factors can influence the COR levels. The sampling was conducted in August which is a pre-spawning period for Arctic char, and it might be that their COR levels are increased during this reproductive state and would not have reflected their basal COR levels. Additionally, stress exposure studies conducted on teleost fish have been conducted on captive fish, and wild fish may experience stress differently from captive fish [157, 155]. Captive fish exposed to confinement experiments are exposed to unnatural stress, whereas natural stressors such as food limitation, contamination, and increased water temperatures are more modest and might increase COR levels over time.

The internal QA and QC in sample analysis for steroid hormones included laboratory procedural blanks and spiked matrix samples. The recoveries of TA were controlled with the use of isotope-labeled IS that was introduced into samples before extraction. The choice of IS for steroid hormone TA was based on similarity in retention time. The IS ^{13}C3-CORNE with a retention time of 2.83 minutes was excluded due to inconsistent signals. The two other IS that were applied, ^{13}C3-DHT and ^{13}C3-17α-OHP, have retention times of 1.68 minutes and 2.37 minutes, respectively. Steroid hormone TA had retention times in the range of 1.69 minutes (DHT) to 3.29 minutes (COR). The use of IS is usually recommended to reduce the matrix effect, however, there might be a slight downside of using IS if a limited amount of IS is used for multi-compound analysis [163]. This is mainly attributed to the fact that a few IS are not enough to cover the whole range of retention times for TA with a wide range

of retention times. Therefore the IS used will not be optimal for all TA. Moreover, if the IS produces inconsistent signals, this might lead to uncertainty in the quantification of the analyte concentrations.

Recoveries are considered as acceptable in the range of 70-120% [177, 189]. Overall, acceptable relative recoveries were obtained for 5 out of 18 steroids; 17α-OHP, P4, DHT, AN, and DHEA (Figure C1). Matrix effects indicated strong matrix suppression during ionization for most steroid TA except for AN and P4 which had weak negative matrix effects of -19% and -2.0%, respectively (Figure C2). DHT had a positive matrix effect of 22%, indicating a slight matrix enhancement of the signals of this steroid hormone. COR, CORNE, COS, 11-deoxyCOR, 17α-OHP, DOC, 11-KetoTS, TS, and 17 OH-P5 had strong negative matrix effects; -98%, -93%, -100%, -91%, -57%, -37%, -92%, -65%, and -68%, respectively. This indicates that co-extracted matrix components are strongly interfering with the ionization of these compounds at the ESI interface, causing an underestimation of the signal response. A previous study has indicated that matrix effects of less than $\pm$ 30% are considered acceptable without leading to considerable inaccurate results [209]. Two of the compounds that were observed, 11-KetoTS and TS, had high recoveries ($>$ 120%). Therefore, the quantification of these compounds might be biased and uncertain due to high recoveries and a strong matrix effect. Additionally, 11-Keto TS was only observed in one plasma sample. The quantified concentrations of these compounds should therefore be taken into consideration before being applied in any way. DHT and AN on the other hand had acceptable recoveries and weak matrix effects of 22% and -19%, respectively. This indicated that the signal response of DHT was slightly overestimated and that the signal response of AN was slightly underestimated. Moreover, when analyzing biological samples, matrix effects are unavoidable and can therefore not be eliminated without considerable loss of the analyte. Similarly to the discussion with COR, the LOD and LOQ estimations of the TA with the calibration curve method provided high LOD/LOQ values for the observed steroid hormones. For example, DHT and 11-KetoTS had LOQ values that were in the upper part of the linear range, almost outside of the linear range (Table C4). Moreover, these two compounds had 4 points in the calibration curve, and therefore the estimation of LOD/LOD with the calibration curve method is not optimal. AN and TS also had high LOD/LOQ values that were estimated from the calibration curve, and these compounds had 7- and 6-point calibration curves, respectively. For all of the observed steroid hormones, LOD/LOQ estimations from the S/N peak height provided lower LOD/LOQ values.

5.2 PFAS in plasma of Arctic char

Mean total PFAS concentration in plasma of Arctic char from Lake Diesetvatent was 26.8±5.98 ng mL^{-1}, and the 9 PFAS compounds that were observed in the plasma were dominated by carbon chain lengths of C8 to C13. Accumulation of longer chain PFAS compounds (6 C $\geq$ for PFSA and 8 C $\geq$ for PFCA) is in accordance with previous studies where increased accumulation has been observed with increasing alkyl chain length [37, 36]. FOSAA, MeFOSAA, and DiSAMPAP were also observed in the plasma, however, due to recoveries <40% and low observation rate these compounds have been excluded due to considerable uncertainty (Table C3). In total 5 of the 9 observed PFAS compounds were PFCAs (carboxylate compounds), and both odd- and even numbers of carbons were detected and included; PFNA (C9), PFDA (C10), PFUnA (C11), PFDoDA (C12), and PFTriDa (C13). In total 3 PFSAs (sulfonate compounds) were detected and included only C8 chain length; PFOS (C8), PFECHS (C8), and PFOSA (C8). Additionally, one fluorotelomer sulfonate compound was observed, namely 6:2 FTS (C8). Four of the PFAS compounds were observed in all individual plasma samples with a mean percentage composition of total PFAS burden: 6:2 FTS (38%), PFUnA (20%), PFOS (20%), and PFNA (8%). The other 5 PFAS compounds were only detected in 1-3 individual samples, and their percentage composition constituted: PFOSA (17%, n=1), PFDA (16%, n=1), PFDoDA (12%, n=2), PFTriDa (11%, n=3), and PFECHS (14%, n=3). Taking only PFAS compounds that were observed in all plasma samples into account, sulfonate and carboxylate compounds accounted for 58% and 28% of the total PFAS burden, respectively. This is in agreement with previous exposure and wildlife studies indicating that PFSA of the same chain length as PFCA have greater accumulative properties. PFOS is more frequently detected than PFOA of the same carbon chain length, which could be confirmed by the present study [37, 36, 6].

Other studies conducted on wild Arctic char from Arctic regions have mainly looked at PFAS in edible muscle, whole body homogenates, or liver (Table A.1). It is worth noting that the concentration in these studies is given as ng g^{-1} wet weight (ww), whereas the present study has measured the concentration of PFAS in ng mL^{-1} plasma ww. Blood plasma has a density close to 1 (approximately 1.025 g mL^{-1}), hence, the concentration in plasma in this study is comparable with other studies without correction for density. One study conducted in the Canadian Arctic by Lescord *et al.* (2015) studied PFAS levels in muscle of Arctic char from six different Lakes [46]. Two of the Lakes; Lake Meretta and Lake Resolute are located downstream of an airport contaminated with PFAS, and Arctic char from these lakes had a total PFAS concentration about two orders of magnitude higher than the other Lakes that receive PFAS from atmospheric deposition. Lake Resolute had mean PFAS concentrations of 122±65 ng g^{-1} ww compared to Lake 9 Mile, Lake North, Lake

Small, and Lake Char which had mean concentrations of 0.28±0.09 ng g^{-1}, 0.32±0.12 ng g^{-1}, 0.36±0.15 ng g^{-1}, and 3.7±2.4 ng g^{-1}, respectively [46]. Moreover, PFOS dominated in Arctic char from contaminated Lakes. For the other Lakes, PFNA was the most dominating sulfonate compound. In juvenile Arctic char, PFOA constituted the biggest fraction in contaminated lakes, while PFNA and total FTS made up the biggest fraction in the non-contaminated Lakes. In this study, they also detected PFECHS in juvenile Arctic char from non-contaminated Lakes, and 6:2 FTS was detected in juvenile char from one of the contaminated lakes. Moreover, PFSA dominated in contaminated Lakes whereas PFCA dominated in non-contaminated Lakes. The study indicates that the difference in PFAS composition is caused by different sources and that the location and the vicinity to point pollution sources are important factors affecting the levels in char. Similarly, Veillette *et al.* (2012) found that PFNA, PFUnA, PFDA, and PFOS dominated in muscle and whole body homogenates of Arctic char from two Lakes, Lake A and Lake C2, in the Candian Arctic [65]. Total PFAS levels were 0.203 ng g^{-1} in Lake A and 0.481 ng g^{-1} in Lake C2. These two lakes are open Lake systems where anadromous Arctic char residents as well. Ahrens *et al.* (2016) observed a similar mean concentration of total PFAS 0.53±0.073 ng g^{-1} ww in the muscle of Arctic char from Linnevatnet at Svalbard, and the major detected PFAS compounds were PFOS, PFUnA, and PFDA [66].

Bossi *et al.* (2014) studied PFAS in the liver of landlocked Arctic char from the Faroe Islands and southwest Greenland [40]. In this study, they found that Arctic char from Lake á Myranar had the highest concentrations of PFTeA and PFTrA, while Arctic char from Greenland had the highest concentration of PFTrA followed by PFUnA, and PFTeA. The mean total PFAS concentration in Arctic char from Faroe Island was 5.67±1.6 ng g^{-1} w.w and 5.27±2.8 ng g^{-1} w.w in Arctic char from Greenland [40]. This study indicated that the concentration fraction of PFAS in the liver to muscle tissue is a factor of about 10 or more. This might be a result of higher protein content in the liver compared to muscle. They also found higher concentrations of odd-number carbon homologs that might be a result of the source from atmospheric input of volatile long-chain FTOH, which have been reported to produce even- and odd-chain-length PFCA when degraded [49]. LRAT is the only pathway for terrestrial and closed Lake systems to receive PFAS contamination. This study also highlighted that ecosystem parameters such as fish age and trophic level must be taken into account together with geographical location and deposition pattern that can modify the input of PFAS compounds. A study conducted by Stock *et al.* (2007) supported the hypothesis that volatile FTOH are transported to the Arctic by the atmosphere and degraded to PFSA and PFCA compounds [210].

To the best of my knowledge, PFAS has not been analyzed in the blood or plasma of

Arctic char previously. However, a few studies have been conducted on other wild fish species. One study conducted by Labadie *et al.* (2011) studied tissue distribution of PFAS in the freshwater fish species European chub and reported the highest total PFAS concentration in plasma, followed by liver > gonad > muscle [211]. In this study they found that PFOS accounted for the greatest proportion of all PFAS analyzed (approx. 70%), followed by PFDoA, PFDA, and PFUnA. PFSA bioaccumulated to a greater extent than PFCA of equivalent perfluoroalkyl chain length, as observed previously [37]. These results are in agreement with an exposure study performed on rainbow trout by Martin *et al.* (2009) who also found the highest total PFAS concentration in blood followed by kidney > liver [37]. Taniyasu *et al.* (2003) also reported higher PFOS concentration in blood compared to the liver for several of the fish species that were studied, however, the concentration of PFOS varied more than two orders of magnitude, and depended on the species and location [212]. Moreover, some of the fish species were piscivorous and might not reflect the same trophic level as Arctic char. Hung *et al.* (2018) also found the highest mean concentration of total PFAS in blood, followed by liver, egg, and muscle [213]. Furthermore, PFOS contributed the greatest to the total PFAS composition, and PFDA and PFUnA were also detected. This study investigated 10 different fish species and found considerable species differences in accumulation levels and PFAS composition [213].

When comparing results across studies conducted on different species one must be careful not to draw any conclusions as there might be considerable species differences in toxicokinetics i.e. absorption versus elimination, metabolic capacities, diet, and location. Moreover, differences in the uptake route i.e. diet or bioconcentration, highly depend on the location and food availability and have shown to affect the tissue distribution [37, 36]. However, PFAS compounds have a high affinity for proteins and are therefore expected to accumulate in tissues with higher protein content. PFAS compounds have shown to exhibit a high binding affinity for albumin, an abundant protein in the blood, and liver fatty acid binding proteins in humans [69]. The elevated levels observed in the plasma of Arctic char in the present study compared to previous studies on Arctic char where PFAS has been analyzed in muscle, whole body, or liver might be explained by the reason that the protein content is higher in matrices such as blood and liver compared to muscle tissue. Labadie *et al.* (2011) analyzed the protein content in the various matrices and found the highest protein content in plasma [211]. In this study they reported that normalizing the PFAS concentration for protein content reduced the PFAS level differences between organs, however, the highest PFAS level was still observed in plasma after protein correction. Moreover, correcting for protein content has been suggested by several studies indicating that it improves comparison across studies when determining the distribution of PFAS in different matrices [214, 211].

Protein correction has not been conducted in the present study, and therefore comparing PFAS levels across studies is challenging. Moreover, other studies conducted on Arctic char mentioned here have not corrected for protein content to the best of my knowledge, and therefore it seems to be different practices among researchers [46, 40]. Similarly, legacy organohalogenated compounds have often been corrected for lipid content due to their affinity for fatty tissues. It is therefore preferred to correct PFAS concentration for the protein content in samples to account for differences in protein content. Additionally, in the study by Labadie *et al.* (2011), they also suggested that it is more appropriate to normalize PFAS concentrations to specific proteins such as fatty acid binding proteins or plasma albumin as these proteins have proven to be important in binding PFAS compounds [211].

In the present study 6:2 FTS, PFOS, PFUnA, and PFNA were the most frequently detected PFAS compounds, and from the studies mentioned above PFOS, PFUnA, and PFNA are compounds that have been detected frequently in Arctic char [46, 40, 66, 65]. In the present study, 6:2 FTS accounted for 38% of the total PFAS burden in plasma of Arctic char, this is in contrast with previous studies where PFOS seems to be the greatest contributor to total PFAS concentration. However, this observation might be biased as PFOS is the PFAS compound that is the most studied. Moreover, there are also some methodological differences between the number of PFAS and which PFAS compounds have been analyzed which hamper the comparison between studies. For example, in the present study plasma samples were analyzed for 43 different PFAS compounds, whereas the study by Lescord *et al.* (2015) analyzed 19 PFAS compounds, and the study by Bossi *et al.* (2014) analyzed 17 PFAS compounds [46, 40]. Even though PFOS almost is a part of the PFAS analyses, analyzing for varying PFAS compounds might affect the PFAS composition and the total PFAS concentration detected. Additionally, different methodologies have been employed for PFAS determination. Amongst different methodologies, are different practices when it comes to extraction and clean-up methods, and analytical techniques. Differences in PFAS composition in Arctic char from different locations might be caused by differences in sources i.e. different air currents might result in LRAT from different sources in Svalbard and Canada as an example. Another important factor that affects the difference in both PFAS levels and PFAS composition is that previous studies in Arctic char have analyzed PFAS in other biological matrices such as muscle, whole body, and liver. It is expected that the affinity and distribution of PFAS compounds are different between various matrices due to protein content. Furthermore, none of the newer PFAS substitutes such as Deca S, PFBA, PFBS, and GenX were detected in the present study. Exposure studies on various teleost fish have shown that the newer PFAS compounds are less bioaccumulative and eliminated faster compared to the legacy PFAS compounds [73, 74].

The levels of total PFAS in the plasma of Arctic char observed in the present study were low. Additionally, the PFAS concentrations were below LOD when the estimation of LOD with the calibration curve method was used. However, concentrations were above LOD if estimated with S/N peak heights (Table C4). The methodological aspects will be discussed later on. Nonetheless, narrow and well-separated peaks were observed which means that Arctic char from Lake Diesetvatnet are exposed to chemicals that are synthesized by humans and not naturally found in the environment. Lake Diesetvatnet is located 35 km North of Ny-Ålesund settlement and this Lake is considered to be remote and not impacted by any human activity. Due to the remote location of Disetvatnet, the Lake is expected to receive input of PFAS contamination mainly from LRAT as there are no point-pollution sources in the vicinity. With the increased rate of global warming, secondary emission from glacial meltwater might contribute to the input of PFAS, as Lake Disetvatnet is connected to several glaciers [54, 53]. These two sources of input are regarded as the main input of PFAS, additionally, other minor sources might contribute to PFAS contamination. In Lake Disetvatnet, both resident and anadromous Arctic char coexist, and anadromous char migrate to the sea in the summer to feed. Some reports state that Arctic char do not migrate any longer than 30 km from the Lake, however, migrating Arctic char might be exposed to different sources of PFAS in the marine environment [128]. It is difficult to predict in which direction or how far the char will migrate, however, if they manage to migrate about 30 km they could reach close to Ny-Ålesund. Therefore, migrating Arctic char could act as a vector for contamination to Lake Diesetvatnet [215]. In Ny-Ålesund PFAS has been measured in the air at the Zeppelin station and there are a few point sources at the settlement that have been identified to contribute to PFAS contamination [28, 6]. Both the FFTS in which fire fighting foams are used as fire extinguishers and the wastewater plant has been identified as PFAS contamination sources in Ny-Ålesund. Moreover, Lake Diesetvatnet is a popular place for people that like to fish in their leisure time. People could potentially bring contamination from the clothes and the equipment they are using. PFAS compounds are used in a wide range of products due to their water- and oil-resistant properties i.e. gore-tex clothing and shoes which are often used by people doing outdoor activities [6]. Additionally, humans could act as a vector for contaminants from one place to another, for example walking with shoes on the contaminated ground could potentially bring the contaminants to Lake Diesetvatnet. Furthermore, during fieldwork seabirds were observed flying over Lake Diesetvatnet to find food, and they were especially interested when we caught the fish. This might be expected as Lake Diesetvatent is only located 3-4 km away from the Ocean. Previous studies on the highly contaminated Lake Ellasjøen at Bjørnøya have identified seabirds as a source of contamination [12]. In this Lake, seabird colonies are nesting and breeding during the

spring and will therefore leave behind nutrients and contamination from the guano and other excretory materials. Both Hg and PCB levels are elevated in Lake Ellasjøen due to high seabird activities, and high levels of these contaminants have been found in Arctic char from this Lake. Unlike Ellasjøen, no known seabird colonies are located close to Lake Diesetvatnet. However, if seabirds are flying over Lake Disetvatnet now and then they might contribute with minor input of both nutrients and contamination. All of these mentioned potential sources of PFAS contamination are only minor sources, however, it is uncertain how much they contribute to the total contamination load in Lake Disetvatnet. Moreover, Lakes are closed aquatic ecosystems that have minimal movement and replacement of water compared to marine ecosystems. Contaminants might accumulate easier in these ecosystems and might become a deposit of a mixture of contaminants.

PFAS compounds were quantified based on the IS method with three different isotopically labeled IS; PFOA $^{13}C_8$, PFOS $^{13}C_8$, and 6:2 FTS $^{13}C_2$ (Table B6) with retention times of approximately 1.46, 1.60, and 1.45 minutes, respectively. The PFAS TA had retention times ranging from 0.89 minutes (PFBA) to 3.68 minutes (diSAMPAP). PFOS $^{13}C_8$ was used as IS for most of the PFAS TA except for PFOA and 6:2 FTS in which the respective PFOA $^{13}C_8$ and 6:2 FTS $^{13}C_2$ IS were used. Most (35 out of 43) of the PFAS TA had acceptable relative recoveries within the range of 70-120% (Figure C3) [177, 189], the method, therefore, proved to be suitable. A few PFAS compounds; FOSAA, MeFOSAA, and diSAMPAP had relative recoveries of 1.4%, 11%, and 11%. Even though these PFAS compounds were observed in a few plasma samples, they were excluded from the concentration of the total sum of PFAS (Table C2) and from the percentage PFAS composition in plasma (Figure 13) due to the high uncertainty of recoveries $< 40\%$. Percentage matrix effects for PFAS TA were either slightly positive or negative. The majority of PFAS compounds that were observed in plasma had matrix effects $< \pm 20\%$, except for PFDA which had a negative matrix effect of -39% indicating that this compound was suppressed during ionization which might have led to underestimation when the compound was quantified. A previous study indicated that matrix effects below $\pm 30\%$ are acceptable without resulting in considerable errors in the quantification [209].

QA and QC steps have been employed during the analytical procedure to avoid contamination, analyte loss, and erroneous quantification. Concentrations were corrected for recovery and matrix effect by quantification based on the IS method, and background contamination has been corrected by subtracting the method blank [163]. Polypropylene tubes and equipment are recommended to use for PFAS determination and were therefore used during the extraction as some PFAS compounds have proven to adsorb irreversibly to glass materials [216]. Moreover, samples were stored at -20°C until sample preparation and anal-

ysis to avoid any degradation or loss of analytes as some precursor PFAS compounds can degrade into the more stable PFAS compounds PFOS and PFOA if stored inappropriately. Moreover, a suitable method for extraction and analysis of PFAS was selected. The hybrid SPE technique has proven to reduce matrix effects in plasma matrix compared to protein precipitation and SPE methods [217]. Hybrid SPE is effective in removing phospholipids which often can interfere with the ionization of analytes [163, 164, 165, 162].

LOD and LOQ were estimated from the calibration curve method. This method uses the standard deviation of the y-intercept of the regression line from the calibration curve divided by the slope of the regression line which is subsequently multiplied by 3.3 or 10 for LOD and LOQ, respectively [180, 182, 179]. Some limitations with this LOD/LOQ estimation method are that it depends on the number of concentration points in the calibration curve, the concentration range, the number of measurements, and the variability of the data points in the calibration curve [181]. In the present study, all PFAS compounds were below LOD when this method was used for the estimation of LOD. However, most studies use the S/N peak height or standard deviation of the blanks to estimate LOD/LOQ, therefore LOD and LOQ were also estimated based on S/N peak heights to compare the values the two different methods provide. Estimations of LOD/LOQ provided considerably lower values (about 1 to 5 orders of magnitude) when S/N peak heights were used (Table C4). All observed PFAS compounds in the present study would have been above LOD if the S/N peak height were used to estimate LOD/LOQ. Moreover, in the present study, the number of calibration points for observed PFAS compounds were ranging from 8 to 10, and the linear concentration range was from 0-0.2 ppb in the lower range and 50 ppb in the upper range (Table C4). Therefore, the number of calibration points and the concentration range should not limit the calibration curve method for the estimation of LOD/LOQ to a great extent. Nonetheless, the calibration curve method provides higher estimations for LOD/LOQ, which might explain why the PFAS compounds were below LOD. Therefore, this method might not be the most suitable method for the estimation of LOD and LOQ. However, these methods are estimates that are used to predict the sensitivity of the analytical method, and there are no standard practices that are used among researchers. Therefore comparison across studies is challenging when different LOD/LOQ estimation methods are used. It is also challenging to determine which method provides the most accurate and true values for LOD/LOQ. These values should therefore not be blindly trusted and preferably evaluated together with other parameters. An issue with the S/N peak height estimation is that it provided LOQ values that were below the linear range for several of the PFAS compounds (PFOSA, PFDA, MeFOSAA, PFDoDA, PFTriDA, DiSAMPAP, and PFECHS), which is not optimal. LOQ should be the lowest concentration in the linear range or within the linear range. On the contrary, the calibration

curve method produced LOQ values that were considerably high. This might indicate that none of these estimates is a good fit. Nevertheless, the observed PFAS compounds in the plasma of Arctic char had symmetrical, narrow, and well-separated peaks, which indicates that Arctic char in Lake Diesetvatnet are exposed to PFAS compounds.

However, there are some limitations with the methodology used in this study as well as challenges with analyzing PFAS compounds. Equipment used in the laboratory may introduce PFAS contamination as they are ubiquitous, and controlling the source of contamination can be challenging [218]. Furthermore, the use of isotopically labeled IS has been recommended to reduce matrix effects. Matrix effects are a problem that is evident and possibly inevitable in biological samples, however, strong matrix effects can hamper the quantification considerably. In the present study, only three isotopically labeled IS were available for the analysis of 43 different PFAS compounds. The effect of IS might be biased when using a small number of IS for a large number of compounds. The IS might not be a suitable match for all PFAS compounds due to a wide range of retention times. It is preferable to use IS that is close in retention time to the compounds that are analyzed [161]. The retention times of IS did not cover the whole range of retention times for PFAS compounds. Therefore, quantification of PFAS TA with considerably lower or higher retention times than the IS might lead to inaccurate quantification compared to the PFAS compounds with a more similar retention time to the IS. Moreover, IS are expensive and it is not always feasible to have an IS for each PFAS compound, and not all PFAS compounds on the market have an available IS [216]. Besides, exogenous matrix effects i.e. compounds that are not a part of the sample matrix, can contribute to the matrix effect when analyzing plasma samples. For instance, polymers contained in different brands of plastic tubes and the anticoagulant lithium heparin have proven to produce matrix effects when analyzing PFAS in blood or plasma as heparin is often used to wash the syringe before blood sampling to avoid the blood from coagulating. Lithium heparin was also used in the present study to wash the syringe and tube prior to blood sampling of Arctic char [219].

5.3 Method test for extraction of steroid hormones and PFAS in liver samples

The purpose of the method test for extraction of steroid hormones and PFAS was to find the most suitable extraction technique to apply on more complex matrices as there are no standardized extraction techniques for steroid hormones and PFAS in biological tissues such as the liver. The purpose of sample preparation is to maximize the extraction efficiency of TA from a sample matrix and minimize matrix effects. In the following subsections, the

different protocols will be discussed based on performance. The emphasis will be directed to the extraction efficiency and matrix effects, as well as the time efficiency of the extraction and clean-up techniques. The analytical techniques used will be discussed briefly.

Several authors have described that a recovery ranging from 70-120% is considered acceptable [177]. The same recovery requirement is recommended for the analysis of pesticide residues in food by the Swedish National Food Administration [189]. Therefore this requirement will be used when evaluating the recoveries obtained in this study. Moreover, environmental and biological samples are complex matrices that contain trace amounts of the target analyte(s) of interest, therefore matrix effect might cause inaccurate results if they are strong. Matrix effects will not be considered significant if ionization is enhanced or suppressed by less than ±30% as this was suggested by a previous study [209]. This will be the basis when the results in the present study are evaluated based on extraction method performance.

5.3.1 Steroid hormones

The IS $^{13}C_3$-CORNE had to be excluded due to inconsistent signals. Therefore IS $^{13}C_3$-DHT and $^{13}C_3$-17α-OHP were applied to the steroid target analytes, with retention times of approximately 1.68 minutes and 2.28 minutes, respectively. The 18 steroid hormone TA had retention times ranging from 1.69 minutes (DHT) to 3.29 minutes (COR), and the choice of IS was based on similarity in retention times. For the Hybrid SPE extraction and clean-up with 0.1% AF in MeOH, 7 out of 18 steroids including 17α-OHP, DOC, P4, DHT, TS, AN, DHEA were within the acceptable range for relative recoveries, while only 11-deoxyCOR had an absolute recovery within this range (Figure C5). The same extraction and clean-up protocol with 0.5% CA in ACN had in total 9 steroids within the acceptable range for relative recoveries including; COR, CORNE, ALDO, 17α-OHP, 11-KetoTS, DHT, AN, DHEA, and 17 OH-P5 (Figure C6), and 8 steroids were within this range for absolute recoveries (COR, CORNE, ALDO, 17α-OHP, P4, 11-KetoTS, DHT, and TS). For the SPE extraction and clean-up protocol, 3 steroids were within 70-120% recovery range for relative recoveries; 11-deoxyCOR, 17α-OHP, and DOC, while 5 steroids (P4, DHT, TS, AN, and DHEA) were within the range for absolute recoveries (Figure C7). For the SLE extraction protocol, 6 steroids were within the acceptable range for relative recoveries including ALDO, COS, 17α-OHP, DOC, P4, and 11-KetoTS, while 8 steroids were within the acceptable range for absolute recoveries (COR, CORNE, ALDO, 11-deoxyCOR, 17α-OHP, 11-KetoTS, TS, 17 OH-P5 (Figure C8). For all of the extraction techniques, strong negative matrix effects ($>$ -30%) were evident for most compounds (Figure C9, C10, C11, and C12). This indicates that there was a strong negative suppression of the signal response due to the presence of co-

extracted matrix components. In general, recoveries were improved when using IS compared to external standards, but the results might be biased as only two IS were available. The two IS did not cover the whole range of retention times for the steroid hormone TA, especially for the TA with the highest retention times such as COR. In summary, the best relative recoveries were obtained for Hybrid SPE extraction and clean-up with 0.5% CA in ACN concerning the number of steroid hormones with acceptable recoveries. However, it is worth noting that the signals for this method were low which might be caused by suppression of the signal due to the presence of citric acid. Moreover, this extraction method also provided strong matrix effects. The overall performance of all extraction methods based on extraction efficiency and matrix effects was not optimal for steroid hormones in liver samples. The sample preparation step, therefore, needs further improvements.

The use of UPSFC-MS/MS for analysis of steroid hormones has increased recently [173]. Previously more traditional techniques such as immunoassays have been used for the quantification of steroid hormones. The advantage of immunoassays is that they are simple, quick, and cost-effective, as well as sensitive and specific analytical techniques. However, the disadvantage of immunoassays is the cross-reactivity of the antibodies used in the assays that can react to several endogenous steroid hormones [155]. Additionally, the application is limited to analyzing one hormone at a time, and the technique is prone to matrix effects i.e. the presence of lipids can interfere with the estimation of steroid hormone levels. Gas chromatography with mass spectrometric (GC-MS) detection has been a commonly used analytical technique for the determination of steroid hormones. The advantage of chromatographic methods is that they offer simultaneous determination of several steroid compounds. However, analyzing steroid hormones with GC-MS requires time-consuming sample preparation steps. Derivatization of steroid hormones is necessary due to the active hydrogen in hydroxyl- and phenolic groups, and to increase the volatility of steroid hormones [176]. On the other hand, GC-MS is environmentally friendly as only inert carrier gas such as nitrogen and helium are used. During the last decades, LC-MS has become more popular as derivatization steps are not needed prior to analysis. However, GC-MS provides increased resolution compared to LC-MS [161]. In addition, LC-MS is not able to separate all isomeric endogenous steroid hormones. The recently increased use of UPSFC-MS/MS provides a combination of LC and GC properties, with efficient separation, high resolution, and reduction in analytical time, due to supercritical fluids properties. Several authors have recently highlighted the use of UPSFC-MS/MS in steroid profiling due to the increased sensitivity and chromatographic efficiency compared to UPLC-MS/MS [173, 174, 175]. Moreover, UPSFC-MS/MS has proven to improve the separation of isomers and enantiomers. This is an important feature of UPSFC-MS/MS because steroid hormones are similar in structure

as they share the same basic four-ring structure, and the only distinct differences in their chemical structure are functional groups and their location, and double bonds on the ring structure [149].

5.3.2 PFAS

The IS PFOS $^{13}C_8$ had inconsistent and missing signals and was therefore not applied. IS PFOA $^{13}C_8$ was applied for all PFAS TA except for 6:2 FTS in which the respective IS 6:2 FTS $^{13}C_2$ was applied. For the Hybrid SPE extraction and clean-up with 0.1% AF in MeOH, 18 out of 43 PFAS TA had relative recoveries in the acceptable range 70-120%, whereas 21 PFAS TA had absolute recoveries within that range (Figure C13). For the same extraction method with the solvent 0.5% CA in ACN, both absolute and relative recoveries of the majority of PFAS TA were below 70% except for PFHpS and PFTDA which had relative and absolute recoveries within the acceptable range (Figure C14). A similar trend was observed for the SPE extraction and clean-up technique that had 5 PFAS TA (6:2 FTS, PFUnA, PFDoDA, 10:2 FTS, and PFDS) with both absolute and relative recoveries in the acceptable range (Figure C15). For the SLE method, 4 and 5 PFAS TA had relative and absolute recoveries in the acceptable range, respectively (Figure C16). Another observation is that absolute recoveries were higher than relative recoveries in general for all the extraction methods, this is the opposite trend of steroid hormones. However, only two isotopically labeled IS were available; PFOA $^{13}C_8$ and 6:2 FTS $^{13}C_2$, which had similar retention times, 1.44 minutes and 1.43 minutes, respectively. The use of IS, therefore, provided a limitation in that the retention times of PFAS TA were not covered. Percentage matrix effects were strong negative for most PFAS TA ($>$ -30%) on all extraction and clean-up techniques, with the exception of Hybrid SPE with 0.5% CA in ACN which provided strong positive matrix effects (Figure C17, C18, C19, and C20). In summary, the best relative recoveries were obtained for Hybrid SPE extraction and clean-up with 0.1% AF in MeOH concerning the number of PFAS compounds with acceptable recoveries. However, this extraction method also provided strong matrix effects. The overall performance of all extraction methods based on extraction efficiency and matrix effects was not optimal for PFAS in liver samples, and therefore needs further improvements.

The use of HPLC/(UPLC)-ESI-MS/MS has shown to be applicable for analyzing a broad range of PFAS in biological samples due to high sensitivity and selectivity and is by far the most used technique for PFAS in environmental and biological samples [171, 172, 163, 220]. However, the inherent downside of the analytical techniques is that ESI ionization is prone to matrix effects [216].

5.3.3 Discussion of extraction methods and improvements

Biological samples are complex matrices that contain high amounts of proteins and phospholipids that can interfere with the ionization of TA during the ESI ionization. A proper sample preparation method is required to provide accurate results. Extraction and clean-up are important parts of sample preparation that can affect the recovery and matrix effect if inappropriate.

Low recovery of the steroid hormones and PFAS in the present study might be attributed to several factors. Firstly, insufficient homogenization might have affected the extraction negatively. The pooled liver samples were homogenated by hand with a mortar and a pestle. This way of homogenizing the sample may not have provided small enough pieces. The liver samples were homogenized as wet tissue which made it challenging to crush the samples into small pieces. The extraction efficiency is dependent on the surface area of the sample. Smaller sample particles will facilitate improved extraction [166, 83]. Moreover, the extraction is influenced by the choice of solvent as the solvent used should dissolve the analytes of interest. In the present study, the different extraction methods used various solvents: Hybrid SPE used MeOH and ACN, and during the SPE method a mix of H_2O and MeOH was used. During SLE, the MTBE solvent was used for extraction. Organic solvents will cause proteins to precipitate from the solution, removing some of the interfering matrix components. Steroid hormones are lipophilic compounds that are soluble in non-polar solvents (*n*-hexane and octanol), however, the use of highly non-polar solvents will also cause more matrix components to be co-extracted, such as lipids present in the liver [220]. Alcohols such as MeOH and EtOH are usually good at solving steroid hormones, and are therefore often used as fewer lipid matrix components will co-extract [220]. PFAS compounds are amphiphilic compounds that consist of a non-polar fluorinated carbon chain and a small polar functional group. Moreover, PFAS are regarded as both hydrophobic and lipophobic compounds. In the review by Valsecchi *et al.* (2013) that summarized different methods used in the analysis of PFAS in aquatic organisms, solvents such as MTBE, ACN, and MeOH or a mix of MeOH and H_2O were frequently used among researchers [220]. However, the use of AF in MeOH or a mix of MeOH and H_2O often resulted in poorer extraction and lower recovery of long-chained PFAS. This was also observed for some of the PFAS in the present study; PFNA, PFUnA, and PFDS had a low recovery for the Hybrid SPE extraction method with AF in MeOH (Table C13). Moreover, matrix effects have also been reported to occur when MeOH was used for extraction [220]. ACN is a good solvent for protein precipitation of biological samples, whereas the use of MTBE as a solvent might cause analyte loss because solvent evaporation and exchange are required before the chromatographic analysis. In the review by Valsecchi *et al.* (2013) they also reported that using alkaline digestion before extraction

enhanced the recovery of PFAS, as the PFAS binding to proteins in tissues is broken when using alkaline solutions. Additionally, a mix of THF and water also proved to produce good recoveries for a wide range of PFAS compounds. On the contrary, poor recoveries in the present study might reflect suppression of the signal response during the ionization i.e. matrix effects. Techniques that were implemented during the sample preparation that is known to enhance the extraction are agitation of the sample mixture by vortexing and ultrasonication, and these were applied to all of the extraction methods in the present study [166].

Hybrid SPE is a novel extraction and clean-up method that is simple and time efficient. This method has previously been used in biological samples for analysis of PFAS and has proven to be efficient in removing phospholipids, and reducing ME [163, 164, 165]. Before the sample extract is applied to the Hybrid SPE cartridge, the sample is mixed with a PP agent. In the present study, 0.1% AF in MeOH and 0.5% CA in ACN were used to remove proteins and to inhibit the analytes of interest from co-retaining with the phospholipids on the Zr sorbent [165]. The Hybrid SPE method has been recommended for use on biological liquid samples such as plasma and serum by the manufacturer, and not for solid matrices. However, a recent study that extracted PFAS with Hybrid SPE in liver samples provided good recoveries, however, positive matrix effects were evident for some PFAS compounds [163]. In the present study, recoveries were low and matrix effects were strong negative when Hybrid SPE was used on liver sample extracts. It might be that this method is not designed to tackle the greater amount of matrix components present in solid samples compared to liquid samples, resulting in less efficient removal of interfering matrix components. Moreover, hydrophilic interaction liquid chromatography (HILIC) interactions have been observed for Hybrid SPE when using ACN as a PP agent i.e. the analyte interacts with the sorbent in the Hybrid SPE cartridge, and this could potentially lead to lower recoveries [165]. This might explain the low recoveries provided by the Hybrid SPE extraction with CA in ACN for the PFAS compounds. On the contrary, there are several advantages of using the Hybrid SPE method; it is simple and fast, and the consumption of solvents is minimal. Moreover, authors have reported that this method is less expensive compared to the traditional SPE method.[162].

The more traditional SPE extraction and clean-up method is a more time-consuming method compared to the Hybrid SPE as several conditioning steps of the cartridge need to be conducted before the sample can be loaded onto the cartridge [161, 83]. The solvent consumption is greater and requires different types of solvents from non-polar to polar. However, the SPE method is widely used, as it efficiently separates target analytes from interfering compounds. There are different sorbents available for SPE, however, reversed-phase is ap-

plied to non-polar and moderately polar compounds. However, as the reversed-phase sorbent is based on hydrophobic interactions, other hydrophobic and C-H-rich compounds such as phospholipid can be retained as well [162]. Therefore, SPE removes proteins and only small amounts of phospholipids. This can also be observed in the present study where strong negative matrix effects were evident for both steroid hormones and PFAS in liver samples prepared with the SPE method.

SLE is an easy but more time-consuming extraction method as repeated extractions of a solid sample are carried out. SLE is an inexpensive method that removes most protein in a sample, but the consumption of solvents is greater compared to Hybrid SPE and SPE. However, the absence of a clean-up step to remove matrix components such as phospholipids other than centrifugation is not included. Therefore, this method will mainly remove proteins. Additionally, this method also included a critical step; evaporation and solvent change from MTBE to a mix of MeOH and H_2O which can cause analyte loss. Moreover, the extraction efficiency of SLE is dependent on the choice of solvent, extraction time, and sample particle size [166]. In the review by Valsecchi *et al.* (2013) suggestion for clean-up of the extracts after SLE is to include a freezer incubation step that facilitates the precipitation of both proteins and phospholipids and to combine the SLE with SPE [220].

In the present study, both steroid hormones and PFAS compounds demonstrated strong negative matrix effects except for a few compounds, and the Hybrid SPE method with 0.5% CA in ACN produced mostly positive matrix effects for PFAS compounds. Matrix effects are often related to insufficient clean-up of the sample solution extract, and therefore co-eluting matrix components can interfere with the ESI ionization causing suppression or enhancement of the signal response [219]. The problem with matrix effect is that it negatively affects the quantification, linearity, accuracy, and precision of the method. Co-extracted matrix components can also affect the chromatography by modifying the retention time and the peak shape compared to the analyte in a pure solvent [221]. Moreover, both steroid hormones and PFAS were analyzed with the use of ESI ionization. ESI is a soft ionization technique that is prone to matrix effect [219]. For example, sometimes it is necessary to derivatize the steroid hormones due to poor ionization of some steroids, such as estrogens [176]. In addition, ionization of steroids can be difficult due to carbonyl- and hydroxyl-groups that have low proton affinity [173]. In biological samples, matrix effect derives mainly from proteins and phospholipids that interfere with ESI ionization. There are several methods available for the removal of proteins; the addition of organic solvents and PP agents, and SPE. However, few methods are available to remove phospholipids which are the major reason for ion suppression during chromatographic analyses [162]. Another way to reduce the matrix effect is to modify and optimize the chromatographic and mass spectrometric parameters to shift the retention

time of target analytes from the area where the chromatogram is affected by matrix effect, and to enhance the separation of chromatographic peaks [219]. However, this is beyond the scope of this project, and will therefore not be discussed further. Another way that could reduce the matrix effect is to simply reduce the injection volume or to dilute the sample [185]. However, the analytical methods used in the present study for both steroid hormones and PFAS compounds with UPSFC-MS/MS and UPLC-MS/MS, respectively, have been optimized previously for these compounds. Furthermore, the application of the IS method has been recommended to reduce matrix effects and to correct for loss of analytes during extraction and the analytical method [219]. In the present study, two isotopically labeled were available for the analysis of steroid hormones and PFAS, which might have been insufficient for the multi-compound analysis of 18 steroid hormones and 43 PFAS compounds. A further improvement could therefore be to implement a few more IS. However, having a IS for every compound is not feasible as isotopically labeled IS are expensive and do not exist for all compounds. Moreover, the analysis of CRM of the analytes could have been implemented for better quality control, and to verify the performance of the method [83]. However, CRM was not available to use for this project. In the present study, steroid hormones and PFAS in the liver samples were not quantified as no calibration curves were analyzed, though, the use of matrix-matched calibration curves has been recommended to reduce the effects of matrix effects.

To summarize, both SPE and SLE extraction methods are more time-consuming, and the consumption of solvents is greater compared to the Hybrid SPE method. Additionally, SPE and SLE extraction methods are inadequate at removing phospholipids compared to Hybrid SPE which are designed to remove phospholipids. However, Hybrid SPE has been recommended to use for liquid samples and in the present study, the method did not prove to improve matrix effects compared to the other methods. None of the tested extraction methods can therefore be recommended. The results indicated the need for improvements in both extraction efficiency and matrix removal. However, as ion suppression of the signal response might cause the impression of low recoveries, implementing an additional clean-up step might improve the performance outcome. Due to time limitations in the present study, further investigation were not conducted.

5.4 Trace elements in Arctic char

Several trace elements in Lake Diesetvatnet might derive from both natural and anthropogenic sources, however, the relative contributions are difficult to ascertain. In high arctic areas such as Svalbard, natural sources due to erosion of the bedrock and sediment may rep-

resent an important source for some trace elements. The bedrock at Mitrahalvøya constitutes metamorphic rock types such as marble, phyllite, metapelitic schist, and small amounts of quartzite [88]. These types of rock consist of several major elements and trace elements. A study conducted in Svalbard by a previous Master's student that analyzed elemental composition in soil from Lake Nordre Diesetvatent found that trace elements such as As, Ni, Pb, and Zn were elevated compared to other locations at Svalbard [222]. Additionally, trace elements such as Cd, Cr, and Cu were also measured in the soil close to Lake Nordre Diesetvatnet. Therefore, the local bedrock geology, sediment, and soil environment might contribute to elevated levels of some trace elements found in Arctic char at Lake Diesetvatnet. Due to the special bedrock on Svalbard, several Artic Lakes have a high content of dissolved ions [10].

The anthropogenic input mainly derives from the atmospheric deposition from LRAT of contaminants from distant sources at lower latitudes. The main sources that contribute to trace element contamination are the combustion of fossil fuels such as coal, oil, and gasoline, non-ferrous metal production, and waste incineration [84]. The industrial activities in Svalbard are limited. However, Ny-Ålesund which is in proximity to Mitrhalvøya, about 35 km South, has a previous history of coal mining and burning. Similarly, Longyearbyen has mine 7 in operation, and the local power generation derives from coal burning. The anthropogenic activities at Svalbard might have a minor contribution to the total LRAT at Lake Diesetvatnet. Coal combustion can contribute to the emission of elements such as Cr, Hg, Pb, Mn, Sb, Se, Sn, and Tl [84]. Moreover, some studies have suggested that the size of the Lake catchment area is an indicator for the input of atmospheric wet and dry deposition to Artic Lakes that can affect the bioaccumulation of trace elements in Arctic char [94, 95, 91]. Atmospheric deposition is thought to be the main input of Hg to Arctic Lakes. Hg is mainly released as gaseous elemental mercury and can be transported to the Artic within a few days by LRAT [1]. In addition to LRAT of contaminants, secondary sources such as thawing glaciers, permafrost, and snow might contribute with the input of water and sediment particles that contain trace elements to Lake Diesetvatnet. Additionally, the accumulation and distribution of trace elements in fish are influenced by the total concentrations in the aquatic environment as well as physiological factors inherent in the fish [14, 15].

The main focus in the following subsections will be to discuss the distribution of non-essential trace elements: Hg, Cd, Pb, and As, and a selection of essential elements in tissues of Artic char. Moreover, the distribution pattern and levels will be compared with previous studies. However, comparison across studies can be challenging as there are great variations in trace elements and tissues of fish that have been analyzed. Moreover, species differences and variations in trace element concentrations and speciation between locations make comparison difficult.

5.4.1 Mercury

The distribution of Hg in organs of Arctic char from Lake Diesetvatnet can be ranked accordingly from highest to lowest based on mean Hg concentration; kidney > liver > gonad > brain > RBC > hard roe > plasma. From Figure 14 it can be observed that Hg concentration is enriched in the kidney (0.0966±0.079 μg g $^{-1}$ dw) and liver (0.0786±0.12 μg g $^{-1}$ dw) compared to the other tissues, however, there was only statistically significant difference in the median Hg concentration between the kidney and plasma. This might be explained by the great variation in the dataset, and that there are several outliers in the Hg concentration of all tissues which increases the concentration range.

There is a limited number of studies that have analyzed the distribution of Hg in various organs of Arctic char and other fish species. Most of the existing studies have analyzed Hg in muscle tissue as this is of high relevance for human consumption. A study conducted in Russia on salmon trout, a species from the same Salmonidae family as Arctic char, measured the highest Hg concentration in kidney and liver 0.197±0.028 μg g^{-1} dw and 0.196±0.034 μg g^{-1} dw, respectively [92]. The Hg concentration measured in the kidney and liver was one order of magnitude greater than what was measured in the muscle tissue of salmon trout. This study also examined other fish species indicating that Hg accumulation was species-specific and that the overall accumulating properties of Hg for all fish species analyzed were liver > muscle > kidney > gills. Another study that looked at heavy metal distribution in various tissues of different freshwater fish species found that Hg concentrations were highest in muscle tissue (0.031-0.159 μg g^{-1} ww), and lowest in the gonad (0.005-0.01 μg g^{-1} ww) [223]. Hg concentrations found in kidney and liver ranged from 0.021-0.081 μg g^{-1} ww and 0.011-0.072 μg g^{-1} ww, respectively. Moreover, the distribution of Hg in tissues was as follows across all five species; muscle > gills > kidney > liver > gonad. In some freshwater species, Hg muscle concentration can be higher than in the kidney and liver. A study conducted on different freshwater fish species; roach, perch, and chub from both a low and high contaminated location found that Hg was differently distributed between the liver and muscle tissue from the different locations [224]. Fish from the highly contaminated location had higher levels of Hg in the liver compared to muscle, whereas in fish from the low contaminated location the distribution between the two tissues was opposite. The distribution of Hg in muscle and internal organs might depend on the degree of contamination in the surrounding environment. The liver plays an important role in the storage, redistribution, metabolism, and detoxification of contaminants, and might become more involved if the contaminant load in the surrounding environment is high. Additionally, Hg has shown to accumulate in muscle tissues over time. For example, an exposure study on fish demonstrated that initially after exposure to MeHg, concentrations are highest in the blood, kidney, and liver. After

a few weeks, MeHg is redistributed and accumulates in muscle tissue bound to cysteine, a sulfur-rich amino acid [101, 102].

A study by Adams *et al.* (2010) found the following Hg distribution in tissues of spotted seatrout; kidney > liver > muscle > brain > gonad > RBC [225]. This distribution trend is similar to what was detected in the present study, where the highest Hg concentration was found in the kidney followed by the liver, and the lowest concentrations were found in RBC, gonad, and plasma. The Hg concentration in the RBC was 0.07±0.01 μg g $^{-1}$ in spotted seatrout from the contaminated location and 0.02±0.01 μg g $^{-1}$ in the reference site [225]. The Hg concentration in RBC from the reference site is similar to what was detected in RBC in Arctic char from Lake Diesetvatenet; 0.0165 μg g $^{-1}$ ww. In the present study and the study by Adams *et al.*, a higher concentration of Hg was observed in the brain compared to RBC. This might indicate the potential of Hg to cross the BBB. MeHg is a known neurotoxic compound that can cross the BBB due to the ability of MeHg to mimic the amino acid methionine [122, 34]. However, the MeHg content was not examined in the present study, but the presence of Hg in the brain might indicate that Artic char from Lake Diesetvatnet are exposed to MeHg.

In the present study, the mean Hg concentration was lower in hard roe (0.008±0.003 μg g $^{-1}$ dw) compared to the gonad (0.02±0.03 μg g $^{-1}$ dw). This might indicate that a limited amount of Hg is transferred from the ovaries to the hard roes. The critical review by Crump and Trudeau (2009) found that the amount of Hg transferred maternally is low, approximately 0.2-3% of the total body burden [122]. Additionally, maternal transfer of Hg is mainly in the form of MeHg (> 90%), and the study indicated that the diet of the fish during egg growth and development is the predominant factor determining the MeHg load in hard roes rather than the remobilization of stored MeHg in the body [225]. Similarly, Khadra *et al.* (2019) indicated that MeHg could be maternally transferred to the hard roes [226].

Several of the mentioned studies indicate high concentrations of Hg in muscle tissue and some even higher than in the kidney and liver [227, 223, 224, 101, 102]. Moreover, the distribution of Hg in tissues might depend on the environmental Hg load and speciation [15]. Muscle tissue was not examined in the present study and it is, therefore, difficult to predict whether concentrations would have been higher or lower in the muscle compared to the kidney and liver. A study conducted by Hudleson *et al.* (2019) on landlocked Arctic char in the Canadian Arctic from six different lakes showed great variation in Hg muscle concentration. Arctic char Hg concentration in Amituk Lake (1.28±0.23 μg g^{-1} ww) was significantly higher compared to the other Lakes with concentrations ranging from (0.12-0.43 μg g^{-1} ww) [91]. Additionally, Hg concentration was significantly correlated to dissolved and

particulate organic carbon concentration in the water, which supports the fact that abiotic factors might affect exposure and uptake of Hg in fish.

In the present study, kidney and liver Hg concentrations were measured; 0.0966±0.079 μg g $^{-1}$ and 0.0786±0.12 μg g $^{-1}$ in dry weight, respectively. In the Canadian study, Hg concentrations in Arctic char were measured in wet weight and are still higher than the concentrations in kidney and liver in the present study by one to two orders of magnitude [91]. Even though this comparison is drawn across the same species it is expected to observe different Hg levels between Arctic char populations at different locations. Several confounding factors might affect the difference in Hg levels. First of all, comparing Hg levels between various tissues is challenging due to the two tissues' different accumulation potentials. In addition, concentrations were measured in dry weight in the present study and wet weight in the Canadian study [91]. There might be different water content between individual fish and tissues which complicates the comparison. Additionally, there might be considerable differences in size and age between the Arctic char that was caught at different locations. As previously mentioned, in the study by Hudelson *et al.* (2019) only landlocked Arctic char was caught, whereas in the present study Arctic char was caught from Lake Dieset-vatnet where both landlocked and anadromous Arctic char residents. In the present study, the lifestyle of Arctic char caught was not determined. Several studies have reported that landlocked Arctic char have higher Hg concentrations than anadromous Arctic char. This could be explained by the slower growth and smaller size of landlocked Arctic char [11]. Furthermore, landlocked Artic char often have poorer body conditions because they feed on oligotrophic Lakes which could increase their susceptibility to contaminant accumulation [106, 107, 108, 1]. Several field studies have reported a negative correlation between MeHg concentration in tissue and body condition of the fish [104, 140]. On the contrary, anadromous Arctic char grow quicker due to their annual sea migration where they can double their size after feeding intensively for several weeks [84]. Moreover, Hudelson *et al.* (2019) indicated that the elevated Hg levels found in Amituk Lake could be explained by the difference in the trophic level of Arctic char compared to the other Lakes [91]. A study on Arctic char from Greenland found that landlocked Arctic char had 10-15 times higher Hg muscle concentrations compared to anadromous char [108, 84]. Additionally, landlocked Arctic char have a bimodal growth pattern as some individuals become cannibalistic when they reach a certain size or age. Cannibalistic Arctic char have higher Hg levels as their diet change to a higher trophic level [113, 140]. Furthermore, Arctic char has an opportunistic diet, therefore, the location and their diet could considerably affect the bioaccumulation of Hg. For instance, benthic invertebrates have high Hg levels compared to pelagic invertebrates at some locations [112]. In oligotrophic Arctic Lakes, the food availability could be different

between Lakes at different locations. Additionally, there are also environmental factors that can affect the bioavailability and bioaccumulation of Hg at a location. For example, water parameters such as pH, temperature, organic matter, salinity, ionic strength, and metal speciation can affect the bioavailability of Hg in fish [84, 89, 90, 91, 15].

As mentioned, the speciation of Hg affects its bioavailability and is dependent on several water parameters. Moreover, the bioavailability of Hg is also dependent on the magnitude of methylating bacteria that can transform inorganic Hg to MeHg, which is the more toxic form of mercury [92]. Arctic freshwater ecosystems are considered to be more inorganic systems due to low primary production and less nutrient content, therefore, it is expected that there might be less organic carbon content. Hg methylation has shown to be dependent on organic carbon in the water and sediment, as a consequence, there might be less methylation in freshwaters compared to marine environments [96, 92]. Additionally, some studies have indicated that there is increased evasion of Hg from freshwaters compared to marine ecosystems [97]. Moreover, photochemical reactions can also modify the speciation and mobility of Hg, and the reduction of Hg in freshwaters is mainly caused by photoreduction [97, 98]. Furthermore, higher concentrations of humic acids have shown to favor the transport and retention of Hg in the water phase as organic complexes, which may increase the bioavailability of Hg [84]. The uptake and bioaccumulation of Hg in Arctic char are also affected by Hg speciation. For example, MeHg is mainly absorbed from the diet through the intestine, and the absorption of MeHg is efficient (approximately 80%) [99, 100]. MeHg on the other hand is not efficiently taken up through the gills. In the present study, total Hg was determined, and it is, therefore, difficult to predict whether the Hg is present in organic or inorganic form. However, several studies indicate that MeHg has higher bioaccumulative properties and is more efficiently absorbed. MeHg is also of the highest concern due to the neurotoxic effect and the ability to cross the BBB. A study conducted on landlocked Arctic char from Greenland, found that 72% to 92% of total Hg concentration constituted of MeHg [108]. The relative percentage of MeHg might vary from location and depend on the diet and the abiotic environment.

In the present study, the selenium: mercury (Se:Hg) ratio in various tissues of Arctic char was determined and found to be > 1 in all tissues (Table 15). The highest Se:Hg molar ratio was found in the hard roe and gonads, and the lowest Se:Hg molar ratio was found in RBC. Similar Se:Hg molar ratios were found in the kidney, liver, and brain of approximately 250-300. A previous study analyzed Se:Hg ratio in various tissues in bluefish, and found the highest Se:Hg ratio in the kidney and the lowest in the muscle [228]. Several studies have indicated that excess levels of Se compared to Hg might have protective effects against mercury toxicity. A Se:Hg molar ratio of > 1 has been described as beneficial with regards

to MeHg toxicity [119]. The explanation behind this is that Se binds to Hg with a high binding affinity to form insoluble mercury selenide, which reduces the bioavailability of Hg in an organism [118]. Due to the important role of Se in antioxidant enzymes, an excess of Se is needed to maintain the enzyme activity [118]. However, the Se:Hg ratio in all tissues of Arctic char from Lake Dieesetvatnet was well above 1, ranging from 92-1600. The excess Se levels indicate that Arctic char in the present study might be protected from Hg toxicity. Additionally, the Se distribution in tissues of Arctic char was similar to that of Hg (Figure 14 and C23) except for hard roe in which Se levels were much higher than Hg levels. This might be attributed to the protective effect of Se in the hard roe. Moreover, Se is an essential trace element that is an important cofactor in antioxidant enzymes, which can be beneficial in several ways, including the growth of hard roes. Zhang *et al.* (2020) found a similar trend with high levels of Se in the roes and lower levels of Hg compared to other tissues [229]. Even though Se is an essential trace element, high concentrations could lead to decreased hatching success and survival, and embryo deformities. Covington *et al.* (2018) indicated a Se threshold level for deformities in offsprings from brown trout in the range 21.1-21.8 μg g^{-1} dw [230]. Se levels measured in all tissues in Arctic char from Lake Disetvatnet were below these values indicating no risk for a negative effect of Se. Se is transferred from the liver to the gonads during vitellogenesis, production of a egg yolk protein vitellogenin that is needed for oogenesis growth and development [226]. This is important as early-life stages are particularly sensitive to exposure to contaminants, and could potentially lead to impairment of the development of the fish if they are exposed to high concentrations. However, even though hard roe Hg concentrations were low, exposure of the roes could also occurs in the water after spawning. Furthermore, the different distributions of Se and Hg indicate different accumulation and metabolic pathways of these trace elements. The study also suggested that a lower Se:Hg molar ratio could indicate the increased formation of Hg-Se compounds [118]. For example, in the present study lower Se:Hg molar ratios were observed in the kidney, liver, and brain which might be attributed to the Se binding of Hg.

5.4.2 Cadmium

The distribution of Cd in tissues of Arctic char from Lake Diesetvatnet can be ranked accordingly from highest to lowest based on mean concentrations; kidney > liver > gonad > hard roe > brain > plasma > RBC. From Figure 15 it can be observed that Cd concentration is enriched in the kidney with a mean concentration of 1.98±1.1 μg g $^{-1}$ dw. The median Cd concentration in the kidney was statistically significantly higher than the median Cd concentration in the brain, gonad, and hard roe. Liver Cd concentrations were lower than the kidney Cd concentrations, however, no statistically significant difference between these

tissues was found, probably due to an outlier than increased the Cd concentration range of the liver tissue. Plasma and RBC samples were not included in the distribution plot or statistical test due to low sample numbers (< 4).

A study by Moiseenko *et al.* (2020) found the highest Cd concentration in the kidney of several fish species, followed by liver, gill, skeleton, and muscle tissue [92]. Another study that looked at heavy metal distribution in various tissues of several freshwater fish species found that Cd concentrations were highest in the kidney (0.037-0.498 μg g^{-1} ww). Yin *et al.* (2018) also found the overall highest concentration of Cd in the kidney where 9 different tissues were analyzed in 8 different freshwater fish species [223]. Similarly, Hasyimah *et al.* (2011) found the highest concentration of Cd in the kidney followed by the liver [231]. The kidney is usually regarded as the main target for Cd accumulation, and this argument could be supported by the present study that also observed the highest mean Cd concentration in Arctic char from Lake Diesetvatnet [14, 232]. However, studies report different levels of Cd in the kidney which indicates species differences in the bioaccumulation and differences in the exposure level from the aquatic environment they live. Martyniuk *et al.* (2020) analyzed several trace elements in the liver and dorsal muscle of anadromous Arctic char, and found significantly higher levels of Cd in the liver compared to muscle; 0.52±0.41 μg g $^{-1}$ dw and 0.03±0.03 μg g $^{-1}$ dw [233]. The Cd concentration in the liver of this study is similar to what was found in the liver of the present study; 0.305±0.36 μg g $^{-1}$ dw. Similarly, Jia *et al.* (2017) found that Cd accumulated in the liver of the three freshwater fish species that were analyzed [14]. Elevated uptake of Cd in muscle tissue of fish has been observed to be seasonally dependent, and increased uptake has been observed with elevated water temperatures [233]. Köck *et al.* (1996) also observed increased uptake of Cd in the summer, which could be explained by increased metabolic rate and greater bioavailability of Cd due to changes in water chemistry [90]. However, Cd seems to accumulate in the kidney and liver over time [233, 227]. This observation could be explained by the role the kidney and liver have as metabolic active organs that are responsible for detoxification of contaminants, it is therefore expected to see elevated concentrations of heavy metals in these tissues [15]. Moreover, higher concentrations of Cd observed in the kidney and liver could be attributed to high levels of MT binding proteins in these tissues that sequester Cd [14].

The uptake and bioaccumulation of Cd are dependent on both endogenous and exogenous factors i.e. the physiology of the fish and the aquatic environment. Different water parameters in the aquatic environment affect the speciation and bioavailability of Cd. For example, one study indicated that Cd has increased bioavailability in freshwaters with low pH and Ca^{2+} concentration [92]. Several studies have also shown that Cd accumulation in fish is enhanced in aquatic systems with low concentrations of Ca^{2+} [232, 92, 15]. This might

implicate that Cd is more bioavailable in freshwaters than in marine environments, and that anadromous Arctic char might be less exposed to Cd during their seaward migration. However, the pH in freshwaters is dependent on the bedrock and the surrounding environment. The study by Moiseenko *et al.* (2020) indicated that Cd is present mainly in ionic form in oligotrophic waters with pH $\leq$ 7.3. Moreover, Cd is readily bioavailable in ionic form as Cd^{2+}. In the present study, the pH in Lake Diesetvatnet was measured at 8.03, which might indicate that Cd is less bioavailable as the pH is similar to marine waters (Table 3). Furthermore, the bioaccumulation of Cd depends on the rate of uptake and elimination. Dietary uptake of Cd is low (<5%), whereas Cd is readily taken up by the gills due to the interaction with Ca^{2+} metabolism [92]. Cd is normally slowly excreted, which results in accumulation over time. Additionally, low dietary intake of Ca, Fe, Zn, Cu, and proteins can enhance the uptake of Cd [92, 34]. Therefore, diet is also an important factor that impacts the bioaccumulation of Cd indirectly. Moreover, high levels of Cd in the kidney can lead to nephrotoxicity and growth reduction [14, 92]. Furthermore, Cd has shown to affect the foraging behavior and induce MT gene expression and production in fish [116, 117, 115].

5.4.3 Lead

The distribution of Pb in tissues of Arctic char from Lake Diesetvatnet can be ranked accordingly from highest to lowest based on mean concentrations; brain > kidney > gonad > plasma > liver > hard roe > RBC. From Figure 16, it can be observed that Pb concentrations are enriched in the brain, kidney, and gonad. However, no statistically significant difference was found in the median Pb concentrations between the tissues. This might be caused by the several outliers that increase the concentration range of the tissues. Hard roe and plasma samples were not included in the distribution plot or statistical test due to low sample numbers (< 4).

Interestingly, the highest Pb concentration was measured in the brain of Arctic char in the present study with a mean concentration of 0.298±0.38 μg g $^{-1}$ dw. Pb, therefore, exhibits the ability to cross the BBB from these results. Yin *et al.* (2018) also found the highest concentration of Pb in the brain in several of the freshwater fish species that were analyzed [234]. The author suggested that the accumulation of heavy metals, particularly Pb, in the brain could be attributed to the high lipid content in this tissue. Some trace elements might accumulate in lipid-rich tissue, such as MeHg. Moreover, Pb can mimic other essential elements such as Ca and Fe, which could be another explanation for the observation of Pb in the brain [92]. A similar mimicry of endogenous compounds has been observed with MeHg that bind to cysteine, which can pass the BBB due to the similarity of the amino acid methionine [122, 34, 123]. In the present study, Pb concentrations were

quite high in the kidney of Arctic char; 0.195±0.19 μg g $^{-1}$ dw, however, lower levels were observed in the liver 0.0266±0.043 μg g $^{-1}$ dw. A study conducted in Russia on several fish species found the highest Pb concentration in the kidney followed by the liver [92]. Similarly, Hasyimah *et al.* (2011) detected the highest concentration of Pb in the kidney followed by the liver [231].

On the contrary, Martyniuk *et al.* (2020) analyzed several trace elements in anadromous Arctic char in the liver and dorsal muscle and found no significantly higher levels of Pb in the liver compared to muscle tissue; 0.03±0.02 μg g $^{-1}$ dw and 0.05±0.07 μg g $^{-1}$ dw, a similar Pb concentration that was measured in the liver of Arctic char in the present study [233]. In the study, they indicated that low levels of Pb in the liver could be a result of the uptake of Pb by the gills and that Pb has a higher affinity to mucosal membranes such as gills, skin, fin, and intestine [233]. A study by Has-Schön *et al.* (2006) also indicated no accumulating trend of Pb in any of the tissues of freshwater fish [227]. A study by Jia *et al.* (2017) indicated that Pb accumulates in gills and that this might indicate that the main uptake route of Pb is from the surrounding water [14]. Another study conducted on six freshwater fish species found the highest Pb concentrations in the gills [223]. A similar trend was observed in a study conducted on European catfish where high Pb concentrations were found in the gill, kidney, and liver [232]. Gills are the main site for the uptake of metal species from the water due to their large surface areas that enable the transport of metals. Pb is analogous to Ca^{2+} in processes of uptake and accumulation in the fish. Ca^{2+} is adsorbed and transported through the membrane in the gills. Because of the strong similarity of Pb^{2+} to Ca^{2+}, Pb can penetrate the organism and can get involved in metabolic processes [92]. Additionally, lower pH at the gill surface due to respired carbon dioxide could increase the dissolved Pb leading to enhanced uptake of this metal [232]. Moreover, a short-term exposure study conducted on shorthorn sculpins found the highest levels of Pb in the gills followed by muscle tissue, and liver [145]. Their findings also indicated an elevated level of Pb in the blood after exposure, which might indicate that blood is a good indicator of recent exposure. In the present study, low levels of Pb were measured in RBC and plasma which might indicate that exposure has occurred over time. The liver and kidney are involved in the detoxification of toxic elements, and therefore chronic exposure to high levels of Pb might be reflected in the levels measured in these tissues. In the present study, lower levels of Pb in the liver might indicate that Artic char from Lake Diesetvatent are not exposed to high levels of Pb. However, a higher Pb concentration was detected in the kidney which might indicate that Pb is preferably accumulated in the kidney of Arctic char from Lake Diesetvatnet.

Additionally, in the present study elevated Pb concentration was detected in the gonad, which might indicate the potential for maternal exposure to the hard roes. A study by

Has-Schön *et al.* (2008) conducted on six freshwater fish species also found high levels of Pb in gonads ranging from 0.024 to 0.1 μg g^{-1} ww in the different fish species. However, in the present study higher levels were detected in the gonad with a mean Pb concentration of 0.161±0.14 μg g $^{-1}$ dw [223]. That study also found that Pb is higher in muscle and gonads compared to Cd in these tissues [223]. Moreover, Has-Schön *et al.* (2008) also indicated that Cd accumulated more in the kidney and liver compare to Pb, this was also observed in the present study. A previous study found that Pb accumulated in the gonad and brain of five tissues that were analyzed in two cyprinid freshwater fish [235]. Moreover, the authors indicated that the high trace element load in the gonad negatively affected the steroidogenesis of sex steroid hormones such as estradiol and testosterone. Heavy metals could act directly on the HP-axis or the gonads that produce sex hormones. These effects might disrupt the reproductive success of the fish[235]. Pb has also been suggested to disturb the Ca^{2+}-homeostasis, similar to Cd [92].

The different accumulation and distribution of Pb in organs might be caused by species differences in uptake and excretion, differences in environmental concentration and speciation, and other environmental factors such as diet and habitat use. Moreover, Pb concentrations are generally lower in the marine environment compared to freshwater systems which might lead to less bioaccumulation of Pb in anadromous Arctic char in the summer [233]. Pb bioaccumulation had shown to be dependent on the salinity in the water, with increased uptake at low Ca^{2+} concentrations [92].

5.4.4 Arsenic

The distribution of As in tissues of Arctic char from Lake Diesetvatnet can be ranked accordingly from highest to lowest based on mean concentrations: gonad > kidney > hard roe > liver > brain > plasma > RBC. From Figure 17 it can be observed that As concentrations are enriched in the gonad and kidney. The median As concentration in the gonad and kidney was statistically significantly higher than the median As concentration in the plasma and RBC, but none of the other tissues.

Martyniuk *et al.* (2020) analyzed As in the liver and dorsal muscle of anadromous Arctic char from Canada [233]. The study reported statistically significantly higher As concentrations in the liver than in the dorsal muscle with a mean As concentration in the liver of 2.3±0.75 μg g $^{-1}$ dw. In the present study, As concentrations in the gonad and kidney of Artic char from Lake Diesetvatent were elevated with mean concentrations of 3.51±4.3 μg g $^{-1}$ dw and 1.69±0.46 μg g $^{-1}$ dw, respectively. The reported As concentration in the gonad and kidney of the present study is higher and lower, respectively, compared to the As concentration in the liver of Artic char from the Canadian study [233]. Furthermore,

the Canadian study reported a mean As concentration in the dorsal muscle of 1.93±0.60 μg g $^{-1}$ dw, which is similar to the levels measured in the kidney of the present study. The high levels of As in the gonad of the present study might indicate the potential for maternal transfer and exposure to the hard roes to As. The mean As concentration in the hard roe of the present study was 1.18±1.0 μg g $^{-1}$ dw, higher than the measured As concentration in the liver. However, the As concentration in hard roe was not statistically significantly higher than any of the organs. A previous exposure study conducted on freshwater fish exposed to As through the diet found that As accumulated in the gonads with a mean As concentration of 7.4±0.2 μg g^{-1} dw [236]. On the contrary, a study by Has-Schön *et al.* (2006) found no tendency for As to accumulate in gonads in any of the five freshwater fish species that were analyzed. However, this study indicated that As showed a slight tendency to accumulate in muscle tissue compared to the other analyzed organs (kidney, gills, liver, and gonad) [227]. Similarly, a study conducted on European catfish found the highest levels of As in the muscle tissue [232]. Furthermore, another study conducted on freshwater fish found low levels of As in all tissues that were analyzed with concentrations ranging from 0.003 to 0.161 μg g $^{-1}$ ww [223].

The inconsistent findings of As accumulation in fish might reflect that there are considerable species differences in the accumulation and distribution pattern among tissues. Moreover, most of the presented studies are conducted in different aquatic freshwater environments, in which the levels of As might varyconsiderable. Water parameters in the aquatic environment affect the speciation and bioavailability of As. The speciation of As is important for the bioaccumulation potential and toxicity. The bioavailability of As is often higher in the marine environment as organic complexes which might implicate higher exposure of As for anadromous Arctic char during seaward migration in the summer [233]. Moreover, organic forms of As are less toxic compared to inorganic forms of As such as trivalent arsenic (As^{3+}) or pentavalent arsenic (As^{5+}). However, several studies suggest that the content of inorganic As in fish only accounts for a minor part of the total As levels [14, 15, 237, 238].

5.4.5 Essential trace elements in Arctic char

In contrast to non-essential trace elements that are toxic even at low concentrations, essential elements such as Cu, Zn, Se, Ni, Cr, Mn, Tl, and Co are required in a specific concentration range for an organism to be in homeostasis. Deficiency or exceedance of the required concentration of essential trace elements can potentially have negative implications and lead to toxic effects in fish [34]. Essential trace elements are therefore under strict homeostatic control and do not display large variations in the concentrations [83, 34].

Several factors affect the trace element bioaccumulation and bioconcentration in Arctic

char from Lake Diesetvatent, some of which have been mentioned previously. Firstly, the local bedrock and sediment of the Lake are important factors that influence the input of trace elements [88]. Moreover, the aquatic environment and water parameters determine the speciation and bioavailability of the trace elements [15]. Additionally, some trace elements might be enriched in the Lake due to anthropogenic input from dry and wet deposition of LRAT of trace elements. Trace elements are emitted as aerosols with different particle sizes or in gas form [84]. The potential for LRAT of trace elements, therefore, depends on the particle size. Trace elements emitted as gases have the potential to be transported longer distances, such as Hg [1]. Physiological variables of the fish such as size, age, length, trophic level, body condition, and life stage affect the uptake and bioaccumulation of trace elements [109, 110, 91, 111]. Moreover, trace element concentrations in Arctic char might vary with season and diet. Lake Diesetvatnet is characterized as oligotrophic, the food availability is therefore limited and the diet of Artic char might change during the season [233]. Moreover, the nutrition and trace element content is dependent on the diet. For example, benthic invertebrates might contain higher elemental concentrations compared to pelagic invertebrates due to differences in habitat use. Additionally, the uptake and bioaccumulation might be seasonally dependent. Some studies have suggested that the uptake of trace elements might be more efficient during the summer with higher water temperatures leading to increased feeding, metabolic rate, and growth of the fish [89, 92, 90]. For instance, anadromous Arctic char seasonal migration to the sea might affect the uptake of trace elements due to differences in water chemistry, food availability, and trace element concentration between marine and freshwater environments. Trace element concentrations are lower in marine waters due to the salinity, therefore, migration might reduce the trace element exposure of anadromous char in the summer [15]. However, the trace element concentration might be higher in the food they consume during their sea residency. On the contrary, during the winter when the food is limited, Arctic char might be depleted for energy and essential trace elements. However, emaciation and reduced body condition in the winter might cause increased trace element concentration or redistribution of certain trace elements within the body [11]. Moreover, persistent trace elements might become concentrated with a reduced body mass.

Trace elements except for Hg are understudied in Arctic char, therefore the basis of comparison within this species is scarce. However, Martyniuk *et al.* (2020) analyzed several essential and non-essential trace elements in the liver and dorsal muscle of anadromous Arctic char from Canada [233]. This study found that trace element concentrations of Cu, Ni, and Zn in the liver were statistically significantly greater than in the dorsal muscle. However, no significant differences were found for Cr. In the present study, Cu concentrations in the liver and hard roe; 27.0±10 μg g $^{-1}$ dw and 25.8±17 μg g $^{-1}$ dw, respectively, of Arctic

char were elevated and found to be statistically significantly higher than Cu concentrations in the RBC and plasma. Moreover, the brain also exhibited elevated Cu levels with a mean concentration of 9.72±0.80 μg g $^{-1}$ dw. The brain Cu concentration was found to be statistically significantly higher than the Cu concentration in RBC. Additionally, the mean Cu concentration of 27.0±10 μg g $^{-1}$ dw in the liver of Arctic char from the present study was of similar magnitude to that reported in the liver of Arctic char from Canada; 21.3±64.7μg g $^{-1}$ dw.

Furthermore, the Ni concentration was elevated in the kidney of Arctic char in the present study with a mean Ni concentration of 0.472±0.56 μg g $^{-1}$ dw. The Ni concentration in the kidney was statistically significantly higher than Ni concentrations in the liver, hard roe, and RBC. Moreover, the Ni concentration in the brain was also slightly elevated with a mean concentration of 0.241±0.27 μg g $^{-1}$ dw, which was significantly higher than the Ni concentration in RBC. The mean Ni concentration in the kidney from the present study was higher than the Ni concentration in the liver of Arctic char from Canada with a mean concentration of 0.23±0.14 μg g $^{-1}$ dw, whereas the mean Ni concentration in the brain of Arctic char from the present study was in the same order of magnitude as the liver in Arctic char from Canada [233].

In the present study, elevated levels of Zn were observed in hard roe, kidney, liver, and gonad with mean Zn concentrations of 139±74 μg g $^{-1}$ dw, 110±28 μg g $^{-1}$ dw, 84.4±19 μg g $^{-1}$ dw, and 75.3±47 μg g $^{-1}$ dw, respectively. Zn concentrations in hard roe and kidney were statistically significantly higher than levels in plasma and RBC, whereas Zn concentrations in the liver and gonad were statistically significantly higher than the Zn concentration in RBC. The Zn concentration in the liver of Artic char from Canada; 115.68±28.00 μg g $^{-1}$ dw was similar to what was measured in the kidney of Arctic char from the present study but higher than the Zn concentration in the liver of Artic char from the present study [233].

Moreover, elevated levels of Cr were observed in the brain and kidney of Artic char with mean Cr concentrations of 0.565±0.84 μg g $^{-1}$ dw and 0.242±0.17 μg g $^{-1}$ dw respectively. The kidney Cr level was statistically significantly higher than Cr concentrations in plasma and RCB, whereas the Cr concentration in the brain was statistically significantly higher than the Cr level in RBC. The Cr concentration detected in the kidney of Artic char from the present study is similar to the Cr concentration reported in the liver of Arctic char from Canada; 0.26±0.04 μg g $^{-1}$ dw [233]. The Cr concentration in the liver of Artic char from Lake Diesetvatnet was one order of magnitude lower than the Cr concentration in the liver of Artic char from Canada, which indicate that these two populations have a different distribution pattern of Cr in tissues.

Elevated levels of Tl were also measured in the liver and kidney in Artic char from Lake

Diesetvatnet with mean concentrations of 0.0751±0.10 μg g $^{-1}$ dw and 0.0489±0.070 μg g $^{-1}$ dw, respectively. The Tl concentrations in the kidney and liver were statistically significantly higher than the Tl concentration in RBC but none of the other organs. A previous study by Barst *et al.* (2016) conducted on landlocked Arctic char from four different Lakes in Canada measured Tl in the liver [239]. In the study, Arctic char from Amituk Lake had elevated levels of Tl in the liver with a mean concentration of 0.058 μg g $^{-1}$ ww compared to the other Lakes where the liver Tl concentration ranged from 0.004-0.014 μg g $^{-1}$ ww [239]. In the Canadian study, Tl concentrations are measured in wet weight whereas in the present study concentrations are measured in dry weight. This indicated that Tl concentrations in the liver and kidney of Artic char from Lake Diesetvatnet are higher compared to Artic char from Canada. Barst *et al.* (2016) indicated that higher levels of Tl in the liver of Artic char from Amituk Lake caused histological changes in the liver tissue in the form of hepatic fibrosis which indicates chronic cell injury. Moreover, subcellular analysis of the liver samples of Artic char from Amituk Lake indicated that Tl was detoxified at a greater fraction than in the other Lakes [239]. However, the liver damage was not only caused by the presence of Tl, but also higher concentrations of Hg in the liver of Artic char from Amituk Lake caused the injury of the liver tissue. The results from this study might indicate that the levels of Tl measured in Artic char from Lake Diesetvatent might have the potential to cause liver damage in the presence of other trace elements found at elevated levels in the liver. Moreover, Se was also measured in the liver of Arctic char from the four Canadian Lakes and exhibited the same trend as Hg and Tl with the highest concentrations in Artic char from Amituk Lake [239]. The mean Se concentration measured in the liver of Artic char from the present study was in the same order of magnitude as the Canadian study with a mean Se concentration of 4.09±3.3 μg g $^{-1}$ dw and 3.64 μg g $^{-1}$ ww, respectively [239].

A few studies conducted on different tissues in other freshwater fish species found higher levels of Co in the liver compared to other analyzed tissues (kidney, gill, muscle), this is in contrast to the present study that detected the highest Co concentration in the kidney of Artic char with about one order of magnitude greater than the other tissues [240, 241]. Furthermore, this study also found the high levels of Mn in the kidney, however, in the present study, no significantly higher concentrations were found in this tissue. Moreover, all the analyzed organs had significantly higher Mn concentrations than the plasma in the present study. Yin *et al.* (2018) found elevated levels of several trace elements; Cu, Cr, Ni, and Pb at higher levels in tissues such as kidney, liver, and brain in 8 freshwater fish species in which 9 different tissues were analyzed [234]. Other studies have found that trace elements such as Mn, Co, Cu, Zn, and Cr have higher accumulating potential in liver tissue compared to muscle tissues [240, 232, 242, 241, 243]. Moreover, some studies have also found elevated

levels of the trace elements Zn and Cr in the gonads [242, 241]. Some of these studies have also reported that the gonads were abnormal and found histological changes in this tissue. In the present study, the highest Zn levels were found in the hard roe, kidney, and liver, whereas the highest Cr levels were detected in the kidney and brain.

The different distributions of trace elements in the mentioned studies are affected by several factors. Firstly, different accumulation patterns in fish might reflect species-specific bioaccumulation. Moreover, the aquatic environments in some of the studies are very different from Artic Lakes. The difference in bioaccumulation and bioconcentration might be caused by differences in water parameters and the surrounding bedrock that affect the speciation and bioavailability of trace elements [15]. Moreover, the environmental concentrations are also different between studies, as some of the freshwaters are located at lower latitudes. The exposure of trace elements to these aquatic environments is therefore expected to be different as they are closer to anthropogenic and industrial activities. Additionally, diet and habitat use are also factors that affect the uptake of trace elements in fish [112, 113]. There are methodological differences between studies and high variability in which tissues have been analyzed in fish. Therefore, the different distribution patterns of trace elements in fish are also caused by the various methods used. However, the general trend among studies is that trace elements accumulate to a higher degree in the liver and kidney. These organs are metabolic active organs that are involved in detoxification and excretion of toxic elements, and it is therefore expected to detect higher levels of trace elements in these tissues [15]. Moreover, these organs are the main site for metal storage due to the high content of MT metal binding proteins [14, 233].

5.5 Principal component analysis

The PCA plot was used as an additional tool to study the distribution of trace elements in tissues of Arctic char. PCA can provide information about the trend and similarity of the accumulation of trace elements in tissues of Arctic char. Variables such as body condition, hepatosomatic index, and gender are also included in the PCA. The respective PCA score and loading plots should be used together when interpreting the PCA [196]. The main trends observed in the PCA score and loading plots will be presented and discussed in the following subsections.

5.5.1 PCA loading plot

The PCA loading plot (Figure 18) contains all the variables measured in the samples. In the present study, several selected trace elements were investigated.

Several groupings of trace elements can be observed in the PCA loading plot. Along the first principal component (PC1), which explains 41% of the total variance, a visible grouping of variables is the trace elements Se, Hg, Tl, and Cd that correlate positively. A second grouping is trace elements Pb, V, Cr, Sn, Al, Ti, and Ba that correlates and are strongly loaded on PC1 in the positive direction. Furthermore, trace elements U, Fe, Ni, and Sb are grouped and loaded strongly on PC1 in the positive direction. The last group is the trace elements Mg, Ca, and Mn that are grouped and loaded strongly on PC1 in the positive direction. The other trace elements presented in the PCA plot are more spread out. For example, Cu is loaded on PC1 in the negative direction, opposite of the other trace elements. As is close to origo, and therefore does not display or contribute to a special distribution pattern. Co is loaded on PC1 in the positive direction, same as Se, Hg, Tl, and Cd, and these trace elements, therefore, correlate positively on PC1.

Along the second principal component (PC2), which explains 20% of the total variance, trace elements Se, Hg, Tl, and Cd are loaded strongly in the positive direction. Similarly, the single elements Mo and Zn are also loaded strongly in the positive direction. The trace element grouping Pb, V, Cr, Sn, Al, Ti, and Ba are loaded the strongest along PC2 in the negative direction. These two groupings; Se, Hg, Tl, and Cd and Pb, V, Cr, Sn, Al, Ti, and Ba are negatively correlated on PC2, which might indicate that these elements originate from a different source or that they are distributed differently. The grouping U, Fe, Ni, and Sb are also loaded positively on PC2, while Mg, Mn, and Ca are loaded weakly in the negative direction on PC2.

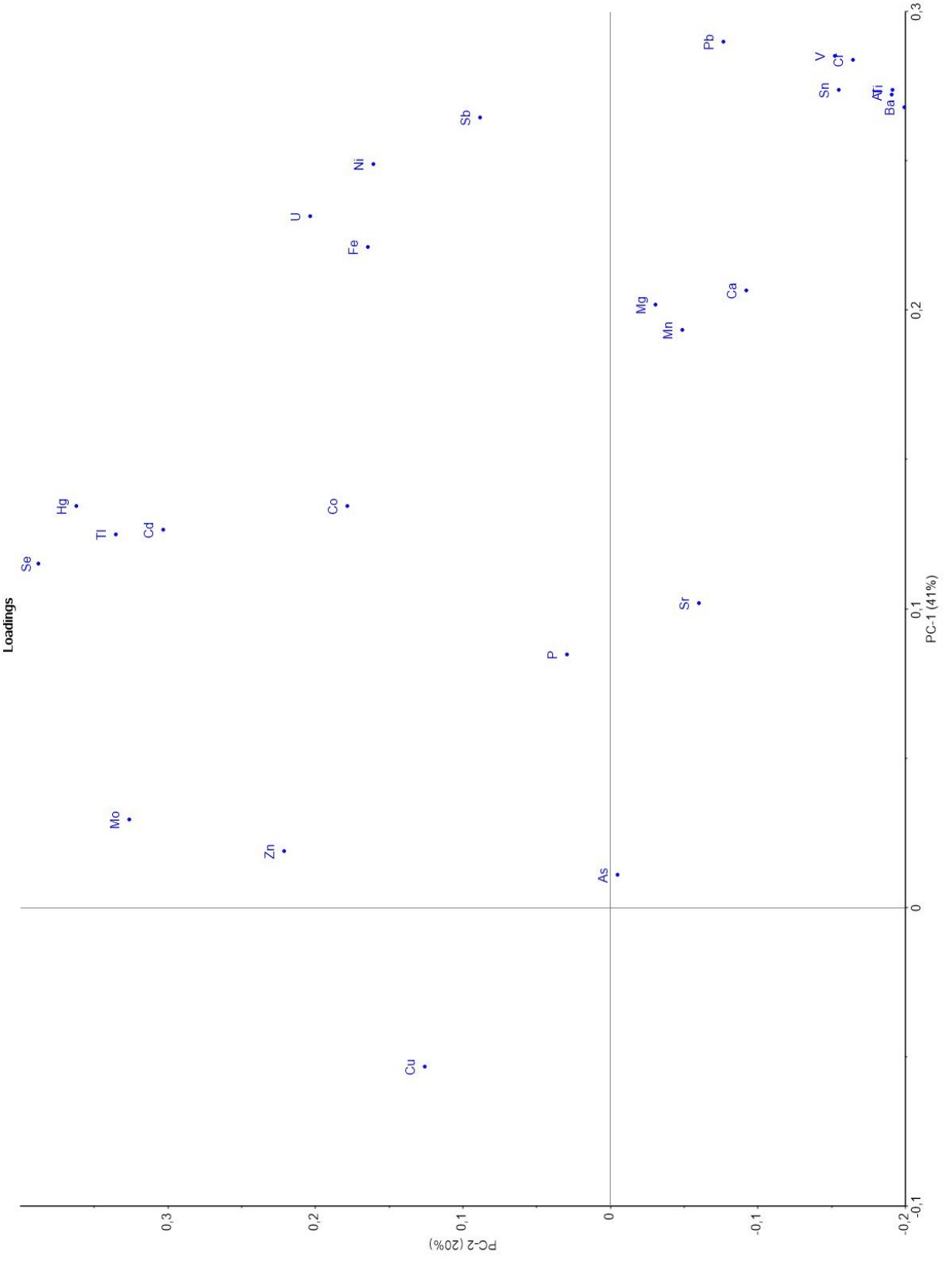

Figure 18: PCA loading plot showing all the variables included in the dataset. PC1 explains 41% of the total variance, and PC2 explains 20% of the total variance.

5.5.2 PCA score plot

The PCA score plot (Figure 19) includes individual samples of Arctic char, and an overview of the samples ID can be found in Appendix (Table D1). The most apparent observation in the score plot is the three outliers R3, R21, and R28 (outside the circle) which are the brain sample of Arctic char number 3, liver sample of Arctic char number 4, and kidney sample of Arctic char number 4, respectively. The outliers were kept as they represent an important part of the data and show that there can be variations between fish from the same freshwater. PC1 explains 41% of the total variance and PC2 explains 20% of the total variance, and the PCA plot, therefore, explains in total 61% of the variance.

Sample R21 and R28 were loaded strongly on PC2 in the positive direction and compared together with the loading plot this sample correlates with trace elements Se, Hg, Tl, and Cd that also are loaded strongly on PC2 in the loading plot. Both of the outliers were from the liver and kidney of the same individual and indicate that these elements are elevated in these two organs. This is as expected as Arctic char number 4 had the highest Hg and Cd concentration in the liver and kidney of all the fish. Interestingly, this was also the smallest individual that was caught with a body mass of 350 grams compared to the other Arctic char with approximately body masses of 1000 grams. Arctic char number 4 also had the poorest body condition and the lowest hepatosomatic index of all the fish (Table B1). Moreover, in Arctic char number 4, tapeworms were observed in the stomach which further supports the poor body condition of this individual (Figure B2). There might be an explanation for this observation, one might be that this individual is older than other Arctic char. Another possible explanation is that this individual might be landlocked Arctic char. As mentioned previously, landlocked Arctic char grow much slower compared to anadromous Arctic char [106, 107, 108]. Landlocked Arctic char is therefore often smaller compared to anadromous Arctic char concerning their age. However, this is a hypothetical explanation that unfortunately cannot be confirmed due to the lack of data on the age and lifestyle of Arctic char that was caught. A previous study conducted on landlocked Arctic char from Canada found that Hg muscle concentrations correlated with fish length, weight, age, and Tl, Pb, and Se in Resolute Lake [111]. However, landlocked populations are different from populations that consist of both anadromous and landlocked Artic char due to their difference in growth. A correlation with age, length, and weight might not exist as anadromous Arctic char grow much faster and are expected to have lower concentration due to body mass dilution [84]. However, the high correlation of Se with Hg is expected as this element is known to bind strongly to Hg, which can protect against Hg toxicity if Se:Hg ratio is > 1. As previously mentioned, a Se:Hg ratio in excess (> 1) was found in all tissues which indicate that Arctic char from Lake Diesetvatnet might be protected from Hg toxicity. Similar to Hg

and Cd, Tl was enriched in the liver and kidney. Pb on the other hand did not correlate with Hg and Cd in the present study, which indicates that Pb is distributed differently in the tissues of Arctic char.

PCA score plot (Figure 20) displays the distribution of the organs but represents the same individual samples shown in the previous PCA score plot. Due to the outliers, the pattern of the other samples does not contribute as strongly. Nonetheless, the observation in this plot is that organs such as the kidney and liver are grouped separately. Kidney samples are loaded on PC1 and PC2 in the positive direction, while liver samples are loaded on PC1 in the negative direction. However, one of the liver samples is loaded positively on PC2. The other organs are more spread out and overlap slightly. However, brain samples seem to contribute in the positive direction of PC1, while gonad samples are slightly loaded on PC1 and PC2 in the negative direction. The egg samples on the other hand are loaded slightly on PC1 in the negative direction, and most of the gonad samples are loaded on PC1 and PC2 in the negative direction.

The main trend from this plot is that Cu from the loading plot seems to correlate with liver samples from the score plot as they both are loaded on PC1 in the negative direction. Similarly, the kidney samples correlate with Se, Hg, Tl, and Cd. PC1 and PC2 seem to represent the loadings and contributions of trace elements in the various tissues. For example, elements loaded strongly on PC2 in the positive direction are elevated in the kidney; Se, Hg, Tl, and Cd, while elements loaded strongly on PC1 in the positive direction are elevated both in the brain and the kidney, since kidney samples are loaded positively on both PC2 and PC1. Furthermore, trace elements in the negative direction of PC1 are elevated in the liver, namely Cu. This observation was confirmed as the highest concentration of Cu was detected in the liver (Figure C21). Elements loaded negatively on PC2 are elevated in the brain, this is attributed to the that brain samples are loaded positively on PC1 and negatively on PC2. Additionally, elements close to origo such as As do not display any special trend or distribution in the tissues of Arctic char. However, elevated levels of As of about one order of magnitude were found in one of the gonad samples R14 (fish number 4), which correlates with As in the loading plot. This is an interesting finding as this correlates with the accumulation of other trace elements in fish number 4, and might reflect that fish with poor body conditions are more prone to accumulate certain trace elements. However, as this only represents one fish, the evidence in the present study is weak. But this assumption can be backed up by previous literature on Arctic char that have found a negative correlation with levels of for example Hg in fish muscle with body condition [109, 110, 91, 111].

Sample R3 is strongly loaded on PC1 in the positive direction, and if compared with the loading plot this sample correlates with trace elements such as Pb, Sn, V, Cr, Al, Ti,

and Ba. Interestingly, Pb levels were quite high in the brain of Arctic char, however, the outlier R3 stands out compared to the other brain samples. Sample R3 had about one order of magnitude higher Pb concentration compared to the other brain samples. In addition, this one sample correlates with trace elements such as Al, Ba, and Ti. Similarly, these elements were also enriched in this one sample compared to the other brain samples. Al, Ba, and Ti are elements that often are enriched in the bedrock [83]. Moreover, the elevated Al concentrations might derive from the alumina foil that the samples were packed in for storage, and as brain samples were small they are more easily contaminated. This one outlier might indicate possible contamination from the surrounding soil. Additionally, Pb did not correlate with Hg and Cd as expected but correlated with other trance elements which might indicate that Pb might originate from another source or that Pb accumulates differently compared to the other non-essential elements. Because of the possibility of contamination from the soil of sample R3, a new score and loading plot where this individual sample was removed has been made. The respective PCA score and loading plot can be found in the appendix (Figure D1, D2, D3).

The trends that can be observed in these PCA loading and score plots without sample R3 are similar to the previous PCA plots, and PC1 now explains 42% of the total variance whereas PC2 explains 17% of the total variance. Kidney samples are loaded strongly on PC1 in the positive direction of the score plot, and compared with the loading plot the kidney samples correlate positively with a big group of trace elements; Cd, Co, Ni, Sb, Pb, V, Cr, Sn, Se, Hg, Tl, and Fe. This agrees well with the observations of elevated concentrations of Cd, Co, Cr, Ni, and Se in the kidney (Table 14). Cu is still the only trace element that is loaded negatively on PC1, and the liver samples correlate with this element. One of the outliers R21, a liver sample of fish number 4, is now loaded strongly on PC2 in the negative direction and correlates with trace elements Mo, Fe, Tl, Se, Hg, and Zn that also are loaded strongly on PC2 in the negative direction. Elevated levels of these elements were also observed in the liver (Table C8). PC1 seems to explain the association of trace elements with the kidney i.e. trace elements that are loaded strongly on PC1 in the positive direction are enriched in the kidney. On the contrary, PC2 in the negative direction seems to explain the association of trace elements that are enriched in both the liver and kidney. Brain, egg, and gonad samples do not contribute to any trend of trace elements except for two brain samples that are loaded in the direction of trace elements Ca, Ba, Ti, and Al. Pb was not as strongly associated with brain samples after the outlier R3 was removed, which might indicate that this sample was contaminated by soil.

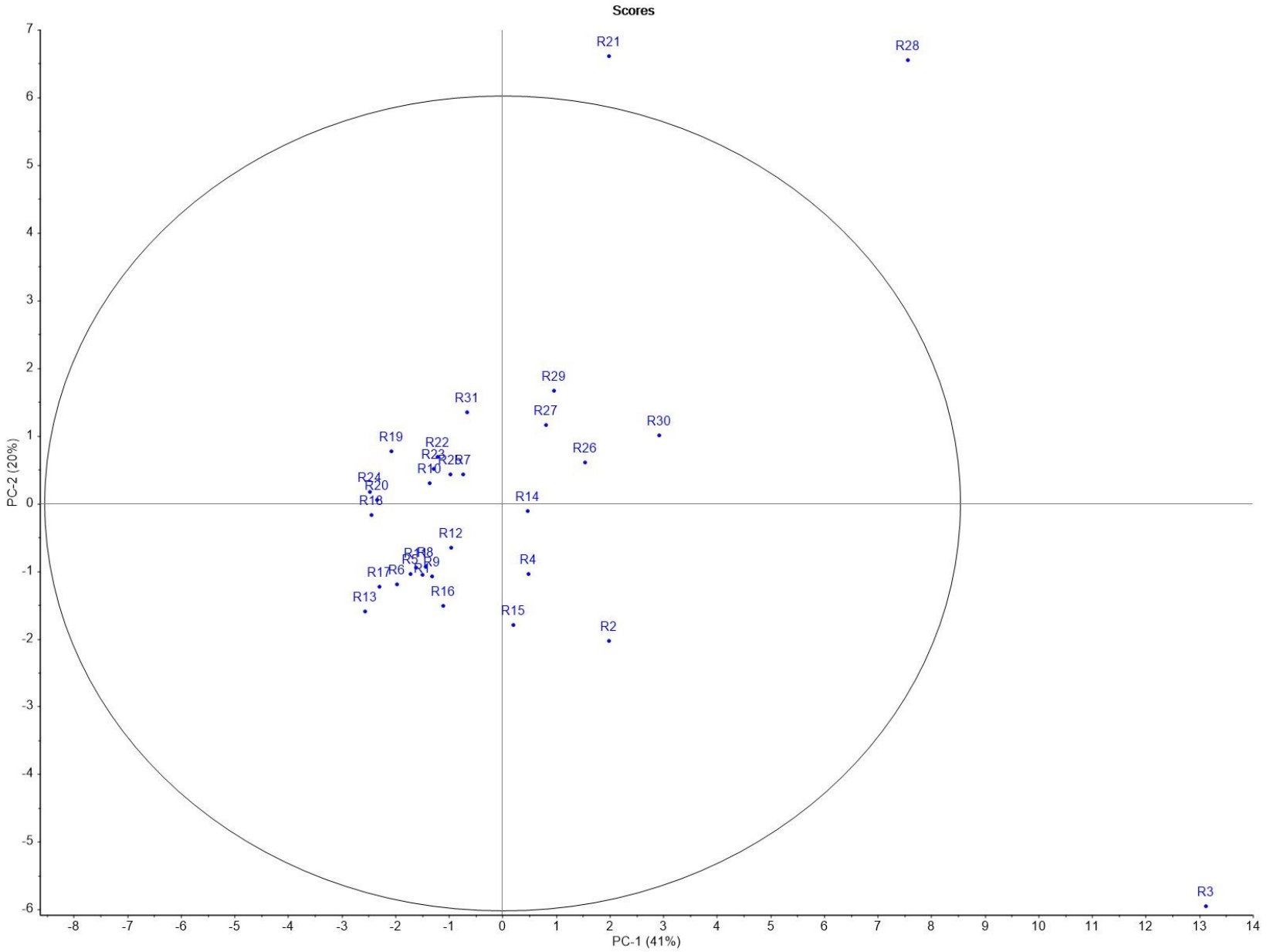

Figure 19: PCA score plot showing all the individual samples included in the dataset displayed as ID-numbers that can be found in Table D1. PC1 explains 41% of the total variance, and PC2 explains 20% of the total variance.

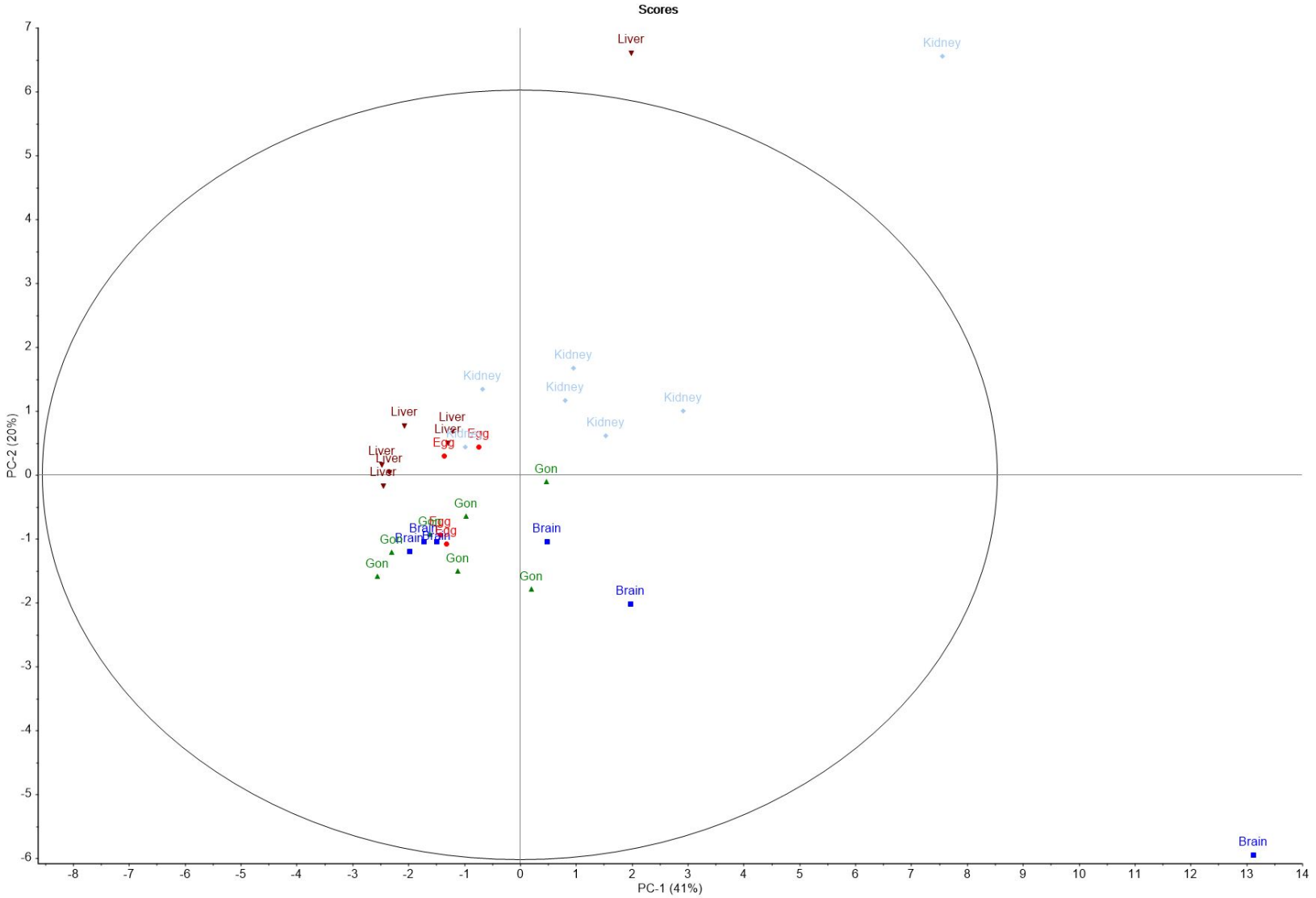

Figure 20: PCA score plot showing all the individual samples included in the dataset displayed as sample type i.e brain, gonad (Gon), hard roe (Egg), liver, and kidney. PC1 explains 41% of the total variance, and PC2 explains 20% of the total variance.

5.5.3 Elemental methodology

Quality control steps included for the elemental analysis in fish tissues included analysis of blanks, analysis of duplicates, and analysis of several reference materials that contain certified ranges of trace elements. The accuracy of elemental analysis was tested using CRM; DORM-5 fish protein, DOLT-3 dogfish liver, Seronorm^{TM} trace elements whole blood L-2, and Seronorm^{TM} trace elements serum containing certified concentrations of trace elements. Percentage recovery (%) of elements concentrations analyzed in CRM and information on which element concentrations measured in CRM that fulfill the range of the certified values are given in Table C10. The detected trace element concentrations in tissues of Arctic char have not been corrected for recovery.

Samples were stored at -20°C until sample preparation to avoid analyte loss. Gloves were used during sample preparation to avoid contamination. During sample preparation, the equipment used was washed in between samples to avoid cross-contamination. Moreover, the sample preparation was conducted starting from the expected lowest to highest levels of trace elements. Additionally, during sample preparation, EtOH was used to wash and dry the knife that was used for cutting the organs into smaller pieces. However, the EtOH used contained small amounts of trace elements ($\leq$ 0.01-0.1 ppm); Al, Ba, Ca, Cd, Co, Cr, Cu, Fe, and Mg, which can potentially constitute a source of contamination. However, as the EtOH was properly evaporated after washing it is only regarded as a minor source. Similarly, the HNO_3 used for digestion of the samples also contains minor amounts of some trace elements such as Si, Ti, Cr, and Fe, however, this was corrected for using method blanks. The use of HNO_3 for digestion is widely used for environmental and biological samples, however, HNO_3 does not dissolve all elements completely, and the recovery for some trace elements might be lower because of that. However, no precipitation was noticed in any of the samples after acid digestion. Some deviations were seen in the levels measured compared to the certified ranges for some elements, however, these differences were not notably great and considered close to the certified value for most elements. However, in the CRMs DORM-5 and DOLT-3 recoveries (%) of Hg were outside the certified range, however, most notably for DOLT-3 with a recovery of 57%. Furthermore, after acid digestion, two of the samples were yellow colored which might have been caused by the high lipid content in some of the samples. Some studies have described that in samples containing a high amount of organic material, improved recovery can be obtained by adding a strong oxidizing agent such as hydrogen peroxide (H_2O_2) in addition to the mineral acids [169, 178, 167]. Furthermore, the agate mortar and pestle used to crush the tissue sample might contribute to small amounts of trace elements but the material is heterogenic therefore differences in the element content of the mortars might occur. Studies have indicated that agate mortar and pestle is considered

a good choice of material for soft samples that do not cause hard abrasion on the material [244, 245, 246].

During sampling, quality control measures from an ISO 23893-1:2007(E) [198] on fish sampling were followed as close as possible. Tissues of Artic char were collected and wrapped in alumina foil for storage. Due to the possibility of contamination of Al from the alumina foil, this element was not included in the results and discussion section [247]. Moreover, Al-foil might contain some other trace elements, which can constitute a source of contamination. Information on other trace elements in the alumina foil was not possible to find. However, food-grade alumina foil has strict requirements concerning purity, and the Al content is usually at least 99%. Therefore, other trace elements from the foil are regarded as a negligible sources.

5.6 Limitations of the study and recommendations for improvements in future work

The main limitation of this study is the number of samples. Seven Arctic char were caught on one day of fieldwork. Due to economical constraints, only one day of fieldwork was possible. Additionally, conducting fieldwork in the Arctic can be challenging sometimes due to unpredictable weather. To get to the sampling location, boat transportation to the west side of Mitrahalvøya was necessary, and from there we went to the sampling location. The transport back and forth took some time, which meant less time for fishing. The small number of samples might not represent the general health status of the Arctic char population in Lake Diesetvatent as there are considerable variations in the fish that was caught. Therefore, several assumptions are made on a small number of samples. An increased number of samples would have improved the understanding of the accumulation patterns in Arctic char from Lake Diesetvatnet. However, this study indicates that fish in remote locations are exposed to contaminants transported from lower latitudes.

Several factors are not accounted for in this study which needs further investigation. During fieldwork, biometric measurements such as the age of the fish were not conducted. The original plan was to bring a biologist to fieldwork but due to an injury, this person could not participate. Age is recommended to determine as it provides useful information when evaluating contaminant levels in fish. Age can be determined by otolith readings [10]. The length is also an indication of the age of the fish, however, the length relationship would most likely be different for landlocked and anadromous Arctic char due to their different growth pattern. One report from the Norwegian Directorate of Water Resources and Energy provided a length- to age relationship (Figure 2-26, p.36) in anadromous and landlocked

Arctic char from Lake Vårfluesjøen at Svalbard [10]. This length-age relationship shows that anadromous Arctic char on a general basis is bigger than landlocked individuals. Landlocked individuals from Vårfluesjøen have a growth that often stagnates at around 12-18 cm, whereas anadromous Arctic char can become up to 50 cm. This might indicate that the Arctic char collected from Lake Disetvatnet were anadromous as most of the individuals were around ±50 cm in length, except for individual number 4 (Table 4). However, these are results that are taken from another Lake at Svalbard, and differences between these Arctic char populations must be taken into account. The results from this report can therefore not be extrapolated directly. Similarly, maternity could not be confirmed for all of the fish due to the lack of a biologist during fieldwork. Moreover, the whole body of the fish could not be brought back to NTNU for evaluation due to weight limitations on the flight from Ny-Ålesund. Maternity was therefore only confirmed for 4 of the fish where hard roe was observed in the body cavity of fish number 3, 5, 6, and 7. Moreover, the determination of anadromous and landlocked Artic char would have provided useful information about their lifestyle, however, this was not conducted. This is recommended to be included in future studies as these two forms of Artic char grow differently. Additionally, anadromous Arctic char are exposed to contaminants differently due to their annual migration to the Ocean. The distinction between anadromous and landlocked forms can be conducted by analysis of the relative abundance of carbon isotope ratio (δ^{13}C), which will provide information about their diet, feeding location, and habitat (marine or terrestrial). Additionally, measurement of nitrogen isotope ratio (δ^{15}N) in muscle or blood samples can provide information about the trophic position of Arctic char [46]. Moreover, the difference in contaminant loads between genders could not be evaluated because only one male fish was caught.

Some additional thoughts on the improvement of the study are the inclusion of muscle samples as it would provide a better foundation for comparison to previous studies conducted on Arctic char. Previous studies on Arctic char have mainly analyzed contaminants in muscle tissue. Additionally, muscle samples would have provided useful regarding human health and consumption of Artic char. However, this study aimed to determine which tissues trace elements accumulate, and therefore metabolic and detoxifying tissues are more relevant. Moreover, several studies suggest that gills are appropriate tissue for monitoring trace elements in the water. Therefore it is recommended to include gills in the sampling as it can provide information on the trace elements in the aquatic environment. Additionally, including a field blank would have improved the quality control of the sampling procedure, and possibly given more information about contamination from the soil and surrounding environment. The dissection of the fish was conducted in the field, contamination from the soil can therefore not be entirely excluded. However, quality control steps were included

during the sampling to avoid contamination. The use of gloves to avoid contamination from the hands, which were exchanged between each fish to avoid cross-contamination. The knife was washed in the water in between each fish, and samples were stored in separate plastic bags during transportation and further stored at -20°C until sample preparation to avoid contaminant loss and degradation of the samples. Furthermore, the inclusion of sediment and water samples would have provided useful information regarding which trace elements are enriched in the bedrock and water, which can provide additional information on which trace elements that accumulate in fish. Water samples from Lake Diesetvatnet were taken, however, these were only analyzed for water parameters such as pH, conductivity, turbidity, and redox conditions. The outcome of this study could therefore be improved by collecting an increased number of Arctic char and including biometric measurements in correlation to contamination levels as well as samples from the abiotic environment that could provide information about the exposure levels for Arctic char.

6 Conclusion

In the present study levels of steroid hormones, PFAS, and trace elements were determined in seven Artic char collected from Lake Diesetvatnet at Svalbard. Steroid hormones and PFAS were quantified in plasma, and a total of 41 trace elements were measured in various tissues of Artic char including the brain, gonad, hard roe, liver, kidney, RBC, and plasma.

Four steroid hormones were observed in the plasma of Arctic char including AN, TS, and DHT with mean concentrations of 6.43±3.55 ng mL^{-1}, 15.3±13.2 ng mL^{-1}, and 20.0±8.50 ng mL^{-1}. Additionally, 11-KetoTS was observed in one plasma sample at a concentration of 18.7 ng mL^{-1}. The observed steroid hormones are androgen hormones that are responsible for male sexual characteristics, and these hormones play an important role in the reproductive cycle [203]. Moreover, androgens are precursors of estrogenic steroid hormones, and therefore present in both male and female Arctic char. Sexual maturation and the reproductive cycle are processes that are associated with an increase in circulating steroid sex hormones, and the timing of sampling coincided with the pre-spawning season of Arctic char which might reflect in the levels of steroid hormones [11].

To the best of my knowledge, this is the first study to report on PFAS contamination in the plasma of Arctic char. Total PFAS concentration detected in the plasma of Arctic char from Lake Diesetvatnet; 26.8±5.98 ng mL^{-1}, was about 5 to 100 times higher compared to previous studies on Arctic char that have analyzed PFAS in liver and muscle tissue. In the present study, the higher levels of PFAS observed in Artic char might be explained by the higher content of proteins in plasma compared to muscle and liver tissues [69, 211]. Previous studies have reported that PFAS tends to accumulate in protein-rich matrices such as plasma. Protein levels in plasma were not measured in the present study, therefore, protein content cannot be concluded to be the main cause of higher levels of PFAS. In total, 9 PFAS compounds were observed in the plasma of Arctic char including 6:2 FTS, PFNA, PFOSA, PFOS, PFDA, PFUnA, PFDoDA, PFTriDA, and PFECHS. The 9 PFAS compounds that were observed in the plasma were dominated by carbon chain lengths of C8 to C13. The observation of long-chain PFAS (6 C $\geq$ for PFSA and 8 C $\geq$ for PFCA) is in accordance with previous literature indicating increased accumulation with increasing alkyl chain length [37, 36]. Four of the PFAS compounds were observed in all individual plasma samples with a mean percentage composition of total PFAS burden: 6:2 FTS (38%), PFUnA (20%), PFOS (20%), and PFNA (8%). Perfluoroalkyl sulfonate and carboxylate compounds accounted for 58% and 28% of the total PFAS burden, respectively. This observation supports the literature indicating that sulfonate compounds are more frequently detected than carboxylate compounds in Arctic animals [6, 37]. Arctic char from Lake Diesetvatnet are exposed to

PFAS mainly from long-range transport due to its remote location. However, secondary sources such as glacial meltwater might contribute to the input of PFAS in Lake Disetvatnet. Moreover, minor sources such as fishermen, migrating anadromous Arctic char, and seabirds might act as vectors for contamination to the Lake.

The concentration of steroid hormones and PFAS in plasma were below LOD estimated from the calibration curve method, however, this method for estimating LOD was not optimal, and provided unreasonable high values for LOD and LOQ. Estimations of LOD based on S/N peak height provided concentrations above LOD. Additionally, extraction method tests were performed to find a suitable extraction method for PFAS and steroid hormones in liver tissue. However, none of the tested methods proved satisfactory regarding method performance. Due to time limitations in the present study, further investigations on method improvements were not conducted. The results indicated the need for improvements for both extraction efficiency and matrix removal. Implementing an additional clean-up step might improve the performance outcome.

Multivariate principal component analysis (PCA) was performed to investigate the distribution of selected trace elements including Hg, Cd, Pb, As, Cu, Zn, Ni, Cr, Se, Mn Co, and Tl in various tissues of Arctic char. The PCA analysis indicated that trace elements were differently distributed within tissues of Arctic char. Kidney samples correlated strongly to trace elements such as Hg, Cd, Se, and Tl, while Cu correlated with liver samples. This could be confirmed by the higher levels measured in these tissues. Moreover, a strong correlation between Hg and Se was found with PCA, this is expected due to the suggested protective effect of Se on Hg toxicity [119]. The molar ratio of Se:Hg were above 1 in all tissues in Arctic char, indicating a protective effect of Se against Hg toxicity.

The PCA also identified outliers, and of special interest elevated levels of Cd and Hg in the kidney and liver of about one order of magnitude were observed in Arctic char number 4. Arsenic indicated no distribution pattern in the tissues of Arctic char. However, As correlated strongly with the gonad sample of Arctic char number 4 which measured the highest As the concentration of all samples. Arctic char number 4 which was the smallest individual had the poorest body condition and hepatosomatic index. Moreover, tapeworms were detected in the stomach of this fish. These findings might indicate that Arctic char with poor body condition is more prone to accumulate contaminants. Another explanation could be the age of this individual. However, this needs to be further investigated as no data were available to conclude this. Pb did not exhibit the same distribution pattern as Hg and Cd but was associated with the brain. However, elevated levels of Pb in the brain might have been caused by one outlier that might have been contaminated by the soil. After removing this outlier from the PCA, trace elements Co, Cr, and Ni were also associated with

elevated levels in the kidney, while Tl, Se, Hg, and Zn correlated more strongly with the liver samples. Interestingly, Co indicated the potential to accumulate in the kidney similar to Cd.

The non-essential trace elements Hg, Cd, Pb, and As were expected to be found at elevated levels in the kidney and liver. This was statistically tested with the non-parametric Kruskal Wallis test followed by multiple pairwise comparisons using Dunn's test for post-hoc analysis with Holm adjustments. Hg concentration in kidney samples was significantly higher than the Hg concentration in plasma ($p < 0.01$), but the Hg concentration in liver samples was not significantly higher than in any of the tissues. The Cd concentration in the kidney was significantly higher than Cd levels in the brain, gonad, and hard roe ($p < 0.01$). The concentration of Cd in the liver was not significantly higher in none of the other tissues. Concentrations of Pb were not significantly higher in the liver or kidney, or any of the other tissues. The concentration of As in kidney samples was significantly higher than As levels in RBC and plasma ($p < 0.01$). As concentration in the liver was not significantly different. However, As concentration in the gonad was found to be significantly higher than the As concentrations in RBC and plasma ($p < 0.01$). The results on trace element levels in Arctic char from Lake Diesetvatnet indicate that Hg, Cd, and As have the potential to accumulate in the kidney. Trace elements in Lake Diesetvatnet might derive from both natural and anthropogenic sources, however, the relative contributions are difficult to determine without samples from the local bedrock and sediment in the Lake.

This project outcome consists of a new batch of innovative data on contamination in Arctic char from Lake Diesetvatnet and supports the scientific research on Arctic freshwater ecosystems. Moreover, this study has contributed with data on elemental levels in various tissues of Arctic char, and observations of PFAS in plasma of Arctic char. The levels of PFAS and trace elements were low, however, the results indicate the presence of contaminants that have been long-range transported to Arctic areas as no point sources have been identified in the vicinity of Lake Diesetvatnet. Due to the low number of samples the results presented in this study only provide preliminary indications, and therefore future studies are suggested to continue the research of Arctic char from Lake Diesetvatnet. Future investigation of biometric variables such as age, gender, length, and lifestyle in correlation to contaminant levels is suggested to be implemented to better understand the accumulation patterns in this population. Additionally, including samples from the Lake water and sediment for analysis of these contaminants can provide a better understanding of the exposure level of Arctic char in Lake Diesetvatnet.

References

[1] AMAP. *AMAP Assessment 2011: Mercury in the Arctic*, page 193. Arctic Monitoring and Assessment Programme (AMAP). Oslo, Norway., 2011.

[2] AMAP. *AMAP Assessment 2018: Biological Effects of Contaminants on Arctic Wildlife and Fish*, page 84. Arctic Monitoring and Assessment Programme (AMAP) Tromsø, Norway, 2018.

[3] I.C Burkow and R Kallenborn. Sources and transport of persistent pollutants to the arctic. *Toxicology letters*, 112:87–92, 2000. doi: https://doi.org/10.1016/S0378-4274(99)00254-4.

[4] United Nations Environment Programme: The Stockholm Convention. The new pops under the stockholm convention, 2009. URL `http://chm.pops.int/TheConvention/ThePOPs/TheNewPOPs/tabid/2511/Default.aspx`.

[5] United Nations Environment Programme: The Stockholm Convention. The new pops under the stockholm convention, 2019. URL `http://chm.pops.int/TheConvention/ThePOPs/TheNewPOPs/tabid/2511/Default.aspx`.

[6] AMAP. *AMAP Assessment 2016: Chemicals of Emerging Arctic Concern*, page 353. Arctic Monitoring and Assessment Programme (AMAP), 2017.

[7] United Nations Environment Programme. Minamata convention on mercury: text and annexes, 2013. URL `https://wedocs.unep.org/20.500.11822/8541`.

[8] AMAP. *AMAP Assessment 2021: Mercury in the Arctic.*, page 324. Arctic Monitoring and Assessment Programme (AMAP), Tromsø, Norway., 2021. ISBN 978-82-7971-106-3.

[9] M.A Svenning. Metodikk for prøvefiske etter røye på svalbard. *NINA rapport*, 2010.

[10] A.K Brittain, J.E Schartau and M.A Svenning. Biologisk mangfold i ferskvann på svalbard: kunnskapsgrunnlag, påvirkninger og forslag til framtidig overvåking. *NVE Rapport 13*, 2020.

[11] E.H Jørgensen and H.K Johnsen. Rhythmic life of the arctic charr: adaptations to life at the edge. *Marine Genomics*, 14:71–81, 2014. doi: https://doi.org/10.1016/j.margen.2013.10.005.

[12] A Evenset, J Carroll, GN Christensen, R. Kallenborn, D Gregor, and G.W Gabrielsen. Seabird guano is an efficient conveyer of persistent organic pollutants (pops) to arctic lake ecosystems. *Environmental Science & Technology*, 41(4):1173–1179, 2007. doi: https://doi.org/10.1021/es0621142.

[13] Henrik Kylin, Johan Hammar, Jacques Mowrer, Henk Bouwman, Carl Edelstam, Mats Olsson, and Sören Jensen. Persistent organic pollutants in biota samples collected during the ymer-80 expedition to the arctic. *Polar Research*, 34(1):21129, 2015.

[14] Yuyu Jia, Lin Wang, Zhipeng Qu, Chaoyi Wang, and Zhaoguang Yang. Effects on heavy metal accumulation in freshwater fishes: species, tissues, and sizes. *Environmental Science and Pollution Research*, 24(10):9379–9386, 2017.

[15] Hazrat Ali and Ezzat Khan. Bioaccumulation of non-essential hazardous heavy metals and metalloids in freshwater fish. risk to human health. *Environmental chemistry letters*, 16(3):903–917, 2018.

[16] K. Halbach, Ø. Mikkelsen, T. Berg, and E. Steinnes. The presence of mercury and other trace metals in surface soils in the norwegian arctic. *Chemosphere*, 188:567–574, 2017. doi: https://doi.org/10.1016/j.chemosphere.2017.09.012.

[17] A Evenset, J Carroll, GN Christensen, R Kallenborn, D Gregor, and GW Gabrielsen. Seabird guano is an efficient conveyer of persistent organic pollutants (pops) to arctic lake ecosystems. *Environmental Science & Technology*, 41(4):1173–1179, 2007. doi: https://doi.org/10.1021/es0621142.

[18] AMAP. *AMAP Assessment 2020: POPs and Chemicals of Emerging Arctic Concern: Influence of Climate Change*, page 134. Arctic Monitoring and Assessment Programme (AMAP), Tromsø, Norway, 2020.

[19] Glenn E Shaw. The arctic haze phenomenon. *Bulletin of the American Meteorological Society*, 76(12):2403–2414, 1995.

[20] PK Quinn, TL Miller, TS Bates, JA Ogren, E Andrews, and GE Shaw. A 3-year record of simultaneously measured aerosol chemical and optical properties at barrow, alaska. *Journal of Geophysical Research: Atmospheres*, 107(D11):AAC–8, 2002.

[21] Ping Gong and Xiaoping Wang. Critical roles of secondary sources in global cycling of persistent organic pollutants under climate change. *Journal of Hazardous Materials Advances*, 6:100064, 2022. doi: https://doi.org/10.1016/j.hazadv.2022.100064.

[22] Karen Y Kwok, Eriko Yamazaki, Nobuyoshi Yamashita, Sachi Taniyasu, Margaret B Murphy, Yuichi Horii, Gert Petrick, Roland Kallerborn, Kurunthachalam Kannan, Kentaro Murano, et al. Transport of perfluoroalkyl substances (pfas) from an arctic glacier to downstream locations: implications for sources. *Science of the total environment*, 447:46–55, 2013. doi: https://doi.org/10.1016/j.scitotenv.2012.10.091.

[23] F. Wania and D. Mackay. Peer reviewed: tracking the distribution of persistent organic pollutants. *Environmental science & technology*, 30(9):390A–396A, 1996.

[24] Alena Dekhtyareva, Kåre Edvardsen, Kim Holmén, Ove Hermansen, and Hans-Christen Hansson. Influence of local and regional air pollution on atmospheric measurements in ny-ålesund. *ATMOPART Final report*, 2016.

[25] Tatiana Drotikova, Aasim M Ali, Anne Karine Halse, Helena C Reinardy, and Roland Kallenborn. Polycyclic aromatic hydrocarbons (pahs) and oxy-and nitro-pahs in ambient air of the arctic town longyearbyen, svalbard. *Atmospheric Chemistry and Physics*, 20(16):9997–10014, 2020.

[26] A. Kalinowska, M. Szopińska, S. Chmiel, M. Kończak, Ż. Polkowska, W. Artichowicz, K. Jankowska, A. Nowak, and A. Łuczkiewicz. Heavy metals in a high arctic fiord and their introduction with the wastewater: A case study of adventfjorden-longyearbyen system, svalbard. *Water*, 12(3):794, 2020. doi: https://doi.org/10.3390/w12030794.

[27] L. Ahrens, J. Rakovic, S. Axelson, and R. Kallenborn. Source tracking and impact of per-and polyfluoroalkyl substances at svalbard–fluorosimpact–. In *Svalbard Final Report Notes 3-17*. UNIS, 2016.

[28] J.S Skaar, E.M. Ræder, J.L. Lyche, L. Ahrens, and R. Kallenborn. Elucidation of contamination sources for poly-and perfluoroalkyl substances (pfass) on svalbard (norwegian arctic). *Environmental Science and Pollution Research*, 26(8):7356–7363, 2019.

[29] H. Dørum and G.W. Gabrielsen. Vadefugler i kongsfjorden, svalbard. 2021.

[30] Maria Granberg, Lisa Winberg von Friesen, Lis Bach, France Collard, Geir Wing Gabrielsen, and Jakob Strand. Anthropogenic microlitter in wastewater and marine samples from ny-ålesund, barentsburg and signehamna, svalbard. 2019.

[31] Lisa W von Friesen, Maria E Granberg, Olga Pavlova, Kerstin Magnusson, Martin Hassellöv, and Geir W Gabrielsen. Summer sea ice melt and wastewater are important local sources of microlitter to svalbard waters. *Environment International*, 139:105511, 2020.

[32] Alessandra Amore, Fabio Giardi, Silvia Becagli, Laura Caiazzo, Mauro Mazzola, Mirko Severi, and Rita Traversi. Source apportionment of sulphate in the high arctic by a 10 yr-long record from gruvebadet observatory (ny-ålesund, svalbard islands). *Atmospheric Environment*, 270:118890, 2022.

[33] Torunn Berg, Roland Kallenborn, and Stein Manø. Temporal trends in atmospheric heavy metal and organochlorine concentrations at zeppelin, svalbard. *Arctic, Antarctic, and Alpine Research*, 36(3):284–291, 2004.

[34] RA Roth and Luyendyk JP JH. Casarett & doull's toxicology: The basic science of poisons. *McGraw-Hill Education, New York*, 2019.

[35] Frank APC Gobas, Barry C Kelly, and Jon A Arnot. Quantitative structure activity relationships for predicting the bioaccumulation of pops in terrestrial food-webs. *QSAR & combinatorial science*, 22(3):329–336, 2003.

[36] Jonathan W Martin, Scott A Mabury, Keith R Solomon, and Derek CG Muir. Dietary accumulation of perfluorinated acids in juvenile rainbow trout (oncorhynchus mykiss). *Environmental Toxicology and Chemistry: An International Journal*, 22(1):189–195, 2003.

[37] Jonathan W Martin, Scott A Mabury, Keith R Solomon, and Derek CG Muir. Bioconcentration and tissue distribution of perfluorinated acids in rainbow trout (oncorhynchus mykiss). *Environmental Toxicology and Chemistry: An International Journal*, 22(1):196–204, 2003.

[38] Marianne Haukås, Urs Berger, Haakon Hop, Bjørn Gulliksen, and Geir W Gabrielsen. Bioaccumulation of per-and polyfluorinated alkyl substances (pfas) in selected species from the barents sea food web. *Environmental Pollution*, 148(1):360–371, 2007.

[39] D.M Lemal. Perspective on fluorocarbon chemistry. *The Journal of organic chemistry*, 69(1):1–11, 2004. doi: https://doi.org/10.1021/jo0302556.

[40] Rossana Bossi, Maria Dam, and Frank F Rigét. Perfluorinated alkyl substances (pfas) in terrestrial environments in greenland and faroe islands. *Chemosphere*, 129:164–169, 2015. doi: https://doi.org/10.1016/j.chemosphere.2014.11.044.

[41] D.A Ellis, J.W Martin, A.O De Silva, S.A Mabury, M.D Hurley, M.P Sulbaek Andersen, and T.J Wallington. Degradation of fluorotelomer alcohols: a likely atmospheric source of perfluorinated carboxylic acids. *Environmental science & technology*, 38(12): 3316–3321, 2004. doi: https://doi.org/10.1021/es049860w.

[42] Kurt R Rhoads, Elisabeth M-L Janssen, Richard G Luthy, and Craig S Criddle. Aerobic biotransformation and fate of n-ethyl perfluorooctane sulfonamidoethanol (n-etfose) in activated sludge. *Environmental science & technology*, 42(8):2873–2878, 2008. doi: https://doi.org/10.1021/es702866c.

[43] J.W. Martin, D.A. Ellis, S.A. Mabury, M.D. Hurley, and T.J. Wallington. Atmospheric chemistry of perfluoroalkanesulfonamides: kinetic and product studies of the oh radical and cl atom initiated oxidation of n-ethyl perfluorobutanesulfonamide. *Environmental science & technology*, 40(3):864–872, 2006. doi: https://doi.org/10.1021/es051362f.

[44] L. Ahrens. Polyfluoroalkyl compounds in the aquatic environment: a review of their occurrence and fate. *Journal of Environmental Monitoring*, 13(1):20–31, 2011. doi: 10.1039/C0EM00373E.

[45] Lutz Ahrens, Sachi Taniyasu, Leo WY Yeung, Nobuyoshi Yamashita, Paul KS Lam, and Ralf Ebinghaus. Distribution of polyfluoroalkyl compounds in water, suspended particulate matter and sediment from tokyo bay, japan. *Chemosphere*, 79(3):266–272, 2010. doi: https://doi.org/10.1016/j.chemosphere.2010.01.045.

[46] Gretchen L Lescord, Karen A Kidd, Amila O De Silva, Mary Williamson, Christine Spencer, Xiaowa Wang, and Derek CG Muir. Perfluorinated and polyfluorinated compounds in lake food webs from the canadian high arctic. *Environmental science & technology*, 49(5):2694–2702, 2015. doi: https://doi.org/10.1021/es5048649.

[47] David A. Ellis, Jonathan W. Martin, Amila O. De Silva, Scott A. Mabury, Michael D. Hurley, Mads P. Sulbaek Andersen, and Timothy J. Wallington. Degradation of fluorotelomer alcohols: A likely atmospheric source of perfluorinated carboxylic acids. *Environmental Science & Technology*, 38(12):3316–3321, 2004. doi: 10.1021/es049860w.

[48] J. W. Martin, D. A. Ellis, S. A. Mabury, M. D. Hurley, and T. J. Wallington. Atmospheric chemistry of perfluoroalkanesulfonamides: Kinetic and product studies of the oh radical and cl atom initiated oxidation of n-ethyl perfluorobutanesulfonamide. *Environmental Science & Technology*, 40(3):864–872, 2006. doi: 10.1021/es051362f.

[49] D.A. Ellis, J.W. Martin, A.O. De Silva, S.A. Mabury, M.D. Hurley, M.P. Sulbaek Andersen, and T.J. Wallington. Degradation of fluorotelomer alcohols: a likely atmospheric source of perfluorinated carboxylic acids. *Environmental science & technology*, 38(12):3316–3321, 2004. doi: https://doi.org/10.1021/es049860w.

[50] N. Yamashita, K. Kannan, S. Taniyasu, Y. Horii, G. Petrick, and T. Gamo. A global survey of perfluorinated acids in oceans. *Marine pollution bulletin*, 51(8-12):658–668, 2005. doi: https://doi.org/10.1016/j.envpol.2012.06.004.

[51] H. Joerss, Z. Xie, C.C Wagner, W.J Von Appen, E.M Sunderland, and R. Ebinghaus. Transport of legacy perfluoroalkyl substances and the replacement compound hfpo-da through the atlantic gateway to the arctic ocean—is the arctic a sink or a source? *Environmental science & technology*, 54(16):9958–9967, 2020. doi: https://doi.org/10.1021/acs.est.0c00228.

[52] Z. Zhao, Z. Xie, A. Möller, R. Sturm, J. Tang, G. Zhang, and R. Ebinghaus. Distribution and long-range transport of polyfluoroalkyl substances in the arctic, atlantic ocean and antarctic coast. *Environmental pollution*, 170:71–77, 2012. doi: https://doi.org/10.1016/j.envpol.2012.06.004.

[53] J. MacInnis, A.O. De Silva, I. Lehnherr, D.C.G. Muir, K.A.S. Pierre, V.L.S. Louis, and C. Spencer. Investigation of perfluoroalkyl substances in proglacial rivers and permafrost seep in a high arctic watershed. *Environmental Science: Processes & Impacts*, 2022. doi: 10.1039/D1EM00349F.

[54] Jack Garnett, Crispin Halsall, Anna Vader, Hanna Joerss, Ralf Ebinghaus, Amber Leeson, and Peter M Wynn. High concentrations of perfluoroalkyl acids in arctic seawater driven by early thawing sea ice. *Environmental science & technology*, 55(16): 11049–11059, 2021. doi: https://doi.org/10.1021/acs.est.1c01676.

[55] C.M Butt, U. Berger, R. Bossi, and G.T. Tomy. Levels and trends of poly-and perfluorinated compounds in the arctic environment. *Science of the total environment*, 408 (15):2936–2965, 2010. doi: https://doi.org/10.1016/j.scitotenv.2010.03.015.

[56] OECD. Toward a new comprehensive global database of per-and polyfluoroalkyl substances (pfass): Summary report on updating the oecd 2007 list of per-and polyfluoroalkyl substances (pfass). *Organisation for Economic Cooperation and Development (OECD)*, Series on Risk Management No. 39, 2018. doi: https://www.oecd.org/officialdocuments/publicdisplaydocumentpdf/?cote=ENV-JM-MONO(2018)7doclanguage=en.

[57] R.C. Buck, S.H. Korzeniowski, E. Laganis, and F. Adamsky. Identification and classification of commercially relevant per-and poly-fluoroalkyl substances (pfas). *Integrated Environmental Assessment and Management*, 17(5):1045–1055, 2021. doi: https://doi.org/10.1002/ieam.4450.

[58] John P Giesy and Kurunthachalam Kannan. Global distribution of perfluorooctane sulfonate in wildlife. *Environmental science & technology*, 35(7):1339–1342, 2001. doi: https://doi.org/10.1021/es001834k.

[59] United Nations Environment Programme: The Stockholm Convention. Chemicals proposed for listing under the stockholm, 2017. URL `http://www.pops.int/TheConvention/ThePOPs/ChemicalsProposedforListing/tabid/2510/De`

[60] H Joerss, Z Xie, C.C Wagner, W.J Von Appen, E.M Sunderland, and R Ebinghaus. Transport of legacy perfluoroalkyl substances and the replacement compound hfpo-da through the atlantic gateway to the arctic ocean—is the arctic a sink or a source? *Environmental science & technology*, 54(16):9958–9967, 2020. doi: https://doi.org/10.1021/acs.est.0c00228.

[61] Z. Wang, I.T. Cousins, M. Scheringer, and K. Hungerbuhler. Fluorinated alternatives to long-chain perfluoroalkyl carboxylic acids (pfcas), perfluoroalkane sulfonic acids (pfsas) and their potential precursors. *Environment international*, 60:242–248, 2013. doi: https://doi.org/10.1016/j.envint.2013.08.021.

[62] John J MacInnis, Igor Lehnherr, Derek CG Muir, Roberto Quinlan, and Amila O De Silva. Characterization of perfluoroalkyl substances in sediment cores from high and low arctic lakes in canada. *Science of the Total Environment*, 666:414–422, 2019.

[63] John J MacInnis, Igor Lehnherr, Derek CG Muir, Kyra A St. Pierre, Vincent L St. Louis, Christine Spencer, and Amila O De Silva. Fate and transport of perfluoroalkyl substances from snowpacks into a lake in the high arctic of canada. *Environmental science & technology*, 53(18):10753–10762, 2019.

[64] R. Kallenborn. *Perfluorinated alkylated substances (PFAS) in the Nordic environment*. Nordic Council of Ministers, 2004.

[65] Julie Veillette, Derek CG Muir, Dermot Antoniades, Jeff M Small, Christine Spencer, Tracey N Loewen, John A Babaluk, James D Reist, and Warwick F Vincent. Perfluorinated chemicals in meromictic lakes on the northern coast of ellesmere island, high arctic canada. *Arctic*, pages 245–256, 2012.

[66] L Ahrens, J Rakovic, S Axelson, and R Kallenborn. Source tracking and impact of per- and polyfluoroalkyl substances at svalbard–fluorosimpact–. In *Svalbard Final Report Notes 3-17*. UNIS, 2016.

[67] WA Bruggeman, LBJM Martron, D Kooiman, and O Hutzinger. Accumulation and elimination kinetics of di-, tri-and tetra chlorobiphenyls by goldfish after dietary and aqueous exposure. *Chemosphere*, 10(8):811–832, 1981.

[68] B Streit. Bioaccumulation processes in ecosystems. *Experientia*, 48(10):955–970, 1992.

[69] Carla A Ng and Konrad Hungerbuhler. Bioconcentration of perfluorinated alkyl acids: how important is specific binding? *Environmental science & technology*, 47(13):7214–7223, 2013.

[70] Geary W Olsen, Jean M Burris, David J Ehresman, John W Froehlich, Andrew M Seacat, John L Butenhoff, and Larry R Zobel. Half-life of serum elimination of perfluorooctanesulfonate, perfluorohexanesulfonate, and perfluorooctanoate in retired fluorochemical production workers. *Environmental health perspectives*, 115(9):1298–1305, 2007.

[71] Sandy Falk, Klaus Failing, Sebastian Georgii, Hubertus Brunn, and Thorsten Stahl. Tissue specific uptake and elimination of perfluoroalkyl acids (pfaas) in adult rainbow trout (oncorhynchus mykiss) after dietary exposure. *Chemosphere*, 129:150–156, 2015.

[72] Yali Shi, Robin Vestergren, Therese Haugdahl Nost, Zhen Zhou, and Yaqi Cai. Probing the differential tissue distribution and bioaccumulation behavior of per-and polyfluoroalkyl substances of varying chain-lengths, isomeric structures and functional groups in crucian carp. *Environmental science & technology*, 52(8):4592–4600, 2018.

[73] Shu Su, Paul D Jones, Jason C Raine, Zilin Yang, Yufeng Gong, Yuwei Xie, Jie Tang, Chao Wang, Xiaoli Zhao, and John P Giesy. Absorption and elimination of per and poly-fluoroalkyl substances substitutes in salmonid species after pre-fertilization exposure. *Science of The Total Environment*, 814:152547, 2022.

[74] Kathryn L Hassell, Timothy L Coggan, Tom Cresswell, Adam Kolobaric, Kathryn Berry, Nicholas D Crosbie, Judy Blackbeard, Vincent J Pettigrove, and Bradley O Clarke. Dietary uptake and depuration kinetics of perfluorooctane sulfonate, perfluorooctanoic acid, and hexafluoropropylene oxide dimer acid (genx) in a benthic fish. *Environmental Toxicology and Chemistry*, 39(3):595–603, 2020.

[75] Yongbing Du, Xiongjie Shi, Chunsheng Liu, Ke Yu, and Bingsheng Zhou. Chronic effects of water-borne pfos exposure on growth, survival and hepatotoxicity in zebrafish: a partial life-cycle test. *Chemosphere*, 74(5):723–729, 2009.

[76] Su Keiter, Lisa Baumann, H Färber, Henrik Holbech, D Skutlarek, Magnus Engwall, and Thomas Braunbeck. Long-term effects of a binary mixture of perfluorooctane sulfonate (pfos) and bisphenol a (bpa) in zebrafish (danio rerio). *Aquatic toxicology*, 118:116–129, 2012.

[77] Lianguo Chen, James CW Lam, Chenyan Hu, Mirabelle MP Tsui, Paul KS Lam, and Bingsheng Zhou. Perfluorobutanesulfonate exposure skews sex ratio in fish and transgenerationally impairs reproduction. *Environmental Science & Technology*, 53 (14):8389–8397, 2019.

[78] Yongming Wu, Mi Deng, Yuanxiang Jin, Xin Liu, Zhaohuan Mai, Hailin You, Xiyan Mu, Xiaoli He, Reem Alharthi, Daniel Joseph Kostyniuk, et al. Toxicokinetics and toxic effects of a chinese pfos alternative f-53b in adult zebrafish. *Ecotoxicology and Environmental Safety*, 171:460–466, 2019.

[79] Gerald T Ankley, Douglas W Kuehl, Michael D Kahl, Kathleen M Jensen, Ann Linnum, Richard L Leino, and Dan A Villeneuve. Reproductive and developmental toxicity and bioconcentration of perfluorooctanesulfonate in a partial life-cycle test with the fathead minnow (pimephales promelas). *Environmental Toxicology and Chemistry: An International Journal*, 24(9):2316–2324, 2005.

[80] Ignacio A Rodríguez-Jorquera, R Cristina Colli-Dula, Kevin Kroll, B Sumith Jayasinghe, Maria V Parachu Marco, Cecilia Silva-Sanchez, Gurpal S Toor, and Nancy D Denslow. Blood transcriptomics analysis of fish exposed to perfluoro alkyls substances: assessment of a non-lethal sampling technique for advancing aquatic toxicology research. *Environmental science & technology*, 53(3):1441–1452, 2018.

[81] Lina Birgersson, Justin Jouve, Elisabeth Jönsson, Noomi Asker, Fredrik Andreasson, Oksana Golovko, Lutz Ahrens, and Joachim Sturve. Thyroid function and immune status in perch (perca fluviatilis) from lakes contaminated with pfass or pcbs. *Ecotoxicology and Environmental Safety*, 222:112495, 2021.

[82] Guohui Shi, Qianqian Cui, Hongxia Zhang, Ruina Cui, Yong Guo, and Jiayin Dai. Accumulation, biotransformation, and endocrine disruption effects of fluorotelomer surfactant mixtures on zebrafish. *Chemical Research in Toxicology*, 32(7):1432–1440, 2019.

[83] Frederick William Fifield and Peter J Haines. *Environmental analytical chemistry*, volume 2. Blackwell science London, 2000.

[84] Arctic Monitoring and Assessment Programme (AMAP). Amap assessment 2002: Heavy metals in the arctic. *Oslo, Norway*, pages xvi + 265 pp, 2005.

[85] William H Schroeder, KG Anlauf, LA Barrie, JY Lu, A Steffen, DR Schneeberger, and T Berg. Arctic springtime depletion of mercury. *Nature*, 394(6691):331–332, 1998.

[86] Raymond G Semkin, Greg Mierle, and Roy J Neureuther. Hydrochemistry and mercury cycling in a high arctic watershed. *Science of the Total Environment*, 342(1-3):199–221, 2005.

[87] Mina Nasr, Jae Ogilvie, Mark Castonguay, Andy Rencz, and Paul A Arp. Total hg concentrations in stream and lake sediments: Discerning geospatial patterns and controls across canada. *Applied geochemistry*, 26(11):1818–1831, 2011.

[88] Winifred K Dallmann. *Geoscience atlas of Svalbard*. Norsk polarinstitutt, 2015.

[89] TI Moiseenko and LP Kudryavtseva. Trace metal accumulation and fish pathologies in areas affected by mining and metallurgical enterprises in the kola region, russia. *Environmental Pollution*, 114(2):285–297, 2001.

[90] G Köck, M Triendl, and R Hofer. Seasonal patterns of metal accumulation in arctic char (salvelinus alpinus) from an oligotrophic alpine lake related to temperature. *Canadian Journal of Fisheries and Aquatic Sciences*, 53(4):780–786, 1996.

[91] K.E. Hudelson, D.C.G. Muir, P.E. Drevnick, G. Köck, D. Iqaluk, X. Wang, J.L. Kirk, B.D. Barst, A. Grgicak-Mannion, R. Shearon, et al. Temporal trends, lake-to-lake variation, and climate effects on arctic char (salvelinus alpinus) mercury concentrations from six high arctic lakes in nunavut, canada. *Science of The Total Environment*, 678: 801–812, 2019.

[92] TI Moiseenko and NA Gashkina. Distribution and bioaccumulation of heavy metals (hg, cd and pb) in fish: Influence of the aquatic environment and climate. *Environmental Research Letters*, 15(11):115013, 2020.

[93] John Chételat, Marc Amyot, Paul Arp, Jules M Blais, David Depew, Craig A Emmerton, Marlene Evans, Mary Gamberg, Nikolaus Gantner, Catherine Girard, et al. Mercury in freshwater ecosystems of the canadian arctic: Recent advances on its cycling and fate. *Science of the Total Environment*, 509:41–66, 2015.

[94] Gretchen L Lescord, Karen A Kidd, Jane L Kirk, Nelson J O'Driscoll, Xiaowa Wang, and Derek CG Muir. Factors affecting biotic mercury concentrations and biomagnification through lake food webs in the canadian high arctic. *Science of the Total Environment*, 509:195–205, 2015.

[95] Nikolaus Gantner, Derek C Muir, Michael Power, Deborah Iqaluk, James D Reist, John A Babaluk, Markus Meili, Hans Borg, Johan Hammar, Wendy Michaud, et al. Mercury concentrations in landlocked arctic char (salvelinus alpinus) from the canadian arctic. part ii: influence of lake biotic and abiotic characteristics on geographic trends in 27 populations. *Environmental Toxicology and Chemistry: An International Journal*, 29(3):633–643, 2010.

[96] Hans Fredrik V Braaten, Heleen A de Wit, Eirik Fjeld, Sigurd Rognerud, Espen Lydersen, and Thorjørn Larssen. Environmental factors influencing mercury speciation in subarctic and boreal lakes. *Science of the Total Environment*, 476:336–345, 2014.

[97] Alexandre J Poulain, Edenise Garcia, Marc Amyot, Peter GC Campbell, Farhad Raofie, and Parisa A Ariya. Biological and chemical redox transformations of mercury in fresh and salt waters of the high arctic during spring and summer. *Environmental science & technology*, 41(6):1883–1888, 2007.

[98] Chad R Hammerschmidt and William F Fitzgerald. Photodecomposition of methylmercury in an arctic alaskan lake. *Environmental science & technology*, 40 (4):1212–1216, 2006.

[99] DW Rodgers. You are what you eat and a little bit more: bioenergetics-based models of methylmercury accumulation in fish revisited. In *Mercury pollution intergration and synthesis*, pages 427–439. 1994.

[100] BD Hall, RA Bodaly, RJP Fudge, JWM Rudd, and DM Rosenberg. Food as the dominant pathway of methylmercury uptake by fish. *Water, Air, and Soil Pollution*, 100(1):13–24, 1997.

[101] C.A Oliveira Ribeiro, C. Rouleau, E. Pelletier, C. Audet, and H. Tjälve. Distribution kinetics of dietary methylmercury in the arctic charr (salvelinus alpinus). *Environmental science & technology*, 33(6):902–907, 1999.

[102] H.H. Harris, I.J. Pickering, and G.N. George. The chemical form of mercury in fish. *Science*, 301(5637):1203–1203, 2003.

[103] Jillian LA Van Walleghem, Paul J Blanchfield, and Holger Hintelmann. Elimination of mercury by yellow perch in the wild. *Environmental science & technology*, 41(16): 5895–5901, 2007.

[104] Mark B Sandheinrich and James G Wiener. Methylmercury in freshwater fish: recent advances in assessing toxicity of environmentally relevant exposures. *Environmental contaminants in biota*, pages 169–192, 2011.

[105] Rune Dietz, Christian Sonne, Niladri Basu, Birgit Braune, Todd O'Hara, Robert J Letcher, Tony Scheuhammer, Magnus Andersen, Claus Andreasen, Dennis Andriashek, et al. What are the toxicological effects of mercury in arctic biota? *Science of the Total Environment*, 443:775–790, 2013.

[106] Heidi Swanson, Nikolaus Gantner, Karen A Kidd, DCG Muir, and James D Reist. Comparison of mercury concentrations in landlocked, resident, and sea-run fish (salvelinus spp.) from nunavut, canada. *Environmental Toxicology and Chemistry*, 30(6): 1459–1467, 2011.

[107] Anton Scheuhammer, Birgit Braune, Hing Man Chan, Héloïse Frouin, Anke Krey, Robert Letcher, Lisa Loseto, Marie Noël, Sonja Ostertag, Peter Ross, et al. Recent progress on our understanding of the biological effects of mercury in fish and wildlife in the canadian arctic. *Science of the Total Environment*, 509:91–103, 2015.

[108] F Riget, G Asmund, and P Aastrup. Mercury in arctic char (salvelinus alpinus) populations from greenland. *Science of the Total Environment*, 245(1-3):161–172, 2000.

[109] S Van der Velden, MS Evans, JB Dempson, DCG Muir, and M Power. Comparative analysis of total mercury concentrations in anadromous and non-anadromous arctic charr (salvelinus alpinus) from eastern canada. *Science of the total environment*, 447: 438–449, 2013.

[110] S Van der Velden, JB Dempson, MS Evans, DCG Muir, and M Power. Basal mercury concentrations and biomagnification rates in freshwater and marine food webs: Effects on arctic charr (salvelinus alpinus) from eastern canada. *Science of the Total Environment*, 444:531–542, 2013.

[111] Derek Muir, Xiaowa Wang, Doug Bright, Lyle Lockhart, and Günter Köck. Spatial and temporal trends of mercury and other metals in landlocked char from lakes in the canadian arctic archipelago. *Science of the Total Environment*, 351:464–478, 2005.

[112] John Chételat, Marc Amyot, Paul Arp, Jules M Blais, David Depew, Craig A Emmerton, Marlene Evans, Mary Gamberg, Nikolaus Gantner, Catherine Girard, et al. Mercury in freshwater ecosystems of the canadian arctic: Recent advances on its cycling and fate. *Science of the Total Environment*, 509:41–66, 2015.

[113] Nikolaus Gantner, Michael Power, Deborah Iqaluk, Markus Meili, Hans Borg, Marcus Sundbom, Keith R Solomon, Greg Lawson, and Derek C Muir. Mercury concentrations in landlocked arctic char (salvelinus alpinus) from the canadian arctic. part i: insights from trophic relationships in 18 lakes. *Environmental Toxicology and Chemistry: An International Journal*, 29(3):621–632, 2010.

[114] Nancy Beckvar, Tom M Dillon, and Lorraine B Read. Approaches for linking whole-body fish tissue residues of mercury or ddt to biological effects thresholds. *Environmental Toxicology and Chemistry: An International Journal*, 24(8):2094–2105, 2005.

[115] E Scherer, RE McNicol, and RE Evans. Impairment of lake trout foraging by chronic exposure to cadmium: a black-box experiment. *Aquatic Toxicology*, 37(1):1–7, 1997.

[116] Marcela Gerpe, Peter Kling, and Per Erik Olsson. Metallothionein gene expression in arctic char (salvelinus alpinus) following metal and pcb exposure. *Marine environmental research*, 46(1-5):551–554, 1998.

[117] Reinhard Dallinger, Margit Egg, Günther Köck, and Rudolf Hofer. The role of metallothionein in cadmium accumulation of arctic char (salvelinus alpinus) from high alpine lakes. *Aquatic Toxicology*, 38(1-3):47–66, 1997.

[118] Nicholas VC Ralston and Laura J Raymond. Mercury's neurotoxicity is characterized by its disruption of selenium biochemistry. *Biochimica et Biophysica Acta (BBA)-General Subjects*, 1862(11):2405–2416, 2018.

[119] Eugen G Sørmo, Tomasz M Ciesielski, Ida B Øverjordet, Syverin Lierhagen, Grethe S Eggen, Torunn Berg, and Bjørn M Jenssen. Selenium moderates mercury toxicity in free-ranging freshwater fish. *Environmental science & technology*, 45(15):6561–6566, 2011.

[120] Helen F Cserr and Magnus Bundgaard. Blood-brain interfaces in vertebrates: a comparative approach. *American Journal of Physiology-Regulatory, Integrative and Comparative Physiology*, 246(3):R277–R288, 1984.

[121] Magnus Bundgaard and N Joan Abbott. All vertebrates started out with a glial blood-brain barrier 4–500 million years ago. *Glia*, 56(7):699–708, 2008.

[122] Kate L Crump and Vance L Trudeau. Mercury-induced reproductive impairment in fish. *Environmental Toxicology and Chemistry: An International Journal*, 28(5):895–907, 2009.

[123] Michael Aschner and Judy Lynn Aschner. Mercury neurotoxicity: mechanisms of blood-brain barrier transport. *Neuroscience & Biobehavioral Reviews*, 14(2):169–176, 1990.

[124] Michael A Miller. Maternal transfer of organochlorine compounds in salmonines to their eggs. *Canadian Journal of Fisheries and Aquatic Sciences*, 50(7):1405–1413, 1993.

[125] J Bytingsvik, M Frantzen, A Götsch, ES Heimstad, G Christensen, and A Evenset. Current status, between-year comparisons and maternal transfer of organohalogenated compounds (ohcs) in arctic char (salvelinus alpinus) from bjørnøya, svalbard (norway). *Science of the Total Environment*, 521:421–430, 2015.

[126] AJ Niimi. Biological and toxicologtcal effects of environmental contaminants in fish and their eggs. *Canadian Journal of Fisheries and Aquatic Sciences*, 40(3):306–312, 1983.

[127] M.A Svenning. Kannibal-og sjørøyebestander på svalbard; genetiske røyemorfer med spesielle forvaltningskrav? *Norsk Institutt for Naturforskning*, 2010.

[128] J.R Hansen and Ø Overrein. Røye på svalbard og jan mayen: en statusoversikt med vekt på forvaltningsrelaterte kunnskapsbehov. *The Norwegian Polar Institute*, 2000.

[129] Arnoldus Schytte Blix. *Arctic animals and their adaptations to life on the edge*. Tapir Academic Press, 2005.

[130] Kjell J Nilssen and Odd A Gulseth. Summer seawater tolerance of small-sized arctic charr, salvelinus alpinus, on svalbard. *Polar Biology*, 20(2):95–98, 1998.

[131] Hans Nordeng. Solution to the" char problem" based on arctic char (salvelinus alpinus) in norway. *Canadian Journal of Fisheries and Aquatic Sciences*, 40(9):1372–1387, 1983.

[132] P-A Amundsen, M-A Svenning, and SI Slikavuoplo. An experimental comparison of cannibalistic response in different arctic charr (salvelinus alpinus (l.)) stocks. *Ecology of Freshwater Fish*, 8(1):43–48, 1999.

[133] Nils Gullestad and Anders Klemetsen. Size, age and spawning frequency of landlocked arctic charr salvelinus alpinus (l.) in svartvatnet, svalbard. *Polar Research*, 16(2): 85–92, 1997.

[134] J.E.T Strand, J.J Aarseth, T.L Hanebrekke, and E.H Jørgensen. Keeping track of time under ice and snow in a sub-arctic lake: plasma melatonin rhythms in arctic charr overwintering under natural conditions. *Journal of pineal research*, 44(3):227–233, 2008. doi: https://doi.org/10.1111/j.1600-079X.2007.00511.x.

[135] Ø Aas-Hansen, M.M Vijayan, H.K Johnsen, C Cameron, and E.H Jørgensen. Resmoltification in wild, anadromous arctic char (salvelinus alpinus): a survey of osmoregulatory, metabolic, and endocrine changes preceding annual seawater migration. *Canadian Journal of Fisheries and Aquatic Sciences*, 62(1):195–204, 2005. doi: https://doi.org/10.1139/f04-186.

[136] H Kalamarz-Kubiak. Cortisol in correlation to other indicators of fish welfare. *Corticosteroids*, page 155, 2018.

[137] NW Pankhurst. The endocrinology of stress in fish: an environmental perspective. *General and comparative endocrinology*, 170(2):265–275, 2011.

[138] Helga Rachel Høgåsen and Patrick Prunet. Plasma levels of thyroxine, prolactin, and cortisol in migrating and resident wild arctic char, salvelinus alpinus. *Canadian Journal of Fisheries and Aquatic Sciences*, 54(12):2947–2954, 1997.

[139] Attila Mozsár, Gergely Boros, Péter Sály, László Antal, and Sándor Alex Nagy. Relationship between f ulton's condition factor and proximate body composition in three freshwater fish species. *Journal of Applied Ichthyology*, 31(2):315–320, 2015.

[140] Jason A Dittman and Charles T Driscoll. Factors influencing changes in mercury concentrations in lake water and yellow perch (perca flavescens) in adirondack lakes. *Biogeochemistry*, 93(3):179–196, 2009.

[141] Glen D Foster and Thomas W Moon. Hypometabolism with fasting in the yellow perch (perca flavescens): a study of enzymes, hepatocyte metabolism, and tissue size. *Physiological Zoology*, 64(1):259–275, 1991.

[142] R Bastrop, K Jürss, and R Wacke. Biochemical parameters as a measure of food availability and growth in immature rainbow trout (oncorhynchus mykiss). *Comparative Biochemistry and Physiology Part A: Physiology*, 102(1):151–161, 1992.

[143] Karina Dale, Fekadu Yadetie, Mette Bjørge Müller, Daniela M Pampanin, Alejandra Gilabert, Xiaokang Zhang, Zhanna Tairova, Ane Haarr, Roger Lille-Langøy, Jan Ludvig Lyche, et al. Proteomics and lipidomics analyses reveal modulation of lipid metabolism by perfluoroalkyl substances in liver of atlantic cod (gadus morhua). *Aquatic Toxicology*, 227:105590, 2020.

[144] Rachel Ann Hauser-Davis, Isabella C Bordon, Kurunthachalam Kannan, Isabel Moreira, and Natalia Quinete. Perfluoroalkyl substances associations with morphometric health indices in three fish species from differentially contaminated water bodies in southeastern brazil. *Environmental Technology & Innovation*, 21:101198, 2021.

[145] Khattapan Jantawongsri, Rasmus Dyrmose Nørregaard, Lis Bach, Rune Dietz, Christian Sonne, Kasper Jørgensen, Syverin Lierhagen, Tomasz Maciej Ciesielski, Bjørn Munro Jenssen, James Haddy, et al. Histopathological effects of short-term aqueous exposure to environmentally relevant concentration of lead (pb) in shorthorn sculpin (myoxocephalus scorpius) under laboratory conditions. *Environmental Science and Pollution Research*, 28(43):61423–61440, 2021.

[146] Thomas M Crisp, Eric D Clegg, Ralph L Cooper, David G Anderson, KP Baetcke, Jennifer L Hoffmann, Melba S Morrow, Donald J Rodier, John E Schaeffer, Leslie W Touart, et al. Special report on environmental endocrine disruption: An effects assessment and analysis. *Washington DC: US Environmental Protection Agency*, 1997.

[147] Mairi Cowan, Clara Azpeleta, and Jose Fernando López-Olmeda. Rhythms in the endocrine system of fish: a review. *Journal of Comparative Physiology B*, 187(8): 1057–1089, 2017.

[148] Mikael Haggstrom. Diagram of the pathways of human steroidogenesis. *WikiJournal of medicine*, 1(1):1–5, 2014.

[149] Walter L Miller and Richard J Auchus. The molecular biology, biochemistry, and physiology of human steroidogenesis and its disorders. *Endocrine reviews*, 32(1):81–151, 2011.

[150] Janina Tokarz, Gabriele Möller, Martin Hrabě de Angelis, and Jerzy Adamski. Steroids in teleost fishes: A functional point of view. *Steroids*, 103:123–144, 2015.

[151] S.E Wendelaar Bonga. The stress response in fish. *Physiological reviews*, 77(3):591–625, 1997. doi: https://doi.org/10.1152/physrev.1997.77.3.591.

[152] Stephen G Reid, Nicholas J Bernier, and Steve F Perry. The adrenergic stress response in fish: control of catecholamine storage and release. *Comparative Biochemistry and Physiology Part C: Pharmacology, Toxicology and Endocrinology*, 120(1):1–27, 1998.

[153] Steve F Perry and Nicholas J Bernier. The acute humoral adrenergic stress response in fish: facts and fiction. *Aquaculture*, 177(1-4):285–295, 1999.

[154] Serge Thomas and Steve F Perry. Control and consequences of adrenergic activation of red blood cell na+/h+ exchange on blood oxygen and carbon dioxide transport in fish. *Journal of Experimental Zoology*, 263(2):160–175, 1992.

[155] Bastien Sadoul and Benjamin Geffroy. Measuring cortisol, the major stress hormone in fishes. *Journal of Fish Biology*, 94(4):540–555, 2019.

[156] NW Pankhurst, SL Ludke, HR King, and RE Peter. The relationship between acute stress, food intake, endocrine status and life history stage in juvenile farmed atlantic salmon, salmo salar. *Aquaculture*, 275(1-4):311–318, 2008.

[157] AD Pickering and Tom G Pottinger. Stress responses and disease resistance in salmonid fish: effects of chronic elevation of plasma cortisol. *Fish physiology and biochemistry*, 7(1):253–258, 1989.

[158] AD Pickering, , and TGl Pottinger. Seasonal and diel changes in plasma cortisol levels of the brown trout, salmo trutta l. *General and Comparative Endocrinology*, 49(2): 232–239, 1983.

[159] Hideaki Yamada, Ri-ichi Satoh, Masashi Ogoh, Keigo Takaji, Yasufumi Fujimoto, Takeshi Hakuba, Hiroaki Chiba, Akira Kambegawa, and Munehico Iwata. Circadian changes in serum concentrations of steroids in japanese char salvelinus leucomaenis at the stage of final maturation. *Zoological science*, 19(8):891–898, 2002.

[160] JE Thorpe, MG McConway, MS Miles, and JS Muir. Diel and seasonal changes in resting plasma cortisol levels in juvenile atlantic salmon, salmo salar l. *General and comparative endocrinology*, 65(1):19–22, 1987.

[161] E Lundanes, L Reubsaet, and T Greibrokk. *Chromatography: basic principles, sample preparations and related methods*. John Wiley & Sons, 2013. ISBN 9783527336203.

[162] Shafeeque Ahmad, Harsh Kalra, Amit Gupta, Bharat Raut, Arshad Hussain, and Md Akhlaquer Rahman. Hybridspe: A novel technique to reduce phospholipid-based

matrix effect in lc–esi-ms bioanalysis. *Journal of pharmacy & bioallied sciences*, 4(4): 267, 2012.

[163] Simone Trimmel, Kristine Vike-Jonas, Susana V Gonzalez, Tomasz Maciej Ciesielski, Ulf Lindstrøm, Bjørn Munro Jenssen, and Alexandros G Asimakopoulos. Rapid determination of per-and polyfluoroalkyl substances (pfas) in harbour porpoise liver tissue by hybridspe®–uplc®–ms/ms. *Toxics*, 9(8):183, 2021. doi: https://doi.org/10.3390/toxics9080183.

[164] Kristine Vike-Jonas, Susana Villa Gonzalez, Åse-Karen Mortensen, Tomasz Maciej Ciesielski, Julia Farkas, Vishwesh Venkatraman, Mikhail V Pastukhov, Bjørn Munro Jenssen, and Alexandros G Asimakopoulos. Rapid determination of thyroid hormones in blood plasma from glaucous gulls and baikal seals by hybridspe®-lc-ms/ms. *Journal of Chromatography B*, 1162:122447, 2021. doi: https://doi.org/10.1016/j.jchromb.2020.122447.

[165] Alexandros G Asimakopoulos and Nikolaos S Thomaidis. Bisphenol a, 4-t-octylphenol, and 4-nonylphenol determination in serum by hybrid solid phase extraction–precipitation technology technique tailored to liquid chromatography–tandem mass spectrometry. *Journal of Chromatography B*, 986:85–93, 2015. doi: https://doi.org/10.1016/j.jchromb.2015.02.009.

[166] Sofia Chanioti, George Liadakis, and Constantina Tzia. Solid-liquid extraction. *Food Engineering Handbook: Food Process Engineering*, 2:247–280, 2014.

[167] MD Mingorance, ML Perez-Vazquez, and M Lachica. Microwave digestion methods for the atomic spectrometric determination of some elements in biological samples. *Journal of Analytical Atomic Spectrometry*, 8(6):853–858, 1993.

[168] E.P Nardi, F. S Evangelista, L Tormen, T.D Saint, A.J Curtius, S.S de Souza, F Barbosa Jr, et al. The use of inductively coupled plasma mass spectrometry (icp-ms) for the determination of toxic and essential elements in different types of food samples. *Food Chemistry*, 112(3):727–732, 2009. doi: https://doi.org/10.1016/j.foodchem.2008.06.010.

[169] Kathryn J Lamble and Steve J Hill. Microwave digestion procedures for environmental matrices. critical review. *Analyst*, 123(7):103R–133R, 1998.

[170] Jet C Van De Steene and Willy E Lambert. Comparison of matrix effects in hplc-ms/ms

and uplc-ms/ms analysis of nine basic pharmaceuticals in surface waters. *Journal of the American Society for Mass Spectrometry*, 19(5):713–718, 2008.

[171] T Groffen, L Bervoets, Y Jeong, T Willems, M Eens, and E Prinsen. A rapid method for the detection and quantification of legacy and emerging per-and polyfluoroalkyl substances (pfas) in bird feathers using uplc-ms/ms. *Journal of Chromatography B*, 1172:122653, 2021. doi: https://doi.org/10.1016/j.jchromb.2021.122653.

[172] M Abdul Mottaleb, Michael C Petriello, and Andrew J Morris. High-throughput uhplc-ms/ms measurement of per-and poly-fluorinated alkyl substances in human serum. *Journal of Analytical Toxicology*, 44(4):339–347, 2020.

[173] N. de Kock, S.R. Acharya, S.J. Ubhayasekera, and J. Bergquist. A novel targeted analysis of peripheral steroids by ultra-performance supercritical fluid chromatography hyphenated to tandem mass spectrometry. *Scientific reports*, 8(1):1–9, 2018. doi: https://doi.org/10.1038/s41598-018-35007-0.

[174] Therina du Toit, Desmaré van Rooyen, Maria A Stander, Stephen L Atkin, and Amanda C Swart. Analysis of 52 c19 and c21 steroids by upc2-ms/ms: Characterising the c11-oxy steroid metabolome in serum. *Journal of Chromatography B*, 1152: 122243, 2020.

[175] Jonathan L Quanson, Marietjie A Stander, Elzette Pretorius, Carl Jenkinson, Angela E Taylor, and Karl-Heinz Storbeck. High-throughput analysis of 19 endogenous androgenic steroids by ultra-performance convergence chromatography tandem mass spectrometry. *Journal of Chromatography B*, 1031:131–138, 2016.

[176] SA Wudy, G Schuler, A Sánchez-Guijo, and MF Hartmann. The art of measuring steroids: principles and practice of current hormonal steroid analysis. *The Journal of steroid biochemistry and molecular biology*, 179:88–103, 2018.

[177] Steven J Lehotay. Comparison of analyte identification criteria and other aspects in triple quadrupole tandem mass spectrometry: Case study using uhplc-ms/ms for regulatory analysis of veterinary drug residues in liquid and powdered eggs. *Analytical and Bioanalytical Chemistry*, 414(1):287–302, 2022.

[178] Michael Krachler, Herbert Radner, and Kurt J Irgolic. Microwave digestion methods for the determination of trace elements in brain and liver samples by inductively coupled plasma mass spectrometry. *Fresenius' journal of analytical chemistry*, 355(2): 120–128, 1996.

[179] ICH Q2B. Validation of analytical procedure: Methoddology. *International Conference on Harmonization of Technical Requirements for Registration of Pharmaceuticals for Human Use, Geneva, Switzerland*, 1996.

[180] Saba Ershadi and Ali Shayanfar. Are lod and loq reliable parameters for sensitivity evaluation of spectroscopic methods? *Journal of AOAC International*, 101(4):1212–1213, 2018.

[181] M Marsin Sanagi, Susie L Ling, Zalilah Nasir, Dadan Hermawan, Wan Aini Wan Ibrahim, and Ahmedy Abu Naim. Comparison of signal-to-noise, blank determination, and linear regression methods for the estimation of detection and quantification limits for volatile organic compounds by gas chromatography. *Journal of AOAC International*, 92(6):1833–1838, 2009.

[182] Jérôme Vial and Alain Jardy. Experimental comparison of the different approaches to estimate lod and loq of an hplc method. *Analytical Chemistry*, 71(14):2672–2677, 1999.

[183] Kapil Kalra. Method development and validation of analytical procedures. *Quality Control of Herbal Medicines and Related Areas*, 4:3–16, 2011.

[184] ICH Harmonised Tripartite Guideline et al. Validation of analytical procedures: text and methodology. *Q2 (R1)*, 1(20):05, 2005.

[185] Wanlong Zhou, Shuang Yang, and Perry G Wang. Matrix effects and application of matrix effect factor, 2017.

[186] Paul J Taylor. Matrix effects: the achilles heel of quantitative high-performance liquid chromatography–electrospray–tandem mass spectrometry. *Clinical biochemistry*, 38 (4):328–334, 2005.

[187] Andrija Ćirić, Helena Prosen, Milena Jelikić-Stankov, and Predrag Đurđević. Evaluation of matrix effect in determination of some bioflavonoids in food samples by lc–ms/ms method. *Talanta*, 99:780–790, 2012.

[188] Erin Chambers, Diane M Wagrowski-Diehl, Ziling Lu, and Jeffrey R Mazzeo. Systematic and comprehensive strategy for reducing matrix effects in lc/ms/ms analyses. *Journal of Chromatography B*, 852(1-2):22–34, 2007.

[189] T. Pihlström. Method validation and quanlity control procedures for pesticide residues analysis in food and feed. *Document N° SANCO/12495/2011*, 2012.

[190] William H Kruskal and W Allen Wallis. Use of ranks in one-criterion variance analysis. *Journal of the American statistical Association*, 47(260):583–621, 1952.

[191] Alexis Dinno. Nonparametric pairwise multiple comparisons in independent groups using dunn's test. *The Stata Journal*, 15(1):292–300, 2015.

[192] Olive Jean Dunn. Multiple comparisons using rank sums. *Technometrics*, 6(3):241–252, 1964.

[193] Rasmus Bro and Age K Smilde. Principal component analysis. *Analytical methods*, 6 (9):2812–2831, 2014. doi: 10.1039/C3AY41907J.

[194] Hervé Abdi and Lynne J Williams. Principal component analysis. *Wiley interdisciplinary reviews: computational statistics*, 2(4):433–459, 2010.

[195] Markus Ringnér. What is principal component analysis? *Nature biotechnology*, 26(3): 303–304, 2008.

[196] Kim H Esbensen, Dominique Guyot, Frank Westad, and Lars P Houmoller. *Multivariate data analysis: in practice: an introduction to multivariate data analysis and experimental design*. Multivariate Data Analysis, 2002.

[197] Monica Sund. Polar hydrology. *Norwegian water resources and Energy Directorate's work in Svalbard. NVE Report*, 2, 2008.

[198] International Organization for Standardization. Water quality — biochemical and physiological measurements on fish — part 1: Sampling of fish, handling and preservation of samples (ISO 23893-1:2007(E)). 2007.

[199] Johan Juhl Weisser, Cecilie Hurup Hansen, Rikke Poulsen, Lizette Weber Larsen, Claus Cornett, and Bjarne Styrishave. Two simple cleanup methods combined with lc-ms/ms for quantification of steroid hormones in in vivo and in vitro assays. *Analytical and bioanalytical chemistry*, 408(18):4883–4895, 2016.

[200] Alexandros G Asimakopoulos, Lei Wang, Nikolaos S Thomaidis, and Kurunthachalam Kannan. A multi-class bioanalytical methodology for the determination of bisphenol a diglycidyl ethers, p-hydroxybenzoic acid esters, benzophenone-type ultraviolet filters, triclosan, and triclocarban in human urine by liquid chromatography–tandem mass spectrometry. *Journal of Chromatography A*, 1324:141–148, 2014.

[201] Standard Norge. Foodstuffs, determination of trace elements, pressure digestion (NS-EN 13805:2014). 2015.

[202] Indrajeet Patil. Visualizations with statistical details: The 'ggstatsplot' approach. *Journal of Open Source Software*, 6(61):3167, 2021. doi: 10.21105/joss.03167. URL `https://doi.org/10.21105/joss.03167`.

[203] B Borg. Androgens in teleost fishes. *Comparative Biochemistry and Physiology Part C: Pharmacology, Toxicology and Endocrinology*, 109(3):219–245, 1994.

[204] Christopher J Martyniuk, Sonja Bissegger, and Valérie S Langlois. Current perspectives on the androgen 5 alpha-dihydrotestosterone (dht) and 5 alpha-reductases in teleost fishes and amphibians. *General and Comparative Endocrinology*, 194:264–274, 2013.

[205] H Tveiten, I Mayer, HK Johnsen, and M Jobling. Sex steroids, growth and condition of arctic charr broodstock during an annual cycle. *Journal of Fish Biology*, 53(4): 714–727, 1998.

[206] Luigi Margiotta-Casaluci, Frédérique Courant, Jean-Philippe Antignac, Bruno Le Bizec, and John P Sumpter. Identification and quantification of 5α-dihydrotestosterone in the teleost fathead minnow (pimephales promelas) by gas chromatography–tandem mass spectrometry. *General and Comparative Endocrinology*, 191:202–209, 2013.

[207] Luigi Margiotta-Casaluci and John P Sumpter. 5α-dihydrotestosterone is a potent androgen in the fathead minnow (pimephales promelas). *General and comparative endocrinology*, 171(3):309–318, 2011.

[208] Ø Øverli, RE Olsen, F Løvik, and E Ringø. Dominance hierarchies in arctic charr, salvelinus alpinus l.: differential cortisol profiles of dominant and subordinate individuals after handling stress. *Aquaculture Research*, 30(4):259–264, 1999.

[209] Fei Li, Zhi-ling Zhao, Chun-hua Shen, Qing-ling Zeng, and Shu-po Liu. Elimination of matrix effects during analysis of perfluorinated acids in solid samples by liquid chromatography tandem mass spectrometry. *Journal of Central South University*, 19 (10):2886–2894, 2012.

[210] N.L. Stock, V.I. Furdui, D.C.G. Muir, and S.A. Mabury. Perfluoroalkyl contaminants in the canadian arctic: evidence of atmospheric transport and local contamination. *Environmental science & technology*, 41(10):3529–3536, 2007. doi: https://doi.org/10.1021/es062709x.

[211] P. Labadie and M. Chevreuil. Partitioning behaviour of perfluorinated alkyl contaminants between water, sediment and fish in the orge river

(nearby paris, france). *Environmental pollution*, 159(2):391–397, 2011. doi: https://doi.org/10.1016/j.envpol.2010.10.039.

[212] Sachi Taniyasu, Kurunthachalam Kannan, Yuichi Horii, Nobuyasu Hanari, and Nobuyoshi Yamashita. A survey of perfluorooctane sulfonate and related perfluorinated organic compounds in water, fish, birds, and humans from japan. *Environmental science & technology*, 37(12):2634–2639, 2003.

[213] Mai Duc Hung, Nguyen Hoang Lam, Hui Ho Jeong, Hyeon Ji Jeong, Da Jin Jeong, Gyeong Hwa Park, Pil Jae Kim, Jeong Eun Oh, and Hyeon Seo Cho. Perfluoroalkyl substances (pfass) in ten edible freshwater fish species from major rivers and lakes in korea: distribution and human exposure by consumption. *Toxicology and Environmental Health Sciences*, 10(5):307–320, 2018.

[214] B.C. Kelly, M.G. Ikonomou, J.D. Blair, B. Surridge, D. Hoover, R. Grace, and F.A.P.C. Gobas. Perfluoroalkyl contaminants in an arctic marine food web: trophic magnification and wildlife exposure. *Environmental science & technology*, 43(11):4037–4043, 2009. doi: https://doi.org/10.1021/es9003894.

[215] Jules M Blais, Robie W Macdonald, Donald Mackay, Eva Webster, Colin Harvey, and John P Smol. Biologically mediated transport of contaminants to aquatic systems. *Environmental Science & Technology*, 41(4):1075–1084, 2007.

[216] Jonathan W Martin, Kurunthachalam Kannan, URS Berger, Pim De Voogt, Jennifer Field, James Franklin, John P Giesy, Tom Harner, Derek CG Muir, Brian Scott, et al. Peer reviewed: analytical challenges hamper perfluoroalkyl research. *Environmental science & technology*, 38(13):248A–255A, 2004.

[217] V. Pucci, S. Di Palma, A. Alfieri, F. Bonelli, and E. Monteagudo. A novel strategy for reducing phospholipids-based matrix effect in lc–esi-ms bioanalysis by means of hybridspe. *Journal of pharmaceutical and biomedical analysis*, 50(5):867–871, 2009. doi: https://doi.org/10.1016/j.jpba.2009.05.037.

[218] Marta Villagrasa, Maria López de Alda, and Damià Barceló. Environmental analysis of fluorinated alkyl substances by liquid chromatography–(tandem) mass spectrometry: a review. *Analytical and bioanalytical chemistry*, 386(4):953–972, 2006.

[219] Helga Trufelli, Pierangela Palma, Giorgio Famiglini, and Achille Cappiello. An overview of matrix effects in liquid chromatography–mass spectrometry. *Mass spectrometry reviews*, 30(3):491–509, 2011. doi: https://doi.org/10.1002/mas.20298.

[220] Sara Valsecchi, Marianna Rusconi, and Stefano Polesello. Determination of perfluorinated compounds in aquatic organisms: a review. *Analytical and Bioanalytical Chemi*, 405(1):143–157, 2013. doi: https://doi.org/10.1002/mas.20298stry.

[221] Sheryl A Tittlemier and Eric Braekevelt. Analysis of polyfluorinated compounds in foods. *Analytical and bioanalytical chemistry*, 399(1):221–227, 2011.

[222] Sylvia Weging. Study of trace elements, natural organic matter and selected environmental toxicants in soil at mitrahalvøya, to establish bias correction for studies of long-range atmospheric transported pollutants in ny-ålesund. Master's thesis, NTNU, 2021.

[223] Elizabeta Has-Schön, Ivan Bogut, Valentina Rajković, Stjepan Bogut, Milan Čačić, and Janja Horvatić. Heavy metal distribution in tissues of six fish species included in human diet, inhabiting freshwaters of the nature park "hutovo blato"(bosnia and herzegovina). *Archives of Environmental Contamination and Toxicology*, 54(1):75–83, 2008.

[224] Marcela Havelková, Ladislav Dušek, Danka Némethová, Gorzyslaw Poleszczuk, and Zdeňka Svobodová. Comparison of mercury distribution between liver and musc-a biomonitoring of fish from lightly and heavily contaminated localities. *Sensors*, 8(7): 4095–4109, 2008.

[225] Douglas H Adams, Christian Sonne, Niladri Basu, Rune Dietz, Dong-Ha Nam, Pall S Leifsson, and Asger L Jensen. Mercury contamination in spotted seatrout, cynoscion nebulosus: an assessment of liver, kidney, blood, and nervous system health. *Science of the total environment*, 408(23):5808–5816, 2010. doi: https://doi.org/10.1016/j.scitotenv.2010.08.019.

[226] M. Khadra, A. Caron, D. Planas, D.E Ponton, M. Rosabal, and M. Amyot. The fish or the egg: Maternal transfer and subcellular partitioning of mercury and selenium in yellow perch (perca flavescens). *Science of the total environment*, 675:604–614, 2019. doi: https://doi.org/10.1016/j.scitotenv.2019.04.226.

[227] E Has-Schön, I Bogut, and I Strelec. Heavy metal profile in five fish species included in human diet, domiciled in the end flow of river neretva (croatia). *Archives of environmental contamination and toxicology*, 50(4):545–551, 2006.

[228] J. Burger, C. Jeitner, M. Donio, T. Pittfield, and M. Gochfeld. Mercury and selenium levels, and selenium: mercury molar ratios of brain, muscle and other tissues in bluefish

(pomatomus saltatrix) from new jersey, usa. *Science of the total environment*, 443:278–286, 2013. doi: https://doi.org/10.1016/j.scitotenv.2012.10.040.

[229] Haiyan Zhang, Chenqi Guo, Hongru Feng, Yanting Shen, Yaotian Wang, Tao Zeng, and Shuang Song. Total mercury, methylmercury, and selenium in aquatic products from coastal cities of china: Distribution characteristics and risk assessment. *Science of the Total Environment*, 739:140034, 2020. doi: https://doi.org/10.1016/j.scitotenv.2020.140034.

[230] Sean M Covington, Rami B Naddy, Alan L Prouty, Steven A Werner, and Mark Dunn Lewis. Effects of in situ selenium exposure and maternal transfer on survival and deformities of brown trout (salmo trutta) fry. *Environmental toxicology and chemistry*, 37(5):1396–1408, 2018. doi: https://doi.org/10.1002/etc.4086.

[231] AK Nor Hasyimah, V James Noik, YY Teh, CY Lee, and HC Pearline Ng. Assessment of cadmium (cd) and lead (pb) levels in commercial marine fish organs between wet markets and supermarkets in klang valley, malaysia. *International Food Research Journal*, 18(2), 2011.

[232] S Squadrone, M Prearo, P Brizio, S Gavinelli, M Pellegrino, T Scanzio, S Guarise, A Benedetto, and MC Abete. Heavy metals distribution in muscle, liver, kidney and gill of european catfish (silurus glanis) from italian rivers. *Chemosphere*, 90(2):358–365, 2013.

[233] Mackenzie Anne Clifford Martyniuk, Patrice Couture, Lilian Tran, Laurie Beaupré, Nastassia Urien, and Michael Power. A seasonal comparison of trace metal concentrations in the tissues of arctic charr (salvelinus alpinus) in northern québec, canada. *Ecotoxicology*, 29(9):1327–1346, 2020.

[234] Jiaojiao Yin, Qi Liu, Li Wang, Jian Li, Sai Li, and Xuezhen Zhang. The distribution and risk assessment of heavy metals in water, sediments, and fish of chaohu lake, china. *Environmental earth sciences*, 77(3):1–12, 2018.

[235] Mansour Ebrahimi and Mahnaz Taherianfard. Concentration of four heavy metals (cadmium, lead, mercury, and arsenic) in organs of two cyprinid fish (cyprinus carpio and capoeta sp.) from the kor river (iran). *Environmental monitoring and assessment*, 168(1):575–585, 2010.

[236] A. Ohki, T. Nakajima, and S. Maeda. Metabolism and organ distribution of arsenic

in the freshwater fish tilapia mossambica. *Applied Organometallic Chemistry*, 15(6): 566–571, 2001. doi: https://doi.org/10.1002/aoc.211.

[237] Zdenka Šlejkovec, Zlatka Bajc, and Darinka Z Doganoc. Arsenic speciation patterns in freshwater fish. *Talanta*, 62(5):931–936, 2004. ISSN 0039-9140. doi: https://doi.org/10.1016/j.talanta.2003.10.012.

[238] Kaare Julshamn, Bente M Nilsen, Sylvia Frantzen, Stig Valdersnes, Amund Maage, Kjell Nedreaas, and Jens J Sloth. Total and inorganic arsenic in fish samples from norwegian waters. *Food Additives and Contaminants: Part B*, 5(4):229–235, 2012.

[239] Benjamin D Barst, Maikel Rosabal, Peter GC Campbell, Derek GC Muir, Xioawa Wang, Günter Köck, and Paul E Drevnick. Subcellular distribution of trace elements and liver histology of landlocked arctic char (salvelinus alpinus) sampled along a mercury contamination gradient. *Environmental Pollution*, 212:574–583, 2016.

[240] Eisa Solgi, Hossein Alipour, and Farshid Majnooni. Investigation of the concentration of metals in two economically important fish species from the caspian sea and assessment of potential risk to human health. *Ocean Science Journal*, 54(3):503–514, 2019.

[241] Ahmet R Oğuz and Aslı Yeltekin. Metal levels in the liver, muscle, gill, intestine, and gonad of lake van fish (chalcalburnus tarichi) with abnormal gonad. *Biological Trace Element Research*, 159(1):219–223, 2014.

[242] Qiao-qiao Chi, Guang-wei Zhu, and Alan Langdon. Bioaccumulation of heavy metals in fishes from taihu lake, china. *Journal of Environmental Sciences*, 19(12):1500–1504, 2007.

[243] D.W. Evans, D.K Dodoo, and P.J. Hanson. Trace element concentrations in fish livers: implications of variations with fish size in pollution monitoring. *Marine pollution bulletin*, 26(6):329–334, 1993. doi: https://doi.org/10.1016/0025-326X(93)90576-6.

[244] Tsuyoshi Tanaka and Hikari Kamioka. Trace element abundance in agate. *Geochemical Journal*, 28(4):359–362, 1994.

[245] Toru Yamasaki. Contamination from mortars and mills during laboratory crushing and pulverizing. *Bulletin of the Geological Survey of Japan*, 69(3):201–210, 2018.

[246] Francesco Cubadda, Massimo Baldini, Marina Carcea, Luigi Alberto Pasqui, Andrea Raggi, and Paolo Stacchini. Influence of laboratory homogenization procedures on

trace element content of food samples: an icp-ms study on soft and durum wheat. *Food Additives & Contaminants*, 18(9):778–787, 2001.

[247] Kathrin Ertl and Walter Goessler. Aluminium in foodstuff and the influence of aluminium foil used for food preparation or short time storage. *Food Additives & Contaminants: Part B*, 11(2):153–159, 2018. doi: 10.1080/19393210.2018.1442881.

A Appendix - Theoretical background

A.1 Levels of PFAS in Arctic char

Table A1: Levels of PFAS in Arctic char from previous studies. Matrix and number of samples (n), total PFAS concentration ($\sum$PFAS) given in ng g^{-1} wet weight, the main detected PFAS compounds, location and Lake, and the reference of the study.

Matrix (n)	**$\sum$PFAS**	**Main detected PFAS**	**Location**	**Reference**
Liver (10)	5.67±1.6	PFTeA, PFTrA, PFOS, PFUnA, PFDoA	Lake a Myrarnar (Faroe Islands)	[40]
Liver (10)	5.27±2.8	PFTrA, PFUnA, PFTeA, PFDoA, PFOS	Greenland	[40]
Muscle (21)	27±6.8	PFOS, PFNA, PFDS	Lake Meretta (Canada)	[46]
Muscle (18)	122±65	PFOS, PFNA, PFDS	Lake Resolute (Canada)	[46]
Muscle (13)	3.7±2.4	PFNA, PFDS, PFDA	Lake Char (Canada)	[46]
Muscle (20)	0.36±0.15	PFNA, PFDS	Lake Small (Canada)	[46]
Muscle (25)	0.32±0.12	PFNA, PFDS, PFDA	Lake North (Canada)	[46]
Muscle (23)	0.28±0.09	PFNA, PFDS	Lake 9 Mile (Canada)	[46]
Whole body (27), muscle (5)	0.203	PFNA, PFUnA, PFOS/PFDA	Lake A (Canada)	[65]
Muscle (14)	0.481	PFNA, PFOS, PFUnA, PFDA	Lake C2 (Canada)	[65]
Muscle (6)	0.53±0.073	PFOS, PFUnDA, PFDA	Lake Linnevatnet (Svalbard)	[66]

B Appendix - Method and Materials

B.1 Sampling

Table B1: Biometric measurements of Arctic char collected from Lake Diesetvatnet. The length of the fish is given in centimeters, and the body mass and weight of organ samples are given in grams. Organ samples include liver, kidney, and gonad (weight of the eggs are included for fish number 3, 5, 6, and 7). Brain samples and kidney and gonad sample 4 were weighed on a precision scale. The brain sample of fish number 5 is missing. Body condition (K), gender of the fish are given as female (F) or male (M), and hepatosomtic index (HSI).

Fish	Length	Body mass	Liver	Kidney	Gonad	Brain	Gender	K	HSI
1	45.0	900	13	7	43	0.2236	F	0.99	1.44
2	47.5	1050	20	9	8	0.2543	F	0.98	1.90
3	51.5	1350	37	12	13	0.3672	F	0.99	2.74
4	36.0	350	4	0.65	0.39	0.2340	M	0.75	1.14
5	49.0	950	22	5	99		F	0.81	2.32
6	49.0	1040	25	7	96	0.3437	F	0.88	2.40
7	52.5	1390	30	10	17	0.3928	F	0.96	2.16

Figure B1: Photos of individual Arctic char that was sampled at Lake Disetvatnet with their corresponding numbers (same as in Table B1).

Figure B2: Tapeworms were observed in the stomach of Artic char number 4 from Lake Diesetvatnet.

Figure B3: Observations of small circled spots on the liver of Arctic char number 6 which might be nematode paracites.

B.2 Sample ID

Table B2: Sample-ID of Arctic char tissue samples including whole blood (WB), red blood cells (RBC), brain, gonad, hard roe (eggs), liver, and kidney.

Fish	WB	Plasma	RBC	Brain	Gonad	Roe	Liver	Kidney
1	WB-1	P-1a, P-1b, P-1c	RBC-1	B-1	G-1		L-1	K-1
2	WB-2	P-2a, P-2b, P-2c, P-2d, P-2e	RBC-2	B-2	G-2		L-2	K-2
3	WB-3A, WB-3B	P-3Aa, P-3Ab, P-3Ac, P-3Ba, P-3Bb, P-3Bc, P-3Bd, P-3Be, P-3Bf, P-3Bg	RBC-3A, RBC-3B	B-3	G-3	E-3	L-3	K-3
4	WB-4	P-4a, P-4b	RBC-4	B-4	G-4		L-4	K-4
5	WB-5	P-5a, P-5b, P-5c, P-5d	RBC-5		G-5	E-5	L-5	K-5
6	WB-6A, WB-6B	P-6Aa, P-6Ab, P-6Ac, P-6Ad, P-6Ae P-6Ba, P-6Bb, P-6Bc, P-6Bd, P-6Be	RBC-6A, RBC-6B	B-6	G-6	E-6	L-6	K-6
7	WB-7	P-7a, P-7b, P-7c, P-7d, P-7e	RBC-7	B-7	G-7	E-7	L-7	K-7

B.3 List of chemicals and equipments used during sampling and sample preparation

Table B3: List of chemicals and equipments used during sampling and sample preparation.

Chemical/Equipment	Specification	CAS-number	Supplier
Sampling			
Heparin lithium salt	From porcine intestinal mucosa	9045-22-1	Sigma-Aldrich
Alumina foil	Kitchen foil. 45cmx10m 16,5my. Product-ID: 52012		Lyreco
Extraction of steroid hormones/PFAS			
Milli-Q water (Type I)	Ultrapure. Resitivity>18MΩ·cm, TOC<0.5 ppb. Elga Purelab Flex Elga Chorus Millipore Elix5/Elix10/MilliQ		
Methanol	Assay (on anhydrous substance) 100%, HPLC grade, suitable for UPLC/UHPLC	67-56-1	VWR International
Acetonitrile	Assay (on anhdrous substance) ≥ 99.9%, HPLC grade, suitable for UPLC/UHPLC	75-05-8	VWR International
Acetone	Assay (on anhydrous substances) 100%, HPLC grade	67-64-1	VWR International
Methyl tert-butyl ether	Assay 100%	1634-04-4	VWR International
n-Heptane	Assay 99.3%	142-82-5	VWR International
Ammonium formate	Anhydrous, free-flowing Redi-Dri TM, reagent grad 97%	540-69-2	Sigma-Aldrich
Citric acid	ASC reagent ≥ 99.5%	77-92-9	Sigma-Aldrich
Supelco HybridSPE® Phospholipid	Cartridge: 30 mg, 1 mL. 55261-U		Sigma-Aldrich
HyperSep™ C18 SPE column	Cartridge: 50 mg, 1 mL. Particle size: 40-60 micro m		Thermo Fisher Scientific

Table B3 continued from previous page

Standards and internal standards used for extraction and analysis of steroid hormones/PFAS			
Steroid hormones target analytes	1) DHEA (99.8%), AN (99.7%), TS (99.7%), DHT (99.9%), DOC (99.1%), 11-deoxyCOR (98.6%), ALDO (99.1%), COS (99.5%), 17a-OHP (98.2%), COR (98.9%), CORNE (97.8%), 17a-OH-P5 (96.6%),PREG (99.6%), P4 (99.5%), E1 (99.1%), E2 (99.7%). 2) 11-KetoTS (> 98%) 3) A5	Table B5	1) Cerilliant (Texas, USA) 2) Sigma-Aldrich (Steinheim, Germany) 3) Toronto Reserch Chemicals, Inc. (New York, ON, Canada)
Steroid hormones internal standards	purity ≥ 98%	Table B7	Cambridge Isotope Laboratories, Inc. (Tewksbury, MA, USA)
PFAS target analytes	purity ≥ 98 %	Table B4	Wellington Laboratories Inc. (Guelph, ON, Canada)
PFAS internal standards	purity ≥ 99 %	Table B6	Cambridge Isotope Laboratories, Inc. (Tewksbury, MA, USA)
Freeze drying, homogenization			
Nitric acid (50%, 68%, 1M)	Scanpure. Acid purification in sub-boiling distillation system, Milestone, SubPur, Sorisole, BG, Italy	7697-37-2	VWR Chemicals
Milli-Q water (Type I)	Ultrapure. Resitivity>18MΩ·cm, TOC<0.5 ppb. Elga Purelab FlexElga Chorus Millipore Elix5/Elix10/MilliQ		
Ethanol absolute	AnalaR NORMAPUR	64-17-5	VWR Chemicals
Mortar and pestle	Material: agate		VWR
Cell counter cups, Coulter®	Cup: polystyren (PS) and lid: polyethylen (PE). Article nr: 720-0812		VWR
Certified reference materials for ICP-MS analysis			
DORM-5	Fish protein. Trace elements and species content.		National Research Council Canada (NRC)

Table B3 continued from previous page

DOLT-3	Dogfish liver. Trace elements and methylmercury.	National Research Council Canada (NRC)
Seronorm whole blood L-2	Trace elements. LOT: 1406264, REF: 210205	Sero AS
Seronorm serum	Trace elements. LOT: 704121, Article no: 201405	Sero AS

B.4 Standards of PFAS target analytes

Table B4: Standards of PFAS target analytes with information of PFAS sub-group, full compound name, abbreviation, molecular formula, and CAS-number.

Compound	**Abbreviation**	**Molecular formula**	**CAS-number**
Sodium 1-decanesulfonate	DecaS	$C_{10}H_{21}O_3S$	13419-61-9
Perfluorocarboxylic acids (PFCAs)			
Perfluorobutanoic acid	PFBA	$C_4HF_7O_2$	375-224
Perfluoropentanoic acid	PFPeA	$C_5HF_9O_2$	2706-90-
Perfluorohexanoic acid	PFHxA	$C_6HF_{11}O_2$	307-24-4
Perfluoroheptanoic acid	PFHpA	$C_7HF_{13}O_2$	375-85-9
Perfluorooctanoic acid	PFOA	$C_8HF_{15}O_2$	335-67-1
Perfluorononanoic acid	PFNA	$C_9HF_{17}O_2$	375-95-1
Perfluorodecanoic acid	PFDA	$C_{10}HF_{19}O_2$	335-76-2
Perfluoroundecanoic acid	PFUnA	$C_{11}HF_{21}O$	2058-94-8
Perfluorododecanoic acid	PFDoDA	$C_{12}HF_{23}O_2$	307-55-1
Perfluorotridecanoic acid	PFTriDA	$C_{13}HF_{25}O_2$	72629-94-8
Perfluorotetradecanoic acid	PFTDA	$C_{14}HF_{27}O_2$	376-06-7
Perfluoro-n-hexadecanoic acid	PFHxDA	$C_{16}HF_{31}O_2$	67905-19-5
Perfluorooctadecanoic acid	PFOcDA	$C_{18}HF_{35}O_2$	16517-11-6
Perfluoro-3,7-dimethyloctanoic acid	P37DMOA	$C_{10}HF_{19}O_2$	172155-07-6
7H-Dodecafluoroheptanoic acid	PFHeA	$C_{10}HF_{19}O_2$	172155-07-6
Perfluoroalkyl Sulfonates (PFSA)			
Perfluorobutanoic acid sulfonate	PFBS	$C_4F_9SO_3$	108427-52-7
Perfluoropentane sulfonic acid	PFPeS	$C_5HF_{11}SO_3$	2706-91-4
Perfluorohexane sulfonic acid	PFHxS	$C_6HF_{13}SO_3$	355-46-4
Perfluoro-1-heptanesulfonate	PFHpS	$C_7F_{15}SO_3$	146689-46-5
Perfluorooctano sulfonic acid	PFOS	$C_8F_{17}SO_3$	1763-23-1
Perfluorononane sulfonic acid	PFNS	$C_9HF_{19}SO_3$	68259-12-1
Perfluorodecane sulfonic acid	PFDS	$C_{10}HF_{21}SO_3$	335-77-3

Table B4 – **Continued from previous page**

Perfluorododecane sulfonic acid	PFDoDS	$C_{12}HF_{25}SO_3$	79780-39-5
Perfluoroethylcyclohexane sulfonic acid	PFECHS	$C_8HF_{15}SO_3$	335-24-0
Fluorotelomer Sulfonates (FTS)			
1H,2H-Perfluorohexane sulfonate (4:2)	4:2 FTS	$C_6H_5F_9SO_3$	757124-72-4
1H,2H-Perfluorooctane sulfonate (6:2)	6:2 FTS	$C_8H_5F_{13}SO_3$	27619-97-2
1H,2H-Perfluorodecane sulfonate (8:2)	8:2 FTS	$C_{10}H_5F_{17}SO_3$	39108-34-4
1H,2H-Perfluorododecan sulfonate (10:2)	10:2 FTS	$C_{12}H_{521}SO_3$	120226-60-0
Perfluorooctanesulfonamidoacetic Acids (FOSAA)			
Perfluoro-1-octanesulfonamidoacetic acid	FOSAA	$C_{10}H_4F_{17}NO_4S$	2806-24-8
2-(N-methylPerfluoro-1-octansulfonamido)acetic acid	MeFOSAA	$C_{11}H_6F_{17}NO_4S$	2355-31-9
N-ethylPerfluoro-1-octanesulfonamide acetic acid	EtFOSAA	$C_{12}H_8F_{17}NO_4S$	1336-61-4
Perfluorooctanesulfonamides (FOSA)			
Perfluorooctane sulfonamide	PFOS	$C_8H_2F_{17}NO_2S$	754-91-6
N-methylPerfluoro-1-octanesulfonamide	MeFOSA	$C_9H_4F_{17}NO_2S$	31506-32-8
Sulfluramid	EtFOSA	$C_{10}H_6F_{17}NO_2S$	4151-50-2
Perfluorooctanesulfonamido Ethanols (FOSE)			
N-(2-hydroxyethyl)-N-methylperfluorooctane sulfonamide	MeFOSE	$C_{11}H_8F_{17}NO_3S$	24448-09-7
N-ethyl-N-(2-hydroxyethyl)-N-methylperfluorooctane sulfonamide	EtFOSE	$C_{12}H_{10}F_{17}NO_3S$	1691-99-2
Fluoropolymers			
2,3,3,3-tetrafluoro-2-(1,1,2,2,3,3,3-heptafluoropropoxy)propanoate	Gen X	$C_6H_4F_{11}NO_3$	62037-80-3
Dodecafluoro-3H-4,8-dioxanonoate	ADONA	$C_7H_5F_{12}NO_4$	958445-44-8
9-Chlorohexadecafluoro-3-oxanonane-1-sulfonate	9Cl-PF3ONS	$C_8ClF_{16}SO_4K$	73606-19-6
SaMPAP			
2-(N-ethylperfluorooctane-1-sulfonamido)ethyl phosphate	SaMPAP	$C_{12}H_9F_{17}NO_6PS$	
bis[2-(N-ethylperfluorooctane-1-sulfonamido)ethyl] phosphate	diSaMPAP	$C_{24}H_{22}F_{34}N_3O_8PS_2$	30381-98-7

B.5 Standards of steroid hormone target analytes

Table B5: Standards of steroid hormone target analytes include information on steroid class, the full name of steroid hormone, abbreviation, molecular formula (MF), and CAS-number.

Steroid class	Steroid	Abbreviation	MF	CAS-number
Androgens	Dehydroepiandrosterone	DHEA	$C_{19}H_{28}O_2$	53-43-0
	Androstenedione	AN	$C_{19}H_{26}O_2$	63-05-8
	Androstenediol	A5	$C_{19}H_{30}O_2$	521-17-5
	Testosterone	TS	$C_{19}H_{28}O_2$	58-22-0
	5α-Dihydrotestosterone	DHT	$C_{19}H_{30}O_2$	521-18-6
	11-Ketotestosterone	11-KetoTS	$C_{19}H_{26}O_3$	564-35-2
Corticosteroids	11-deoxycorticosterone	DOC	$C_{21}H_{30}O_3$	64-85-7
	11-deoxycortisol	11-deoxyCOR	$C_{21}H_{30}O_4$	152-58-9
	Aldosterone	ALDO	$C_{21}H_{28}O_5$	52-39-1
	Corticosterone	COS	$C_{21}H_{28}O_5$	50-22-6
	Cortisol	COR	$C_{21}H_{30}O_5$	50-23-7
	Cortisone	CORNE	$C_{21}H_{28}O_5$	53-06-5
Progestogens	Pregnenolone	PREG	$C_{21}H_{32}O_2$	145-13-1
	17α-Hydroxypregnenolone	17α-OH-P5	$C_{21}H_{32}O_3$	387-79-1
	Progesterone	P4	$C_{21}H_{30}O_2$	57-83-0
	17α-hydroxyprogesterone	17α-OHP	$C_{21}H_{30}O_3$	68-96-2
Estrongens	Estrone	E1	$C_{18}H_{22}O_2$	53-16-7
	17β-Estradiol	E2	$C_{18}H_{24}O_2$	50-28-2

B.5.1 Internal standards of PFAS

Table B6: Isotopically labeled internal standards of PFAS including PFAS compound, abbreviation, molecular formula, and CAS-number.

Compound	Abbreviation	Molecular formula	CAS-number
Perfluro-n-octanoic acid $^{13}C_{18}$	PFOA $^{13}C_8$	$^{13}C_8HF_{15}O_2$	335-67-1
Sodium perfluoro-1-octanesulfonate	PFOS $^{13}C_8$	$^{13}C_8F_{17}SO_3$	4021-47-0
1H,2H-Perfluorooctane sulfonic acid (6:2) $^{13}C_2$	6:2 FTS $^{13}C_2$	$C_6{}^{13}C_2H_5F_{13}SO_3$	

B.5.2 Internal standards of steroid hormones

Table B7: Isotopically labeled internal standards of steroid hormones including steroid compound, abbreviation, molecular formula, and CAS-number.

Compound	Abbreviation	Molecular formula	CAS-number
2,3,4-Cortisone-^{13}C3	$^{13}C_3$-CORNE	$C_{18}{}^{13}C_3H_{28}O_5$	112925-31-2
2,3,4-Dihydrotestosterone-^{13}C3	$^{13}C_3$-DHT	$C_{16}{}^{13}C_3H_{30}O_2$	521-18-6
2,3,4-17α-hydroxyprogesterone-^{13}C3	$^{13}C_3$-17α-OHP	$C_{18}{}^{13}C_3H_{30}O_3$	68-96-2

C Appendix - Results

C.1 Steroid hormones in plasma

Table C1: Limit of detection (LOD), limit of quantification (LOQ), absolute recovery (R_{abs}(%)), relative recovery (R_{rel}(%)), and matrix effect (ME (%)) of steroid target analytes analysed in Arctic char plasma (n=9). Samples were spiked with 20 ng mL^{-1} target analytes and 20 ng mL^{-1} internal standard. The instrument LOD and LOQ are calculated from the calibration curve. Some compunds were not detected and is written as NA (Not applicable).

Steroid	**LOD**	**LOQ**	**R_{abs}(%)**	**R_{rel}(%)**	**ME (%)**
COR	3.67	11.12	727	500	-97.5
CORNE	1.02	3.11	264	180	-92.8
ALDO	NA	NA	NA	NA	NA
COS	NA	NA	12300	464	-99.8
11-deoxyCOR	14.2	NA	241	152	-91.0
17α-OHP	1.43	4.33	133	91.6	-57.4
DOC	1.91	5.80	60.2	41.5	-37.4
P4	6.71	20.3	52.3	71.3	-2.00
11-KetoTS	7.00	21.2	297	193	-92.1
DHT	6.41	19.4	64.8	88.7	21.6
TS	5.30	16.1	148	202	-65.9
AN	2.93	8.88	75.8	103	-19.2
PREG	NA	NA	NA	NA	NA
A5	NA	NA	NA	NA	NA
DHEA	NA	NA	44.9	75.1	49.1
17α-OH-P5	NA	NA	139	201	-67.7
E1	NA	NA	NA	NA	NA
E2	NA	NA	NA	NA	NA

C.1.1 Recoveries of steroid hormones in plasma

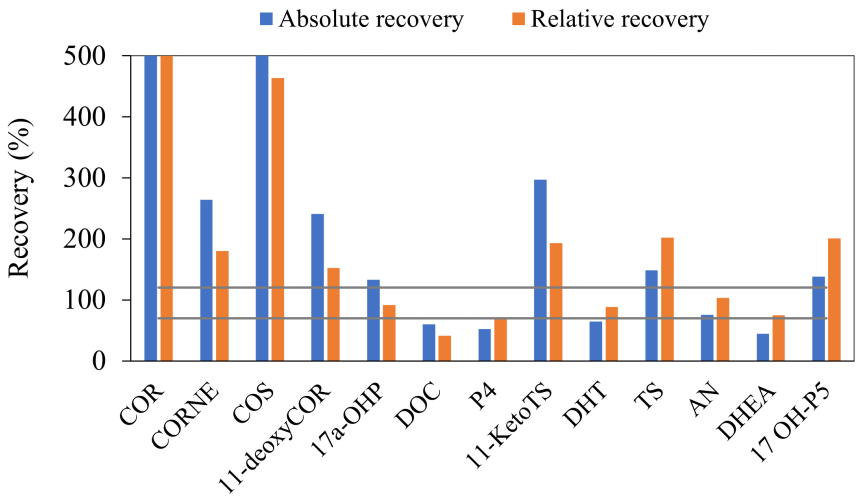

Figure C1: Recoveries of steroid hormones analysed in plasma. The two horisontal lines indicate recoveries between 70-120%.

C.1.2 Matrix effects of steroid hormones in plasma

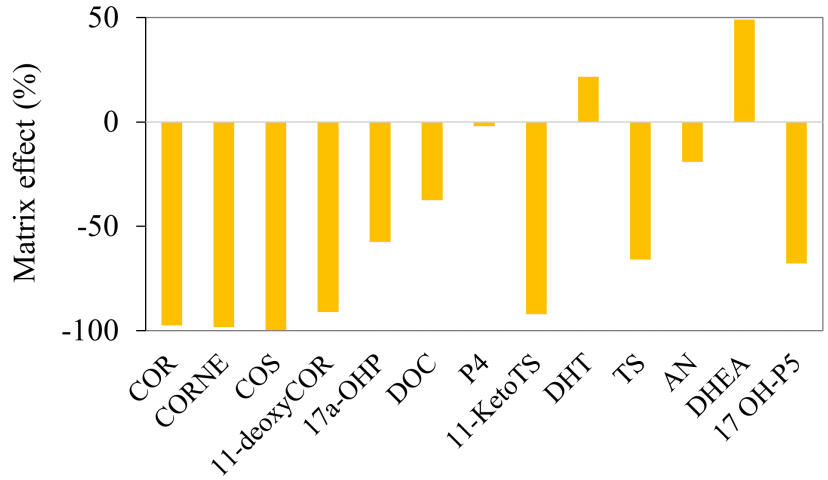

Figure C2: Matrix effects (%) of steroid hormones analysed in plasma.

C.2 PFAS in plasma

Table C2: Concentrations of PFAS compounds observed in individual plasma samples (ng mL^{-1}). Total ΣPFAS concentrations are based on calculations of observed PFAS compounds, however, PFAS compounds with recoveries < 40% (marked with asteriks) are excluded from the total ΣPFAS concentration.

Sample ID	6:2 FTS	PFNA	PFOSA	PFOS	PFDA	FOSAA	PFUnA	MeFOSAA	PFDoDA	PFTriDA	DiSAMPAP	PFECHS	ΣPFAS
P-1b	9.51	2.00		8.98		*4.87	6.12		4.17	3.81	*5.74	4.05	38.7
P-2b	9.28	1.87		6.43			5.18	*5.36		3.49			26.2
P-3Ab	9.79	2.09		1.93		*4.64	4.20					4.19	22.2
P-3Bb	9.97	2.03	5.54	5.23		*4.35	5.13					4.01	32.0
P-4b	9.77	1.98		4.63	4.30		6.06						26.7
P-5b	9.48	1.85		4.83			4.60						20.8
P-6Ab	9.83	2.02		4.48			5.06						21.4
P-6Bb	9.61	1.88		4.98			4.56						21.0
P-7b	9.51	1.85		7.03			6.48		4.06	3.52			32.5

*Values are based on relative recoveries <40%

Table C3: Absolute recovery (R_{abs} (%)), relative recovery (R_{abs} (%)), matrix effect (ME (%)), limit of detection (LOD) and limit of quantification (LOQ) of PFAS target analytes analysed in Arctic char plasma (n=9). Samples were spiked with 20 ng mL^{-1} target analytes and 20 ng mL^{-1} internal standard. The instrument LOD and LOQ are calculated from the calibration curve. Some compunds were not detected and is written as NA (Not applicable).

Compound	**R_{abs} (%)**	**R_{abs} (%)**	**ME (%)**	**LOD**	**LOQ**
DecaS	74.0	87.6	-64.8	3.84	11.6
GenX	87.9	104	-34.2	5.33	16.2
PFPeA	92.0	109	-64.7	4.46	13.5
PFHxA	84.6	100	-34.8	3.36	10.2
4:2 FTS	76.8	90.9	3.50	0.47	1.43
7H-PFHpA	77.8	92.1	-25.1	0.28	0.84
NaDONA	79.6	94.3	-1.30	0.32	0.97
TriDeHFxSA	131	-82.1	-112	NA	NA
PFOA	91.4	98.3	-1.30	6.23	18.9
6:2 FTS	78.9	99.2	18.4	4.96	15.0
PFHpS	77.4	91.7	12.4	2.52	7.63
PFNA	84.6	100	0.60	3.12	9.47
P37DMOA	81.1	96.0	12.9	4.90	14.9
PFOSA	77.9	92.2	5.50	6.17	18.7
PFOS	81.7	96.9	16.1	4.40	13.3
MeFOSA	74.6	88.3	8.90	6.43	19.5
PDFA	85.2	101	-38.6	4.14	12.5
EtFOSA	74.5	88.2	9.10	6.15	18.7
EtFOSAA	75.9	89.9	7.10	6.69	20.3
8:2 FTS	77.7	92.0	1.70	3.24	9.82
9Cl-PF3ONS	78.4	92.9	12.8	5.24	15.9
FOSAA	1.20	1.40	1.20	4.80	14.5
PFUnA	82.5	97.6	8.30	4.72	14.3
MeFOSAA	8.90	10.5	-6.60	6.22	18.9
EtFOSE	77.8	92.2	9.00	10.6	32.0
PFDoDA	87.0	103	-16.8	4.32	13.1
MeFOSE	75.6	89.5	11.5	11.5	34.7
10:2 FTS	80.7	95.5	-23.8	6.29	19.1
PFTriDA	79.5	94.1	-2.50	3.42	10.4
DiSAMPAP	9.20	10.9	-3.60	6.20	18.8

Table C3: Absolute recovery (R_{abs} (%)), relative recovery (R_{abs} (%)), matrix effect (ME (%)), limit of detection (LOD) and limit of quantification (LOQ) of PFAS target analytes analysed in Arctic char plasma (n=9). Samples were spiked with 20 ng mL^{-1} target analytes and 20 ng mL^{-1} internal standard. The instrument LOD and LOQ are calculated from the calibration curve. Some compunds were not detected and is written as NA (Not applicable).

Compound	**R_{abs} (%)**	**R_{abs} (%)**	**ME (%)**	**LOD**	**LOQ**
PFTDA	84.2	99.7	25.0	7.75	23.5
PFHxA	66.1	78.3	-7.50	4.58	13.9
PFBA	94.8	112	-88.0	2.08	6.29
PFBS	81.1	96.0	21.9	0.29	0.87
PFPeS	86.8	103	-16.3	1.47	4.45
PFHpA	92.8	110	-18.9	0.25	0.75
PFHxS	102	120	-9.70	NA	NA
PFECHS	78.8	93.3	6.80	0.46	1.38
PFNS	NA	NA	NA	NA	NA
PFDS	NA	NA	NA	NA	NA
SaMPAP	NA	NA	NA	NA	NA
PFDoDS	NA	NA	NA	NA	NA
PFOcDA	NA	NA	NA	NA	NA

C.2.1 Recoveries of PFAS in plasma

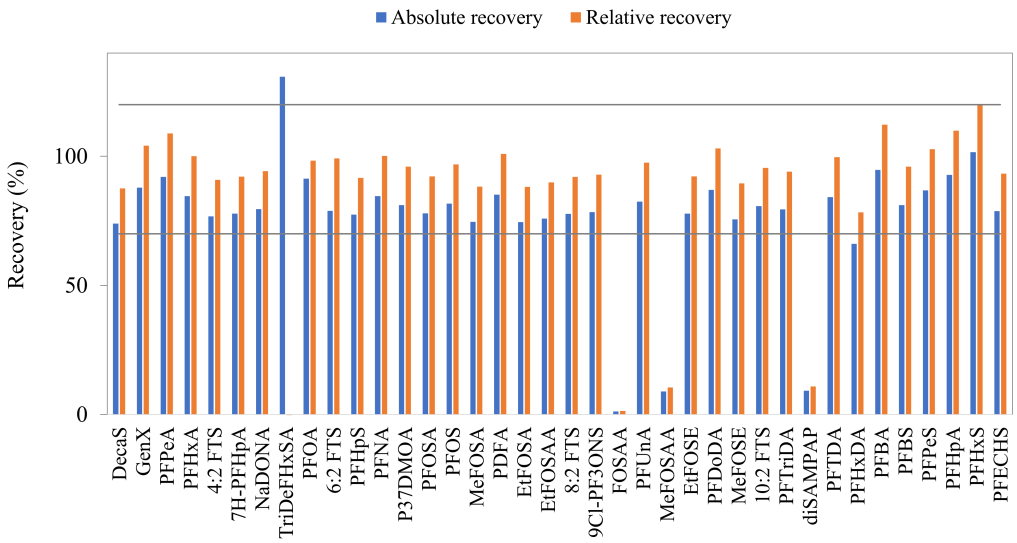

Figure C3: Absolute and relative percentage recoveries (%) of PFAS target analytes in plasma of Arctic char for 38 out 43 analysed PFAS. The PFAS that are not reported here were not detected or had poor separation. The two grey horizontal lines indicate recovery between 70-120%.

C.2.2 Matrix efects of PFAS in plasma

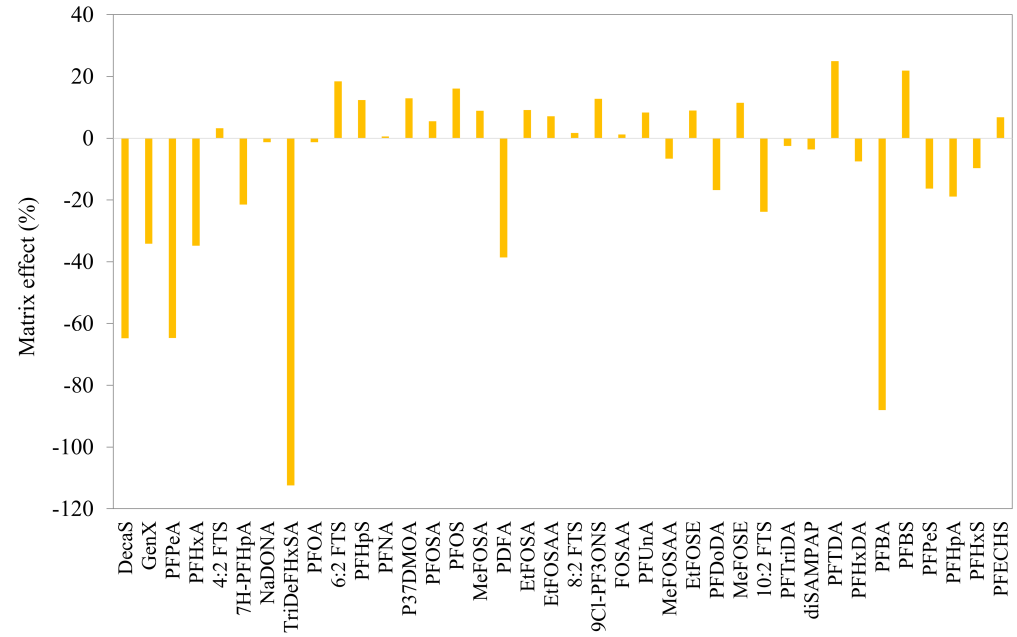

Figure C4: Percentage matrix effect (%) of PFAS target analytes in plasma of Arctic char for 38 out of 43 analysed PFAS. The PFAS that are not reported here were not detected or had poor separation.

C.3 Comparison of LOD and LOQ estimations

Table C4: Comparison of LOD and LOD calculated based on the calibration curve (LOD_{cal} and LOQ_{cal}) and from S/N peak heights ($LOD_{S/N}$ and $LOQ_{S/N}$), 3 times S/N and 10 times S/N for LOD and LOQ, respectively. Information on the linear range and number of calibration points (cal. points) used for the calibration curve method.

Compound	**LOD_{cal}**	**LOQ_{cal}**	**$LOD_{S/N}$**	**$LOQ_{S/N}$**	**Linear range**	**Cal. points**
Steroids						
COR	3.67	11.1	$1.11 \cdot 10^{-3}$	$3.69 \cdot 10^{-3}$	5-20	3
11-KetoTS	7.00	21.2	1.95	6.49	2-20	4
DHT	6.41	19.4	3.24	16.2	2-20	4
TS	5.30	16.1	0.765	2.55	0.5-20	6
AN	2.93	8.88	0.0192	0.0638	0.2-20	7
PFAS						
6:2 FTS	4.96	15.0	$7.56 \cdot 10^{-5}$	$2.52 \cdot 10^{-4}$	0-50	10
PFNA	3.12	9.47	0.333	1.11	0.2-50	8
PFOSA	6.17	18.7	$4.49 \cdot 10^{-5}$	$1.50 \cdot 10^{-4}$	0.1-50	9
PFOS	4.40	13.3	$8.31 \cdot 10^{-5}$	$2.77 \cdot 10^{-4}$	0-50	10
PDFA	4.14	12.5	$1.37 \cdot 10^{-4}$	$4.58 \cdot 10^{-4}$	0.2-50	8
FOSAA	4.80	14.5	0.112	0.373	0.1-50	9
PFUnA	4.72	14.3	0.280	0.935	0.1-50	9
MeFOSAA	6.22	18.9	$2.84 \cdot 10^{-5}$	$9.48 \cdot 10^{-5}$	0.1-50	9
PFDoDA	4.32	13.1	$3.22 \cdot 10^{-5}$	$1.07 \cdot 10^{-4}$	0.1-50	9
PFTriDa	3.42	10.4	$2.95 \cdot 10^{-5}$	$9.83 \cdot 10^{-5}$	0.2-50	8
DiSAMPAP	6.20	18.8	$4.91 \cdot 10^{-5}$	$1.64 \cdot 10^{-4}$	0.1-50	9
PFECHS	0.46	1.38	$5.25 \cdot 10^{-6}$	$1.75 \cdot 10^{-5}$	0.1-50	9

C.4 Method test for extraction of steroid hormones and PFAS in liver samples

Table C5: Absolute and relative recoveries (%) of steroid hormones and PFAS target analytes with four different extraction and clean-up methods; Hybrid SPE with 0.1% AF in MeOH (Hybrid SPE_{AF}), Hybrid SPE with 0.5% CA in ACN (Hybrid SPE_{CA}), solid-phase extraction (SPE_{C18}), and solid-liquid extraction (SLE).

	Absolute recovery (%)				**Relative recovery (%)**			
Compound	Hybrid SPE_{AF}	Hybrid SPE_{CA}	SPE_{C18}	SLE	Hybrid SPE_{AF}	Hybrid SPE_{CA}	SPE_{C18}	SLE
Steroid hormones								
COR	148	85.2	19.4	98.8	284	103	31.1	147
CORNE	138	90.2	19.1	107	256	108	30.3	158
ALDO	NA	80.6	24.1	76.3	NA	96.3	38.4	113
COS	190	38.3	30.9	48.3	372	48.8	53.3	72.2
11-deoxyCOR	81.7	42.7	63.4	97.5	155	67.2	106	146
17a-OHP	53	83.7	68	77.6	99.8	100	108	115
DOC	41.4	54.9	65.4	69.3	77.0	66.3	104	102
P4	60.7	80.4	71.0	28.9	109	130	133	86.0
11-KetoTS	136	85.2	37.6	79.6	257	104	60.9	117
DHT	65.5	71.5	79.8	48.4	118	117	155	144
TS	56.3	99.6	71.6	72.7	101	162	134	216
AN	60.1	66.2	73.7	52.5	108	107	138	156
DHEA	39.5	39.7	93.1	21.4	117	85.4	NA	63.6
17 OH-P5	61.1	64.1	206	81.3	122	118	2510	242
P5	NA	NA	NA	NA	NA	NA	NA	NA
E1	NA	NA	NA	NA	NA	NA	NA	NA
E2	NA	NA	NA	NA	NA	NA	NA	NA
PREG	NA	NA	NA	NA	NA	NA	NA	NA

Table C5 continued from previous page

	Absolute recovery (%)				Relative recovery (%)			
Compound	Hybrid SPE_{AF}	Hybrid SPE_{CA}	SPE_{C18}	SLE	Hybrid SPE_{AF}	Hybrid SPE_{CA}	SPE_{C18}	SLE
PFAS								
DecaS	91.0	508	60.4	113	73.8	482	59.8	78.4
GenX	NA	NA	NA	114	NA	NA	NA	78.4
PFPeA	242	61.4	0.10	46.1	103	58.2	NA	32.0
PFHxA	230	38.3	2.25	51.6	108	36.4	2.18	35.8
4:2 FTS	44.7	25.8	3.04	53.2	36.3	24.5	3.02	36.5
7H-PFHpA	98.7	53.6	0.93	49.3	79.9	50.8	0.88	33.9
NaDONA	117	56.3	10.9	84.6	94.6	53.4	10.8	58.1
TriDeFHxSA	98.6	21.5	41.7	106	79.9	20.4	66.5	118
PFOA	184	63.6	16.5	NA	148	60.3	16.1	126
6:2 FTS	162	44.6	91.5	142	116	48.8	100	86.6
PFHpS	100	109	24.8	86.2	81.1	103	24.7	59.2
PFNA	13.3	47.7	14.6	7.01	32.5	45.2	14.4	5.69
P37DMOA	73.1	27.4	17.0	11.8	59.2	26.0	16.9	8.16
PFOSA	68.2	55.3	161	2.89	55.3	55.7	160	1.99
PFOS	78.1	29.0	14.1	5.67	529	27.5	13.9	3.89
MeFOSA	78.9	60.7	10.9	6.76	64.0	57.6	10.8	4.64
PDFA	87.7	34.1	29.7	7.44	71.1	32.4	29.5	5.11
EtFOSA	77.3	63.8	7.82	5.25	62.6	60.5	7.76	3.61
EtFOSAA	81.4	45.9	12.3	6.01	66.0	43.5	12.2	4.13
8:2 FTS	133	53.3	26.6	7.21	108	50.5	26.1	4.96
9Cl-PF3ONS	91.2	39.3	11.2	8.81	74.2	37.3	11.1	6.06
FOSAA	112	35.4	54.6	1.68	NA	33.6	54.1	2.09

Table C5 continued from previous page

	Absolute recovery (%)				Relative recovery (%)			
Compound	Hybrid SPE_{AF}	Hybrid SPE_{CA}	SPE_{C18}	SLE	Hybrid SPE_{AF}	Hybrid SPE_{CA}	SPE_{C18}	SLE
PFUnA	57.2	37.1	77.4	12.7	46.4	35.2	76.8	8.99
MeFOSAA	61.3	34.2	159	3.19	49.7	32.4	158	2.70
EtFOSE	111	71.2	9.78	5.0	90.0	67.5	9.71	3.47
PFDoDA	108	60.3	96.8	8.76	85.5	57.2	96.1	6.42
MeFOSE	92.1	68.4	19.8	10.2	74.7	64.8	19.7	6.98
10:2 FTS	30.4	54.1	92.8	9.80	24.7	51.3	92.1	6.76
PFTriDA	92.1	73.5	129	14.2	74.6	69.7	128	9.90
DiSAMPAP	NA	NA	NA	8	NA	NA	NA	5.72
PFTDA	80.3	76.7	33.5	12.1	65.2	72.8	33.3	8.42
PFHxDA	87.0	55.7	2.23	6.77	70.5	52.8	2.20	4.84
PFBA	245	38.2	NA	272	199	42.3	NA	187
PFBS	151	38.2	0.22	42.6	123	36.2	0.22	29.4
PFPeS	85.9	32.6	3.50	48.5	69.6	30.9	3.47	33.3
PFHpA	222	53.8	5.35	62.5	180	51.0	5.32	43.3
PFHxS	128	47.6	2.36	65.6	104	45.2	2.34	45.1
PFECHS	156	51.8	16.3	247	126	49.1	16.2	169
PFNS	60.3	16.0	26.2	13.5	48.8	15.1	26.0	9.25
PFDS	21.5	32.0	78.8	12.4	17.4	30.4	78.2	8.65
SAMPAP	54.3	45.9	65.6	336	44.0	43.6	64.5	NA
PFDoDS	58.9	71.5	50.8	14.2	47.8	67.8	50.4	9.77
PFOcDA	83.6	21.6	0.16	12.6	67.8	20.5	0.13	8.81

Table C6: Matrix effects (%) for steroid hormones and PFAS target analytes with four different extraction and clean-up methods; Hybrid SPE with 0.1% AF in MeOH (Hybrid SPE_{AF}), Hybrid SPE with 0.5% CA in ACN (Hybrid SPE_{CA}), solid-phase extraction (SPE_{C18}), and solid-liquid extraction (SLE).

	Matrix effect (%)			
Compound	Hybrid SPE_{AF}	Hybrid SPE_{CA}	SPE_{C18}	SLE
Steroid hormones				
COR	-57.8	-91.2	-65.4	-86.6
CORNE	-46.2	-94.5	-72.4	-90.0
ALDO	-100	6.10	-69.1	-85.3
COS	-49.5	-84.5	-68.0	-56.7
11-deoxyCOR	-7.10	-93.0	-71.8	-79.4
17a-OHP	-1.50	-84.1	-52	-55.5
DOC	-6.30	-74.2	-34.1	-39.6
P4	-62.2	-78.1	-58.4	-11.7
11-KetoTS	-47.6	-95.4	-72.2	-88.8
DHT	-60.5	-71.6	-43.1	6.2
TS	70.1	-86.1	-59.1	-65.8
AN	-72.1	-49.7	-60.5	-44.2
DHEA	-42.3	-6.10	-71.0	115
17 OH-P5	-29.6	-29.6	-83.3	-48.5
P5	NA	NA	NA	NA
E1	NA	NA	NA	NA
E2	NA	NA	NA	NA
PREG	NA	NA	NA	NA
PFAS				
DecaS	-78.6	-70.0	-51.3	-17.7
GenX	NA	NA	-43.5	-92.2
PFPeA	-99.9	-55.7	1.63	-81.0
PFHxA	-99.9	-11.2	-39.1	-83.9
4:2 FTS	-99.4	18.9	33.1	-64.4
7H-PFHpA	-99.6	-21.9	-12.6	-85.9
NaDONA	-99.0	-30.9	-57.3	-84.4
TriDeFHxSA	-88.8	NA	-150	-334
PFOA	-91.8	55.9	-56.2	-120
6:2 FTS	-81.9	96.1	-247	23.3

Table C6 continued from previous page

	Matrix effect (%)			
Compound	Hybrid SPE_{AF}	Hybrid SPE_{CA}	SPE_{C18}	SLE
PFHpS	-98.7	-57.7	-70.9	-84.9
PFNA	-99.9	0.45	-79.4	-90.9
P37DMOA	-99.9	-9.31	-78.7	-93.3
PFOSA	-99.4	101	-86.6	-91.4
PFOS	-100	-47.9	-73.0	-88.7
MeFOSA	84	24300	1300	187
PDFA	-99.9	-1.87	-75.2	-84.3
EtFOSA	142	58900	1430	149
EtFOSAA	-80.0	1360	-25.2	-79.4
8:2 FTS	-99.9	193	-32.7	-63.0
9Cl-PF3ONS	-99.9	-61.3	-84.2	-94.9
FOSAA	-101	52.1	-75.7	-83.7
PFUnA	-99.6	125	-80.1	-83.2
MeFOSAA	-99.7	165	-80.1	-87.4
EtFOSE	-66.3	5890	681	45.0
PFDoDA	-99.8	87.2	-85.3	-89.8
MeFOSE	-42.5	44000	526	43.9
10:2 FTS	-99.3	312	-70.1	-81.6
PFTriDA	-72.5	5450	130	-81.2
DiSAMPAP	-101	NA	41.1	-49.5
PFTDA	-84.7	3620	92.4	88.9
PFHxDA	71.8	39200	330	-75.7
PFBA	NA	211	NA	113
PFBS	-99.7	-46.5	3.58	-79.0
PFPeS	-99.6	-18.1	-27.1	-81.3
PFHpA	-99.6	-40.8	-56.5	-83.9
PFHxS	-99.5	-2.80	-47.1	-82.9
PFECHS	-91.3	-24.9	-69.3	-73.6
PFNS	-99.9	111	-70.6	-84.3
PFDS	-99.6	21.8	-82.9	-85.8
SAMPAP	2.28	17700	73.1	-103
PFDoDS	-53.6	4650	160	-82.7
PFOcDA	-73.7	2780	-64.9	-79.7

C.4.1 Recoveries of steroid hormones in liver samples

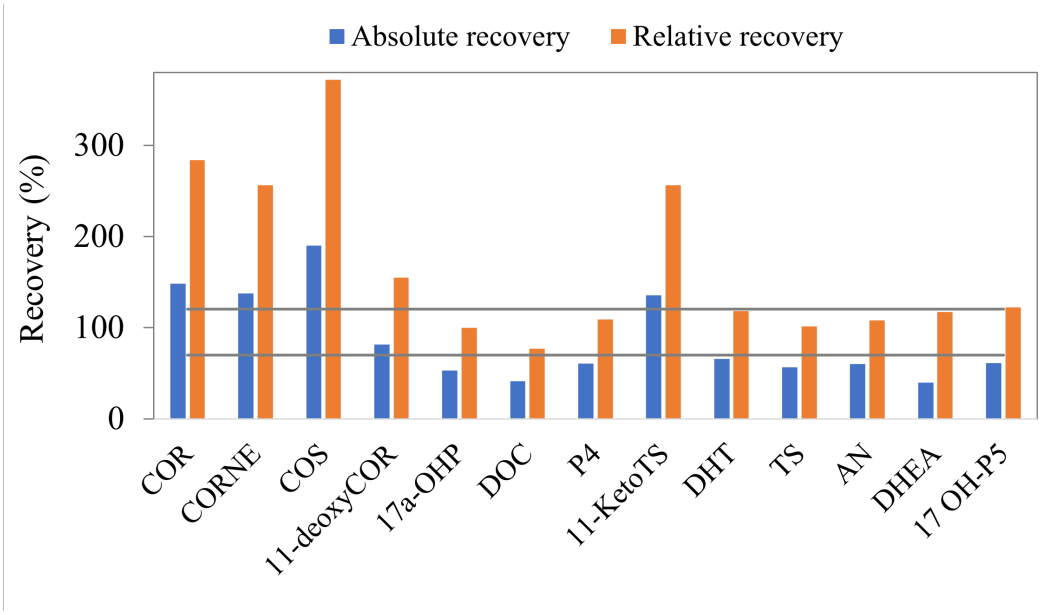

Figure C5: Absolute and relative recoveries (%) of steroid hormones extracted with Hybrid SPE with 0.1% AF in MeOH in liver samples. The two grey horizontal lines indicate recovery between 70-120%.

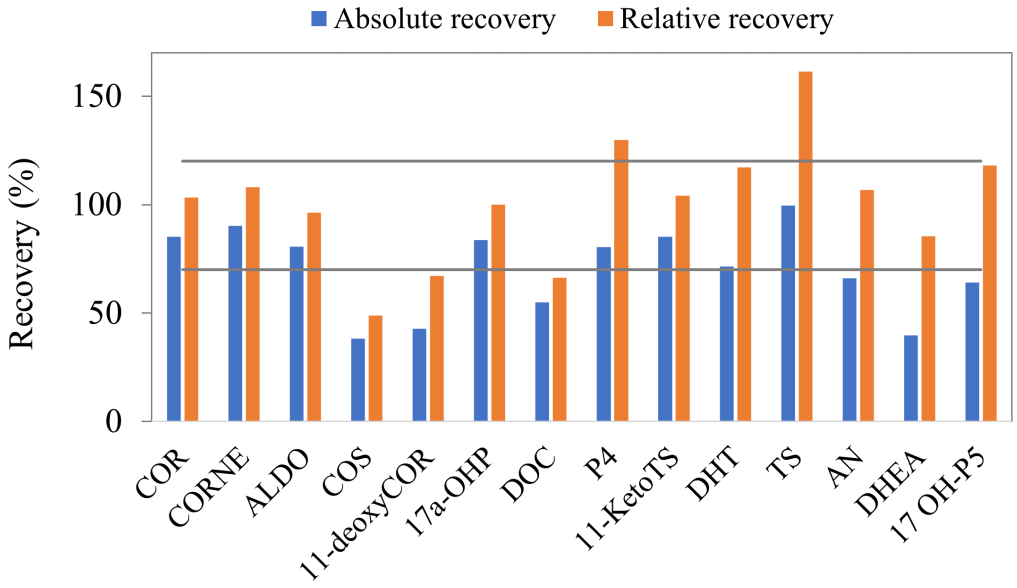

Figure C6: Absolute and relative recoveries (%) of steroid hormones extracted with Hybrid SPE with 0.5% CA in ACN in liver samples. The two grey horizontal lines indicate recovery between 70-120%.

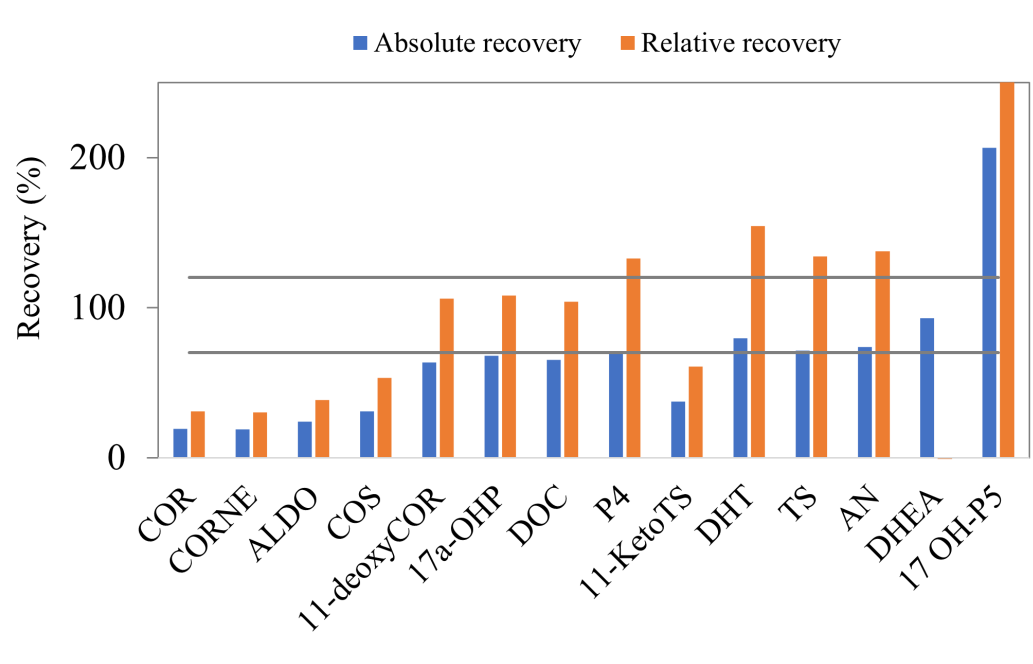

Figure C7: Absolute and relative recoveries (%) of steroid hormones extracted with reversed phase (C18) SPE in liver samples. The two grey horizontal lines indicate recovery between 70-120%.

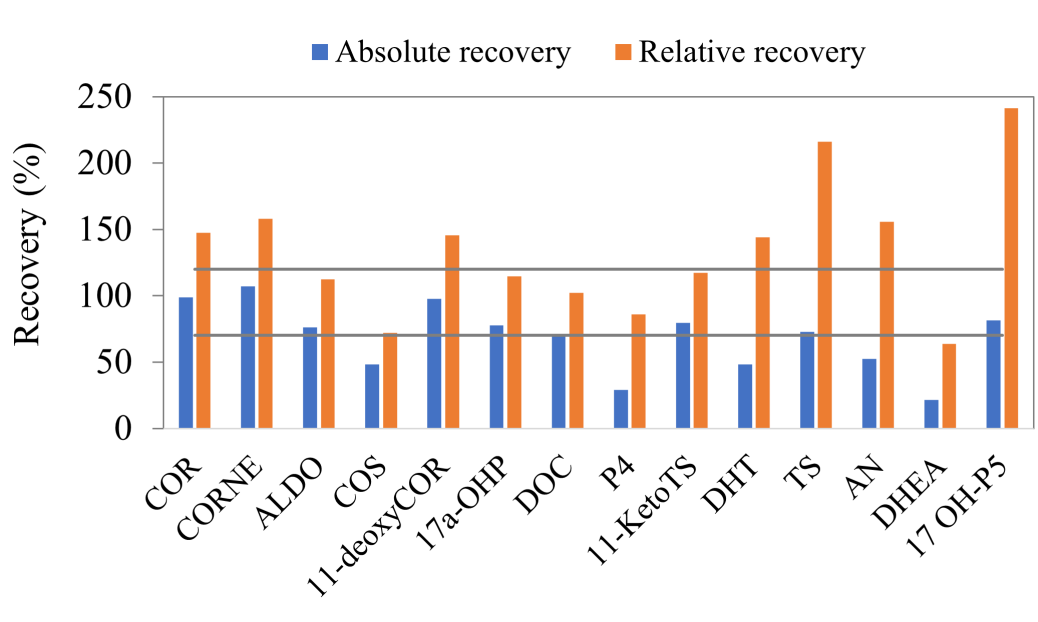

Figure C8: Absolute and relative recoveries (%) of steroid hormones extracted with SLE liver samples. The two grey horizontal lines indicate recovery between 70-120%.

C.4.2 Matrix effects of steroid hormones in liver samples

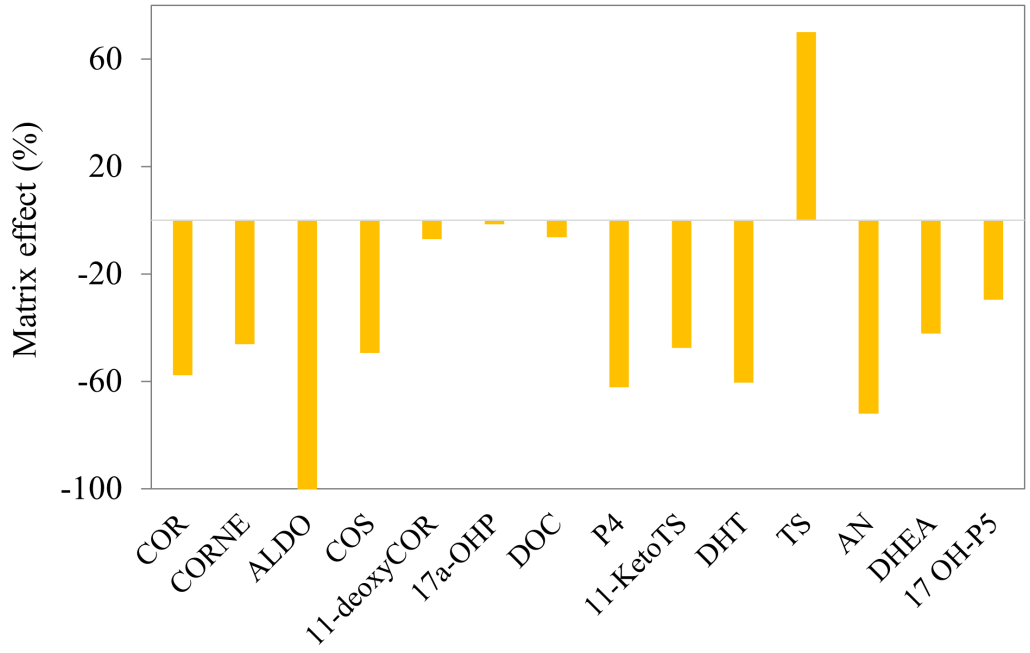

Figure C9: Matrix effects (%) of steroid hormones extracted with Hybrid SPE with 0.1% AF in MeOH in liver samples.

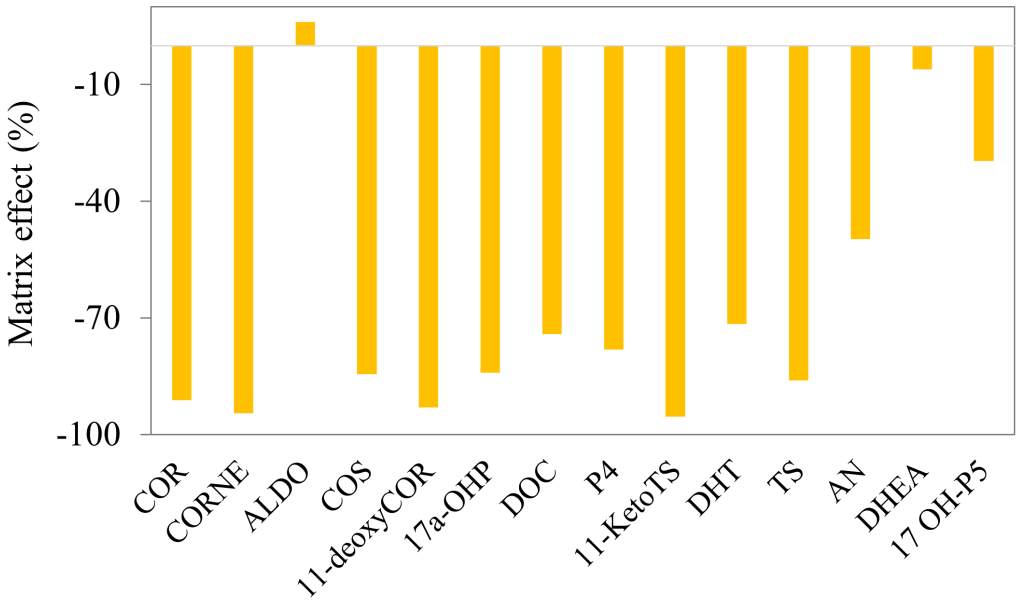

Figure C10: Matrix effects (%) of steroid hormones extracted with Hybrid SPE with 0.5% CA in ACN in liver samples.

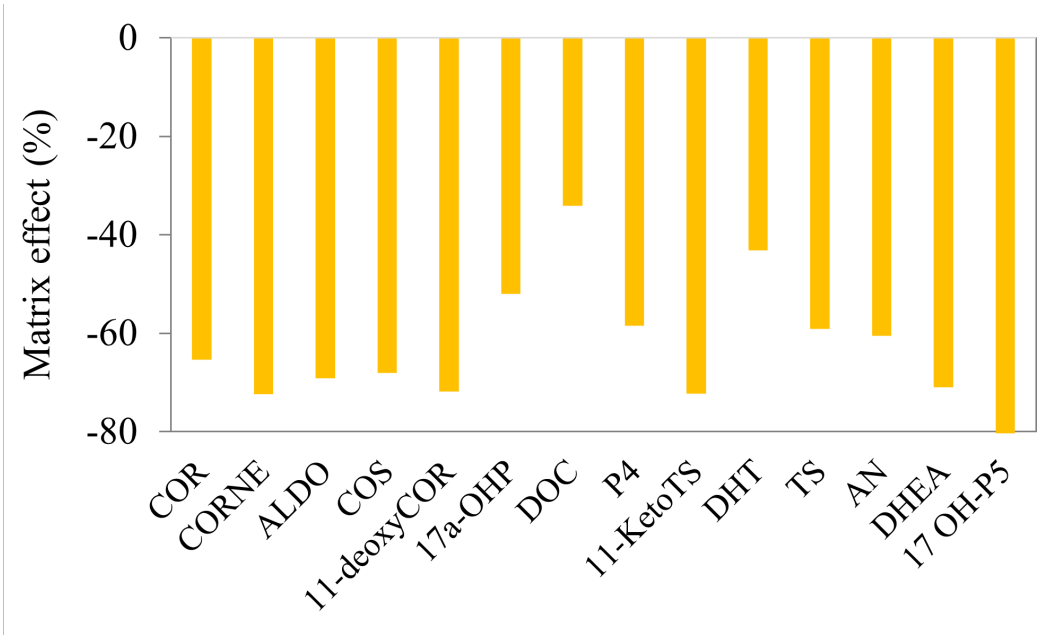

Figure C11: Matrix effects (%) of steroid hormones extracted with reversed phase (C18) SPE in liver samples.

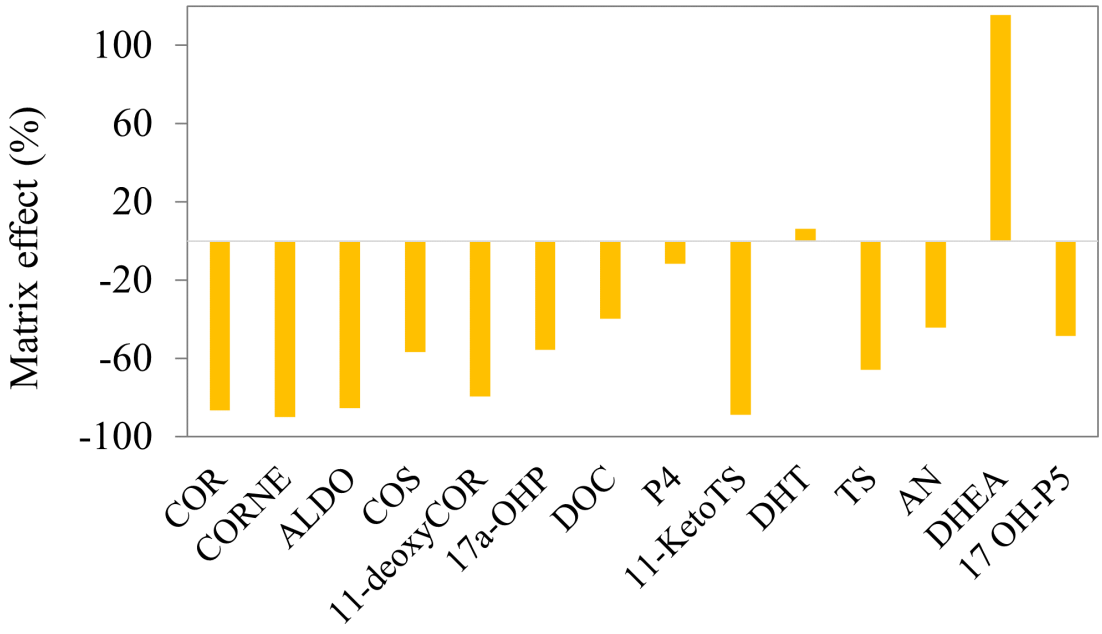

Figure C12: Matrix effects (%) of steroid hormones extracted with SLE in liver samples.

C.4.3 Recoveries of PFAS in liver samples

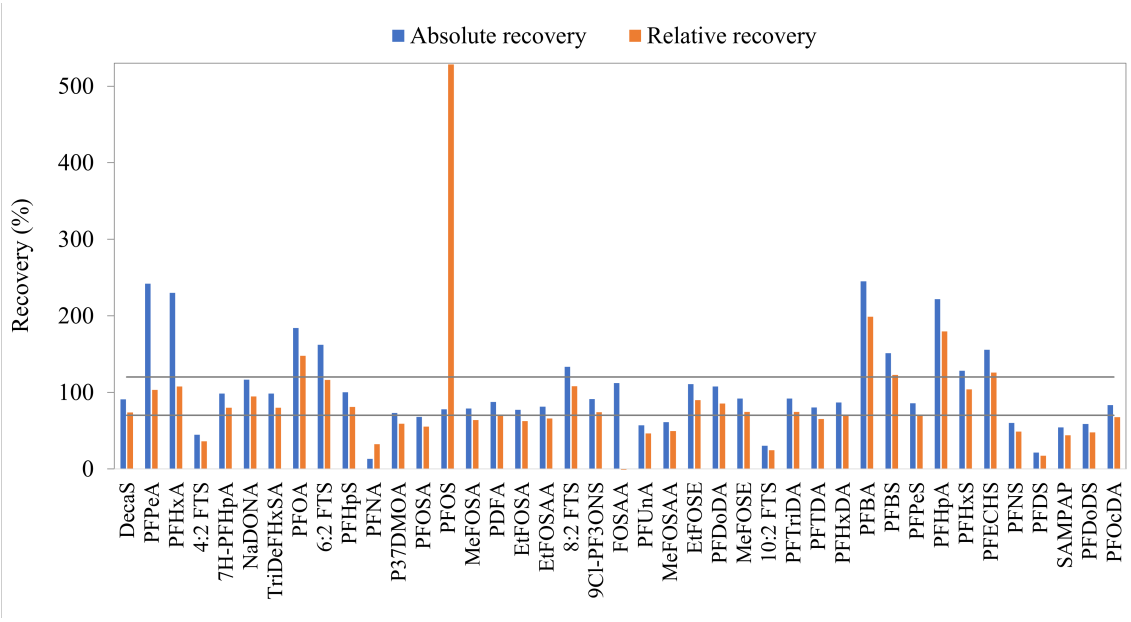

Figure C13: Absolute and relative recoveries (%) of PFAS extracted with Hybrid SPE with 0.1% AF in MeOH in liver samples. The two grey horizontal lines indicate recovery between 70-120%.

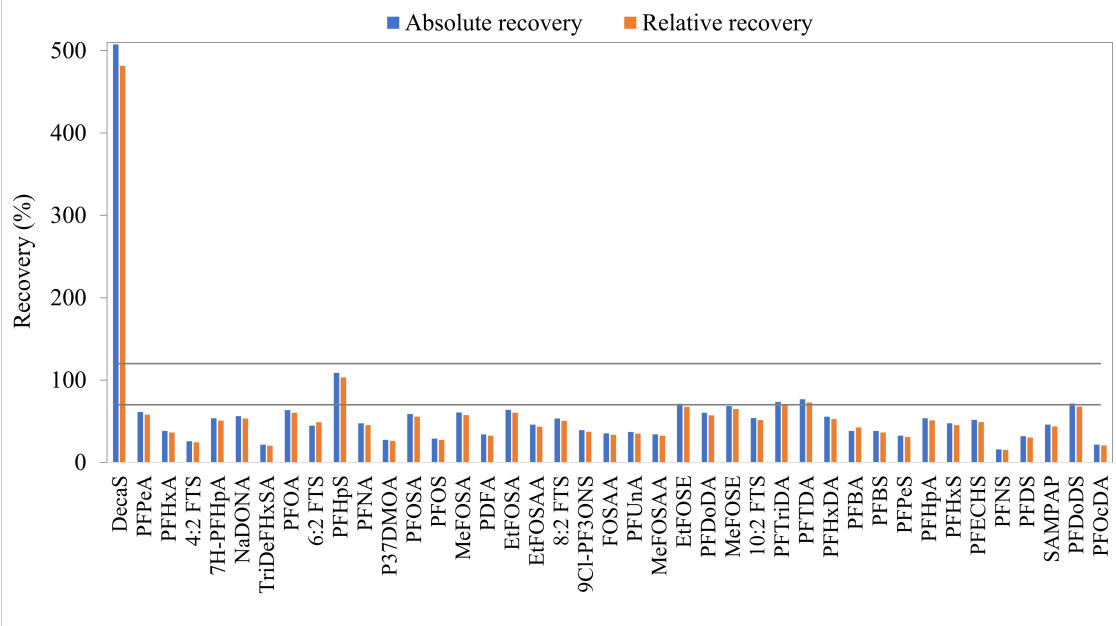

Figure C14: Absolute and relative Recoveries (%) of PFAS extracted with Hybrid SPE with 0.5% CA in ACN in liver samples. The two grey horizontal lines indicate recovery between 70-120%.

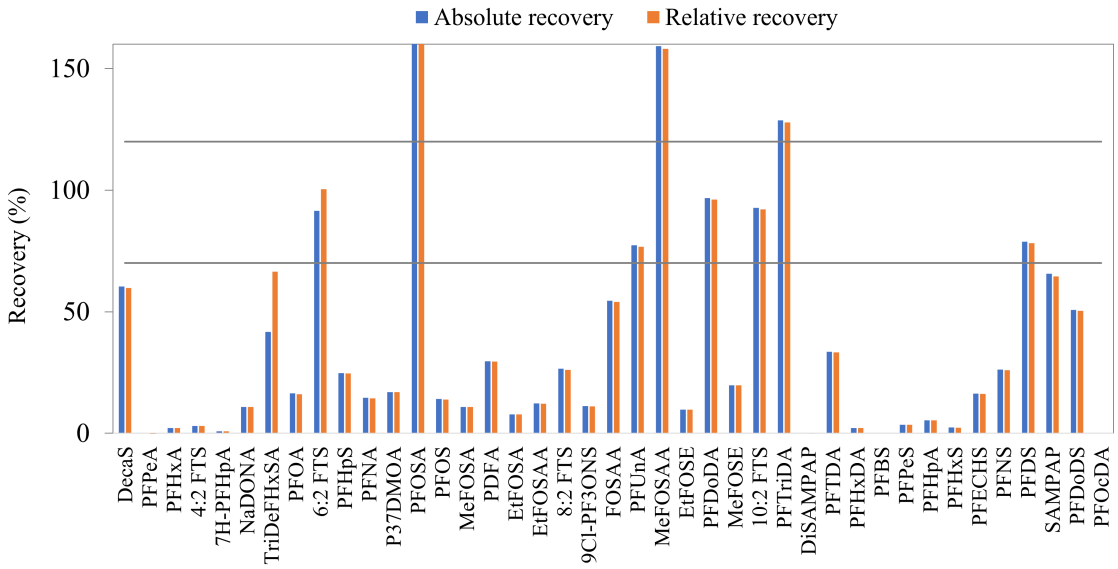

Figure C15: Absolute and relative Recoveries (%) of PFAS extracted with reversed phase (C18) SPE in liver samples. The two grey horizontal lines indicate recovery between 70-120%.

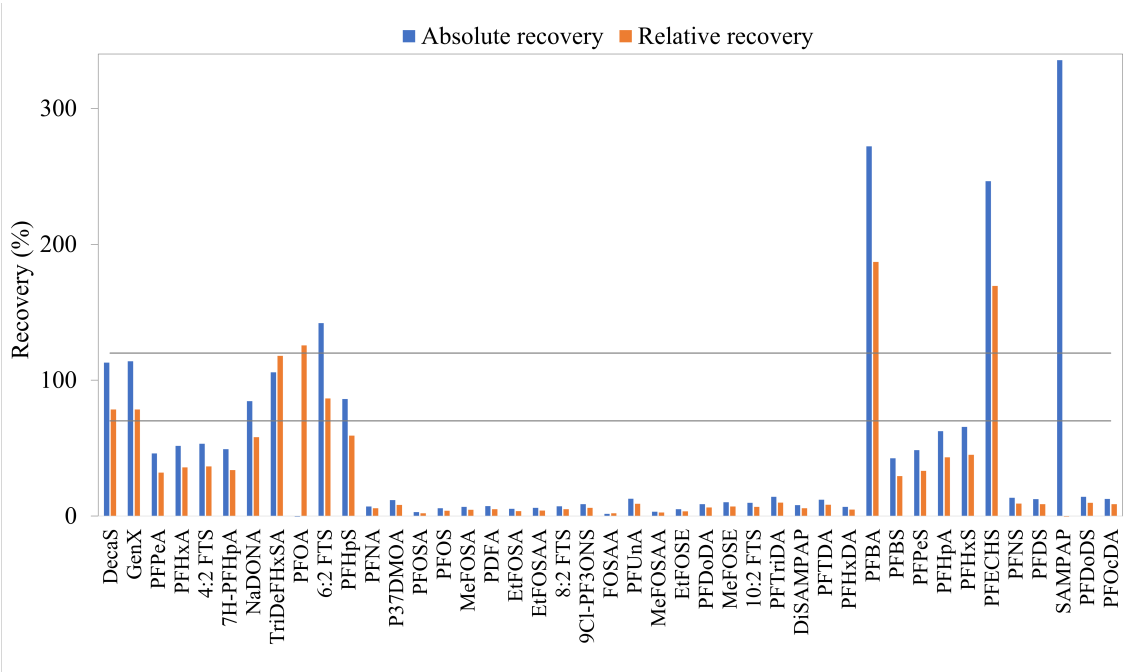

Figure C16: Absolute and relative Recoveries (%) of PFAS extracted with SLE in liver samples. The two grey horizontal lines indicate recovery between 70-120%.

C.4.4 Matrix Effects of PFAS in liver samples

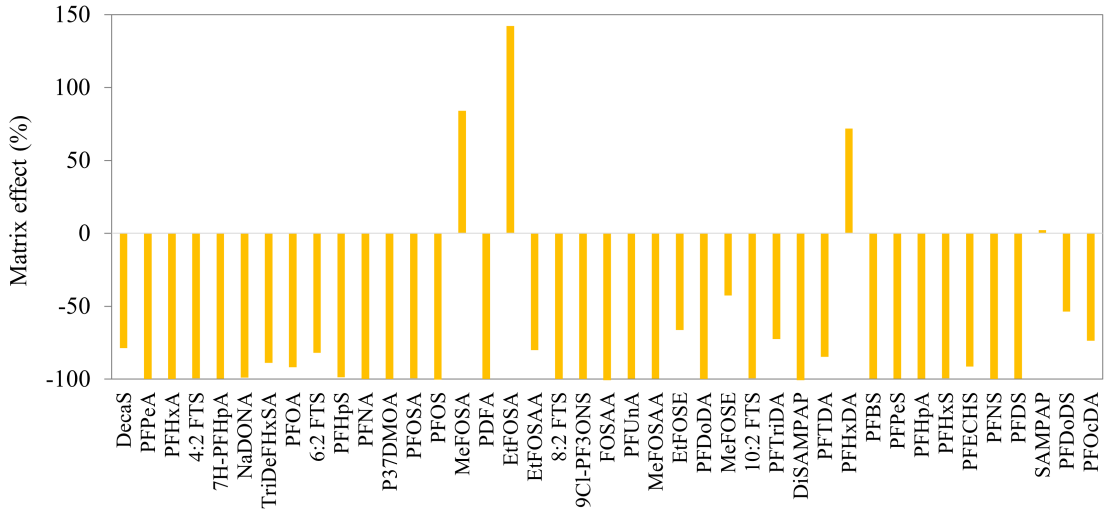

Figure C17: Matrix effects (%) of PFAS extracted with Hybrid SPE with 0.1% AF in MeOH in liver samples.

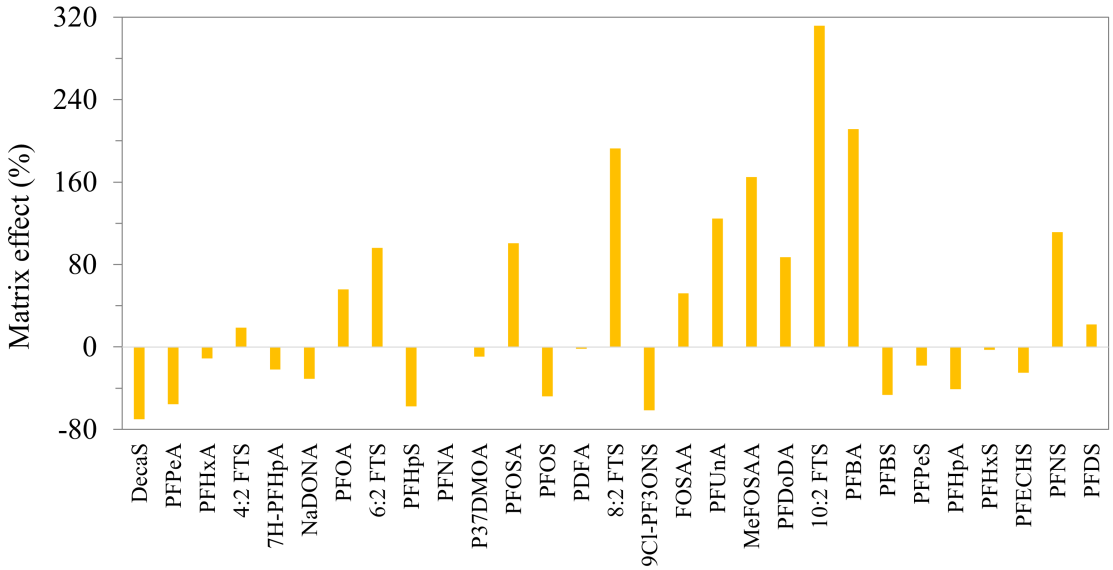

Figure C18: Matrix effects (%) of PFAS extracted with Hybrid SPE with 0.5% CA in ACN in liver samples.

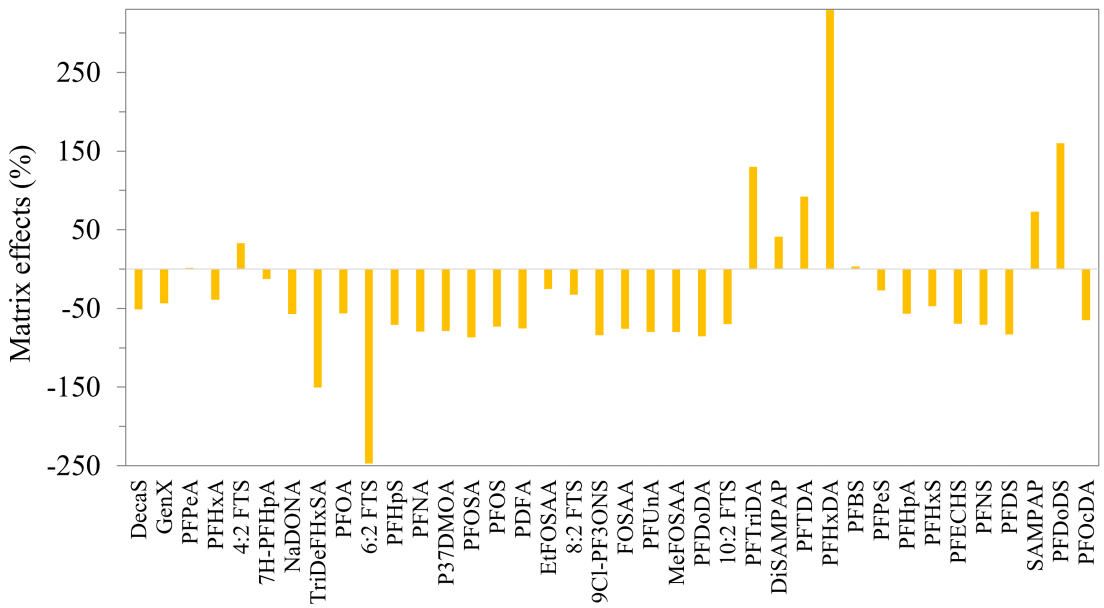

Figure C19: Matrix effects (%) of PFAS extracted with reversed phase (C18) SPE in liver samples.

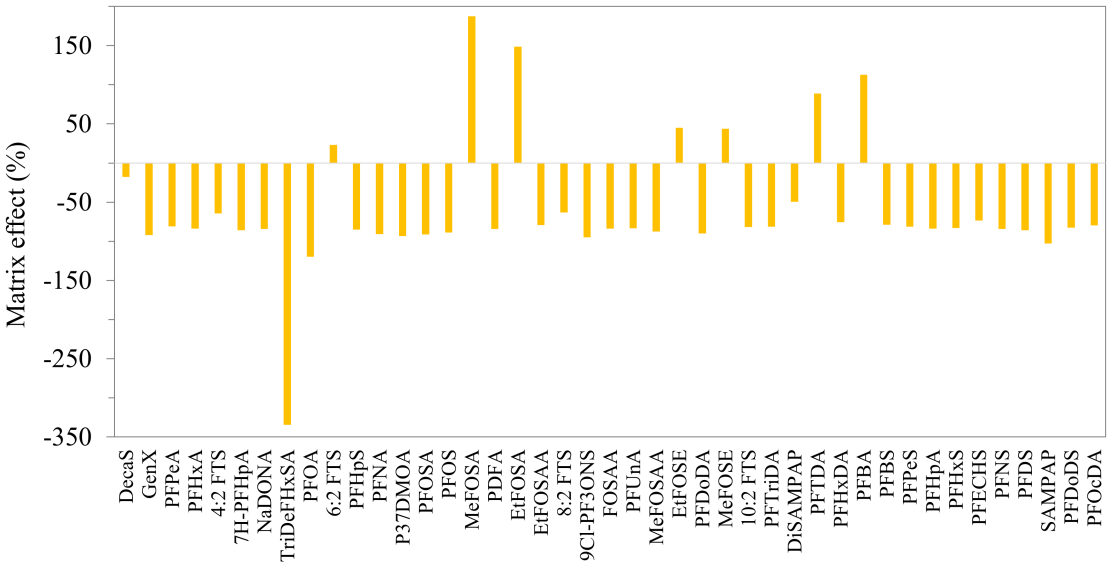

Figure C20: Matrix effects (%) of PFAS extracted with SLE in liver samples.

C.5 Water content (%) in organ samples

Table C7: Mean±SD percentage water content (%) of the different sample matrices, where n is the number of samples. The water content was determined by weighing the samples before and after freeze-drying, as described in the method section 3.3.2. Formula used for calulation of the water concent is provided in the theory section 2.12.

Matrix (n)	**Water content (%)**
Brain (6)	77.2±20.0
Gonad (7)	65.4±27.3
Eggs (4)	62.8±1.15
Liver (7)	64.6±9.16
Kidney (7)	78.4±6.43

C.6 Elemental composition in organs of Arctic char

Table C8: Concentrations of 41 elements in samples from Arctic char. Mean, median, and minium (Min), and maximum (Max) of elemental concentrations in μg g^{-1} for tissue samples in Arctic char from Lake Disetvatnet, and the relative standard deviation (RSD %) of the mean concentrations. Sample matrix and number of samples above LOD (n > LOD). Sample matrices with less than two samples above LOD are given as < LOD. Concentrations for brain, gonad, hard roe, liver, and kidney are given in dry weight and concentrations in red blood cells (RBC) and plasma are given in wet weight.

Element	Matrix	n >LOD	Mean	RSD (%)	Median	Min	Max
Mg	Brain	6	875	1.19	663	510	1890
	Gonad	7	582	1.25	493	89.9	1060
	Hard roe	4	1090	0.86	1150	524	1550
	Liver	7	642	0.86	526	338	1060
	Kidney	7	851	1.23	853	534	1090
	RBC	9	75.4	0.99	72.0	54.2	117
	Plasma	7	36.2	0.95	38.4	24.8	52.1
Ca	Brain	6	1200	2.57	1030	521	2370
	Gonad	7	825	2.56	576	120	2100
	Hard roe	4	1190	2.12	1140	1050	1450
	Liver	7	169	3.35	102	56.0	447
	Kidney	7	979	2.20	686	350	2210
	RBC	9	47.9	3.49	40.3	33.4	107
	Plasma	7	118	3.41	121	61.5	178
P	Brain	6	17100	1.43	17500	15400	18200
	Gonad	7	8940	2.17	6300	905	29200
	Hard roe	4	9700	0.85	9950	8880	10100
	Liver	7	10600	1.57	8350	5620	18300
	Kidney	7	12800	1.39	14100	6370	14900
	RBC	9	1330	2.08	1220	803	2490
	Plasma	7	654	1.26	612	555	828
Li	Brain	3	0.379	3.45	0.192	0.0652	0.880
	Gonad	3	0.0617	7.38	0.0535	0.0379	0.0937
	Hard roe	2	0.0614	7.86		0.0416	0.0812
	Liver	0	< LOD	< LOD	< LOD	< LOD	< LOD
	Kidney	6	0.0702	6.06	0.0466	0.00933	0.146
	RBC	8	0.0426	3.22	0.0354	0.00732	0.0913
	Plasma	5	0.0421	14.1	0.0190	0.00264	0.107

Table C8 continued from previous page

Element	Matrix	n >LOD	Mean	RSD (%)	Median	Min	Max
B	Brain	1	< LOD	< LOD	< LOD	< LOD	< LOD
	Gonad	1	< LOD	< LOD	< LOD	< LOD	< LOD
	Hard roe	0	< LOD	< LOD	< LOD	< LOD	< LOD
	Liver	0	< LOD	< LOD	< LOD	< LOD	< LOD
	Kidney	0	< LOD	< LOD	< LOD	< LOD	< LOD
	RBC	0	< LOD	< LOD	< LOD	< LOD	< LOD
	Plasma	1	< LOD	< LOD	< LOD	< LOD	< LOD
Al	Brain	6	634	1.10	194	3.24	2770
	Gonad	7	92.6	1.24	38.1	8.79	288
	Hard roe	4	16.1	0.898	6.83	1.90	48.9
	Liver	7	19.9	1.73	11.7	0.929	89.9
	Kidney	7	197	2.36	143	16.6	432
	RBC	9	0.145	2.95	0.0274	0.0117	0.427
	Plasma	6	0.367	3.08	0,135	0.0667	1.47
Si	Brain	5	721	2.60	429	48.8	2230
	Gonad	7	127	3.82	49.6	2.26	419
	Hard roe	4	20.9	4.41	6.26	1.56	69.6
	Liver	5	36.0	2.46	14.0	7.88	129
	Kidney	7	292	2.68	228	624	16.4
	RBC	6	1.00	2.29	0.981	0.526	1.59
	Plasma	4	0.832	2.43	0.666	0.612	1.38
Pb	Brain	5	0.298	16.4	0.131	0.00661	1.02
	Gonad	5	0.161	3.28	0.132	0.0118	0.418
	Hard roe	2	0.0176	17.2		0.00237	0.0328
	Liver	6	0.0266	61.3	0.00739	000239	0.122
	Kidney	7	0.195	34.5	0.0935	0.00169	1,64
	RBC	9	0.00525	5.33		0.00299	0.00942
	Plasma	2	0.0602	5.61		0.0251	0.0952
Hg	Brain	6	0.0229	87.0	0.0176	0.00533	0.0561
	Gonad	6	0.0233	94.9	0.00855	0.00180	0.0877
	Hard roe	4	0.00804	43.5	0.00706	0.00506	0.0130
	Liver	7	0.0786	24.5	0.0392	0.0118	0.365
	Kidney	7	0.0966	30.0	0.0668	0.0117	0.272
	RBC	9	0.0165	32.7	0.0127	0.00776	0.0246
	Plasma	4	0.00457	93.1	0.00343	0.000796	0.0106

Table C8 continued from previous page

Element	Matrix	n >LOD	Mean	RSD (%)	Median	Min	Max
Cd	Brain	6	0.0181	49.9	0.0153	0.00630	0.0468
	Gonad	7	0.0481	24.0	0.0177	0.00255	0.142
	Hard roe	4	0.0344	25.4	0.0214	0.00148	0.0931
	Liver	7	0.305	4.89	0.169	0.0913	1.17
	Kidney	7	1.98	2.26	1.73	0.861	4.20
	RBC	3	0.000325	112	0.000319	0.000183	0.000473
	Plasma	3	0000594	156	0.000588	0.000510	0.000685
Se	Brain	6	1.54	9.84	1.33	1.11	2.82
	Gonad	7	1.76	8.47	1.42	0.348	3.60
	Hard roe	4	4.24	2.93	3.98	3.46	5.52
	Liver	7	4.09	5.86	2.73	1.95	12.1
	Kidney	7	6.77	6.37	5.65	3.47	14.9
	RBC	9	0.810	5.82	0.723	0.383	1.82
	Plasma	7	0.444	17.3	0.381	0.0338	0.974
As	Brain	6	0.619	6.76	0.478	0.293	1.20
	Gonad	7	3.51	3.34	1.86	0.421	14.0
	Hard roe	4	1.18	3.97	0.972	0.204	2.56
	Liver	7	0.787	4.50	0.748	0.199	1.25
	Kidney	7	1.69	4.63	1.59	1.09	2.52
	RBC	9	0.0581	11.9	0.0555	0.0107	0.124
	Plasma	7	0.101	14.7	0.0812	0.0235	0.201
Cu	Brain	6	9.72	0.94	9.90	8.60	10.6
	Gonad	7	6.60	1.76	2.00	0.183	30.3
	Hard roe	4	25.8	0.58	21.5	9.20	51.2
	Liver	7	27.0	0.62	29.6	8.54	40.7
	Kidney	7	5.34	1.07	5.10	2.31	7.68
	RBC	9	0.212	1.95	0.201	0.158	0.280
	Plasma	7	0.416	6.34	0.407	0.223	0.807
Zn	Brain	6	44.6	1.25	43.9	38.4	51.1
	Gonad	7	75.3	0.87	61.0	8.04	168
	Hard roe	4	139	0.43	126	62.8	243
	Liver	7	84.4	1.07	82.1	59.3	122
	Kidney	7	110	0.63	95.2	86.1	157
	RBC	9	7.67	1.18	6.71	5.80	14.0
	Plasma	7	13.6	1.45	11.7	7.66	22.8

Table C8 continued from previous page

Element	Matrix	n >LOD	Mean	RSD (%)	Median	Min	Max
Ni	Brain	6	0.241	29.4	0.147	0.0340	0.803
	Gonad	6	0.0745	40.6	0.0653	0.00976	0.159
	Hard roe	4	0.0202	185	0.0143	0.00280	0.0494
	Liver	4	0.0467	187	0.00711	0.00105	0.172
	Kidney	7	0.472	34.1	0.327	0.0724	1.81
	RBC	9	0.00849	21.3	0.00587	0.00410	0.0214
	Plasma	6	0.0278	40.8	0.0145	0.00747	0.0925
Co	Brain	6	0.200	3.95	0.118	0.0455	0.548
	Gonad	7	0.157	4.51	0.107	0.0213	0.634
	Hard roe	4	0.0463	1.33	0.198	0.0869	0.707
	Liver	7	0.150	3.30	0.120	0.0955	0.391
	Kidney	7	1.20	1.23	1.25	0,0823	1.73
	RBC	9	0.0278	5.10	0.0150	0.00754	0.118
	Plasma	7	0.109	12.1	0.0493	0.0328	0.474
Cr	Brain	6	0.565	6.81	0.186	0.00294	2.40
	Gonad	7	0.0832	7.37	0.0580	0.00819	0.261
	Hard roe	1	< LOD	13.3	< LOD	< LOD	< LOD
	Liver	2	0.0518	34.3		0.000563	0.103
	Kidney	7	0.242	5.79	0.197	0.0263	0.559
	RBC	8	0.00613	15.2	0.00361	0.00196	0.0166
	Plasma	4	0.00677	22.7	0.00379	0.000241	0.0193
V	Brain	6	0.793	10.4	0.269	0.00389	0.732
	Gonad	7	0.107	4.56	0.0577	0.00506	0.339
	Hard roe	4	0.0329	8.84	0.0159	0.00693	0.0964
	Liver	7	0.0540	14.8	0.0203	0.00496	0.269
	Kidney	7	0.335	3.54	0.244	0.0529	0.851
	RBC	1	< LOD	< LOD	< LOD	< LOD	< LOD
	Plasma	4	0.00528	19.0	0.00574	0.0000835	0.00956
Fe	Brain	6	379	1.76	160	48.7	1500
	Gonad	7	96.3	1.00	74.7	23.9	199
	Hard roe	4	160	1.26	162	50.4	267
	Liver	7	494	1.09	221	66.5	1950
	Kidney	7	426	1.01	344	148	812
	RBC	9	357	0.96	357	233	432
	Plasma	7	51.9	5.05	15.6	3.33	222

Table C8 continued from previous page

Element	Matrix	n >LOD	Mean	RSD (%)	Median	Min	Max
Mn	Brain	6	6.62	1.10	3.34	1.22	21.2
	Gonad	7	6.38	1.13	2.93	0.413	26.4
	Hard roe	4	5.14	0.91	5.20	2.55	7.61
	Liver	7	4.31	1.11	2.67	1.71	7.72
	Kidney	7	4.95	0.99	4.74	2.51	8.48
	RBC	9	0.0527	3.43	0.0533	0.0163	0.130
	Plasma	6	0.0320	35.3	0.0244	0.0149	0.0645
Ti	Brain	6	21.9	5.31	8.88	0.207	89.2
	Gonad	7	2.99	5.07	1.63	0.144	8.79
	Hard roe	4	0.649	12.6	0.416	0.123	1.64
	Liver	7	0.285	10.6	0.223	0.0335	1.03
	Kidney	7	7.07	3.28	5.01	0.591	16.4
	RBC	9	0.00923	21.8	0.00596	0.00214	0.0245
	Plasma	6	0.0220	26.1	0.0132	0.00815	0.0686
Sc	Brain	6	0.127	22.8	0.0438	0.000556	0.557
	Gonad	5	0.0230	9.73	0.01546	0.00427	0.0533
	Hard roe	4	0.00519	16.3	0.00331	0.00252	0.0116
	Liver	4	0.00487	44.0	0.00100	0.000122	0.0174
	Kidney	7	0.0364	15.1	0.0257	0.00110	0.0852
	RBC	1	< LOD	< LOD	< LOD	< LOD	< LOD
	Plasma	2	0.000341	267	0.000322		0.000359
Rb	Brain	6	3.73	1.17	2.64	1.26	7.55
	Gonad	7	5.07	1.54	3.19	0.355	15.5
	Hard roe	4	3.45	0.941	3.42	3.45	4.84
	Liver	7	7.98	1.11	2.46	1.65	17.9
	Kidney	7	7.11	1.19	5.42	3.20	18.3
	RBC	9	0.574	1.32	0.421	0.305	1.47
	Plasma	7	0.139	5.09	0.111	0.0187	0.271
Sr	Brain	6	1.45	1.70	1.13	0.441	3.03
	Gonad	7	0.927	0.904	0.648	0.116	2.57
	Hard roe	4	1.73	1.00	1.74	1.42	2.02
	Liver	7	0.136	5.28	0.120	0.0371	0.313
	Kidney	7	2.12	1.28	1.04	0.353	8.77
	RBC	9	0.0830	2.95	0.0418	0.0117	0.253
	Plasma	7	0.182	3.71	0.175	0.0550	0.296

Table C8 continued from previous page

Element	Matrix	n >LOD	Mean	RSD (%)	Median	Min	Max
Y	Brain	6	0.175	13.5	0.0603	0.000686	0.712
	Gonad	7	0.0248	9.64	0.0211	0.000192	0.0714
	Hard roe	4	0.0113	13.6	0.00725	0.00181	0.0287
	Liver	7	0.00870	16.5	0.00426	0.00114	0.0343
	Kidney	7	0.0714	5.20	0.0566	0.00623	0.188
	RBC	6	0.0000515	227	0.0000308	5.64E-06	0.000142
	Plasma	3	0.0000952	106	0.0000414	2.06E-05	0.000223
Zr	Brain	6	0.163	10.3	0.109	0.00598	0.486
	Gonad	7	0.0119	32.9	0.0135	0.000299	0.0312
	Hard roe	4	0.00314	37.1	0.00104	0.000925	0.00956
	Liver	3	0.0273	35.9	0.00304	0.000504	0.00465
	Kidney	7	0.0501	31.1	0.0115	0.00561	0.260
	RBC	7	0.000141	62.1	0.000145	0.0000634	0.000226
	Plasma	6	0.000889	32.9	0.000609	0.000161	0.00251
Mo	Brain	6	0.0318	21.7	0.0328	0.0243	0.0391
	Gonad	7	0.0146	48.9	0.0168	0.00142	0.0276
	Hard roe	4	0.0281	9.30	0.0258	0.0158	0.0451
	Liver	7	0.456	4.86	0.398	0.283	0.862
	Kidney	7	0.233	5.27	0.217	0.111	0.425
	RBC	0	< LOD	< LOD	< LOD	< LOD	< LOD
	Plasma	0	< LOD	< LOD	< LOD	< LOD	< LOD
In	Brain	5	0.000801	124	0.000154	0.0000436	0.00307
	Gonad	6	0.000244	72.1	0.000154	0.0000419	0.000540
	Hard roe	2	0.0000561	238		0.0000136	0.0000987
	Liver	2	0.000138	1600		0.00000236	0.000274
	Kidney	6	0.000277	140	0.000203	0.0000332	0.000717
	RBC	3	0.0000111	124	0.0000114	0.0000121	0.00000975
	Plasma	2	0.0000364	179		0.0000321	0.0000407
Sn	Brain	3	0.0409	8.38	0.00680	0.00650	0.109
	Gonad	6	0.0112	16.3	0.0108	0.00105	0.0216
	Hard roe	3	0.00547	10.3	0.00553	0.000928	0.00995
	Liver	0	< LOD	< LOD	< LOD	< LOD	< LOD
	Kidney	7	0.0130	21.4	0.00982	0.00160	0.0316
	RBC	7	0.000432	92.7	0.000374	0.000181	0.000772
	Plasma	7	0.00242995	124	0.00102	0.000507	0.00733

Table C8 continued from previous page

Element	Matrix	n >LOD	Mean	RSD (%)	Median	Min	Max
Sb	Brain	6	0.00513	60.4	0.00497	0.000773	0.0111
	Gonad	7	0.00234	109	0.00273	0.000912	0.00399
	Hard roe	3	0.00132	34.1	0.00101	0.000372	0.00258
	Liver	4	0.00191	69.8	0.00118	0.00103	0.00425
	Kidney	7	0.00767	79.5	0.00726	0.00211	0.0178
	RBC	0	< LOD	< LOD	< LOD	< LOD	< LOD
	Plasma	0	< LOD	< LOD	< LOD	< LOD	< LOD
Cs	Brain	6	0.136	4.31	0.0796	0.0404	0.399
	Gonad	7	0.0503	5.22	0.0433	0.0142	0.104
	Hard roe	4	0.0913	2.65	0.0838	0.0221	0.176
	Liver	7	0.0567	4.81	0.0511	0.0261	0.0980
	Kidney	7	0.108	3.42	0.115	0.0797	0.134
	RBC	9	0.00400	10.4	0.00441	0.00112	0.00516
	Plasma	5	0.00265	47.6	0.00270	0.000263	0.00495
Ba	Brain	6	6.44	2.94	2.98	0.671	26.1
	Gonad	7	0.759	5.38	0.390	0.0311	2.44
	Hard roe	4	0.165	5.30	0.125	0.0869	0.376
	Liver	7	0.144	29.2	0.0580	0.00299	0.678
	Kidney	7	1.64	2.71	1.20	0.154	3.81
	RBC	4	0.00560	18.5	0.00526	0.000932	0.0109
	Plasma	3	0.00182	42.5	0.000977	0.000278	0.00421
La	Brain	6	0.309	5.47	0.0949	0.00252	1.21
	Gonad	7	0.0703	4.12	0.0362	0.00207	0.190
	Hard roe	4	0.0306	2.22	0.0244	0.00731	0.0662
	Liver	7	0.0977	5.89	0.0237	0.0150	0.524
	Kidney	7	0.162	3.66	0.118	0.0191	0.385
	RBC	9	0.000101	95.2	0.0000638	0.0000146	0.000348
	Plasma	6	0.000358	75.4	0.000258	0.0000602	0.000855
Ce	Brain	6	0.676	5.33	0.198	0.00148	2.70
	Gonad	7	0.145	5.21	0.0644	0.00273	0.414
	Hard roe	4	0.0401	5.62	0.0272	0.00606	0.100
	Liver	7	0.118	4.26	0.0300	0.00988	0.657
	Kidney	7	0.330	2.03	0.250	0.0246	0.752
	RBC	4	0.000190	66.2	0.000131	0.0000691	0.000428
	Plasma	5	0.000125	173	0.000102	0.0000572	0.000193

Table C8 continued from previous page

Element	Matrix	n >LOD	Mean	RSD (%)	Median	Min	Max
Lu	Brain	5	0.00230	30.8	0.00145	0.000251	0.00768
	Gonad	5	0.488	29.5	0.000404	0.000170	2.44
	Hard roe	3	0.0000789	240	0.0000360	0.0000114	0.000189
	Liver	4	0.000213	132	0.000157	0.0000229	0.000514
	Kidney	6	0.000810	33.8	0.000579	0.0000733	0.00197
	RBC	1	< LOD	< LOD	< LOD	< LOD	< LOD
	Plasma	1	< LOD	< LOD	< LOD	< LOD	< LOD
Hf	Brain	6	0.0106	26.3	0.00738	0.00118	0.0367
	Gonad	7	0.000808	76.3	0.000763	0.000383	0.00171
	Hard roe	4	0.000438	82.6	0.000454	0.000326	0.000518
	Liver	7	0.000289	123	0.000232	0.0000823	0.000496
	Kidney	7	0.00186	85.9	0.000562	0.000266	0.00871
	RBC	9	0.000238	59.3	0.000265	0.000136	0.000383
	Plasma	7	0.00111	81.9	0.000473	0.000154	0.00311
Ta	Brain	4	0.00175	51.4	0.00202	0.000507	0.00245
	Gonad	3	0.000694	32.5	0.000701	0.000353	0.00103
	Hard roe	1	< LOD	< LOD	< LOD	< LOD	< LOD
	Liver	0	< LOD	< LOD	< LOD	< LOD	< LOD
	Kidney	6	0.000648	55.2	0.000876	0.000214	0.00188
	RBC	3	0.0000121	408	0.0000109	0.0000105	0.0000148
	Plasma	2	0.000229	268		0.0000142	0.000444
W	Brain	6	0.0254	14.7	0.0109	0.00160	0.102
	Gonad	7	0.00298	43.9	0.00209	0.000781	0.00739
	Hard roe	4	0.00176	51.3	0.00179	0.000864	0.00260
	Liver	5	0.00115	132	0.000872	0.000438	0.00194
	Kidney	7	0.00824	39.0	0.00624	0.000753	0.0138
	RBC	7	0.000426	109	0.000291	0.000168	0.00116
	Plasma	5	0.00276	134	0.000478	0.000128	0.0123
Tl	Brain	6	0.0175	12.2	0.0104	0.00498	0.0383
	Gonad	7	0.0158	18.2	0.00467	0.000692	0.0789
	Hard roe	4	0.00406	18.2	0.00426	0.00277	0.00497
	Liver	7	0.0751	6.13	0.0208	0.319	0.0103
	Kidney	7	0.0489	9.17	0.0151	0.00912	0.217
	RBC	7	0.000246	127	0.000125	0.0000214	0.00106
	Plasma	2	0.000319	194		0.0000131	0.000624

Table C8 continued from previous page

Element	Matrix	n >LOD	Mean	RSD (%)	Median	Min	Max
Th	Brain	6	0.0852	17.2	0.0852	0.000549	0.358
	Gonad	7	0.0138	25.6	0.00776	0.000398	0.0364
	Hard roe	3	0.00308	124	0.00166	0.0000475	0.00754
	Liver	6	0.00273	70.1	0.00137	0.000196	0.0100
	Kidney	7	0.0318	17.2	0.0260	0.00322	0.0769
	RBC	2	0.000484	193		0.000295	0.000672
	Plasma	0	< LOD	< LOD	< LOD	< LOD	< LOD
U	Brain	5	0.0140	29.7	0.00915	0.00205	0.0371
	Gonad	5	0.00428	37.1	0.00332	0.000567	0.00851
	Hard roe	3	0.00287	133	0.000488	0.000141	0.00799
	Liver	7	0.00311	95.3	0.00104	0.0000967	0.0161
	Kidney	7	0.0332	15.8	0.0228	0.00474	0.117
	RBC	0	< LOD	< LOD	< LOD	< LOD	< LOD
	Plasma	1	< LOD	< LOD	< LOD	< LOD	< LOD

C.6.1 Elemental distribtuion of selected elements in tissues of Arctic char

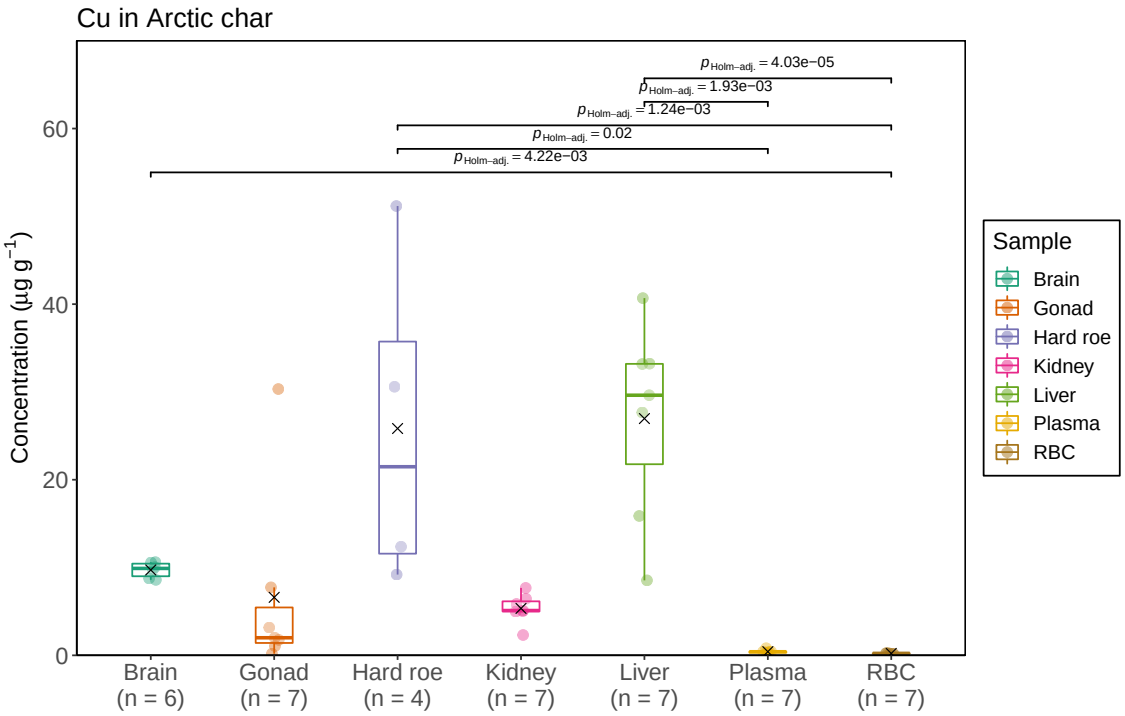

Figure C21: Distribution of Cu in tissues of Arctic char from Lake Diesetvatnet. Box and whisker plot shows minimum and maximum (whiskers), interquartile range (box), and median (horizontal line) concentrations of Cu in μg g $^{-1}$ in each sample type (n indicates the number of samples for each tissue). The cross indicates the mean concentration, and the bar indicates groups that are statistically significantly different with the corresponding p-value.

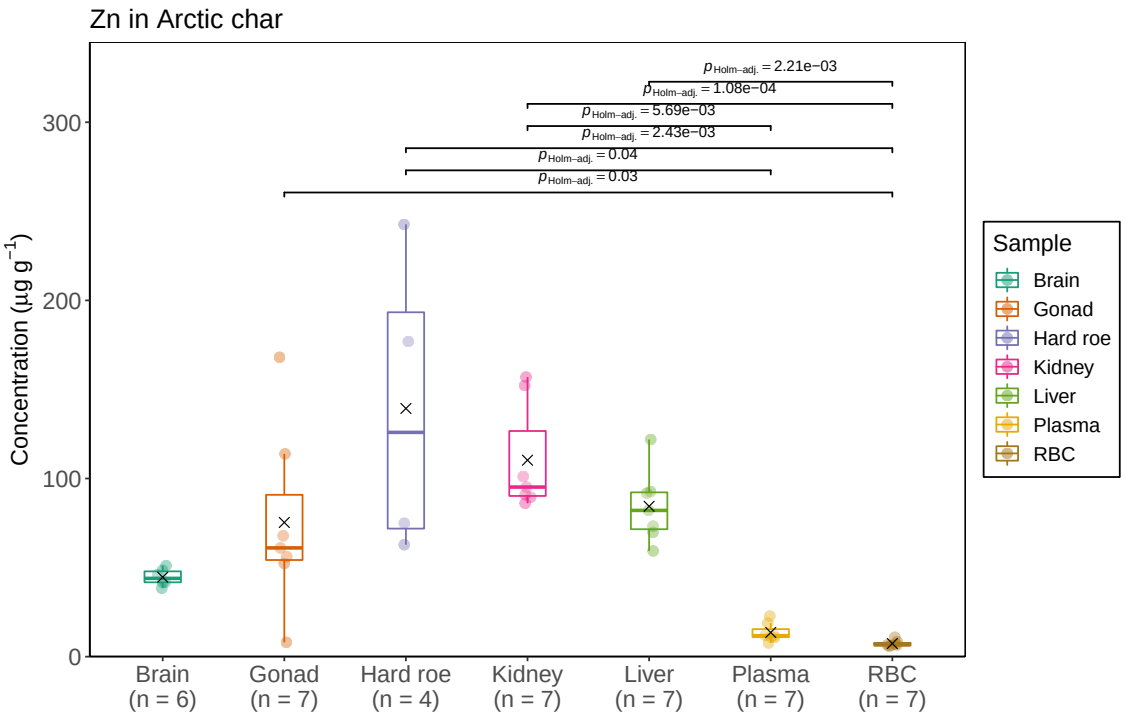

Figure C22: Distribution of Zn in tissues of Arctic char from Lake Diesetvatnet. Box and whisker plot shows minimum and maximum (whiskers), interquartile range (box), and median (horizontal line) concentrations of Zn in μg g $^{-1}$ in each sample type (n indicates the number of samples for each tissue). The cross indicates the mean concentration, and the bar indicates groups that are statistically significantly different with the corresponding p-value.

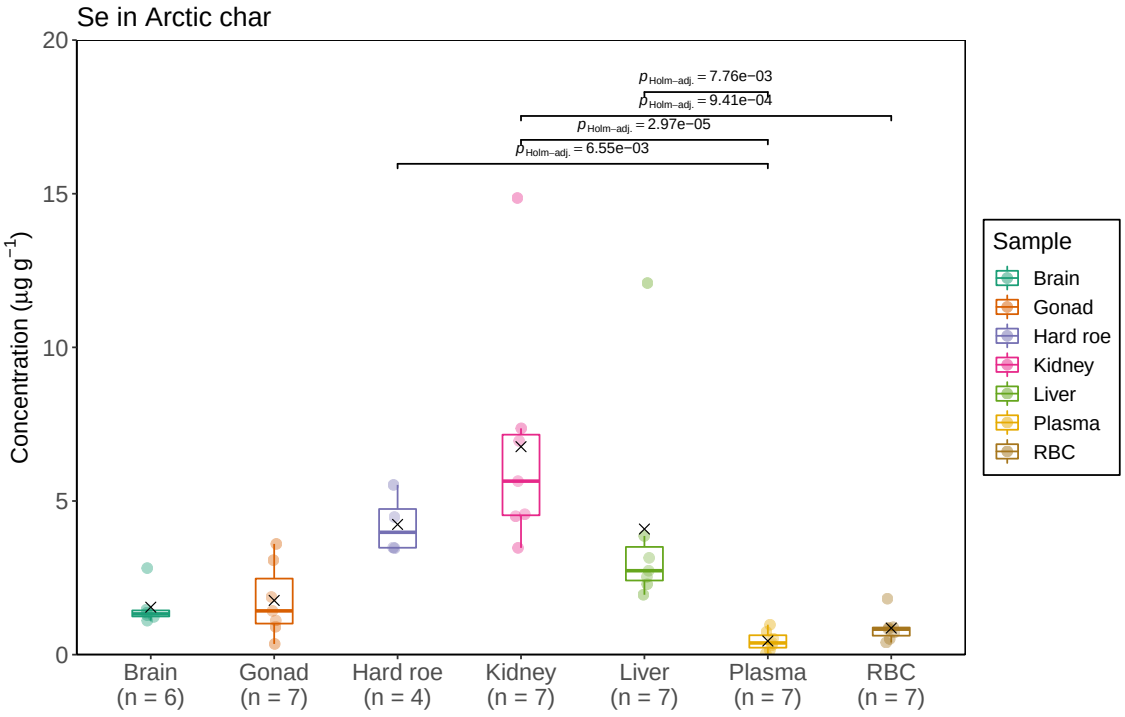

Figure C23: Distribution of Se in tissues of Arctic char from Lake Diesetvatnet. Box and whisker plot shows minimum and maximum (whiskers), interquartile range (box), and median (horizontal line) concentrations of Se in μg g $^{-1}$ in each sample type (n indicates the number of samples for each tissue). The cross indicates the mean concentration, and the bar indicates groups that are statistically significantly different with the corresponding p-value.

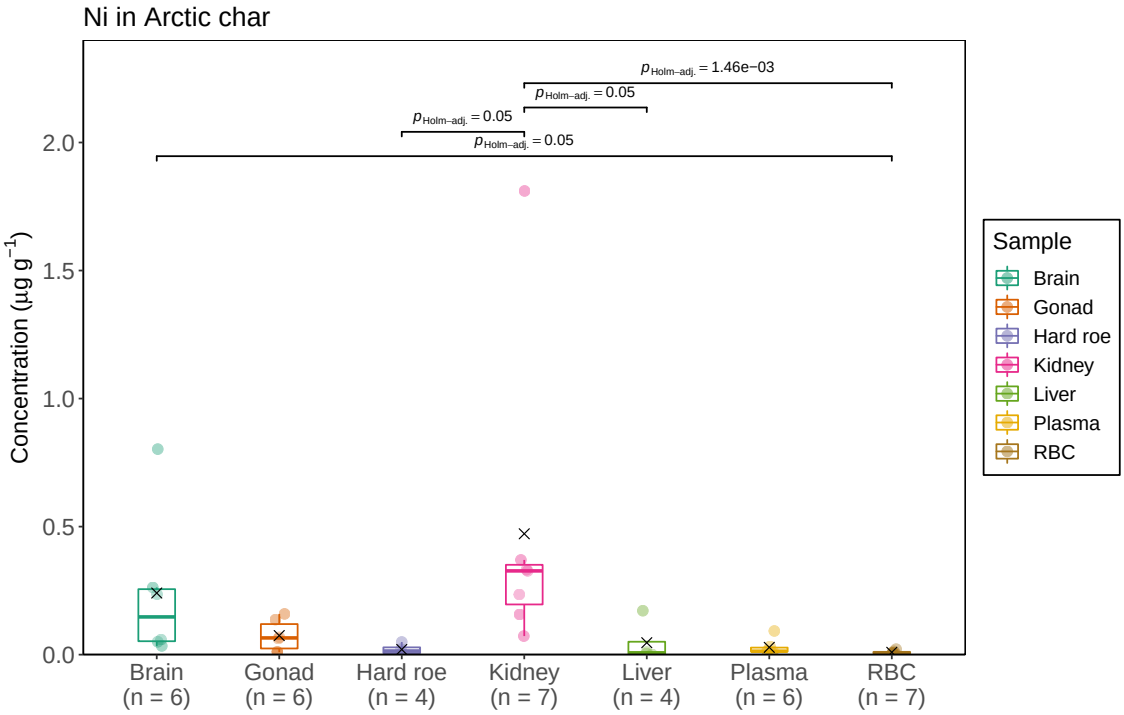

Figure C24: Distribution of Ni in tissues of Arctic char from Lake Diesetvatnet. Box and whisker plot shows minimum and maximum (whiskers), interquartile range (box), and median (horizontal line) concentrations of Ni in μg g $^{-1}$ in each sample type (n indicates the number of samples for each tissue). The cross indicates the mean concentration, and the bar indicates groups that are statistically significantly different with the corresponding p-value.

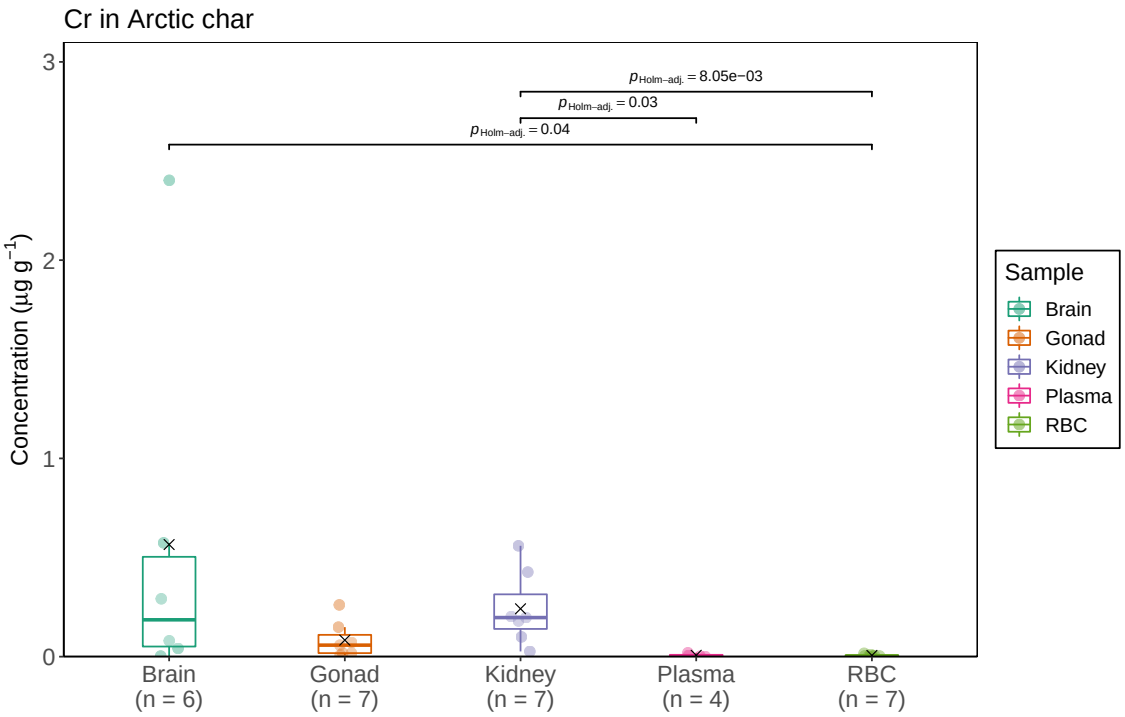

Figure C25: Distribution of Cr in tissues of Arctic char from Lake Diesetvatnet. Box and whisker plot shows minimum and maximum (whiskers), interquartile range (box), and median (horizontal line) concentrations of Cr in μg g $^{-1}$ in each sample type (n indicates the number of samples for each tissue). The cross indicates the mean concentration, and the bar indicates groups that are statistically significantly different with the corresponding p-value.

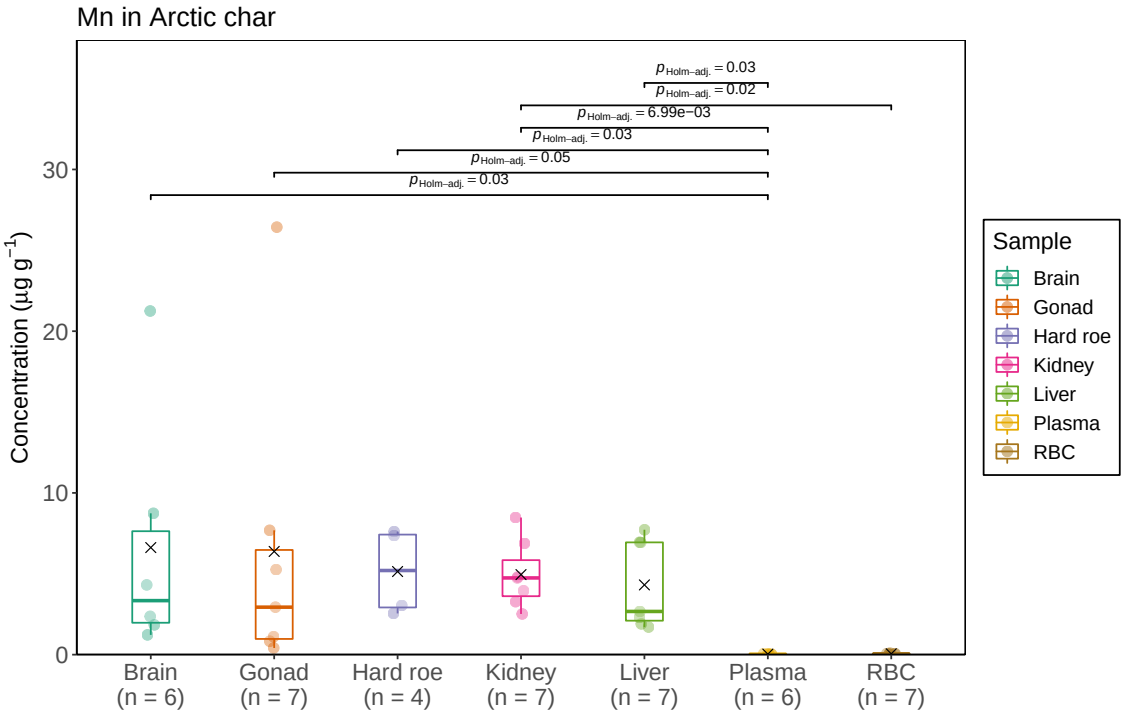

Figure C26: Distribution of Mn in tissues of Arctic char from Lake Diesetvatnet. Box and whisker plot shows minimum and maximum (whiskers), interquartile range (box), and median (horizontal line) concentrations of Mn in μg g $^{-1}$ in each sample type (n indicates the number of samples for each tissue). The cross indicates the mean concentration, and the bar indicates groups that are statistically significantly different with the corresponding p-value.

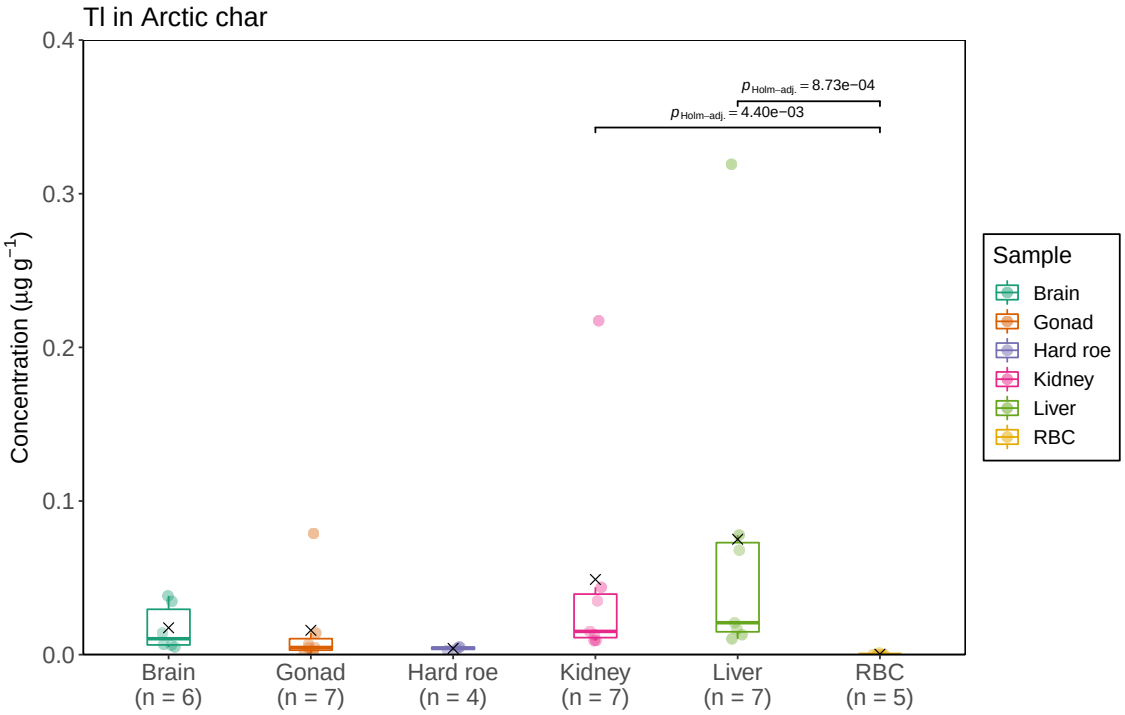

Figure C27: Distribution of Tl in tissues of Arctic char from Lake Diesetvatnet. Box and whisker plot shows minimum and maximum (whiskers), interquartile range (box), and median (horizontal line) concentrations of Tl in μg g $^{-1}$ in each sample type (n indicates the number of samples for each tissue). The cross indicates the mean concentration, and the bar indicates groups that are statistically significantly different with the corresponding p-value.

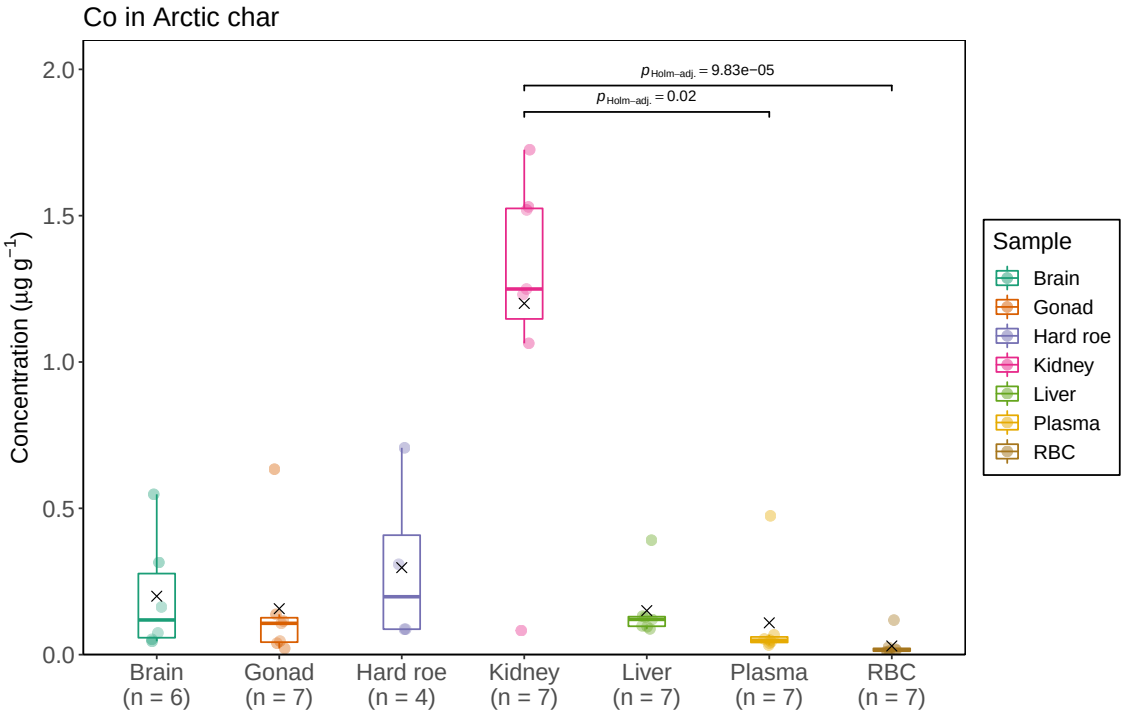

Figure C28: Distribution of Co in tissues of Arctic char from Lake Diesetvatnet. Box and whisker plot shows minimum and maximum (whiskers), interquartile range (box), and median (horizontal line) concentrations of Co in μg g $^{-1}$ in each sample type (n indicates the number of samples for each tissue). The cross indicates the mean concentration, and the bar indicates groups that are statistically significantly different with the corresponding p-value.

C.7 Limit of detection for elemental analysis with ICP-MS

Table C9: Limit of detection (LOD) for elements in μg L^{-1} analysed in fish tissue samples with ICP-MS. LOD_a for elements analysed in Artic char tissues including brain, hard roe, gonad, liver, and kidney. LOD_b for elements analysed in Artic char plasma and red blood cells.

Element	**LOD_a**	**LOD_b**
Li	4.23E-04	2.74E-03
B	2.59E-02	2.70E-02
Mg	1.96E-02	5.54E-03
Al	1.13E-02	7.81E-03
Si	2.80E-01	3.22E-01
P	5.70E-02	4.22E-02
Ca	1.54E-01	3.43E-01
Sc	2.63E-04	4.23E-04
Ti	2.59E-03	7.98E-04
V	4.22E-04	5.05E-05
Cr	4.86E-03	1.68E-03
Mn	3.58E-03	1.12E-03
Fe	9.39E-02	4.66E-02
Co	1.80E-03	6.04E-04
Ni	1.67E-03	1.97E-03
Cu	1.97E-03	4.18E-03
Zn	9.68E-03	1.02E-02
As	9.33E-04	8.41E-04
Se	6.34E-03	1.10E-02
Rb	1.09E-03	2.85E-03
Sr	6.91E-03	3.15E-04
Y	4.84E-05	9.55E-05
Zr	1.32E-04	2.24E-04
Mo	1.44E-03	3.13E-03
Cd	3.25E-04	6.31E-04
In	3.81E-05	5.54E-05
Sn	1.33E-03	1.59E-03
Sb	9.97E-04	2.48E-03
Cs	6.28E-04	2.59E-04
Ba	2.34E-03	1.85E-03

Table C9 continued from previous page

Element	LOD_a	LOD_b
La	1.02E-04	7.59E-05
Ce	4.75E-05	1.72E-04
Lu	3.37E-05	4.53E-05
Hf	9.91E-05	1.02E-04
Ta	8.91E-05	3.48E-05
W	4.00E-04	6.24E-04
Hg	6.22E-03	1.14E-03
Tl	1.80E-04	2.13E-04
Pb	8.35E-04	1.35E-03
Th	1.84E-04	3.28E-04
U	7.02E-05	3.35E-04

C.8 Recovery of elemental concentrations in certified reference materials

Table C10: Percentage recovery (%) of elements in different certified reference materials DORM-5 fish protein (DORM-5), DOLT-3 dogfish liver (DOLT-3), Seronorm^{TM} trace elements whole blood L-2 (Seronorm WB L-2), and Seronorm^{TM} trace elements serum (Seronorm S). Recoveries outside the certified range are marked with one asteriks (*). Recoveries calculated based on approximate values only are marked with two asteriks (**).

	Recovery (%)			
Element	**DORM-5**	**DOLT-3**	**Seronorm WB-L2**	**Seronorm S**
Li	87.3	-	-	-
B	*82.8	-	**30.6	-
Mg	*132	-	**111	102
Al	96.4	-	104	95.8
P	*95.7	-	**107	*93.4
Ca	93.7	-	**114	97.3
Ti	-	-	**107	-
V	101	-	83.8	-
Cr	95.3	-	106	107
Mn	*92.7	-	104	*49.9
Fe	103	102	**103	*124
Co	95.8	-	106	*313
Ni	*81.1	*86.1	106	*127
Cu	*93.1	97.8	101	*93.8
Zn	*94.3	102	108	*91.7
As	96.4	*86.9	86.7	-
Se	*91.1	96.6	95.4	93.1
Rb	*89.7	-	**103	-
Sr	*97.1	-	**114	-
Y	-	-	**92.9	-
Zr	-	-	**130	-
Mo	89.8	-	*41.6	-
Cd	103	97.4	*126	-
Sn	*88.2	-	108	-
Sb	98.3	-	116	-
Cs	-	-	**111	-
La	-	-	**147	-
Ce	-	-	**92.3	-

Table C10 continued from previous page

	Recovery (%)			
Element	**DORM-5**	**DOLT-3**	**Seronorm WB-L2**	**Seronorm S**
Hf	-	-	**2300	-
W	-	-	**587	-
Ba	99.0	-	-	-
Hg	*91.4	*56.9	98.3	-
Tl	-	-	*127	-
Pb	-	85.6	106	-
U	*229	-	-	-

D Appendix - Discussion

D.1 PCA loading and score plots

Table D1: Sample ID for data used in PCA analysis. Sample ID and the corresponding number of individual Arctic char and sample matrix.

Sample-ID	Fish	Matrix
R1	1	Brain
R2	2	Brain
R3	3	Brain
R4	4	Brain
R5	6	Brain
R6	7	Brain
R7	3	Egg
R8	5	Egg
R9	6	Egg
R10	7	Egg
R11	1	Gonad
R12	2	Gonad
R13	3	Gonad
R14	4	Gonad
R15	5	Gonad
R16	6	Gonad
R17	7	Gonad
R18	1	Liver
R19	2	Liver
R20	3	Liver
R21	4	Liver
R22	5	Liver
R23	6	Liver
R24	7	Liver
R25	1	Kidney
R26	2	Kidney
R27	3	Kidney
R28	4	Kidney
R29	5	Kidney
R30	6	Kidney
R31	7	Kidney

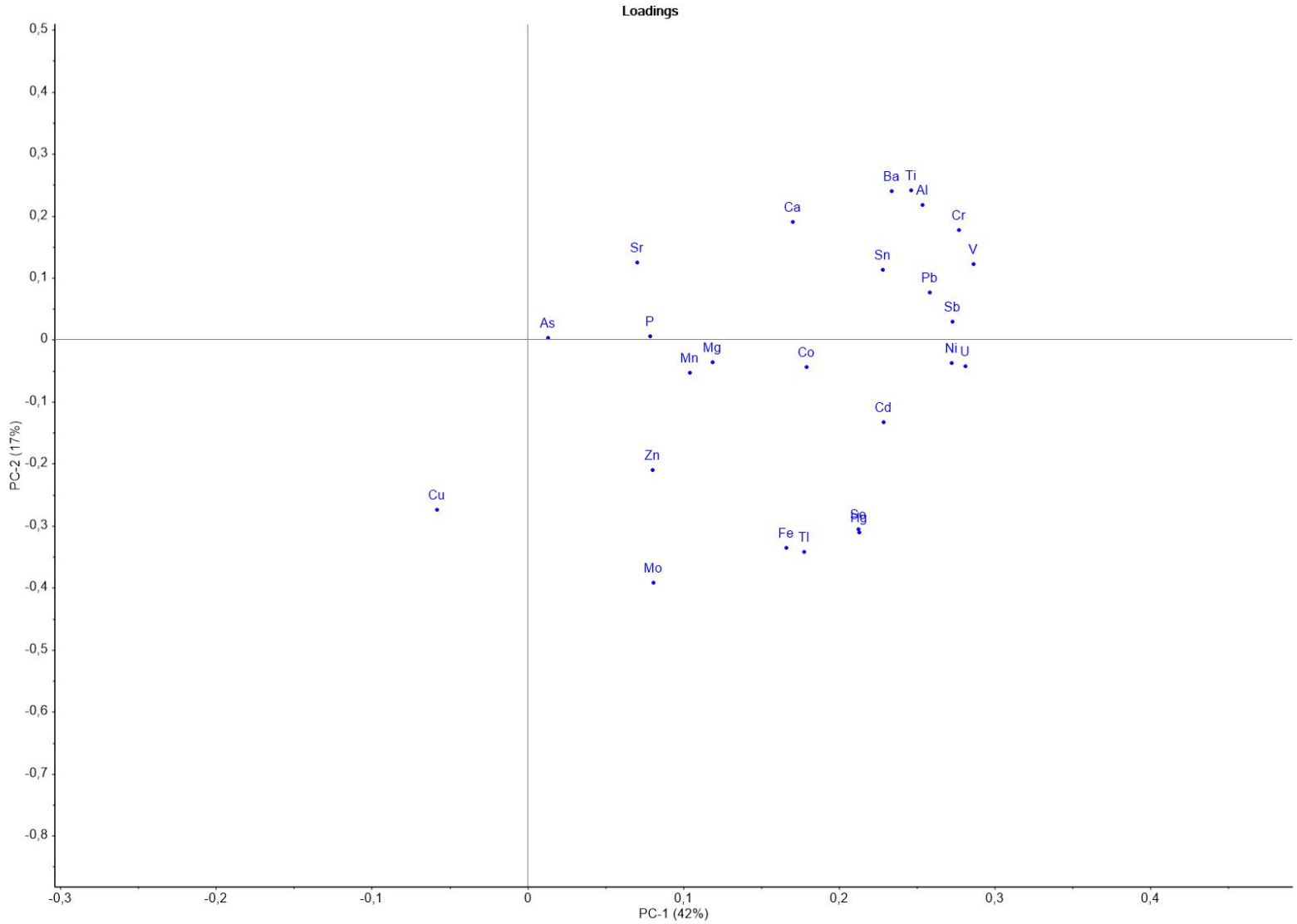

Figure D1: PCA loading plot showing all the variables included in the dataset. PC1 explains 42% of the total variance, and PC2 explains 17% of the total variance.

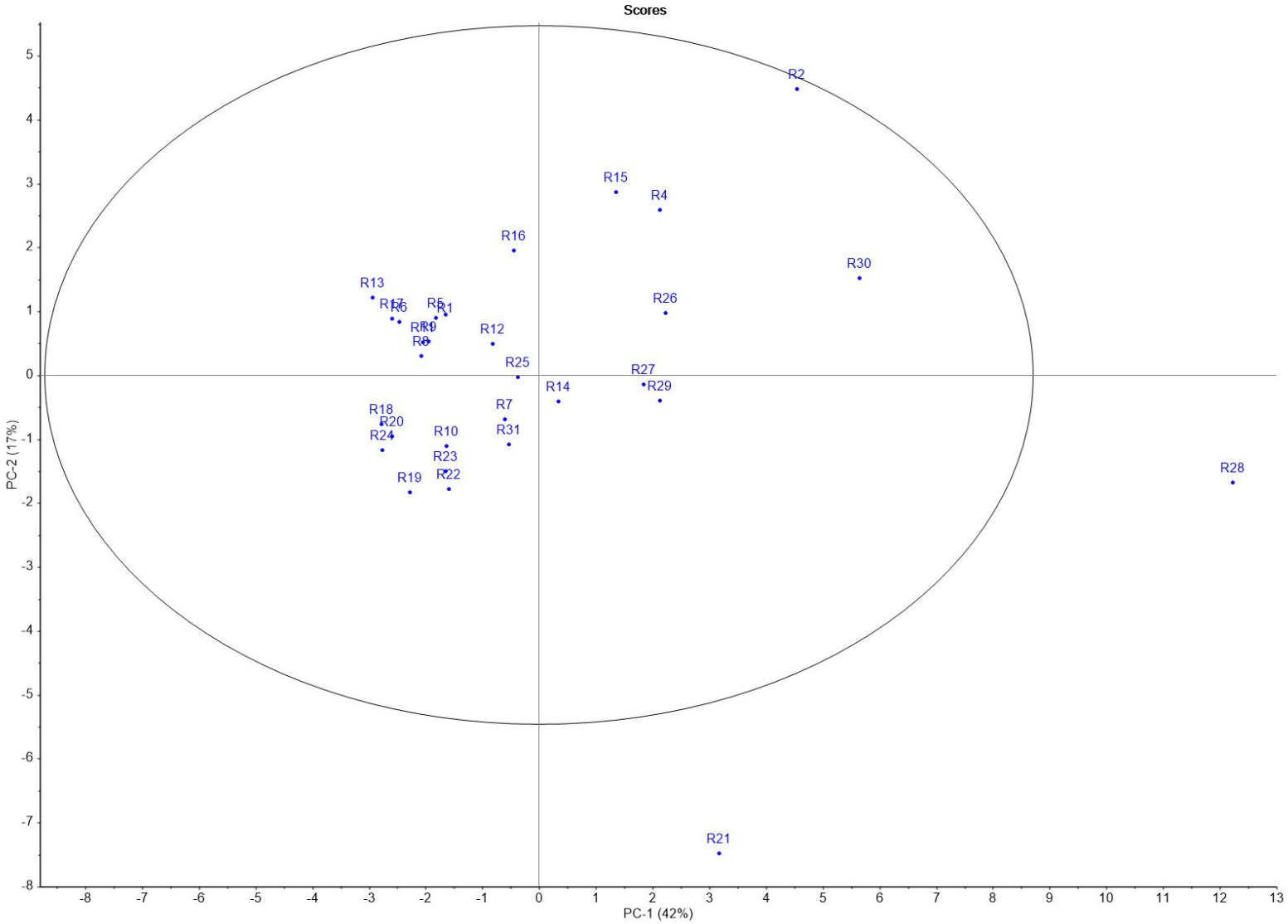

Figure D2: PCA score plot showing all the individual samples included in the dataset displayed as ID-numbers that can be found in Table D1. The outlier number R3 is removed from this PCA. PC1 explains 42% of the total variance, and PC2 explains 17% of the total variance.

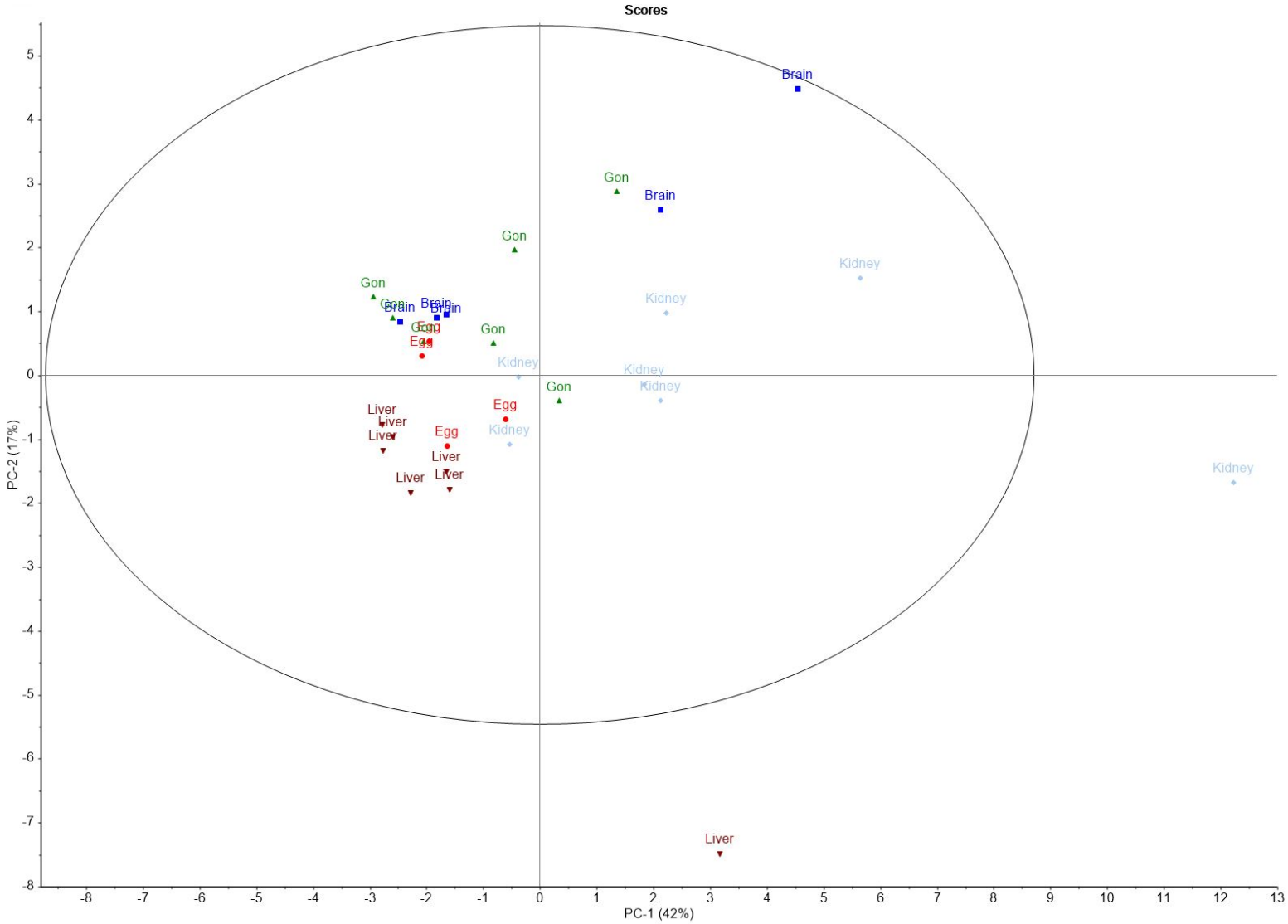

Figure D3: PCA score plot showing all the individual samples included in the dataset displayed as sample type i.e brain, gonad (Gon), hard roe (Egg), liver, and kidney. The outlier number R3 is removed from this PCA. PC1 explains 42% of the total variance, and PC2 explains 17% of the total variance.

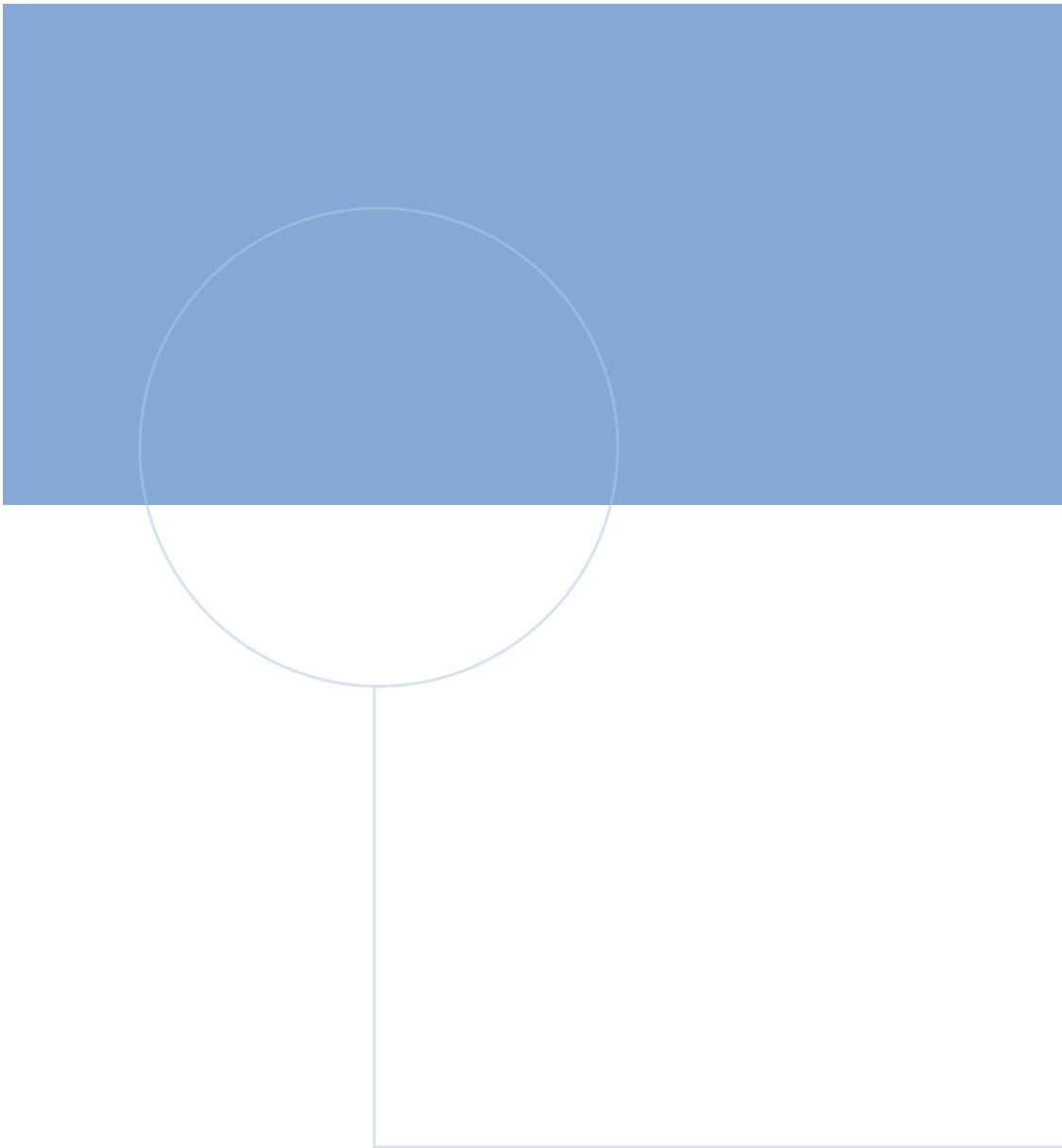

NTNU

Norwegian University of
Science and Technology